The Author

Driven by an interest in climate and earth system functioning, Maria Ansari studied Geosciences (B. Sc. and M. Sc.) with a focus on soil science at the University of Hamburg. During this time, she became particularly fascinated by soil processes, such as soil organic carbon dynamics. Building on that, she pursued her doctorate in the Department of Earth System Science (Soil Science), where she investigated the potential of combined biochar and silicate rock powder application for carbon dioxide removal and soil fertility improvement as part of an interdisciplinary research project.

Verein zur Förderung der Bodenkunde Hamburg
c/o Institut für Bodenkunde - Universität Hamburg
https://www.geo.uni-hamburg.de/de/bodenkunde.html

Hamburger Bodenkundliche Arbeiten

2026

M. Ansari

Band 110

HBA

Maria Ansari

Influence of the combination of biochar and rock powder on soil properties and soil organic carbon dynamics

Band 110
2026

ISSN: 0724-6382

Hamburger Bodenkundliche Arbeiten

Influence of the combination of biochar and rock powder on soil properties and soil organic carbon dynamics

Dissertation

with the aim of achieving a doctoral degree
at the Faculty of Mathematics, Informatics and Natural Sciences
Department of Earth System Sciences
at University of Hamburg

submitted by

Maria Ansari

Hamburg, 2026

Accepted as Dissertation at the Department of Earth System Sciences

Date of Oral Defense:	23rd June 2026
Supervision Committee:	Prof. Dr. Annette Eschenbach Dr. Joscha Becker Prof. Dr. Jörn Peckmann
Reviewers:	Prof. Dr. Annette Eschenbach Dr. Joscha Becker
Members of the Examination Commission:	Prof. Dr. Annette Eschenbach Dr. Joscha Becker Prof. Dr. Jörn Peckmann Prof. Dr. Gerhard Schmiedl Prof. Dr. Felix Ament
Chair of the Subject Doctoral Committee Earth System Sciences:	Prof. Dr. Dirk Notz
Dean of Faculty MIN:	Prof. Dr.-Ing. Norbert Ritter

Published as

Hamburger Bodenkundliche Arbeiten, Volume 110

ISSN: 0724-6382

Editor: Verein zur Förderung der Bodenkunde Hamburg
Allende-Platz 2, 20146 Hamburg
https://www.geo.uni-hamburg.de/bodenkunde/
ueber-das-institut/hba.html

Editorship: Dr. Klaus Berger

Abstract

Carbon dioxide removal (CDR) is a crucial approach to mitigate anthropogenic climate change and to achieve long-term climate targets. Biochar and silicate rock powder for enhanced rock weathering are two promising soil-based technologies, combining CDR with potential soil fertility improvement. Despite their possible synergies, most studies have investigated the effects of the separate application of both amendments. To address this gap, this dissertation compared the effects of pure and combined applications of biochar and basanite, a silicate rock powder, as soil amendments for CDR and soil fertility improvement. Combined applications included both a co-application of biochar and basanite as well as rock-enhanced biochar produced from co-pyrolysis of biomass and basanite.

Amendment applications were investigated in different experimental settings across timescales and soil types to capture potential amendment effects on soil fertility and soil organic carbon (SOC) dynamics, affecting the amendments' CDR potential. A nine-week field-based lysimeter experiment with a temperate sandy soil planted with cabbage turnip (*Brassica oleracea* var. *gongylodes* L.) was used to assess amendment effects on soil properties and processes, affecting soil fertility, as well as SOC stabilization under near-field conditions. Three laboratory-based incubations, each conducted with three contrasting agricultural soils, were used to investigate amendment effects on specific aspects of SOC dynamics: a 17-day incubation with ^{13}C-glucose to assess amendment effects on the response of SOC mineralization to labile carbon input (glucose-induced priming); a 66-day incubation with ^{13}C-labeled biochar-containing amendments to determine the mineralization and stabilization of native and amendment-derived SOC; and an 874-day incubation to quantify SOC stability over time, allowing long-term extrapolation of SOC pools. The three soils differed in their initial carbon and nitrogen contents, texture, and pH and represented common agricultural soils from temperate and tropical regions. To account for the impact of feedstock on amendment effects, biochar-containing amendments derived from woody biomass and wheat straw were included in the incubations.

Soil fertility of the temperate sandy soil in the lysimeter experiment was improved by all biochar-containing amendments, reflected by increased water holding capacity, reduced bulk density, elevated soil pH, and enhanced nutrient availability. These changes in chemical and physical soil properties affected extracellular enzyme kinetics, indicating a shift from sole phosphorus limitation towards a more balanced nutrient acquisition, resulting in a relative increase of microbial nitrogen demand.

The effects of the applied amendments on SOC dynamics were time- and feedstock-dependent and partly differed between the three investigated soils. Across soils, wood-derived amendments were less strongly mineralized, consistently reduced overall SOC mineralization over time, and resulted in larger long-term stable SOC pools, while wheat-derived amendments had more variable and soil-dependent effects. These soil-dependent amendment effects on SOC mineralization were predominantly controlled by soil texture and pH, with a stronger native SOC mineralization following wheat-derived amendment application (positive amendment-induced priming) in both low-pH sandy soils. All biochar-containing amendments increased SOC stabilization in aggregates and mineral associations in the three soils, partly due to the stabilization of amendment-derived carbon, thereby enhancing the overall CDR potential of these biochar-containing amendments. The effects of basanite rock powder on SOC dynamics intensified progressively, while remaining negligible on shorter timescales under laboratory and field conditions. On longer time scales, basanite enhanced SOC mineralization and thus CO_2 release from the neutral-pH temperate silty soil, while ongoing basanite weathering in both low-pH sandy soils resulted in a reduced CO_2 release and thus a visible CDR potential of basanite.

Co-application of biochar and basanite largely mirrored the effects of pure biochar on both soil fertility and SOC dynamics, showing no clear advantages over pure biochar application under the investigated conditions. Rock-enhanced biochar, in contrast, resulted in less pronounced short-term improvements in soil fertility than pure or co-applied biochar, while often more strongly affecting SOC dynamics. Rock-enhanced biochar had a higher inherent stability, resulting in reduced short-term mineralization, larger long-term stable SOC pools, greater resistance to physical breakdown, and pronounced formation of mineral-associated organic matter. The higher short- and long-term stability is likely caused by the occlusion of basanite particles in the pores of rock-enhanced biochar, reducing the accessible surface area, thus limiting amendment-soil-interactions, and improving the CDR potential of rock-enhanced biochar. The pronounced formation of mineral-associations occurred either during co-pyrolysis or in soils due to the higher release of dissolved organic carbon, which can be adsorbed directly to mineral surfaces. Notably, co-pyrolysis of wheat straw with basanite elevated the long-term stable SOC pool to levels comparable to or exceeding those of wood-derived biochar across all soils, demonstrating that co-pyrolysis can compensate for inherent feedstock limitations in long-term amendment stability enhancing the amendments' CDR effect.

In conclusion, all investigated amendments demonstrated potential for CDR and soil fertility improvement, though the magnitude of effects varied with amendment and soil type and over the considered timeframe. The application of basanite had visible effects on SOC dynamics over longer timespans, underlining the suitability of silicate rock powder application for long-term CDR and likely also for soil fertility improvement, especially in low-pH soils that are promoting weathering. Pure and co-applied biochar were better suited for rather rapid soil fertility improvement, while rock-enhanced biochar was most beneficial to improve short- and long-term SOC stability and stabilization while showing the potential for comparably strong soil fertility improvements over longer timescales. Overall, these findings underline that amendment selection should be guided by desired amendment goals, target timescales, and soil conditions.

Zusammenfassung

Die Entnahme von atmosphärischem Kohlenstoffdioxid (engl. carbon dioxide removal (CDR)) ist ein zentraler Ansatz zur Minderung des anthropogenen Klimawandels und zur Erreichung langfristiger Klimaziele. Pflanzenkohle und die beschleunigte Gesteinsverwitterung von Silikatgesteinsmehl stellen zwei vielversprechende Technologien dar, die potenziell CDR mit Verbesserungen der Bodenfruchtbarkeit kombinieren. Trotz ihrer potentiellen Synergien wurden die Effekte beider Bodenzusätze in den meisten bisherigen Studien getrennt voneinander untersucht. Um diese Forschungslücke zu schließen, vergleicht diese Dissertation die Effekte der puren und kombinierten Applikation von Pflanzenkohle und Basanit, einem Silikatgesteinsmehl, auf ihr Potential für CDR und für die Verbesserung der Bodenfruchtbarkeit. Die kombinierten Applikationen umfassten sowohl die Co-Applikation von Pflanzenkohle und Basanit (engl. co-application) als auch gesteinsangereicherte Pflanzenkohle (engl. rock-enhanced biochar), die durch Co-Pyrolyse von Biomasse und Basanit hergestellt wurde.

Die Applikationen der Bodenzusätze wurden in verschiedenen experimentellen Ansätzen über unterschiedliche Zeitskalen und in verschiedenen Bodentypen untersucht. So konnten die möglichen Effekte der Bodenzusätze auf die Bodenfruchtbarkeit und die Dynamik des organischen Bodenkohlenstoffs (engl. soil organic carbon (SOC)), welche das CDR-Potenzial der Zusätze steuert, erfasst werden. Ein neunwöchiges, feldnahes Lysimeterexperiment mit einem sandigen Boden der gemäßigten Klimazone, vermengt mit den jeweiligen Bodenzusätzen und bepflanzt mit Kohlrabi (*Brassica oleracea* var. *gongylodes* L.), wurde durchgeführt. In diesem Experiment wurden die Effekte der Bodenzusätze auf bodenchemische und -physikalische Eigenschaften und Prozesse, die die Bodenfruchtbarkeit beeinflussen, sowie die Stabilisierung von SOC unter feldnahen Bedingungen untersucht. Zusätzlich wurden in drei laborbasierten Inkubationsversuchen mit jeweils drei unterschiedlichen landwirtschaftlichen Böden die Effekte der Bodenzusätze auf spezifische Aspekte der SOC-Dynamik untersucht: eine 17-tägige Inkubation mit ^{13}C-Glukose zur Untersuchung des Einflusses der Bodenzusätze auf den Abbau von SOC nach der Zugabe von leicht verfügbarem Kohlenstoff (glukose-induzierter Priming-Effekt); eine 66-tägige Inkubation mit ^{13}C-markierten pflanzenkohle-basierten Bodenzusätzen zur Bestimmung der Mineralisierung und Stabilisierung von bodeneigenem und aus den Bodenzusätzen stammenden SOC; und eine 874-tägige Inkubation zur Quantifizierung der SOC-Stabilität über die Zeit und zur langfristigen Extrapolation der Inkubationsdaten in SOC-Pools. Die drei verwendeten Böden stehen stellvertretend für typische landwirtschaftliche Böden gemäßigter und tropischer

Regionen und unterschieden sich in ihrem initialen Kohlenstoff- und Stickstoffgehalt, ihrer Textur und ihrem pH-Wert. Um den Einfluss der Ausgangsbiomasse der pflanzenkohle-basierten Bodenzusätze zu berücksichtigen, wurden in den Inkubationen Bodenzusätze aus holziger Biomasse und Weizenstroh untersucht.

Die Bodenfruchtbarkeit des gemäßigten sandigen Bodens im Lysimeterexperiment wurde durch alle pflanzenkohle-basierten Bodenzusätze verbessert, erkennbar in einer erhöhten Wasserhaltekapazität, einer reduzierten Lagerungsdichte, einem erhöhten pH-Wert und einer verbesserten Nährstoffverfügbarkeit. Diese Veränderungen der chemischen und physikalischen Bodeneigenschaften beeinflussten die extrazelluläre Enzymkinetik, welche eine Verschiebung von einer reinen Phosphorlimitierung hin zu einer ausgewogeneren Nährstoffaufnahme zeigte, was in einem erhöhten relativen mikrobiellen Stickstoffbedarf resultierte.

Die Effekte der eingesetzten Bodenzusätze auf die SOC-Dynamik waren zeit- und ausgangsmaterialabhängig und unterschieden sich teilweise zwischen den drei untersuchten Böden. In allen drei Böden wurden holz-basierte Zusätze weniger stark abgebaut, reduzierten den Abbau des gesamten SOC über den Inkubationszeitraum hinweg und resultierten in einem größeren langfristig stabilen SOC-Pool, während weizenbasierte Zusätze variablere und stärker vom Bodentyp abhängige Effekte hatten. Diese bodenspezifischen Effekte auf den Abbau von SOC wurden hauptsächlich durch die Bodentextur und den pH-Wert gesteuert, wobei in den Sandböden mit niedrigem pH mehr bodeneigener SOC aufgrund der Zugabe der weizen-basierten Bodenzusätze abgebaut wurde (positiver bodenzusatz-induzierter Priming-Effekt). Die pflanzenkohle-basierten Bodenzusätze erhöhten die SOC-Stabilisierung in Aggregaten und an Mineraloberflächen in allen drei Böden, teilweise durch die Stabilisierung von Kohlenstoff aus den Bodenzusätzen, wodurch sich das CDR-Potential dieser pflanzenkohle-basierten Bodenzusätze erhöhte. Die Effekte des Basanitgesteinsmehls auf die SOC-Dynamik und somit auf CDR nahmen im Laufe der Zeit zu, während die kurzfristigen Effekte von Basanit sowohl in Labor- als auch in Feldexperimenten vernachlässigbar waren. Längerfristig erhöhte Basanit den SOC-Abbau und somit die CO_2-Freisetzung aus dem schluffigen Boden mit neutralem pH, während die fortschreitende Basanitverwitterung in beiden sandigen Böden mit niedrigem Ausgangs-pH zu einer Reduktion der CO_2-Emissionen führte und das CDR-Potential von Basanit aufzeigte.

Die Co-Applikation von Pflanzenkohle und Basanit hatte sowohl auf die Bodenfruchtbarkeit als auch auf die SOC-Dynamik meist ähnliche Effekte wie die Applikation der puren Pflanzenkohle und zeigte somit unter den untersuchten Bedingungen keine klaren Vorteile gegenüber purer Pflanzenkohle. Gesteinsangereicherte Pflanzenkohle zeigte hingegen eine weniger stark ausgeprägte kurzfristige Verbesserung der Bodenfruchtbarkeit im Vergleich zu purer oder co-applizierter Pflanzenkohle, während sie die SOC-Dynamik häufig stärker beeinflusste. Gesteinsangereicherte Pflanzenkohle hatte eine höhere inhärente Stabilität, was zu einer geringeren kurzfristigen Mineralisierung, größeren langfristig stabilen SOC-Pools, einer höheren physikalischen Stabilität und einer vermehrten Stabilisierung von SOC an Mineraloberflächen führte. Die erhöhte kurz- und langfristige Stabilität steigerte das CDR-Potential der gesteinsangereicherten Pflanzenkohle und wurde wahrscheinlich verursacht durch den Einschluss von Basanitpartikeln in den Poren der gesteins-angereicherten Pflanzenkohle, wodurch deren Oberfläche reduziert und somit die Interaktion mit dem Boden eingeschränkt wurde. Die vermehrte Bildung von Mineralassoziationen entstand entweder während der Co-Pyrolyse oder in Boden durch die vermehrte Freisetzung von gelöstem organischem Kohlenstoff, welcher direkt an Mineraloberflächen gebunden werden kann. Die Co-Pyrolyse von Weizenstroh mit Basanit zu gesteinsangereicherter Pflanzenkohle erhöhte die Größe des langfristig stabilen SOC-Pools auf ein ähnliches oder höheres Niveau als das mit holz-basierter Pflanzenkohle. Somit kann Co-Pyrolyse inhärente Einschränkungen der Ausgangsbiomasse auf die langfristige Stabilität der Bodenzusätze kompensieren.

Zusammenfassend zeigten alle untersuchten Bodenzusätze ein Potenzial für CDR und die Verbesserung der Bodenfruchtbarkeit, wobei das Ausmaß dieser Effekte je nach Bodenzusatz, Bodentyp und betrachteter Zeitspanne variierte. Die Anwendung von Basanit zeigte insbesondere über längere Zeiträume sichtbare Effekte auf die SOC-Dynamik, was die Eignung von Silikatgesteinsmehlen für langfristige CDR und wahrscheinlich auch für die Verbesserung der Bodenfruchtbarkeit, insbesondere in sauren Böden, zeigt. Pure und co-applizierte Pflanzenkohle sind gut geeignet für eine vergleichsweise schnelle Verbesserung der Bodenfruchtbarkeit. Gesteinsangereicherte Pflanzenkohle ist hingegen besonders vorteilhaft, um die kurz- und langfristige SOC-Stabilität und -Stabilisierung zu erhöhen, während sie gleichzeitig das Potenzial für vergleichbar starke Verbesserungen der Bodenfruchtbarkeit auf längeren Zeitskalen aufweist. Insgesamt zeigen diese Ergebnisse, dass die Auswahl von Bodenzusätzen entsprechend den angestrebten Zielen, den relevanten Zeitskalen und den jeweiligen Bodenbedingungen erfolgen sollte.

Manuscripts related to this dissertation

Study A:

Maria Ansari*, Joscha N. Becker, Susanne E. Hamburger, Claudia I. Kammann, Johannes Meyer zu Drewer, Nikolas Hagemann, Annette Eschenbach: Effect of combined biochar and basanite applications on chemical and physical properties of a sandy agricultural soil.

Submitted

Author's contributions:
Maria Ansari: Conceptualization, Formal analysis, Investigation, Methodology, Visualization, Writing – original draft; Joscha N. Becker: Conceptualization, Funding acquisition, Methodology, Supervision, Writing - Review & Editing; Susanne E. Hamburger: Resources; Claudia I. Kammann: Funding acquisition, Resources; Johannes Meyer zu Drewer: Resources, Writing - Review & Editing; Nikolas Hagemann: Funding acquisition, Resources; Annette Eschenbach: Conceptualization, Funding acquisition, Resources, Methodology, Supervision.

Study B:

Maria Ansari*, Svenja Stock, Michaela A. Dippold, Susanne E. Hamburger, Claudia I. Kammann, Johannes Meyer zu Drewer, Nikolas Hagemann, Annette Eschenbach, Joscha N. Becker: Biochar dominated the combined effect of silicate rock powder and biochar application on extracellular enzyme kinetics and nutrient dynamics in a sandy soil.

Published in Soil and Tillage Research (https://doi.org/10.1016/j.still.2026.107234)

Author's contributions:
Maria Ansari: Conceptualization, Formal analysis, Investigation, Visualization, Writing - original draft preparation; Svenja Stock: Methodology, Writing - review and editing; Michaela A. Dippold: Resources, Writing - review and editing; Susanne E. Hamburger: Resources, Writing - review and editing; Claudia I. Kammann: Funding acquisition, Resources, Writing - review and editing; Johannes Meyer zu Drewer: Resources; Nikolas Hagemann: Funding acquisition, Resources, Writing - review and editing; Annette Eschenbach: Funding

acquisition, Resources, Supervision, Writing - review and editing; Joscha N. Becker: Conceptualization, Funding acquisition, Supervision, Writing - review and editing.

Study C:

Maria Ansari*, Annette Eschenbach, Xavier Rodriguez Lloveras, Johannes Meyer zu Drewer, Nikolas Hagemann, Christian Beer, Joscha N. Becker: Effects of combined biochar and basanite application on short-term glucose-priming and long-term soil carbon stability.

In preparation for submission

Author's contributions:
Maria Ansari: Conceptualization, Formal analysis, Investigation, Methodology, Visualization, Writing – original draft; Annette Eschenbach: Conceptualization, Funding acquisition, Resources, Supervision, Writing – review and editing; Xavier Rodriguez Lloveras: Methodology; Johannes Meyer zu Drewer: Resources; Nikolas Hagemann: Funding acquisition, Resources; Christian Beer: Funding acquisition; Joscha N. Becker: Conceptualization, Funding acquisition, Methodology, Supervision, Writing – review and editing.

Study D:

Maria Ansari*, Annemarie Lübeck, Johannes Meyer zu Drewer, Nikolas Hagemann, Annette Eschenbach, Joscha N. Becker: Rock-enhanced biochar has similar priming effect as pure biochar application, but improves short-term carbon stabilization in agricultural soils.

Submitted

(Meanwhile published as Ansari et al. (2026). Rock-enhanced biochar exhibits similar priming effect as pure biochar application while improving short-term carbon stabilization in agricultural soils. Biology and Fertility of Soils: https://doi.org/10.1007/s00374-026-02030-7)

Author's contributions:
Maria Ansari: Conceptualization, Formal analysis, Investigation, Methodology, Visualization, Writing – original draft; Annemarie Lübeck: Investigation;

Johannes Meyer zu Drewer: Resources, Writing – review and editing; Nikolas Hagemann: Funding acquisition, Resources, Writing – review and editing; Annette Eschenbach: Conceptualization, Funding acquisition, Resources, Supervision, Writing – review and editing; Joscha N. Becker: Conceptualization, Funding acquisition, Methodology, Supervision, Writing – review and editing.

* corresponding author

Further contributions to manuscripts

Maria-Elena Vorrath*, Thorben Amann, Johannes Meyer zu Drewer, Nikolas Hagemann, Cierra Aldrich, Janine Börker, Maria Seedtke, Joscha N. Becker, Mathilde Hagens, Annette Eschenbach, Jens Hartmann: Pyrogenic carbon and carbonating minerals for carbon capture and storage (PyMiCCS) part II: organic and inorganic carbon dioxide removal in an Oxisol.

Published in Frontiers in Climate (https://doi.org/10.3389/fclim.2025.1592454).

Mikita Maslouski*, Maria Ansari, Susanne E. Hamburger, Johannes Meyer zu Drewer, Nikolas Hagemann, Annette Eschenbach, Christian Beer, Joscha N. Becker, Claudia I. Kammann, Maria-Elena Vorrath, Philipp Porada: Long-term carbon dioxide removal potential from the application of wood biochar and basanite rock powder in sandy soil using the LiDELSv2 process-based modeling approach.

Published in Environmental Research Letters (https://doi.org/10.1088/1748-9326/ae21f6).

Johannes Meyer zu Drewer*, Maria-Elena Vorrath, Thorben Amann, Jens Hartmann, Maria Ansari, Marcela Cárcamo Pérez, Nikolas Hagemann*: Combining biochar and basanite rock powder enhances carbon dioxide removal by carbonate alkalinity production.

Meanwhile published in Frontiers in Climate (https://doi.org/10.3389/fclim.2026.1853116)

* corresponding author

Table of contents

Unifying essay

Manuscripts

List of figures

Unifying essay

Manuscript A

Manuscript B

Manuscript C

Manuscript D

List of tables

Unifying essay

Manuscript A

Manuscript B

Manuscript C

Manuscript D

Unifying essay

1 Introduction

1.1 Background and motivation

1.1.1 Biochar and silicate rock powder application for carbon dioxide removal

Land use change and the combustion of fossil fuels have driven the long-term emission of greenhouse gases to the atmosphere, primarily causing anthropogenic climate change (IPCC, 2023). To mitigate climate change and to reach long-term climate targets, carbon dioxide removal (CDR) technologies are a critical tool to limit global warming to 2 °C compared to pre-industrial times (FUSS et al., 2018; RIAHI et al., 2022). These CDR technologies include promising soil-based approaches, such as the application of biochar and silicate rock powder for enhanced rock weathering. Both have the potential to remove atmospheric carbon dioxide (CO_2) while improving soil fertility (BUSS et al., 2021; JOSEPH et al., 2021; BEERLING et al., 2025). Unlike land-intensive CDR approaches, such as afforestation, both biochar and enhanced rock weathering of silicate rock powder require no dedicated land use change, as both can be integrated into existing land management systems as soil amendments (FUSS et al., 2018; SMITH et al., 2024).

Biochar is the carbon-rich solid produced by the thermochemical conversion of biomass during oxygen-free or -limited pyrolysis (BOATENG et al., 2015; HAGEMANN et al., 2018; LEHMANN & JOSEPH, 2024) and is traditionally used as a soil amendment globally (ALLEN, 1847; GLASER et al., 2001; WIEDNER et al., 2015). In recent years, biochar has been increasingly researched due to its potential to store carbon (C) in the long-term while improving soil properties determining soil fertility (LEHMANN & JOSEPH, 2024; SMITH et al., 2024). Due to its high aromaticity, approximately 97% of the biochar-C is barely bioavailable (AMELOOT et al., 2013; KUZYAKOV et al., 2014; WANG et al., 2016) and thus contributes to long-term CDR (RECHBERGER et al., 2017; LEHMANN et al., 2021). Overall, biochar has the potential to remove 0.5 to 2 Gt of CO_2 per year (FUSS et al., 2018). The stability of biochar is strongly influenced by pyrolysis temperature and feedstock. Biochar produced at high temperatures (> 500°C) (JOSEPH et al., 2010; AMELOOT et al., 2013; GRUNWALD et al., 2017) from woody feedstock is generally more stable and thus associated with a longer-lasting CDR potential (ZHAO et al., 2013; WANG et al., 2016) compared to low-temperature biochar from lignin-poor biomass, such as agricultural residues (VAUGHN et al., 2013; HAN et al., 2020; WANG et al., 2022). Additionally, soil properties, such as texture and soil organic C (SOC) content, determine the actual stability of biochar in soils (WANG et al., 2016; LENG & HUANG, 2018).

Silicate rock weathering is a naturally occurring process central to the C cycle, removing atmospheric CO_2 over geological time scales (WALKER et al., 1981). During weathering, silicate minerals react with carbonic acid, formed through the dissolution of CO_2 in water, yielding carbonate and bicarbonate (BUSS et al., 2023; ABDALQADIR et al., 2024; BEERLING et al., 2025). These inorganic C forms can either be stored as pedogenic carbonates for centuries or transported via rivers to the ocean, where they can be stored over geological time scales (MARTIN, 2017; BEERLING et al., 2018; VICCA et al., 2022). For enhanced rock weathering, the natural weathering process is accelerated by crushing silicate rock, such as basanite, to powder, thereby increasing its reactive surface area and thus enhancing its weathering rate (HARTMANN et al., 2013; BUSS et al., 2021). High moisture and CO_2 partial pressure, as present in soils, can additionally promote the weathering (HARTMANN et al., 2013). Overall, enhanced weathering of silicate rocks has a CDR potential of 2 to 4 Gt of CO_2 per year (FUSS et al., 2018). The actual rate of weathering and thus the associated CDR depend, among other factors, on soil properties (SCHIEDUNG et al., 2026; TE PAS et al., 2026) and mineralogical composition of the rocks (RENFORTH, 2012; CONG et al., 2024). Basaltoids, such as basanite, contain mafic minerals (HARTMANN et al., 2013) and have relatively low weathering rates compared to other materials potentially used for enhanced rock weathering (HAMMES et al., 2025), thus sustaining its CDR potential over time. Despite the strong interactions between applied silicate rock powder and the amended soils, a systematic understanding of enhanced rock weathering dynamics in soils is currently missing (HARTMANN et al., 2013; SMITH et al., 2024; SCHIEDUNG et al., 2026).

This direct CDR effects of biochar and silicate rock powder is affected by their influence on SOC dynamics. Both amendments can enhance the stabilization of native SOC in aggregates and on mineral-surfaces (WANG et al., 2017; XU et al., 2025) and particularly biochar can influence SOC turnover by either stimulating or reducing the mineralization of native SOC (WHITMAN et al., 2015; YU et al., 2018). These changes can result in an enhanced SOC sequestration and storage, thereby likely increasing the overall CDR potential of both amendments (MANNING et al., 2024; RATHNAYAKE et al., 2024).

To date, most research has investigated the separate application of biochar and silicate rock powder. However, their combined application could maximize CDR per unit land area, offering additive or even synergistic effects (AMANN & HARTMANN, 2019; BUSS et al., 2024b; TE PAS et al., 2026). Such a combined application can include a co-application of biochar and silicate rock powder, such as basanite, as well as the co-pyrolysis of biomass and rock powder to produce rock-enhanced biochar (MEYER ZU DREWER et al., 2025). When co-applied, biochar can stimulate rock powder weathering, probably due to the uptake of weathering products by biochar preventing saturation of the soil solution (SOHNG et al., 2025; TE PAS et al., 2026). While the CDR potential of the co-application of biochar and rock powder is currently increasingly researched (ANTHONY et al., 2025; TE PAS et al., 2026), the effect of rock-enhanced biochar has rarely been investigated. Existing studies indicate potential interactions between biomass and minerals during co-pyrolysis, such as occlusion of rock powder particles in biochar pores (MEYER ZU DREWER et al., 2025) and an increased C yield of the pyrolysis product (BUSS et al., 2024b), pointing to an enhanced stability and thus potentially pronounced CDR potential of rock-enhanced biochar.

1.1.2 Effects of biochar and silicate rock powder application on soil fertility

Beyond their CDR potential, biochar and silicate rock powder have been increasingly recognized due to their potential to improve soil fertility (FIEDLER & HEINZE, 1990; DING et al., 2016), which in turn can determine the amendments' CDR potential (HARTMANN et al., 2013; OELKERS et al., 2018). Soil fertility includes physical, chemical, and biological processes and properties of soils that support the productivity and growth of microorganisms and plants and thus facilitate yield (FIEDLER & HEINZE, 1990). Both biochar and silicate rock powder can trigger physical, chemical, and biological reactions in soils (DUPLA et al., 2024; JOSEPH et al., 2010), with amendment effects on soil fertility depending on both the amendments' inherent physicochemical properties and soil properties (DING et al., 2016; SCHIEDUNG et al., 2026). While the agronomic use of biochar is well established (GLASER et al., 2001; WIEDNER et al., 2015), the effects of silicate rock powder on soil fertility remain poorly understood (HARTMANN et al., 2013; SCHIEDUNG et al., 2026).

Physical soil properties, such as plant-available water or bulk density, are important parameters for soil fertility (FIEDLER & HEINZE, 1990). The application of biochar can improve soil water dynamics, especially in sandy soils (STEINER et al., 2007; LEHMANN et al., 2011; BUSS et al., 2021), and soil aeration by reducing bulk density (ZANUTEL et al., 2024), especially in heavy, clayey soils (LEHMANN et al., 2011; BLANCO-CANQUI, 2017). In contrast to the largely beneficial effects of biochar, effects of silicate rock powder application on soil structure and water dynamics seem to be ambiguous (SCHIEDUNG et al., 2026). On the one hand, the incorporation of small silicate rock particles into soil pores can lead to soil compaction and clogged pores, which reduce water conductivity, especially in clayey soils (VORRATH et al., 2025; SCHIEDUNG et al., 2026). This impairs soil fertility and, given weathering's strong dependence on water movement, limits the CDR potential of enhanced rock weathering (VORRATH et al., 2025; SCHIEDUNG et al., 2026). On the other hand, the formation of secondary minerals, such as clays, during weathering can enhance the soil capacity to hold water, which can be especially beneficial in sandy soils (SCHIEDUNG et al., 2026). When biochar and silicate rock powder are applied together, biochar could reduce this clogging effect of silicate rock powder (ZANUTEL et al., 2024; VORRATH et al., 2025) while improving water retention (STEINER et al., 2007; BLANCO-CANQUI, 2017), which could enhance the weathering and thus the CDR effect of the applied rock powder (TE PAS et al., 2026).

In addition to these effects on physical soil properties, biochar and silicate rock powder application can influence chemical soil properties (ZHANG et al., 2021; SWOBODA et al., 2022). Both amendments can supply nutrients, such as potassium (K) and phosphorus (P), released from dissolving biochar ash and silicate minerals (ANGST & SOHI, 2013; MUKHERJEE & ZIMMERMAN, 2013; AMANN et al., 2020). Additionally, both amendments can increase soil pH, particularly in acidic soils (DAI et al., 2017; AMANN et al., 2020). This can further increase the availability of nutrients, such as P, beyond what is directly released by mineral weathering (SWOBODA et al., 2022; BEERLING et al., 2025) and biochar ash solution (ATKINSON et al., 2010). Due to the high cation exchange capacity of biochar, it often increases nutrient retention (LIANG et al., 2006; VAN ZWIETEN et al., 2010) and reduces nutrient leaching (LAIRD & ROGOVSKA, 2015). Also silicate rock powder can develop a certain cation exchange capacity over time through the formation of secondary minerals during weathering, which is particularly beneficial in highly weathered soils (ANDA et al., 2015). When applying biochar and rock powder together, biochar may retain nutrients released from weathered minerals, thereby reducing leaching losses (AMANN & HARTMANN, 2019). Furthermore, first results of MEYER ZU DREWER et al. (2025) indicate that rock-enhanced biochar from co-pyrolysis of biomass and silicate rock powder has a higher plant-available nutrient content compared to conventional biochar. Combined with the potentially greater long-term stability of rock-enhanced biochar (MEYER ZU DREWER et al., 2025), it could be used as a slow-release fertilizer, improving soil fertility (LAMMIRATO et al., 2011; BUSS et al., 2022). This supply of nutrients via soil amendments is especially beneficial in soil with low fertility, such as sandy or highly weathered soils (JOSEPH et al., 2021; SCHIEDUNG et al., 2026). However, rock powder can also release potentially toxic trace metals, such as nickel and chromium, which makes a careful selection of the applied rock type necessary (Schiedung et al., 2026). Basanite has a relatively low heavy metal concentration, which makes it suitable for agricultural application (Beerling et al., 2020).

Biological soil processes and properties are especially sensitive to change (Burns et al., 2013) and directly affected by alterations of chemical and physical soil properties (Schimel et al., 2007). The applications of both biochar and silicate rock powder often result in an increased microbial activity and an altered microbial community composition (Carson et al., 2007; Lehmann et al., 2011), which may in turn affect nutrient dynamics (Schimel et al., 2007). To meet their nutrient demand, microorganisms produce and release extracellular enzymes (Allison et al., 2011; Jin et al., 2024). Once released into the soil, these enzymes catalyze the breakdown of complex organic substances associated with C, nitrogen (N), P, and other elements into smaller molecules (Shi, 2011), thereby enhancing nutrient availability for microbial uptake (Allison et al., 2011; Jin et al., 2024). Increased nutrient availability often reduces microbial investment in enzyme production, while nutrient limitation can stimulate enzyme release (Allison et al., 2011; Burns et al., 2013). Even though extracellular enzymes can be adsorbed to reactive particle surfaces, such as soil organic matter (Allison, 2006; Burns et al., 2013; Luo et al., 2017a) or biochar (Lehmann et al., 2011), adsorbed enzymes remain a significant reservoir of potential enzyme activity, responding rapidly to changes in nutrient availability (Burns et al., 2013). Consequently, extracellular enzymes serve as valuable indicators for nutrient cycling and availability in soils (Luo et al., 2017a). Both biochar and silicate rock powder can affect extracellular enzyme kinetics by enhancing nutrient supply and availability (Angst & Sohi, 2013; Mukherjee & Zimmerman, 2013; Amann et al., 2020). This could be especially pronounced following the application of rock-enhanced biochar, which has a higher nutrient content compared to conventional biochar (Meyer zu Drewer et al., 2025). Since soil moisture is a key driver of microbial activity and extracellular enzyme kinetics, increased soil water retention following biochar application (Steiner et al., 2007; Lehmann et al., 2011) and rock powder weathering (Amann & Hartmann, 2019; Schiedung et al., 2026) could stimulate microbial nutrient dynamics. Additionally, higher soil moisture could accelerate rock powder weathering in combined applications, potentially releasing additional nutrients and thus further improving enzyme kinetics.

The effects following the pure applications of biochar and silicate rock powder on soil fertility are diverse, mostly beneficial, and can eventually result in an increased yield (Jeffery et al., 2011; Swoboda et al., 2022), which makes both amendments attractive for agricultural use. The beneficial potential of a combined application of both amendments has been discussed in several previous studies (AMANN & HARTMANN, 2019; BUSS et al., 2021; BUSS et al., 2022). First studies addressing the co-application of biochar and silicate rock powder have begun to investigate changes in physical and chemical soil properties, indicating mainly additive responses (HONVAULT et al., 2024; COSTANZO et al., 2025). However, the underlying mechanisms remain poorly understood, and particularly the effects of co-application on biological processes as well as the effects of rock-enhanced biochar on overall soil fertility have not been investigated. A better understanding of these amendment-driven processes is therefore crucial to assess how combined amendment applications influence soil fertility.

1.1.3 Soil organic carbon dynamics and their response to biochar and silicate rock powder application

Most physical, chemical, and biological soil properties and processes and thus overall soil fertility are affected by soil organic matter (WEIL & BRADY, 2017). The stability of this soil organic matter describes its resistance to microbial decomposition and is determined by biochemical recalcitrance, physical protection through spatial inaccessibility, and chemical stabilization via interactions with mineral surfaces (VON LÜTZOW et al., 2006; CONANT et al., 2011; SCHIMEL & SCHAEFFER, 2012). This stability can be assessed by quantifying the mineralization of SOC to CO_2 (PLANTE et al., 2011). Important factors influencing SOC mineralization are soil properties, such as texture and pH (KEMMITT et al., 2006; RASMUSSEN et al., 2006), and environmental factors, such as temperature and moisture (DAVIDSON & JANSSENS, 2006; CONANT et al., 2011). Due to the low degradability of biochar, it generally contributes to the stable SOC pool (KUZYAKOV et al., 2014; WANG et al., 2016). The actual stability of biochar, however, depends on soil and biochar properties. Both texture and native SOC content are important soil properties affecting biochar stability, since higher clay (BRUUN et al., 2014) and SOC contents (WHITMAN et al., 2015) can reduce biochar mineralization. Inherent biochar stability, determined by the quantity and quality of C, depends among other factors on feedstock (ZHAO et al., 2013; LEHMANN et al., 2015; LENG & HUANG, 2018). Biochars produced from woody feedstock contain more aromatic C, while biochars from agricultural residues decompose more easily (AMELOOT et al., 2013; VAUGHN et al., 2013; HAN et al., 2020). Co-pyrolyzing biomass with minerals increased the C yield of the produced rock-enhanced biochar (BUSS et al., 2022) and led to the occlusion of rock particles in biochar pores (MEYER ZU DREWER et al., 2025), which could enhance the long-term stability of rock-enhanced biochar.

How susceptible SOC generally is to decomposition is closely linked to the formation pathway and stabilization mechanisms of this SOC (VON LÜTZOW et al., 2006; KLEBER et al., 2015). Free particulate organic matter (fPOM) resembles the initial plant litter (VON LÜTZOW et al., 2008) and is stabilized only by its biochemical recalcitrance (SOLLINS et al., 1996). Particulate organic matter can be further stabilized by spatial inaccessibility through the occlusion in aggregates (oPOM) (VON LÜTZOW et al., 2006). Mineral-associated organic matter (MAOM) is formed by the adsorption of dissolved organic C (DOC) to mineral surfaces or by microbial processing (MANZONI & COTRUFO, 2024), and is stabilized via physicochemical protection (KLEBER et al., 2015). This limited accessibility of oPOM and MAOM to microbes reduces its biodegradability and enhances its stability (VON LÜTZOW et al., 2006; KLEBER et al., 2015).

The application of both silicate rock powder and biochar can affect the stabilization of native SOC (WANG et al., 2017; BUSS et al., 2024a). Rock powder weathering can enhance aggregate formation by releasing bivalent cations, such as Ca^{2+} and Mg^{2+}, which promote cation bridging and flocculation of soil particles (CLOUGH & SKJEMSTAD, 2000; BUSS et al., 2024a; XU et al., 2025). Additionally, fresh mineral surfaces and reactive secondary minerals, which are formed during weathering, contribute to MAOM formation through the adsorption of DOC (REICHENBACH et al., 2021; BUSS et al., 2024a). Thus, rock powder weathering may facilitate the formation of oPOM and MAOM, which may be particularly beneficial in clay-poor soils with limited reactive mineral surfaces (SCHWEIZER et al., 2019; YAN et al., 2025). Similarly, also biochar application can accelerate the formation of aggregates and the stabilization of native SOC as MAOM, possibly through ligand exchange or cation bridging (WANG et al., 2017; WENG et al., 2017; XU et al., 2024). While most biochar-derived SOC remains as highly recalcitrant fPOM (KALU et al., 2024), it can also be further stabilized by occlusion in aggregates (YOO et al., 2017; JOSEPH et al., 2021) or mineral-association (YANG et al., 2016; YANG et al., 2021). When silicate rock powder is applied together with biochar, its mineral surfaces could contribute to the further stabilization and thus reduced mineralization of biochar-derived SOC (TE PAS et al., 2026). The stabilization of native and biochar-derived SOC by both amendments can additionally increase their CDR potential when reducing SOC mineralization losses (MANNING et al., 2024; RATHNAYAKE et al., 2024).

Another important SOC pool is microbial biomass C, which both responds to amendment application and regulates the potential of amendment-driven CDR and soil fertility improvement. Microorganisms govern the mineralization of SOC (SCHIMEL, 2013) and both biochar and silicate rock powder can increase microbial biomass, enhance microbial activity, and even shift microbial community composition (CARSON et al., 2007; LEHMANN et al., 2011). Such an enhanced microbial activity can on the one hand enhance the biogeochemical cycling of SOC and nutrients, resulting in an increased mineralization of native and biochar-derived SOC (WHITMAN et al., 2015). On the other hand, enhanced microbial activity can increase the incorporation of microbial necromass as stable MAOM (CHEN et al., 2023; YAN et al., 2025) and stimulate rock weathering (LI et al., 2025; REGINATO, 2025).

An important microbially mediated aspect of the SOC cycle is the response of the soil system to the input of labile C (KUZYAKOV et al., 2000; BLAGODATSKAYA & KUZYAKOV, 2008). This reaction is described as the priming effect, inducing short-term changes in the mineralization of SOC following the addition of a labile C source (KUZYAKOV et al., 2000). Those changes can range from a reduction (negative priming) to an increase in SOC mineralization (positive priming) (KUZYAKOV et al., 2000; BASTIDA et al., 2019). Even though biochar mainly consists of highly stable C, it also contains a minor proportion of easily degradable C (BRUUN et al., 2014; BAKSHI et al., 2018), potentially triggering a biochar-induced priming effect of native SOC in soil (WHITMAN et al., 2015; YU et al., 2018). Whether the application of biochar results in negative or positive priming depends on soil and biochar properties (ZIMMERMAN et al., 2011; WHITMAN et al., 2015; JOSEPH et al., 2021). Positive priming is most likely to occur following the application of biochars rich in easily degradable C compounds, such as those made from agricultural residues, to nutrient-poor and acidic soils (WHITMAN et al., 2015). Even though silicate rock powder does not contain labile C to directly induce a priming effect, its application can indirectly affect the mineralization of SOC (SCHIEDUNG et al., 2026), e.g. via an increase in soil pH (AMANN et al., 2020; LEI et al., 2025) or nutrient availability (HARLEY & GILKES, 2000; HARTMANN et al., 2013). Changes in SOC mineralization following amendment application can in turn affect the cycling of nutrients included in soil organic matter, which could alter nutrient availability and enzyme kinetics (WHITMAN et al., 2015).

In addition to amendment-derived labile C inputs, SOC dynamics in soils are affected by natural inputs of easily degradable C, such as root exudates (KUZYAKOV et al., 2000). Those processes are commonly simulated using glucose and described as the glucose-induced priming effect (KUZYAKOV et al., 2009; KUZYAKOV, 2010; WHITMAN et al., 2015). Such labile C inputs can cause the co-metabolic mineralization of native and biochar-derived SOC (HAMER et al., 2004; LEHMANN et al., 2009; KUZYAKOV, 2010). This glucose-induced priming is often positive, but the magnitude can differ strongly between soils and is often highest in low-fertility soils (BASTIDA et al., 2019; WU et al., 2020). The application of biochar can affect the direction and magnitude of glucose-induced priming (LUO et al., 2017b), varying with biochar and soil properties (HAMER et al., 2004;

KUZYAKOV et al., 2009; LEHMANN et al., 2015). How the combined application of biochar and basanite might affect glucose-induced priming, however, remains unknown.

The effects of applied amendments on SOC dynamics vary strongly over time. The mineralization of both native SOC (biochar-induced priming) and biochar-derived SOC is often highest shortly after biochar application and declines over time (KUZYAKOV et al., 2009; AMELOOT et al., 2013; WHITMAN et al., 2015), varying strongly between soils depending mainly on soil texture and SOC content (MAESTRINI et al., 2015; WANG et al., 2016; LENG & HUANG, 2018). While also varying between soils (CONG et al., 2024), the effects of rock powder application on SOC mineralization and stabilization generally increase over time, since they require weathering of the applied rock powder (HARTMANN et al., 2013; BUSS et al., 2024a). Thus, early mineralization rates may not reflect long-term SOC stability (LEHMANN et al., 2015). To extrapolate the available data and assess long-term SOC dynamics, modelling approaches can be used to determine long-term dynamics and mean residence times of SOC pools (LENG et al., 2019; HAN et al., 2020; AZZI et al., 2024).

Given the strong effects of biochar and silicate rock powder application on SOC dynamics, it is crucial to understand the potential of their combined applications. First studies focusing on the co-application of biochar and silicate rock powder observed effects ranging from stimulated SOC mineralization due to pH increases (TE PAS et al., 2026) to an inhibiting effect of rock powder on biochar-induced SOC stabilization (SOHNG et al., 2025) to additive effects of both amendments on SOC sequestration (HONVAULT et al., 2024). The variety of these first results emphasizes the need to understand the underlying processes following a combined application of biochar and silicate rock powder. Whether co-application and rock-enhanced biochar exhibit favorable effects on SOC dynamics (AMANN & HARTMANN, 2019; JOSEPH et al., 2021) – through mechanisms such as enhanced aggregate formation, increased MAOM stabilization, or altered priming responses – compared to pure applications remains poorly understood.

1.2 Thesis objectives and outline

The aim of this dissertation was to determine the effects of combined biochar and basanite rock powder applications on soil fertility and SOC dynamics, affecting the amendments' CDR potential. These combined applications included a co-application of biochar and basanite and the equivalent rock-enhanced biochar produced from co-pyrolysis of biomass and basanite. Understanding the effects of combined compared to pure applications could enhance the potential of these amendments for soil fertility improvement (Study A and B) and CDR via SOC dynamics (Study A, C, and D). To address this, the dissertation is structured around four major research objectives (Figure 1): (I) assessing amendment effects on chemical and physical soil properties (Study A), (II) evaluating amendment effects on microbially mediated nutrient dynamics (Study B), (III) investigating the amendment effects on SOC stability and mineralization over time, including responses to labile C input (Study C), and (IV) determining the mineralization (Study D) and stabilization (Study A and D) of native and amendment-derived SOC following amendment application. Across all studies, comparing the effects of pure biochar or basanite application, their co-application, and rock-enhanced biochar represented the focus of this dissertation. The specific objectives of the studies related to this dissertation were:

Study A

The objective of Study A was to determine the potentials of pure and combined amendments for soil improvements under near-field conditions by (I) investigating chemical and physical soil properties and (II) quantifying stabilization mechanisms for SOC in a field-based lysimeter experiment.

Study B

The objective of Study B was to assess microbial nutrient demands following the application of pure and combined amendments by (I) quantifying kinetics of extracellular enzymes related to C-, N-, and P-cycle, to (II) gain insights into potential nutrient limitations in a field-based lysimeter experiment.

Study C

The objective of Study C was to understand the effects of pure and combined amendments on SOC dynamics by (I) quantifying SOC mineralization over time, (II) extrapolating SOC mineralization dynamics into distinct SOC pools with associated mean residence times, and (III) assess how amendments influence the short-term soil system's response to labile C input (glucose) on SOC mineralization (glucose-induced priming). Throughout, (IV) the influence of feedstock and (V) soil properties on these amendment effects was considered.

Study D

The objective of Study D was to compare the effect of pure and combined amendments on (I) the mineralization of native SOC (amendment-induced priming) and (II) the stabilization of native SOC in aggregates and mineral-associations. Accordingly, the (III) mineralization and stabilization of amendment-derived SOC was quantified. Additionally, (IV) the influence of soil properties on those native and amendment-derived SOC dynamics was included.

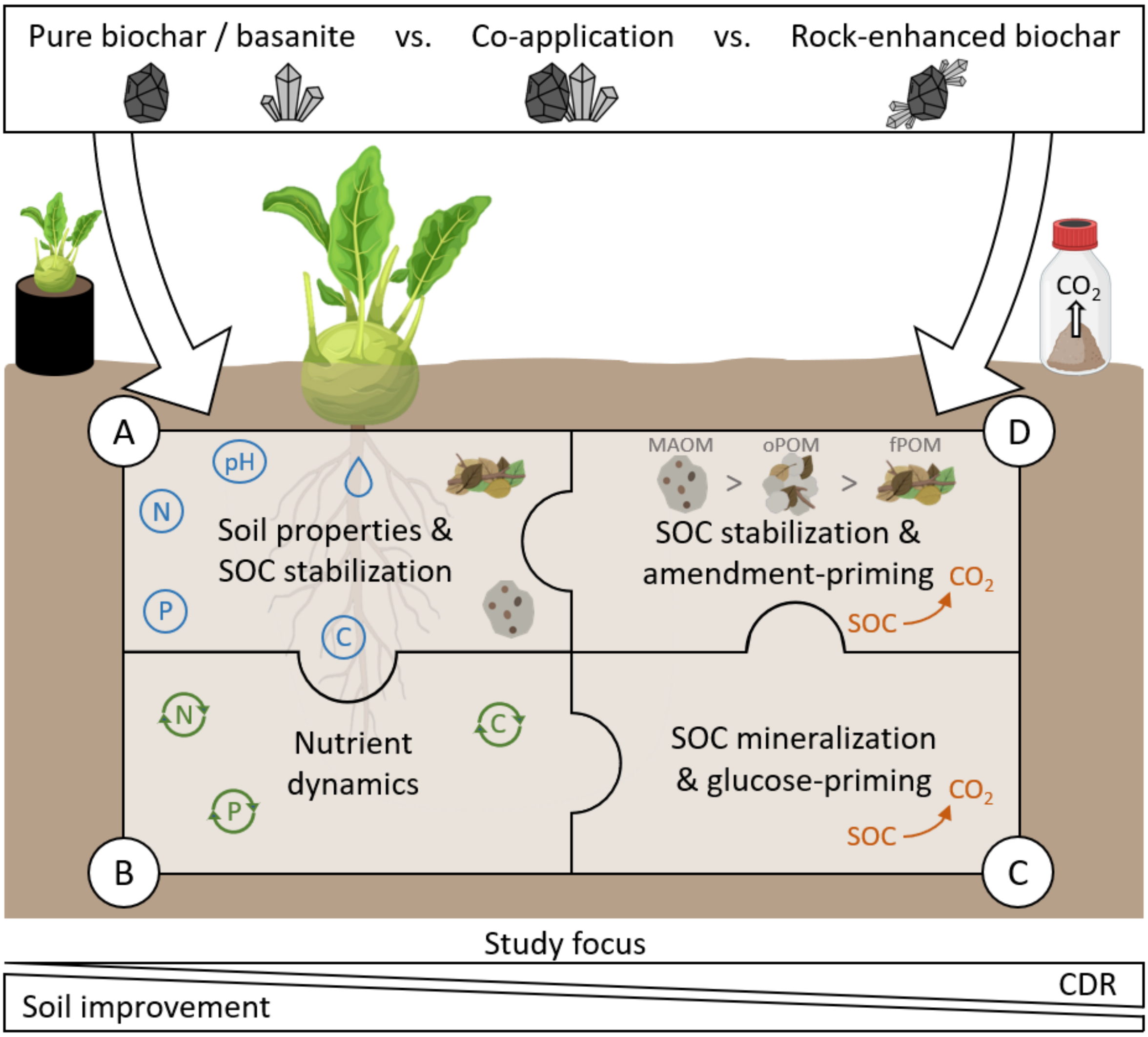

Figure 1: Scheme of the studies related to this dissertation focusing on the effects of pure biochar and silicate rock powder (basanite) applications compared to their combined applications (co-application of biochar and basanite; rock-enhanced biochar from co-pyrolysis of biomass and basanite) for soil fertility improvement and carbon dioxide removal (CDR), focusing on soil organic carbon (SOC) dynamics, in field-based lysimeters (Study A and B) and laboratory incubation experiments (Study C and D). C = carbon, CO_2 = carbon dioxide, fPOM = free particulate organic matter, MAOM = mineral-associated organic matter, N = nitrogen, oPOM = occluded particulate organic matter, P = phosphorus.

Embedment within the PyMiCCS project

This doctorate is embedded in the PyMiCCS project (Pyrogenic carbon and carbonating Minerals for enhanced plant growth and Carbon Capture and

Storage). The project involves an interdisciplinary group of researchers, including soil science, geochemistry, ecology, and biogeochemical modelling from the University of Hamburg, Ithaka Institute, Hochschule Geisenheim University, and Potsdam Institute for Climate Impact Research. The project is funded by the German Federal Ministry of Research, Technology and Space (FKZ: 01LS2109). The shared research objective of the PyMiCCS project is to combine biochar and enhanced rock weathering to maximize the potential of these amendments for CDR, soil fertility improvement, and yield enhancement.

2 Material and methods

2.1 Agricultural topsoils and soil amendments

Three agricultural topsoils (0-30 cm) were used for the experiments within this dissertation, exemplary for temperate and tropical soil properties, differing in C and N contents, texture, and soil pH (Table 1). These soils included a temperate silty soil from central Germany (Goldbach, Germany, 49°59'32.4"N 9°09'53.8"E), a temperate sandy soil from northern Germany (Gartow, Germany, 53°01'26.9"N 11°27'12.7"E), and a tropical sandy soil from central Kenya (Machanga, Kenya, 0°27'26.8"S 37°39'37.4"E). Soils in the respective areas are classified as Cambisol (LFU, 2025), Podzol (LBEG, 2017), and Nitisol (FAO & UNESCO, 1974) according to the world reference base (IUSS WORKING GROUP WRB, 2022). For each of the studies, a selection of the three topsoils was mixed with different soil amendments, tailored to answer the specific research questions of the respective study. This set up, including three soils, allowed investigating the amendment effects in soils with differing properties and in turn the impact of soil properties on amendment effects. The investigated amendments included at least one pure biochar, pure basanite rock powder, at least one co-application of biochar and basanite, and the equivalent rock-enhanced biochar produced from co-pyrolysis of biomass and basanite. Detailed information on the applied amendments is given in the respective studies.

Table 1: Initial properties of temperate silty, temperate sandy, and tropical sandy agricultural topsoils.

Properties	Temperate silty soil	Temperate sandy soil	Tropical sandy soil
C [g kg^{-1}]	18.5 ± 0.0	12.4 ± 0.0	4.7 ± 0.0
TOC [g kg^{-1}]	13.3 ± 0.1	12.0 ± 0.0	4.6 ± 0.0
TIC [g kg^{-1}]	5.2 ± 0.1	0.4 ± 0.0	0.1 ± 0.0
N [g kg^{-1}]	1.3 ± 0.0	1.1 ± 0.0	0.3 ± 0.0
C:N	13.9 ± 0.0	11.6 ± 0.0	15.0 ± 0.0
$\delta^{13}C$ [‰]	-23.2 ± 0.1	-26.7 ± 0.0	-19.2 ± 0.0
pH [$CaCl_2$]	6.9 ± 0.0	4.7 ± 0.0	4.7 ± 0.0
Sand [%]	28.2 ± 1.0	93.8 ± 0.7	68.9 ± 0.6
Silt [%]	58.0 ± 1.0	2.5 ± 0.4	20.4 ± 0.6
Clay [%]	13.8 ± 0.3	3.7 ± 0.3	10.7 ± 0.2

Data is presented as mean ± standard error (n = 3). C = total carbon, N = total nitrogen, TOC = total organic carbon, TIC = total inorganic carbon.

2.2 Study design

The studies related to this dissertation aimed to determine how the effects of combined biochar and basanite powder applications, including co-application and rock-enhanced biochar, differ from those of the pure amendment applications. The main investigated aspects were the potential of these amendments to improve physical, chemical, and biological soil properties and processes, determining soil fertility, as well as the CDR potential of these amendments, focusing on their effect on SOC dynamics. To achieve this aim, the four studies of this dissertation were each specifically designed to investigate at least one of the described aspects. The studies included in this dissertation range from field-based lysimeter-experiments including plants, representing near-natural conditions, to laboratory experiments under controlled conditions, allowing the targeted investigation of individual processes with regard to SOC dynamics.

Field-based lysimeter experiment (Study A & B)

To represent near-natural conditions, 45 lysimeters (each 20 cm inner diameter, 30 cm soil depth, sealed with stainless-steel mesh at the bottom allowing drainage into a catchment vessel below) were embedded in sand beds (Figure 2), ensuring soil temperatures close to field conditions. Inside the lysimeters, PVC bags were installed, containing the soil samples of the different treatments (n=9). As control, lysimeter bags were filled with temperate sandy soil. For the amended treatments, the soil was mixed with either pure biochar produced from woody biomass, pure basanite powder, a co-application of both amendments, or the equivalent rock-enhanced biochar from co-pyrolysis of woody biomass and basanite. All lysimeters were arranged in a randomized complete block design (scheme of lysimeter arrangement in Appendix of Study A and B). Each lysimeter was watered and planted with a cabbage turnip seedling (*Brassica oleracea* var. *gongylodes* L.). To follow plant inputs into SOC fractions, a pulse-labeling was conducted using 99% ^{13}C-CO_2. After nine weeks of plant growth, the soils of the lysimeter experiment were carefully harvested in July 2024 to determine amendment effects on soil fertility. Soil cores were taken in each lysimeter to determine physical soil properties in undisturbed samples (Study A). The remaining soil sample was sieved (2 mm) to remove coarse fragments and roots, air-dried, and used to analyze chemical and further physical soil properties as well as SOC stabilization. A subsample of the fresh sieved soil was cooled and used to determine amendment effects on extra-cellular enzyme kinetics and microbial biomass C (Study B).

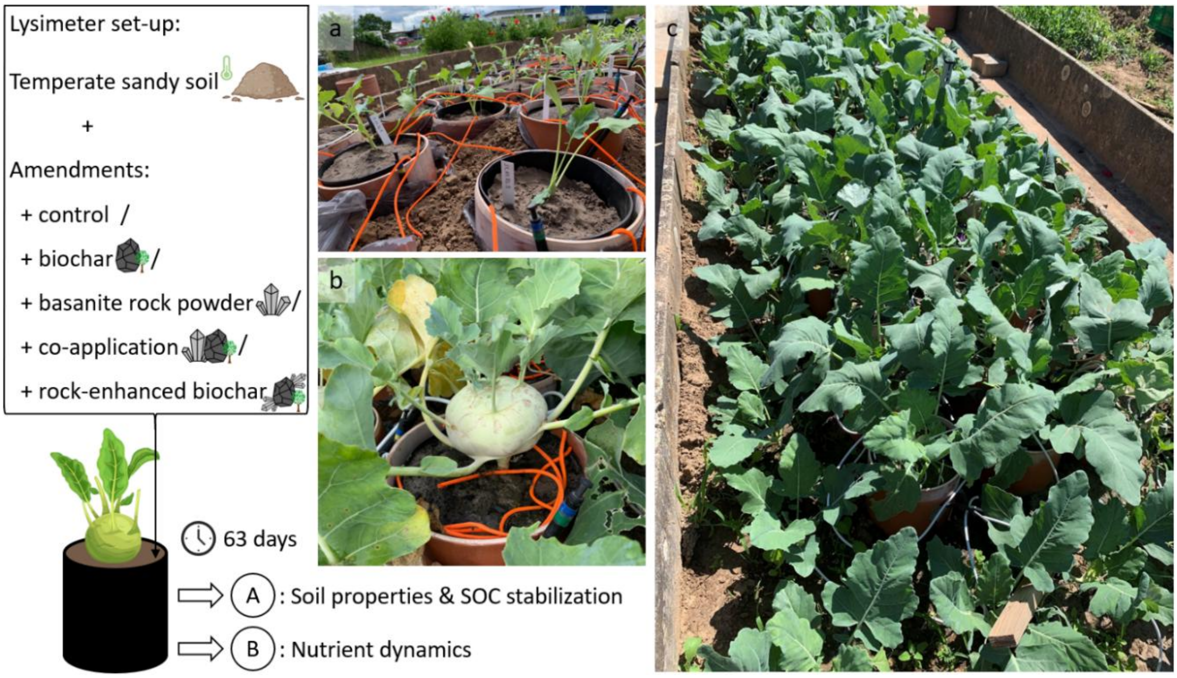

Figure 2: Field-based lysimeter experiment consisting of 45 lysimeters planted with cabbage turnip (*Brassica oleracea* var. *gongylodes* L.) related to Study A and B. Early (a) and late (b) growth stage of cabbage turnip in lysimeters placed in a sand bed (c). SOC = soil organic carbon.

Laboratory-based incubation experiments (Study C & D)

Three different incubation experiments were set up to investigate the effect of amendment applications on different aspects of SOC dynamics (Figure 3). These incubations included the three agricultural topsoils, allowing to assess whether amendment effects depend on soil properties.

A long-term incubation (874 days) was set up to observe the effects of the different soil amendments on the stability and mineralization of SOC over time, measured as the release of CO_2 (Study C). Therefore, the three agricultural topsoils were mixed with pure biochar derived from willow wood (*Salix viminalis* L.) or wheat straw (*Triticum aestivum* L.), pure basanite powder, the co-application of the biochars and basanite powder, or the equivalent rock-enhanced biochars from co-pyrolysis (n=4). This set up allowed for a comparison of pure and combined application effects as well as to investigate the impact of feedstock on the effects of those biochar-containing amendments.

A short-term incubation (17 days) was set up to investigate how the amendment applications altered the system's response to input of labile C, represented by glucose (Study C). This glucose addition could potentially affect the mineralization of both native and amendment-derived SOC, referred to as glucose-induced priming. Therefore, the three agricultural topsoils were mixed with pure biochar derived from willow wood (*Salix viminalis* L.) or wheat straw

(*Triticum aestivum* L.), pure basanite powder, the co-application of the biochars and basanite powder, or the equivalent rock-enhanced biochars from co-pyrolysis in two sets. One set (n=4) was incubated with and another set (n=4) without the addition of ^{13}C-labeled glucose. The ^{13}C-glucose-label allowed distinguishing between glucose- and SOC-derived CO_2 and thus determine the mineralization of those C sources during the incubation.

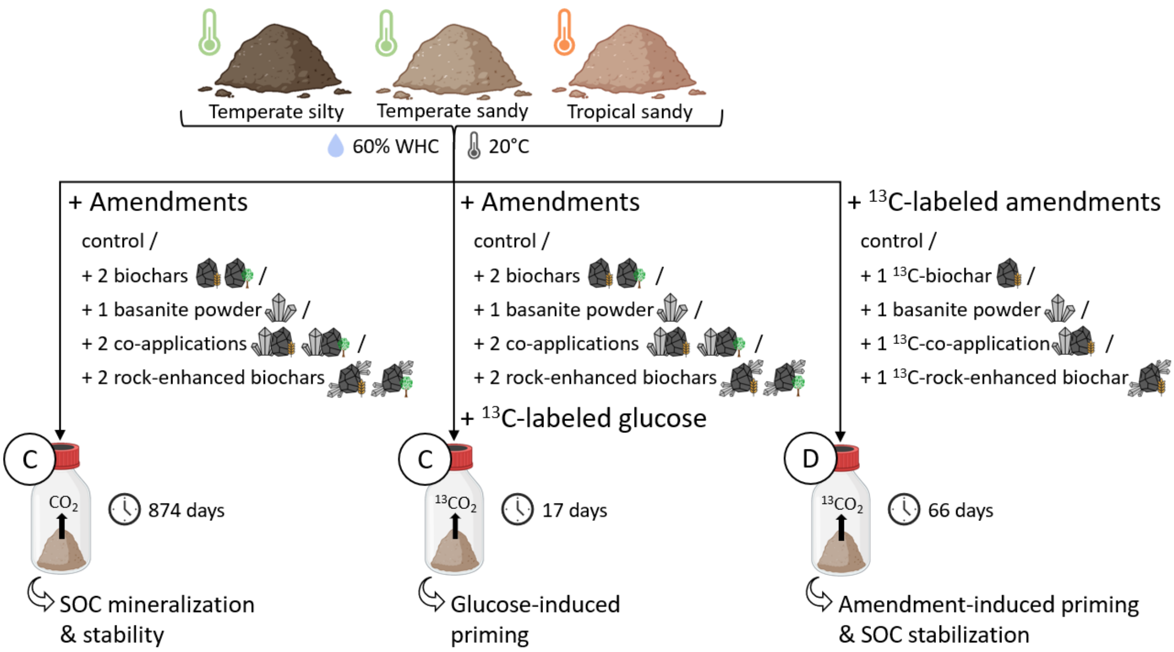

Figure 3: Three incubation experiments related to Study C (874- and 17-day incubations) and D (66-day incubation). Biochar-containing amendments were derived from wheat straw or willow wood. CO_2 = carbon dioxide, SOC = soil organic carbon, WHC = water holding capacity.

To gain further insights into the effects of the applied amendments on SOC dynamics, a 66-day incubation was set up to investigate the amendment-induced priming effect on the mineralization of native SOC, the stabilization of native and amendment-derived SOC, and the mineralization of the amendments themselves (Study D). Therefore, the three agricultural topsoils were mixed with pure ^{13}C-labeled wheat straw biochar (*Triticum aestivum* L.), pure basanite powder, the co-application of the ^{13}C-labeled biochar and basanite powder, or the equivalent ^{13}C-labeled rock-enhanced biochar from co-pyrolysis (n=4). The ^{13}C-label of the applied biochar-containing amendments allowed distinguishing between CO_2 from native and amendment-derived SOC and thus the mineralization of those C sources during the incubation. After the incubation, the stabilization of native and amendment-derived SOC in aggregates and on mineral surfaces was determined.

2.3 Chemical and physical soil properties

General soil and amendment characterization

Initial properties of the soils and amendments were determined prior to the experiments (Study A, B, C, and D). Initial C and N content, pH, and electric conductivity of the soil-amendment-mixtures were determined prior to the incubation experiments, allowing to track amendment-induced effects during the incubations (Study C and D). To compare amendment-induced effects on C and N content, soil pH, and electric conductivity at the end of the respective experiments, these parameters were also determined after the experiments (Study A, B, C, and D). For samples derived from the field-based lysimeter experiment, total and organic C were considered equivalent due to the slightly acidic soil pH of all treatments (< 6.6) (Study A and B). The C in samples derived from the incubation experiments was distinguished between organic and inorganic C (Study C and D).

Physical soil properties

The amendment effects on physical soil properties, focusing on soil water dynamics and soil structure, were analyzed based on soil samples taken at the end of the nine-week field-based lysimeter experiment (Study A). A sieved soil sample (2 mm) was used to determine the water holding capacity as the amount of water the soil can hold against gravity for 24 hours. Soil water retention was determined on undisturbed, water saturated 100 cm^3 soil cores using the pressure plates method (DIN, 2014). Saturated and unsaturated hydraulic conductivity were determined based on 250 cm^3 soil cores using a KSAT device and HYPROP®, respectively (both Meter Group Inc., Munich, Germany). All soil-core data were processed in HYPROP® SoilView based on the van Genuchten bimodal PDI model (IDEN & DURNER, 2014; PETERS, 2014) to calculate air capacity (pF 0-1.8), plant-available water (pF 1.8-4.2), and unavailable water (> pF 4.2). The soil bulk density was determined by relating the volume of the undisturbed 100 cm^3 soil cores to the dry soil weight it contained.

Cation exchange capacity and plant-available nutrients

To assess amendment effects on soil nutrient content and availability, soil samples from the lysimeter experiment were analyzed for their cation exchange capacity and contents of plant-available P and K (VDLUFA, 1991) (Study A and B). Additionally, contents of mineral N in soil (DIN, 2005) were determined (Study B).

2.4 Extracellular enzyme kinetics

To determine amendment effects on soil nutrient dynamics, extracellular enzyme kinetics were determined using fluorogenic substrates, following the protocol of MARX et al. (2001) (Study B). Those investigated enzymes include ß-glucosidase related to the C cycle, chitinase related to C and N cycle, leucine-aminopeptidase related to the N cycle, and acid phosphatase related to the P cycle. The kinetic parameters were calculated following MICHAELIS & MENTEN (1913). To more easily compare microbial nutrient demands, extracellular enzyme stoichiometry was calculated as the ratio of C- (ß-glucosidase), N- (leucine-aminopeptidase), and P-related (acid phosphatase) enzyme kinetics following the concept of SINSABAUGH et al. (2008). While a ratio of C:N:P of 1:1:1 represents an equilibrated system, a value >1 indicates a limitation of the respective nutrient.

2.5 Soil organic carbon dynamics

Soil organic carbon mineralization and pools

To quantify the effect of amendment application on potentially mineralizable native SOC and the mineralization of the amendment-derived SOC, soil samples were incubated for up to 874 days under optimum water and temperature conditions in sealed flasks (Study C and D). The accumulation of CO_2 in the flask headspace was monitored as a proxy for SOC mineralization. A double first-order exponential decay model (ANDRÉN & KÄTTERER, 1997) based on the CO_2 release during the 874-day incubations was used to distinguish fast and intermediate SOC pools, containing native and more labile amendment-derived SOC, and their mean residence times (Study C). A third, long-term stable SOC pool was distinguished to extrapolate the amount of SOC present over time. This pool contains the stable SOC derived from biochar-containing amendments, determined by hydropyrolysis (HAGEMANN et al., 2025; MEYER ZU DREWER et al., 2025).

Priming effect induced by glucose or biochar-containing amendments

To trace the mineralization of native SOC, amendment-derived SOC, and glucose and to investigate amendment- and glucose-induced priming effects, $\delta^{13}C$ values of the initial materials and of the CO_2 released during the incubations were measured. The $\delta^{13}C$ (‰) describes the abundance of ^{13}C, representing the ratio of ^{13}C:^{12}C relative to the Vienna-PeeDee-Belemnite Standard.

To investigate glucose-induced priming effects (Study C), the isotopic signatures of ^{13}C-labeled glucose and SOC were used to partition the CO_2 released during the 17-day incubation into glucose- and SOC-derived by applying a two-pool mixing model following BAMMINGER et al. (2014) and FANG et al. (2015). The glucose-induced priming effect was calculated as the relative difference in SOC mineralization between glucose-amended and -unamended samples.

To investigate amendment effects on the mineralization and stabilization of native and amendment-derived SOC (Study D), the use of ^{13}C-labeled biochar-containing amendments allowed the distinction between amendment-derived and native SOC in CO_2 and SOC fractions (KUZYAKOV, 2011) by applying a two-pool mixing model following BAMMINGER et al. (2014) and FANG et al. (2015). Amendment-induced priming effects were calculated as the difference in native SOC mineralization between amended and unamended samples.

Soil organic carbon stabilization

To determine the amendment effects on SOC stabilization, the SOC was divided into fractions stabilized by different mechanisms. After the nine-week lysimeter experiment, a sieve fractionation of the soil samples was conducted following JUST et al. (2021) and LUGATO et al. (2021) (Study A). A 53 µm sieve was used to separate particulate organic matter (POM), defined as >53 µm, from MAOM, defined as <53 µm, by size. The $\delta^{13}C$ value of the sieve fractions allowed to trace the incorporation of ^{13}C-labeled plant material into the SOC.

Following the 66-day incubation using ^{13}C-labeled amendments, a density fractionation was conducted following GOLCHIN et al. (1994) and VIRET & GRAND (2019) (Study D). In comparison to the sieve fractionation, the density fractionation additionally distinguishes fPOM and oPOM. This is especially useful in soils with finer texture, which are more likely to form aggregates. A sodium polytungstate ($3\ Na_2WO_4 \cdot 9\ WO_3 \cdot H_2O$) solution with a density of 1.8 g cm^{-3} allowed the density-based differentiation between fPOM, oPOM stabilized in aggregates, and MAOM. The $\delta^{13}C$ value of the density fractions allowed to trace SOC from native and biochar-containing amendments in these fractions.

Microbial biomass and dissolved organic carbon

Microbial biomass C was determined using the chloroform fumigation extraction method adapted from VANCE et al. (1987) (Study A, B, C, and D). The difference between the extracted C in fumigated and non-fumigated samples was interpreted as microbial biomass C (Joergensen, 1996). The C in the non-fumigated samples is considered as DOC. The use of ^{13}C-labeled amendments (Study D) allowed to trace the incorporation of native and amendment-derived C in the microbial biomass.

2.6 Statistical analyses

Differences in target variables ($p < 0.05$) were evaluated by analysis of variance (Study A, B, C, and D) or, for repeated measurements, by linear mixed-effects models (Study B, C, and D). Both analysis of variance and linear mixed-effects models were followed by a Tukey HSD post-hoc test for pairwise comparison. Prior to analysis, model residuals were checked visually for normality and homogeneity of variance. All statistical analyses were performed in RStudio 4.5.1, using 'dplyr' package (Wickham et al., 2023) for data handling, 'lme4' package (Bates et al., 2015) for linear mixed-effects models computing, 'emmeans' (Lenth et al., 2025) and 'multcomp' (Hothorn et al., 2008) for pairwise comparison and compact letter display, 'ggplot2' package (Wickham, 2016) and 'gridExtra' (Auguie & Antonov, 2017) for data visualization.

3 Key findings

Table 2: Overview of objectives and key findings of the studies related to this dissertation.

Study	Objectives	Key findings
Study A: *Effect of combined biochar and basanite applications on chemical and physical properties of a sandy agricultural soil*	• Comparing effects of pure and combined amendments on soil properties under near-field conditions • Assessing amendment effects on chemical and physical soil properties, affecting soil fertility • Quantifying amendment effects on the stabilization of SOC as particulate and mineral-associated organic C	• Biochar dominated the effect of combined biochar and basanite applications • Biochar-containing amendments improved chemical and physical soil properties and increased both particulate and mineral-associated SOC • Rock-enhanced biochar was more resistant to physical breakdown, but less effective in improving soil fertility in this nine-week timeframe compared to co-applied biochar • Pure basanite rock powder application had no effect on the analyzed parameters, probably due to low weathering rates
Study B: *Biochar dominated the combined effect of silicate rock powder and biochar application on extracellular enzyme kinetics and nutrient dynamics in a sandy soil*	• Comparing effects of pure and combined amendment applications on nutrient dynamics under near-field conditions • Quantifying amendment effects on extracellular enzyme kinetics • Assessing amendment effects on microbial nutrient demands and potential nutrient limitations, affecting soil fertility	• Biochar dominated the effect of combined biochar and basanite applications • Biochar-containing amendments increased P availability and thus reduced microbial P demand, increasing the relative N demand and leading to a shift towards a more balanced microbial nutrient demand • Pure biochar application resulted in the highest short-term P availability, while rock-enhanced biochar potentially results in a more long-term fertility improvement

Study	Objectives	Key findings
		• Pure basanite rock powder application had no effect on nutrient dynamics, probably due to low weathering rates
Study C: *Effects of combined biochar and basanite application on short-term glucose-priming and long-term soil carbon stability*	• Comparing effects of pure and combined amendment applications on SOC dynamics as part of the amendments' CDR potential • Determining effects of feedstock and soil properties on amendment effects • Investigating amendment effects on short-term glucose-induced priming • Quantifying amendment effects on SOC mineralization over time • Assessing amendment effects on SOC pools and their mean residence times	• Biochar dominated the effect of combined biochar and basanite applications • Effects of amendments on short-term glucose-induced priming differed between soils • Combined applications partly reduced SOC mineralization less strongly than pure biochar over time • Wood-derived amendments more strongly reduced SOC mineralization over time and resulted in higher long-term stable SOC pools, beneficial for CDR, compared to wheat-derived amendments • Co-pyrolysis to wheat-derived rock-enhanced biochar increased the long-term stable SOC pool to similar or higher levels as wood-derived biochar • Effects of wheat-derived amendments on SOC mineralization over time were likely determined by initial soil pH • Effect of basanite rock powder application on SOC dynamic intensified over time due to progressive weathering and was more pronounced in low-pH sandy soils

Study	Objectives	Key findings
Study D: *Rock-enhanced biochar has similar priming effect as pure biochar application, but improves short-term carbon stabilization in agricultural soils*	• Comparing effects of pure and combined amendment applications on mineralization (amendment-induced priming) and stabilization of native SOC in aggregates and mineral-associations • Quantifying mineralization and stabilization of amendment-derived SOC from pure and combined applications • Understanding effects of soil properties on SOC dynamics, affecting the amendments' CDR potential	• Biochar dominated the effect of combined biochar and basanite applications • Short-term priming effects induced by biochar-containing amendments were triggered by low-pH and sandy texture • Amendment-derived SOC was incorporated in aggregates and mineral-associations • Amendment-derived SOC incrporation exceeded occasional losses of native SOC in mineral-associations • Rock-enhanced biochar had a higher short-term stability and increased mineral-associated SOC stronger than pure and co-applied biochar • Pure basanite rock powder application had no effect on SOC mineralization and stabilization, probably due to low weathering rates

C = carbon, CDR = carbon dioxide removal, N = nitrogen, P = phosphorous, SOC = soil organic carbon.

3.1 Effects of combined and pure amendment applications on soil fertility

The application of biochar-containing amendments (pure biochar, co-application, rock-enhanced biochar) affected soil physical, chemical, and biological properties and processes and thus improved overall soil fertility of the investigated temperate sandy soil during the nine-week field-based lysimeter experiment (Study A and B). Biochar-containing amendments partly improved physical properties by increasing water holding capacity and reducing bulk density (Study A). These improvements are especially beneficial in sandy soils (BLANCO-CANQUI, 2017; RAZZAGHI et al., 2020; ZHANG et al., 2021), such as the temperate sandy soil investigated in this study. However, air capacity and plant-available water, two important physical soil parameters relevant for plant growth (RITCHIE, 1981), remained unaffected by the application of biochar-containing amendments. Air capacity is generally high in sandy soils (ARCHER & SMITH, 1972), explaining the limited additional benefit of biochar-containing amendment application. In contrast, plant-available water is often relatively scarce in organic-poor sandy soils, which typically makes biochar particularly effective at improving water availability in such soils (RAZZAGHI et al., 2020; BUSS et al., 2021). The absence of a short-term improvement in plant-available water may be attributed to the high ash content (AURANGZEIB et al., 2025) and larger particle size (IBRAHIMI & ALGHAMDI, 2022) of the biochar-containing amendments. Since process-derived changes in physical soil properties may take years to become measurable (COSTANZO et al., 2025), positive long-term effects of the biochar-containing amendments remain likely (BLANCO-CANQUI, 2017).

The application of biochar-containing amendments altered several chemical soil properties, including the supply of nutrients. Due to the high C content of biochar-containing amendments (JOSEPH et al., 2010; GROSS et al., 2021; QIU et al., 2023), the soil C content increased more strongly than its N content, resulting in a widened C:N ratio. The dissolution of biochar ash increased the content of available nutrients, such as P (JIN et al., 2016; GLASER & LEHR, 2019; WANG et al., 2025), by releasing P_2O_5 over time (GHODSZAD et al., 2021; BUSS et al., 2022). The increased soil pH following the biochar-containing amendment application likely additionally enhanced P availability, potentially exceeding the amount of P released via biochar ash dissolution, and reduced P leaching (SHEPHERD et al., 2017; GHODSZAD et al., 2021). These changes in nutrient availability were directly reflected in extracellular enzyme kinetics (Study B), indicating a shift in microbial nutrient demand following the application of biochar-containing amendments. The increase in plant-available P allowed microorganisms to down-regulate the production of acid phosphatase, a P-acquiring enzyme (SINSABAUGH et al., 2008; ALLISON et al., 2011). Simultaneously, the biochar-containing amendment applications increased the relative microbial demand for N, reflected in an enhanced investment in the N-acquiring enzyme leucine-aminopeptidase (SINSABAUGH et al., 2008; ALLISON et al., 2011). This increased N demand was likely a consequence of the widened soil C:N ratio and the potential adsorption of mineral N on the surfaces of biochar-containing amendments (CLOUGH et al., 2013). While P remained the primary limiting nutrient for microorganisms, the application of biochar-containing amendments appeared to shift the soil system towards a more balanced nutrient demand with a relative increase in N demand.

The observed increase in microbial biomass, a key driver for biological soil processes (SINGH & GUPTA, 2018), likely reflects improved microbial habitat and growth conditions (GHODSZAD et al., 2021) following the application of biochar-containing amendments (Study A and B). These improvements were probably driven by increases in soil pH, nutrient and water retention capacity, and labile C availability (VAN ZWIETEN et al., 2010; LIU et al., 2015), e.g. through DOC released from biochar-containing amendments (AZEEM et al., 2023; CHEN et al., 2024).

The improved soil fertility following the application of biochar-containing amendments can increase plant growth and yield (JOSEPH et al., 2021; ZHANG et al., 2021), making those amendments a suitable option for agricultural use. However, the magnitude of biochar-containing amendment effects on soil fertility differed between application types (Study A and B). The co-application of biochar and basanite rock powder largely mirrored the effects of pure biochar, indicating that co-application did not compromise the beneficial effects of biochar while synergistic effects remain possible over time (HONVAULT et al., 2024). Indeed, the increase in soil pH and electrical conductivity was most pronounced following co-application, suggesting a synergistic effect driven by the combined liming and ionic contributions of both amendments. In contrast, rock-enhanced biochar partly resulted in comparatively smaller short-term improvements of soil fertility. However, this attenuated short-term response during the field-based lysimeter experiment suggests the use of rock-enhanced biochar as a potential slow-release amendment for long-term soil improvement (LAMMIRATO et al., 2011; BUSS et al., 2022).

In contrast to the biochar-containing amendments, pure basanite rock powder application neither improved nor impaired soil fertility, likely due to limited basanite weathering during the nine-week field-based lysimeter experiment (Study A and B). Basanite can have comparatively low weathering rates given its mineralogical composition (HAMMES et al., 2025). Consistent with previous studies reporting positive effects of silicate rock powder over longer time scales (KAHNT et al., 1986; DUPLA et al., 2024; RICHARDSON, 2025), beneficial effects on soil fertility are likely in the long term.

3.2 Effects of combined and pure amendment applications on soil organic carbon dynamics

The application of biochar-containing amendments affected all investigated SOC dynamics (Study A, C, and D). Soil properties were one of the dominant factors controlling the stability and mineralization of amendment-derived SOC as well as the amendment-induced priming effect on the mineralization of native SOC (Study D). The mineralization of amendment-derived and native SOC were higher in both sandy soils compared to the temperate silty soil during the 66-day incubation, likely driven by the low initial pH (4.7) and coarse texture of these soils. The strong pH increase following the application of biochar-containing amendments in both sandy soils from 4.7 to 7.2-7.4 during pre-incubation, compared to the weaker increase in the temperate silty soil from 6.9 to 7.5 during pre-incubation, likely promoted microbial activity and modified the microbial community composition (LUO et al., 2011; ZHANG et al., 2018; XU et al., 2021). The input of labile C compounds from the biochar-containing amendments potentially amplified this effect, particularly in sandy soils that are poor in organic matter (ZIMMERMAN et al., 2011; WANG et al., 2016). Clay-poor or sandy soils commonly experience positive priming following biochar application (FANG et al., 2015; LIU et al., 2015; WANG et al., 2016), whereas clay-rich soils often show negative priming (BRUUN et al., 2014; HERATH et al., 2015; YU et al., 2020). This underlines the role of soil texture and pH in controlling amendment-induced priming (ZIMMERMAN et al., 2011; WANG et al., 2016) and short-term stability of biochar-containing amendments (BRUUN et al., 2014; YANG et al., 2022; SCHMIDT et al., 2025), thus affecting their CDR potential.

The relevance of soil properties for the amendment's effects on the mineralization of SOC (native and amendment-derived) was additionally affected by feedstock type and time (Study C), with the effects of wheat-derived amendments being particularly sensitive to soil properties during the 874-day incubation. The application of the wheat-derived amendments increased the SOC mineralization in the temperate silty soil over time, while reducing it in both sandy soils. This pattern over time is opposing to the short-term mineralization dynamics during the 66-day incubation, indicating time-dependent effects of wheat-derived biochar-containing amendments on SOC mineralization. However, also on longer time scales, the different responses of SOC mineralization to this amendment application was likely linked to the higher soil pH of the temperate silty soil (WANG et al., 2022), as higher pH has been shown to reduce biochar stability (WANG et al., 2022). In contrast, consistently across soils and throughout the 874-day incubation, wood-derived biochar-containing amendments reduced SOC mineralization more strongly than wheat-derived amendments, reflecting the inherently higher stability of woody feedstock (LUO et al., 2011; VAUGHN et al., 2013; WANG et al., 2016). This highlights the potential of biochar-containing amendments, particularly those derived from wood, to lower SOC mineralization and thus to reduce soil-borne CO_2 emissions, directly contributing to CDR.

This feedstock-effect was reflected in the long-term stable SOC pool, which was larger following the application of wood- compared to wheat-derived amendments in all three soils (Study C). This long-term stable SOC pool, which likely has a mean residence time of over 1000 years (KUZYAKOV et al., 2009; LEHMANN et al., 2015; SCHMIDT et al., 2025), consisted of the aromatic compounds of biochar-containing amendments and represents the long-term CDR potential of these amendments. Co-pyrolyzing wheat straw with basanite resulted in similar or even larger stable SOC pools than pure and co-applied wood-derived biochar. This likely results from the higher initial stability of rock-enhanced biochar compared to pure and co-applied biochar (MEYER ZU DREWER et al., 2025). Thus, co-pyrolysis is an equally important factor as feedstock in controlling long-term stability and thereby CDR potential of biochar-containing amendments, likely compensating for inherent feedstock-determined stability limitations. These findings show the need to validate the potential of rock-enhanced biochar from co-pyrolysis in long-term field experiments (WANG et al., 2022; AZZI et al., 2024).

Beyond these general feedstock and soil effects, soil-amendment-interactions can produce irregular SOC dynamics, as observed for wood-derived rock-enhanced biochar applied to the tropical sandy soil. After more than 250 days, the CO_2 release of this soil-amendment-combination started to increase – contrasting to the typical decline of SOC mineralization as labile C compounds are depleted over time (KUZYAKOV et al., 2009; AMELOOT et al., 2013; HAN et al., 2020). This late increase in SOC mineralization suggests a shift in microbial dominance (LIU et al., 2020) toward fungal activity, which intensifies as bacterial mineralization of labile compounds declines and recalcitrant C sources prevail (LEHMANN et al., 2009; AMELOOT et al., 2013; WANG et al., 2022). That this response occurred only in the tropical sandy soil amended with wood-derived rock-enhanced biochar may reflect an inherently higher fungal:bacterial ratio in this soil (MALIK et al., 2016) and/or the high proportion of recalcitrant compounds in woody feedstock (VAUGHN et al., 2013; WANG et al., 2016; WANG et al., 2022) triggering fungal activity. While the underlying mechanisms remain speculative, this observation demonstrates the context-dependency of biochar-containing amendment effects on SOC dynamics.

The stability and mineralization of native and amendment-derived SOC are known to be strongly determined by their stabilization mechanisms (VON LÜTZOW et al., 2006). The application of biochar-containing amendments led to similar or increased SOC contents in fPOM, oPOM, and MAOM compared to the unamended soils following the 66-day incubation (Study D) and the nine-week field-based lysimeter-experiment (Study A). The increase in fPOM content mainly originated from amendment-derived SOC, as biochar has been observed to accumulate in the fPOM fraction (Herath et al., 2014; Singh et al., 2014; Paetsch et al., 2017). The stability of those free biochar-containing amendment particles is mainly determined by their chemical composition, including readily available and highly stable C compounds (Schiedung et al., 2020; Ameloot et al., 2013; Wang et al., 2016). The strong persistence of SOC derived from biochar-containing amendments increased the recalcitrance of overall fPOM, changing the properties of this otherwise rather labile SOC fraction. Amendment-derived SOC was additionally incorporated in oPOM and MAOM in all three soils (Study D), suggesting its further stabilization in aggregates and on mineral-surfaces (Azzi et al., 2024; Brodowski et al., 2006; Singh et al., 2014). This enhances the CDR potential of biochar-containing amendments by further reducing their accessibility to microbes. However, the application of biochar-containing amendments led to a loss of native fPOM and MAOM compared to the unamended temperate soils. The loss of native fPOM following the application of biochar-containing amendments was, at least partly, caused by a shift of native fPOM to oPOM, indicating an enhanced stabilization of native SOC via aggregate occlusion following the application of biochar-containing amendments. The amendment-induced priming of the typically stable MAOM might have been caused by its response to released labile amendment-derived C compounds (Paetsch et al., 2017; Schiedung et al., 2020). These could mobilize native MAOM due to the high sorption affinity of SOC derived from biochar-containing amendments, particularly in sandy soils with limited sorption capacity (Kleber et al., 2015). However, the incorporation of amendment-derived SOC in all SOC fractions compensated for the partial loss of native fPOM and MAOM, resulting in a positive contribution to CDR.

Similarly to SOC mineralization, also SOC stabilization was affected by soil properties (Study D). Particularly the initial native SOC content determined the amendment effects on SOC stabilization, as aggregate-occlusion and mineral-association of SOC was more pronounced in the initially SOC-poor tropical sandy soil. Simultaneously, the incorporation of amendment-derived C in the microbial biomass was more pronounced in this tropical sandy soil. Both could indicate higher microbial turnover of native and amendment-derived SOC, potentially triggering the microbially mediated formation of MAOM (Manzoni & Cotrufo, 2024) in this SOC-poor soil. While Fang et al. (2018) and Schiedung et al. (2020) identified fine soil texture as the main driver of biochar-derived SOC stabilization in column and field experiments, we observed strong interactions between amendment-derived SOC and soil minerals also in coarse textured soils. The magnitude of those interactions within only 66 days suggests the potential of biochar-containing amendments for progressive SOC stabilization and thus CDR.

Another factor influencing SOC dynamics is the input of labile C compounds, which enter the soil naturally via e.g. root exudates (KUZYAKOV et al., 2000), simulated by using glucose (Study C). The addition of glucose as an easily available C source can enhance the mineralization of native SOC (WU et al., 2020; GAUDEL et al., 2022) and SOC derived from biochar-containing amendments (LEHMANN et al., 2009; FANG et al., 2014), since the microbial utilization of glucose can promote the co-metabolic decomposition of SOC (HAMER et al., 2004; KUZYAKOV et al., 2009). However, the glucose-induced priming, as well as its response to amendment application, differed strongly between soils. In the temperate sandy soil, glucose addition had only minor effects on the mineralization of SOC, regardless of whether and which amendment was applied. This absence of glucose-induced priming could be caused by the higher proportion of POM in this soil, which suggests that more easily available substrates were already decomposed, leaving POM as a more recalcitrant fraction that is less likely to be primed (LAVALLEE et al., 2020; ZHENG et al., 2023). In the tropical sandy soil, glucose addition increased the mineralization of SOC, potentially due to the initially low SOC content (4.7 g kg^{-1}) of this soil. In such soils, microbial communities are often C limited and thus respond more strongly to fresh substrate inputs, resulting in a more pronounced glucose-induced priming effect (KUZYAKOV et al., 2009; BASTIDA et al., 2019; WU et al., 2020). Pure and co-applied wood-derived biochar were, however, able to suppress this glucose-induced loss of SOC, potentially due to the adsorption of glucose onto the biochar surface (IPPOLITO et al., 2020; KALU et al., 2024; HAMER et al., 2004), thereby preventing SOC mineralization and enhancing the CDR potential of these amendments. In the temperate silty soil, the application of biochar-containing amendments increased the system's response to glucose addition. While the SOC mineralization of the unamended temperate silty soil did not respond to glucose addition, biochar-containing amendments increased the glucose-induced priming. This might result from an interaction between glucose and biochar-containing amendments (LUO et al., 2017b), potentially combining glucose- and amendment-induced priming (LUO et al., 2017b). Alternatively, biochar-containing amendments could adsorb mineral N onto their surfaces (CLOUGH et al., 2013), thus increasing the microbial N demand, causing an N-mining, and thus enhancing decomposition of native soil organic matter (CRAINE et al., 2007; CHEN et al., 2014). The variability of the amendment effects on glucose-induced priming indicated complex interactions between soil, amendment, and C inputs with implications for the context-dependency of the amendments' CDR potential.

While glucose-induced priming is often a rather short-term effect (KUZYAKOV et al., 2000), the effects of biochar-containing amendments varied over time.

Biochar mineralization is known to decrease over time, once labile compounds are decomposed (KUZYAKOV et al., 2009; AMELOOT et al., 2013). Thus, the amendment-derived SOC mineralized during the 66-day incubation (Study D) probably reflected the more easily available C compounds of the amendments (AZZI et al., 2024; HAGEMANN et al., 2025; SANEI et al., 2025). As already indicated by the decreasing amendment mineralization during this rather short-term incubation, this process is expected to decline over time (AMELOOT et al., 2013; WANG et al., 2016; AZZI et al., 2024). Similarly, also the positive priming of native SOC in both sandy soils following the application of biochar-containing amendments decreased during the first incubation days. As the release of easily available biochar-derived C declines (BRUUN et al., 2008; BRUUN et al., 2014), previous studies showed a shift from positive to negative biochar-induced priming over time (MAESTRINI et al., 2015; DING et al., 2018; JOSEPH et al., 2021). This projected decrease of amendment-derived and native SOC mineralization was already visible in the reduced mineralization of SOC over the course of the 874-day incubation (Study C), supporting the long-term CDR potential of biochar-containing amendments.

While the application of biochar-containing amendments affected SOC dynamics throughout the 874-day incubation, the effects of basanite rock powder application on CO_2 release intensified with increasing incubation duration (Study C). This indicated progressive basanite weathering and subsequent impacts on soil C dynamics, explaining the missing effect of basanite during the more short-term experiments of Study A, B, and D (SOKOL et al., 2024; XU et al., 2025). However, similar to the effects of biochar-containing amendments on SOC mineralization, those of basanite also depended strongly on soil properties, particularly initial soil pH. In both low-pH sandy soils, basanite application reduced cumulative CO_2 release compared to the respective unamended soils over time, while increasing the CO_2 release from the neutral-pH temperate silty soil. The increased CO_2 release from the basanite-amended temperate silty soil indicated stimulated microbial activity enhancing SOC mineralization (BUSS et al., 2021; FANG et al., 2023; LEI et al., 2025) that exceeded CO_2 uptake via weathering (DIETZEN et al., 2018; TE PAS et al., 2026), thereby limiting the CDR potential of basanite in this neutral-pH soil. In contrast, the reduced CO_2 release from both basanite-amended sandy soils indicated either reduced SOC mineralization (BUSS et al., 2023) and/or enhanced CO_2 uptake during weathering (TE PAS et al., 2026). The latter is supported by the steady pH in those two basanite-amended soils, indicating an ongoing alkalinity release (HARTMANN et al., 2013; BEERLING et al., 2020), while all other treatments showed a reduction in pH during the 874-day incubation. Given that increasing pH generally rather promotes than suppresses microbial activity (DIETZEN et al., 2018), a reduced SOC mineralization appears unlikely as the dominant mechanism reducing the CO_2 release from the sandy soils. Thus, the results suggest that measurable basanite weathering was faster or more effective in both sandy soils with initial low pH (HARTMANN et al., 2013; ABDALQADIR et al., 2024).

In both combined applications, the effect of biochar was dominant compared to basanite. However, the stability and stabilization of rock-enhanced biochar repeatedly differed from those of pure and co-applied biochar. Rock-enhanced biochar itself had a higher initial stability (MEYER ZU DREWER et al., 2025). This was reflected in a lower short-term mineralization (Study D), a reduced susceptibility to physical breakdown during sieve fractionation (Study A), and a larger long-term stable SOC pool (Study C), directly enhancing the CDR potential of rock-enhanced biochar compared to pure and co-applied biochar. Rock-enhanced biochar released more DOC than pure and co-applied biochar (Study A), probably caused by the pyrogenic coating formed during co-pyrolysis, consisting of rather labile C compounds (MEYER ZU DREWER et al., 2025). Since DOC can be directly adsorbed onto mineral surfaces (YANG et al., 2016; YANG et al., 2021), this higher DOC release likely explained at least a part of the pronounced amendment-derived MAOM formation following rock-enhanced biochar application (Study D) (MANZONI & COTRUFO, 2024). This difference in the short-term stability and stabilization of rock-enhanced biochar highlights the potential of co-pyrolyzing biomass and basanite to further improve the persistence of amendment-derived C and thus the amendments' CDR potential.

3.3 Comparison of pure and combined amendment application effects

The effects of both combined applications on soil fertility and CDR, reflected as SOC dynamics, generally followed those of pure biochar across all studies, indicating limited effects of basanite rock powder. This likely reflected low basanite weathering rates during the short-term experiments (Study A, B, and D), while synergistic effects remain possible over longer time scales (HONVAULT et al., 2024; TE PAS et al., 2026). In line with this, basanite showed progressive weathering and associated CO_2 uptake in both low-pH sandy soils during the 874-day incubation (Study C). This showed the long-term potential of basanite rock powder as a CDR technology and suggests that the ongoing weathering might also result in a soil fertility improvement (SWOBODA et al., 2022; DUPLA et al., 2024).

While effects of basanite were particularly small in co-application, they became more visible in rock-enhanced biochar. Compared to pure and co-applied biochar, rock-enhanced biochar application resulted in a weaker improvement of several soil properties, ranging from nutrient release over soil pH increase to bulk density reduction, during the nine-week field-based lysimeter experiment (Study A and B). This reduced short-term effectiveness is likely caused by the inclusion of basanite particles within biochar pores during feedstock preparation or co-pyrolysis. As described by MEYER ZU DREWER et al. (2025) and observed in Study D, this inclusion decreased pore space and specific surface area, thereby limiting the interaction between soil and rock-enhanced biochar. While this led to a weaker short-term modification of physical, chemical, and biological soil properties and processes (Study A and B), rock-enhanced biochar could be suitable as a slow-release amendment improving soil fertility over longer time spans (LAMMIRATO et al., 2011; BUSS et al., 2022). Additionally, this reduced reactivity likely protects rock-enhanced biochar against decomposition, potentially improving its stability and CDR effect (ARCHANJO et al., 2017; BUSS et al., 2024b; SCHMIDT et al., 2025). In line with this, rock-enhanced biochar had the highest short-term stability, reflected in the lowest mineralization (Study D), showed a greater resistance to physical breakdown during sieving (Study A), and resulted in the largest long-term stable SOC pool (Study C) compared to pure and co-applied biochar. By co-pyrolysis, this stable SOC pool following the application of wheat-derived rock-enhanced biochar was even similar or higher as that following the application of wood-derived biochar, thereby offsetting inherent feedstock limitations for long-term amendment stability (Study C) and CDR potential. Furthermore, rock-enhanced biochar resulted in a more strongly promoted MAOM formation (Study D) compared to pure and co-applied biochar. Whether this MAOM formation primarily occurred during amendment preparation or after the soil application remains unclear. On the one hand, MEYER ZU DREWER et al. (2025) observed the formation of pyrogenic coating on the rock particles, suggesting MAOM formation during feedstock preparation or co-pyrolysis. On the other hand, this coating mainly consists of rather labile C compounds (MEYER ZU DREWER et al., 2025), which may have promoted the enhanced release of DOC (Study A) and its direct adsorption as MAOM (MANZONI & COTRUFO, 2024). Despite these advantages of rock-enhanced biochar, pure biochar was more effective in reducing overall SOC mineralization on longer time scales compared to rock-enhanced biochar (Study C). Yet, the overall benefits of rock-enhanced biochar for short- and long-term SOC stability and stabilization may largely compensate for this lower effectiveness in reducing overall SOC mineralization. Taken together, inclusion of basanite within biochar pores promoted the stability and stabilization of SOC, but simultaneously limited the short-term reactivity of rock-enhanced biochar. However, the effects of rock-enhanced biochar on soil fertility improvement may progressively increase over time. Thus, the choice between application types depends on the intended management goal – while pure and co-applied biochar are preferable for relatively rapid soil fertility improvement, rock-enhanced biochar may be more suitable for enhancing SOC stability and stabilization, thus increasing its long-term CDR potential, while potentially improving soil fertility to similar extends over time.

4 Conclusions and outlook

4.1 Conclusion

This dissertation advanced the understanding of the effects of combined biochar and basanite rock powder applications compared to pure biochar and basanite applications on soil fertility and SOC dynamics, affecting the amendments' CDR potentials. The combined applications included the co-application of biochar and basanite as well as rock-enhanced biochar from co-pyrolysis of biomass and basanite. The effects of pure and combined amendment applications were assessed in field-based lysimeters with plants and laboratory incubation experiments, with the latter additionally considering the impact of feedstock and different soil properties.

The application of biochar-containing amendments (pure biochar, co-application, rock-enhanced biochar) consistently improved soil fertility of the investigated temperate sandy soil in the field-based lysimeters. These improvements were reflected in increased water holding capacity, reduced bulk density, elevated soil pH, and enhanced plant-available nutrient contents. As a result, these amendments affected extracellular enzyme kinetics, indicating a shift in microbial nutrient demand towards a more balanced acquisition of C, N, and P, driven by the improved P availability and the relative increase in N demand. Together with increased microbial biomass C, these findings indicate enhanced biological activity, while also showing the need for tailored N fertilization strategies to avoid potential nutrient limitations following the application of biochar-containing amendments.

In addition to soil fertility improvements, biochar-containing amendments demonstrated the potential for CDR by affecting short- and long-term SOC stability and improving SOC stabilization in the three investigated soils with differing soil properties. However, direction and magnitude of these effects depended on feedstock and soil type. Wood-derived amendments had a higher short-term stability and consistently reduced SOC mineralization across time and soils. In contrast, wheat-derived amendments showed more variable and soil-dependent responses over time, with stronger short-term amendment-induced positive priming and higher amendment mineralization in low-pH sandy soils. Similarly, the effect of amendments on labile C input in the form of glucose (glucose-induced priming) also differed between soils, potentially determined by SOC content, stability, and stabilization. Additionally, atypical SOC mineralization dynamics in certain soil-amendment-combinations showed the complexity of soil-amendment-interactions and underlined the context-dependency of amendment effects on SOC dynamics and thus on CDR potentials of biochar-containing amendments.

Across all experiments, the type of amendment application affected both soil fertility and SOC dynamics in field and laboratory experiments. Biochar dominated the effect of both combined applications and especially the co-application of biochar and basanite largely resembled the effects of pure biochar, with rare indications of synergistic interactions with basanite during the investigated time frames. However, due to the contrasting temporal dynamics – rather rapid effects of biochar versus weathering-based long-term effects of basanite – co-application may provide complementary benefits over longer timescales. Whether these interactions result in synergistic, additive, or diminishing effects remained unclear and require long-term field validation. In contrast to both pure and co-applied biochar, rock-enhanced biochar had a reduced short-term reactivity under field and laboratory conditions. On the one hand, this reduced reactivity resulted in weaker short-term improvements of soil fertility, but on the other hand enhanced the stability of rock-enhanced biochar simultaneously. The latter was reflected in a reduced short-term mineralization, a larger long-term stable SOC pool, a greater resistance to physical breakdown, and an enhanced stabilization of amendment-derived SOC in mineral associations following the application of rock-enhanced biochar. Overall, rock-enhanced biochar more strongly improved SOC stability and stabilization, increasing its CDR potential compared to pure and co-applied biochar. Notably, co-pyrolysis of wheat straw with basanite to rock-enhanced biochar compensated for feedstock-related limitations in amendment stability, yielding stable SOC pools comparable to or exceeding those of wood-derived biochar across soils. This suggested co-pyrolysis as an equally important factor for long-term amendment stability and thus CDR as feedstock type. Those effects of rock-enhanced biochar are likely explained by the inclusion of basanite particles into biochar pores, reducing surface area and thus limiting interactions with the soil compared to conventional biochar.

Pure basanite application showed, in contrast to the biochar-containing amendments, negligible short-term effects on soil fertility and SOC dynamics, likely reflecting limited weathering during this time frame. However, basanite's increasing effects on SOC mineralization during the 874-day incubation suggested progressive weathering in both low-pH, sandy soils over time, indicating potential long-term effects for CDR and soil fertility.

Overall, the findings of this dissertation demonstrate that all investigated amendments showed potential to improve soil fertility and contribute to CDR and climate change mitigation, while the magnitude and timescale of their effects varied between amendment and soil types. While pure and co-applied biochar were particularly effective for rather rapid improvement in soil fertility, rock-enhanced biochar represented a more stable, slow-release amendment with enhanced short- and long-term SOC stabilization and thus a more sustained climate change mitigation potential. These findings underline that amendment effects on soil fertility and SOC dynamics, affecting CDR, are context-dependent, necessitating amendment selection based on the intended effect, management timescale, and properties of the target soil.

4.2 Further research perspectives

This dissertation is the first study comparing the effects of pure biochar and basanite rock powder with their co-application and their respective rock-enhanced biochar from co-pyrolysis on soil fertility and the amendments' CDR potentials, focusing on SOC dynamics. The complex interactions between amendment type, feedstock type, soil properties, and timescale were demonstrated in a stepwise approach, scaling from mechanistic laboratory incubations to a short-term field-based lysimeter experiment. Building on these findings, further research — spanning both controlled laboratory experiments and long-term field studies across diverse soils and climates — will be required before fully incorporating combined amendments into global CDR strategies.

At the laboratory scale, certain underlying mechanisms determining the effects of combined applications on soil properties and processes remained unclear. The feedstock range investigated in this dissertation was limited to woody biomass and wheat straw, while biochar is often produced from a broad feedstock supply, including manure, grass, and sludge (JOSEPH et al., 2010; HAN et al., 2020). Since feedstock strongly determined the properties and effects of biochar-containing amendments in soils investigated in this dissertation, further investigations of combined applications from various feedstocks are necessary to understand the feedstock-dependent range of potential effects on soil fertility and CDR via SOC dynamics. Additionally, the increased SOC mineralization in the tropical sandy soil amended with wood-derived rock-enhanced biochar, while all other soil-amendment combinations showed the typical decrease over time, potentially indicated a change in microbial community and triggered fungal activity. This underlines that amendment effects on SOC dynamics depended not only on feedstock and soil types, but also on individual interactions between amendments and soil biota. As microbial activity and soil biota emerged as an important potential factor driving SOC dynamics and soil fertility, the microbial community composition should be more thoroughly investigated. Generally when investigating the effect of biochar and basanite, the experimental design must be adapted accordingly, since established soil analytical methods can be limited in fully capturing amendment effects, particularly for biochar (e.g. MUNERA-ECHEVERRI et al., 2018). This could include a combined use of density and sieve fractionation with thermal analysis to gain further information on SOC stabilization, particularly at mineral surfaces (BURGEON et al., 2021; FOUCHÉ et al., 2023), as well as micro- and spectroscopy to investigate inner-pore processes governing the effects of rock-enhanced biochar. Such mechanistic insights from laboratory experiments will be beneficial to conduct field-scale studies and interpret their results.

Beyond the laboratory scale, the time-dependent nature of amendment effects observed in this dissertation – particularly the progressive basanite weathering and the potential slow-release dynamics of rock-enhanced biochar – suggests that short-term experiments may be insufficient to capture the full potential of basanite-containing amendments and underlines the need for long-term field trials with plants (SOKOL et al., 2024; ANTHONY et al., 2025; COSTANZO et al., 2025). Such experiments would allow to understand the effects of combined amendments on plant growth and yield and to test whether the beneficial effects of rock-enhanced biochar observed under controlled conditions translate to field conditions. Given the pronounced soil-dependent effects of most amendments observed in this dissertation, these field trials should include a range of soil types and climatic conditions to assess combined amendment effects on soil properties and processes more comprehensively. Since both biochar and basanite are particularly effective in low-fertility, low-pH soils under tropical conditions (JEFFERY et al., 2017; SWOBODA et al., 2022), future field studies should investigate the effects of combined applications under tropical climate in soils with differing fertility and mineralogy to test where the combined benefits may be most beneficial and where the CDR potential is highest.

Transferring the findings of this dissertation to global CDR approaches requires quantifying the benefits of combined applications compared to pure biochar and basanite application. Rock-enhanced biochar showed higher long-term SOC stability and stabilization, but whether these benefits outweigh the additional efforts and costs of co-pyrolysis compared to pure or co-application remains uncertain (MEYER ZU DREWER et al., 2025). Combined applications may result in trade-offs between soil fertility improvement and CDR potential, since e.g. weathering-stimulated microbial activity could accelerate biochar mineralization (FANG et al., 2023), while biochar-induced pH increases could in turn reduce basanite weathering (HARTMANN et al., 2013; SWOBODA et al., 2022). However, improved microbial habitat and activity following biochar application could enhance rock powder weathering (AMANN & HARTMANN, 2019) and secondary mineral formation following enhanced weathering could improve the stabilization of C derived from biochar-containing amendments (TE PAS et al., 2026). Whether such mutually limiting or synergistic effects are relevant at field scale in the long-term remains unknown. Resolving these uncertainties will be essential to evaluate whether combined biochar and basanite amendments can meaningfully contribute to climate mitigation.

5 References

ABDALQADIR, M., HUGHES, D., REZAEI GOMARI, S. & RAFIQ, U. 2024. A state of the art of review on factors affecting the enhanced weathering in agricultural soil: Strategies for carbon sequestration and climate mitigation. Environ Sci Pollut R. https://doi.org/10.1007/s11356-024-32498-5.

ALLEN, R. L. 1847. A Brief Compend of American Agriculture. Oakland, California, USA, University of California.

ALLISON, S. D. 2006. Soil minerals and humic acids alter enzyme stability: implications for ecosystem processes. Biogeochemistry, 81, 361–373. https://doi.org/10.1007/s10533-006-9046-2.

ALLISON, S. D., WEINTRAUB, M. N., GARTNER, T. B. & WALDROP, M. P. 2011. Evolutionary-economic principles as regulators of soil enzyme production and ecosystem function. *In:* SHUKLA, G. & VARMA, A. (eds.) Soil Enzymology. Berlin, Heidelberg: Springer Berlin Heidelberg. https://doi.org/10.1007/978-3-642-14225-3_12.

AMANN, T. & HARTMANN, J. 2019. Ideas and perspectives: Synergies from co-deployment of negative emission technologies. Biogeosciences, 16, 2949–2960. https://doi.org/10.5194/bg-16-2949-2019.

AMANN, T., HARTMANN, J., STRUYF, E., DE OLIVEIRA GARCIA, W., FISCHER, E. K., JANSSENS, I., MEIRE, P. & SCHOELYNCK, J. 2020. Enhanced Weathering and related element fluxes – a cropland mesocosm approach. Biogeosciences, 17, 103–119. https://doi.org/10.5194/bg-17-103-2020.

AMELOOT, N., GRABER, E. R., VERHEIJEN, F. G. A. & DE NEVE, S. 2013. Interactions between biochar stability and soil organisms: review and research needs. Eur J Soil Sci, 64, 379–390. https://doi.org/10.1111/ejss.12064.

ANDA, M., SHAMSHUDDIN, J. & FAUZIAH, C. I. 2015. Improving chemical properties of a highly weathered soil using finely ground basalt rocks. CATENA, 124, 147–161. https://doi.org/10.1016/j.catena.2014.09.012.

ANDRÉN, O. & KÄTTERER, T. 1997. ICBM: The introductory carbon balance model for exploration of soil carbon balances. Ecol Appl, 7, 1226–1236. https://doi.org/10.1890/1051-0761(1997)007[1226:ITICBM]2.0.CO;2.

ANGST, T. E. & SOHI, S. P. 2013. Establishing release dynamics for plant nutrients from biochar. GCB Bioenergy, 5, 221–226. https://doi.org/10.1111/gcbb.12023.

ANTHONY, T. L., JONES, A. R. & SILVER, W. L. 2025. Supplementing enhanced weathering with organic amendments accelerates the net climate benefit of soil amendments in rangeland soils. AGU Advances, 6, e2024AV001480. https://doi.org/10.1029/2024AV001480.

ARCHANJO, B. S., MENDOZA, M. E., ALBU, M., MITCHELL, D. R. G., HAGEMANN, N., MAYRHOFER, C., MAI, T. L. A., WENG, Z., KAPPLER, A., BEHRENS, S., MUNROE, P., ACHETE, C. A., DONNE, S., ARAUJO, J. R., VAN ZWIETEN, L., HORVAT, J., ENDERS, A. & JOSEPH, S. 2017. Nanoscale analyses of the surface structure and composition of biochars extracted from field trials or after co-composting using advanced analytical electron microscopy. Geoderma, 294, 70–79. https://doi.org/10.1016/j.geoderma.2017.01.037.

ARCHER, J. R. & SMITH, P. D. 1972. The relation between bulk density, available water capacity, and air capacity of soils. J Soil Sci, 23, 475–480. https://doi.org/10.1111/j.1365-2389.1972.tb01678.x.

ATKINSON, C. J., FITZGERALD, J. D. & HIPPS, N. A. 2010. Potential mechanisms for achieving agricultural benefits from biochar application to temperate soils: a review. Plant Soil, 337, 1–18. https://doi.org/10.1007/s11104-010-0464-5.

AUGUIE, B. & ANTONOV, A. 2017. gridExtra: Miscellaneous Functions for "Grid" Graphics - R package version 2.3. [Online].

AURANGZEIB, M., ZHANG, S., YAN, S., WEI, Z., ZHANG, H., NIU, X. & YAN, P. 2025. Does biochar improve acidic soil physical properties and crop yield under varying climatic and soil conditions? A global comprehensive meta-analysis. Soil Use Manage, 41, e70081. https://doi.org/10.1111/sum.70081.

AZEEM, M., SUN, T.-R., JEYASUNDAR, P. G. S. A., HAN, R.-X., LI, H., ABDELRAHMAN, H., SHAHEEN, S. M., ZHU, Y.-G. & LI, G. 2023. Biochar-derived dissolved organic matter (BDOM) and its influence on soil microbial community composition, function, and activity: A review. Crit Rev Env Sci Tec, 1–23. https://doi.org/10.1080/10643389.2023.2190333.

AZZI, E. S., LI, H., CEDERLUND, H., KARLTUN, E. & SUNDBERG, C. 2024. Modelling biochar long-term carbon storage in soil with harmonized analysis of decomposition data. Geoderma, 441, 116761. https://doi.org/10.1016/j.geoderma.2023.116761.

BAKSHI, S., BANIK, C. & LAIRD, D. A. 2018. Quantification and characterization of chemically-and thermally-labile and recalcitrant biochar fractions. Chemosphere, 194, 247–255. https://doi.org/10.1016/j.chemosphere.2017.11.151.

BAMMINGER, C., MARSCHNER, B. & JÜSCHKE, E. 2014. An incubation study on the stability and biological effects of pyrogenic and hydrothermal biochar in two soils. Eur J Soil Sci, 65, 72–82. https://doi.org/10.1111/ejss.12074.

BASTIDA, F., GARCÍA, C., FIERER, N., ELDRIDGE, D. J., BOWKER, M. A., ABADES, S., ALFARO, F. D., ASEFAW BERHE, A., CUTLER, N. A., GALLARDO, A., GARCÍA-VELÁZQUEZ, L., HART, S. C., HAYES, P. E., HERNÁNDEZ, T., HSEU, Z.-Y., JEHMLICH, N., KIRCHMAIR, M., LAMBERS, H., NEUHAUSER, S., PEÑA-RAMÍREZ, V. M., PÉREZ, C. A., REED, S. C., SANTOS, F., SIEBE, C., SULLIVAN, B. W., TRIVEDI, P., VERA, A., WILLIAMS, M. A., LUIS MORENO, J. & DELGADO-BAQUERIZO, M. 2019. Global ecological predictors of the soil priming effect. Nat Commun, 10, 3481. https://doi.org/10.1038/s41467-019-11472-7.

BATES, D., MÄCHLER, M., BOLKER, B. & WALKER, S. 2015. Fitting linear mixed-effects models using lme4. J Stat Softw, 67, 1 – 48. https://doi.org/10.18637/jss.v067.i01.

BEERLING, D. J., KANTZAS, E. P., LOMAS, M. R., TAYLOR, L. L., ZHANG, S., KANZAKI, Y., EUFRASIO, R. M., RENFORTH, P., MECURE, J.-F., POLLITT, H., HOLDEN, P. B., EDWARDS, N. R., KOH, L., EPIHOV, D. Z., WOLF, A., HANSEN, J. E., BANWART, S. A., PIDGEON, N. F., REINHARD, C. T., PLANAVSKY, N. J. & VAL MARTIN, M. 2025. Transforming US agriculture for carbon removal with enhanced weathering. Nature, 638, 425–434. https://doi.org/10.1038/s41586-024-08429-2.

BEERLING, D. J., KANTZAS, E. P., LOMAS, M. R., WADE, P., EUFRASIO, R. M., RENFORTH, P., SARKAR, B., ANDREWS, M. G., JAMES, R. H., PEARCE, C. R., MERCURE, J.-F., POLLITT, H., HOLDEN, P. B., EDWARDS, N. R., KHANNA, M., KOH, L., QUEGAN, S., PIDGEON, N. F., JANSSENS, I. A., HANSEN, J. & BANWART, S. A. 2020. Potential for large-scale CO_2 removal via enhanced rock weathering with croplands. Nature, 583, 242–248. https://doi.org/10.1038/s41586-020-2448-9.

BEERLING, D. J., LEAKE, J. R., LONG, S. P., SCHOLES, J. D., TON, J., NELSON, P. N., BIRD, M., KANTZAS, E., TAYLOR, L. L., SARKAR, B., KELLAND, M., DELUCIA, E., KANTOLA, I., MÜLLER, C., RAU, G. & HANSEN, J. 2018. Farming with crops and rocks to address global climate, food and soil security. Nature Plants, 4, 138–147. https://doi.org/10.1038/s41477-018-0108-y.

Blagodatskaya, E. & Kuzyakov, Y. 2008. Mechanisms of real and apparent priming effects and their dependence on soil microbial biomass and community structure: critical review. Biol Fert Soils, 45, 115–131. https://doi.org/10.1007/s00374-008-0334-y.

Blanco-Canqui, H. 2017. Biochar and soil physical properties. Soil Sci Soc Am J, 81, 687–711. https://doi.org/10.2136/sssaj2017.01.0017.

Boateng, A., Garcia-Perez, M., Mašek, O., Brown, R. & del Campo, B. 2015. Biochar production technology. *In:* Lehmann, J. & Joseph, S. (eds.) Biochar for environmental Management: Science, technology and implementation. 2nd edition ed. London, UK and New York, USA: Routledge. 10.4324/9780203762264

Brodowski, S., John, B., Flessa, H. & Amelung, W. 2006. Aggregate-occluded black carbon in soil. Eur J Soil Sci, 57, 539–546. https://doi.org/10.1111/j.1365-2389.2006.00807.x.

Bruun, S., Clauson-Kaas, S., Bobuľská, L. & Thomsen, I. K. 2014. Carbon dioxide emissions from biochar in soil: Role of clay, microorganisms and carbonates. Eur J Soil Sci, 65, 52–59. https://doi.org/10.1111/ejss.12073.

Bruun, S., Jensen, E. S. & Jensen, L. S. 2008. Microbial mineralization and assimilation of black carbon: Dependency on degree of thermal alteration. Org Geochem, 39, 839–845. https://doi.org/10.1016/j.orggeochem.2008.04.020.

Burgeon, V., Fouché, J., Leifeld, J., Chenu, C. & Cornélis, J.-T. 2021. Organo-mineral associations largely contribute to the stabilization of century-old pyrogenic organic matter in cropland soils. Geoderma, 388, 114841. https://doi.org/10.1016/j.geoderma.2020.114841.

Burns, R. G., DeForest, J. L., Marxsen, J., Sinsabaugh, R. L., Stromberger, M. E., Wallenstein, M. D., Weintraub, M. N. & Zoppini, A. 2013. Soil enzymes in a changing environment: Current knowledge and future directions. Soil Biol Biochem, 58, 216–234. https://doi.org/10.1016/j.soilbio.2012.11.009.

Buss, W., Hasemer, H., Ferguson, S. & Borevitz, J. 2023. Stabilisation of soil organic matter with rock dust partially counteracted by plants. bioRxiv, https://doi.org/10.1101/2023.06.02.543347. 10.1101/2023.06.02.543347.

Buss, W., Hasemer, H., Ferguson, S. & Borevitz, J. 2024a. Stabilisation of soil organic matter with rock dust partially counteracted by plants. Glob Chang Biol, 30, e17052. https://doi.org/10.1111/gcb.17052.

Buss, W., Hasemer, H., Sokol, N. W., Rohling, E. J. & Borevitz, J. 2024b. Applying minerals to soil to draw down atmospheric carbon dioxide through synergistic organic and inorganic pathways. Commun Earth Environ, 5, 602. https://doi.org/10.1038/s43247-024-01771-3.

Buss, W., Wurzer, C., Manning, D. A. C., Rohling, E. J., Borevitz, J. & Mašek, O. 2022. Mineral-enriched biochar delivers enhanced nutrient recovery and carbon dioxide removal. Commun Earth Environ, 3, 67. https://doi.org/10.1038/s43247-022-00394-w.

Buss, W., Yeates, K., Rohling, E. & Borevitz, J. 2021. Enhancing natural cycles in agro-ecosystems to boost plant carbon capture and soil storage. Oxford Open Climate Change, 1, kgab006. https://doi.org/10.1093/oxfclm/kgab006.

Carson, J. K., Rooney, D., Gleeson, D. B. & Clipson, N. 2007. Altering the mineral composition of soil causes a shift in microbial community structure. FEMS Microbiol Ecol, 61, 414–423. https://doi.org/10.1111/j.1574-6941.2007.00361.x.

CHEN, M., LIU, D., SHAO, X., LI, S., JIN, X., QI, J., LIU, H., LI, C., LI, C. & LI, C. 2024. Effect of biochar types and rates on SOC and its active fractions in tropical farmlands of China. Agronomy*,* 14**,** 676. https://doi.org/10.3390/agronomy14040676.

CHEN, R., SENBAYRAM, M., BLAGODATSKY, S., MYACHINA, O., DITTERT, K., LIN, X., BLAGODATSKAYA, E. & KUZYAKOV, Y. 2014. Soil C and N availability determine the priming effect: microbial N mining and stoichiometric decomposition theories. Glob Chang Biol*,* 20**,** 2356–2367. https://doi.org/10.1111/gcb.12475.

CHEN, Y., SUN, K., YANG, Y. & ZHENG, H. 2023. Effects of biochar on the accumulation of necromass-derived carbon, the physical protection and microbial mineralization of soil organic carbon. Crit Rev Env Sci Tec**,** 1–29. https://doi.org/10.1080/10643389.2023.2221155.

CLOUGH, A. & SKJEMSTAD, J. O. 2000. Physical and chemical protection of soil organic carbon in three agricultural soils with different contents of calcium carbonate. Soil Res*,* 38**,** 1005–1016. https://doi.org/10.1071/SR99102.

CLOUGH, T., CONDRON, L. M., KAMMANN, C. & MÜLLER, C. 2013. A review of biochar and soil nitrogen dynamics. Agronomy*,* 3**,** 275–293. https://doi.org/10.3390/agronomy3020275.

CONANT, R. T., RYAN, M. G., ÅGREN, G. I., BIRGE, H. E., DAVIDSON, E. A., ELIASSON, P. E., EVANS, S. E., FREY, S. D., GIARDINA, C. P., HOPKINS, F. M., HYVÖNEN, R., KIRSCHBAUM, M. U. F., LAVALLEE, J. M., LEIFELD, J., PARTON, W. J., MEGAN STEINWEG, J., WALLENSTEIN, M. D., MARTIN WETTERSTEDT, J. Å. & BRADFORD, M. A. 2011. Temperature and soil organic matter decomposition rates – synthesis of current knowledge and a way forward. Glob Chang Biol*,* 17**,** 3392–3404. https://doi.org/10.1111/j.1365-2486.2011.02496.x.

CONG, L., LU, S., JIANG, P., ZHENG, T., YU, Z. & LÜ, X. 2024. CO_2 sequestration and soil improvement in enhanced rock weathering: A review from an experimental perspective. Greenhouse Gas Sci Technol*,* n/a. https://doi.org/10.1002/ghg.2313.

COSTANZO, S. A., HOLZER, I. O., MOONILALL, N. I., DAVENPORT, A., HOULTON, B. Z. & NOCCO, M. A. 2025. Preliminary assessment of crushed rock, compost, and biochar amendments on soil physical properties. Agric Environ Lett*,* 10**,** e70028. https://doi.org/10.1002/ael2.70028.

CRAINE, J. M., MORROW, C. & FIERER, N. 2007. Microbial nitrogen limitation increasases decomposition. Ecology*,* 88**,** 2105–2113. https://doi.org/10.1890/06-1847.1.

DAI, Z., ZHANG, X., TANG, C., MUHAMMAD, N., WU, J., BROOKES, P. C. & XU, J. 2017. Potential role of biochars in decreasing soil acidification - A critical review. Sci Total Environ*,* 581-582**,** 601–611. https://doi.org/10.1016/j.scitotenv.2016.12.169.

DAVIDSON, E. A. & JANSSENS, I. A. 2006. Temperature sensitivity of soil carbon decomposition and feedbacks to climate change. Nature*,* 440**,** 165–173. https://doi.org/10.1038/nature04514.

DIETZEN, C., HARRISON, R. & MICHELSEN-CORREA, S. 2018. Effectiveness of enhanced mineral weathering as a carbon sequestration tool and alternative to agricultural lime: An incubation experiment. Int J Greenh Gas Con*,* 74**,** 251–258. https://doi.org/10.1016/j.ijggc.2018.05.007.

DIN 2005. DIN 19746:2005-06: Soil quality - Determination of mineral nitrogen (nitrat and ammonium) in soil profiles (N_{min} laboratory method). Berlin, Germany: DIN Media GmbH.

DIN 2014. DIN EN ISO 11274:2014-07: Soil quality - Determination of the water-retention characteristic - Laboratory methods. Berlin, Germany: DIN Media GmbH.

DING, F., VAN ZWIETEN, L., ZHANG, W., WENG, Z., SHI, S., WANG, J. & MENG, J. 2018. A meta-analysis and critical evaluation of influencing factors on soil carbon priming following biochar amendment. J Soil Sediment, 18, 1507–1517. https://doi.org/10.1007/s11368-017-1899-6.

DING, Y., LIU, Y., LIU, S., LI, Z., TAN, X., HUANG, X., ZENG, G., ZHOU, L. & ZHENG, B. 2016. Biochar to improve soil fertility. A review. Agron Sustain Dev, 36, 36. https://doi.org/10.1007/s13593-016-0372-z.

DUPLA, X., ROMANE, C., EMMA, B., IRIS, G., RENÉE-CLAIRE, L. B. & STÉPHANIE, G. 2024. Let the dust settle: Impact of enhanced rock weathering on soil biological, physical, and geochemical fertility. Sci Total Environ, 176297. https://doi.org/10.1016/j.scitotenv.2024.176297.

FANG, Q., LU, A., HONG, H., KUZYAKOV, Y., ALGEO, T. J., ZHAO, L., OLSHANSKY, Y., MORAVEC, B., BARRIENTES, D. M. & CHOROVER, J. 2023. Mineral weathering is linked to microbial priming in the critical zone. Nat Commun, 14, 345. https://doi.org/10.1038/s41467-022-35671-x.

FANG, Y., SINGH, B. & SINGH, B. P. 2015. Effect of temperature on biochar priming effects and its stability in soils. Soil Biol Biochem, 80, 136–145. https://doi.org/10.1016/j.soilbio.2014.10.006.

FANG, Y., SINGH, B., SINGH, B. P. & KRULL, E. 2014. Biochar carbon stability in four contrasting soils. Eur J Soil Sci, 65, 60–71. https://doi.org/10.1111/ejss.12094.

FANG, Y., SINGH, B. P., LUO, Y., BOERSMA, M. & VAN ZWIETEN, L. 2018. Biochar carbon dynamics in physically separated fractions and microbial use efficiency in contrasting soils under temperate pastures. Soil Biol Biochem, 116, 399–409. https://doi.org/10.1016/j.soilbio.2017.10.042.

FAO & UNESCO. 1974. Soil map of the world (Scale 1:5.000.000). Rome, Italy: Food and Agriculture Organization (FAO) of the United Nations.

FIEDLER, H. J. & HEINZE, M. 1990. Bodenfruchtbarkeit. *In:* FIEDLER, H. J. (ed.) Bodennutzung und Bodenschutz. Basel: Birkhäuser Basel. https://doi.org/10.1007/978-3-0348-5625-6_3.

FOUCHÉ, J., BURGEON, V., MEERSMANS, J., LEIFELD, J. & CORNELIS, J.-T. 2023. Accumulation of century-old biochar contributes to carbon storage and stabilization in the subsoil. Geoderma, 440, 116717. https://doi.org/10.1016/j.geoderma.2023.116717.

FUSS, S., LAMB, W. F., CALLAGHAN, M. W., HILAIRE, J., CREUTZIG, F., AMANN, T., BERINGER, T., DE OLIVEIRA GARCIA, W., HARTMANN, J., KHANNA, T., LUDERER, G., NEMET, G. F., ROGELJ, J., SMITH, P., VICENTE, J. L. V., WILCOX, J., DEL MAR ZAMORA DOMINGUEZ, M. & MINX, J. C. 2018. Negative emissions - Part 2: Costs, potentials and side effects. Environ Res Lett, 13, 063002. 10.1088/1748-9326/aabf9f.

GAUDEL, G., POUDEL, M., MOSONGO, P. S., XING, L., OLJIRA, A. M., ZHANG, Y., BIZIMANA, F., LIU, B., WANG, Y., DONG, W., UWAMUNGU, J. Y. & HU, C. 2022. Meta-analysis of the priming effect on native soil organic carbon in response to glucose amendment across soil depths. Plant Soil, 479, 107–124. https://doi.org/10.1007/s11104-021-05168-5.

GHODSZAD, L., REYHANITABAR, A., MAGHSOODI, M. R., ASGARI LAJAYER, B. & CHANG, S. X. 2021. Biochar affects the fate of phosphorus in soil and water: A critical review. Chemosphere, 283, 131176. https://doi.org/10.1016/j.chemosphere.2021.131176.

GLASER, B., HAUMAIER, L., GUGGENBERGER, G. & ZECH, W. 2001. The 'Terra Preta' phenomenon: a model for sustainable agriculture in the humid tropics. Naturwissenschaften, 88, 37–41. https://doi.org/10.1007/s001140000193.

GLASER, B. & LEHR, V.-I. 2019. Biochar effects on phosphorus availability in agricultural soils: A meta-analysis. Sci Rep, 9, 9338. https://doi.org/10.1038/s41598-019-45693-z.

GOLCHIN, A., OADES, J., SKJEMSTAD, J. & CLARKE, P. 1994. Study of free and occluded particulate organic matter in soils by solid state ^{13}C Cp/MAS NMR spectroscopy and scanning electron microscopy. Soil Res, 32, 285–309. https://doi.org/10.1071/SR9940285.

GROSS, A., BROMM, T. & GLASER, B. 2021. Soil organic carbon sequestration after biochar application: A global meta-analysis. Agronomy, 11, 2474. https://doi.org/10.3390/agronomy11122474.

GRUNWALD, D., KAISER, M., JUNKER, S., MARHAN, S., PIEPHO, H.-P., POLL, C., BAMMINGER, C. & LUDWIG, B. 2017. Influence of elevated soil temperature and biochar application on organic matter associated with aggregate-size and density fractions in an arable soil. Agr Ecosyst Environ, 241, 79–87. https://doi.org/10.1016/j.agee.2017.02.029.

HAGEMANN, N., SCHMIDT, H.-P., BUCHELI, T. D., GRAFMÜLLER, J., VOSSWINKEL, S., HERDEGEN, V., MEREDITH, W., UGUNA, C. N. & SNAPE, C. E. 2025. Proxies for use in biochar decay models: Hydropyrolysis, electric conductivity, and H/C_{org} molar ratio. PLoS ONE, 20, e0330206. https://doi.org/10.1371/journal.pone.0330206.

HAGEMANN, N., SPOKAS, K., SCHMIDT, H.-P., KÄGI, R., BÖHLER, M. A. & BUCHELI, T. D. 2018. Activated carbon, biochar and charcoal: Linkages and synergies across pyrogenic carbon's ABCs. Water, 10, 182. https://doi.org/10.3390/w10020182

HAMER, U., MARSCHNER, B., BRODOWSKI, S. & AMELUNG, W. 2004. Interactive priming of black carbon and glucose mineralisation. Org Geochem, 35, 823–830. https://doi.org/10.1016/j.orggeochem.2004.03.003.

HAMMES, J. S., HARTMANN, J., BARTH, J. A. C., LINKE, T., SMET, I., HAGENS, M., POGGE VON STRANDMANN, P. A. E., REERSHEMIUS, T., CASIMIRO, B., VIENNE, A., STOECKEL, A. A., STEFFENS, R. & PAESSLER, D. 2025. Soil processes govern alkalinity and cation retention in enhanced weathering for carbon dioxide removal - *preprint*. EGUsphere, 2025, 1–40. https://doi.org/10.5194/egusphere-2025-5402.

HAN, L., SUN, K., YANG, Y., XIA, X., LI, F., YANG, Z. & XING, B. 2020. Biochar's stability and effect on the content, composition and turnover of soil organic carbon. Geoderma, 364, 114184. https://doi.org/10.1016/j.geoderma.2020.114184.

HARLEY, A. D. & GILKES, R. J. 2000. Factors influencing the release of plant nutrient elements from silicate rock powders: a geochemical overview. Nutr Cycl Agroecosys, 56, 11–36. https://doi.org/10.1023/A:1009859309453.

HARTMANN, J., WEST, A. J., RENFORTH, P., KÖHLER, P., DE LA ROCHA, C. L., WOLF-GLADROW, D. A., DÜRR, H. H. & SCHEFFRAN, J. 2013. Enhanced chemical weathering as a geoengineering strategy to reduce atmospheric carbon dioxide, supply nutrients, and mitigate ocean acidification. Rev Geophys, 51, 113–149. https://doi.org/10.1002/rog.20004.

HERATH, H. M. S. K., CAMPS-ARBESTAIN, M., HEDLEY, M., VAN HALE, R. & KAAL, J. 2014. Fate of biochar in chemically- and physically-defined soil organic carbon pools. Org Geochem, 73, 35–46. https://doi.org/10.1016/j.orggeochem.2014.05.001.

HERATH, H. M. S. K., CAMPS-ARBESTAIN, M., HEDLEY, M. J., KIRSCHBAUM, M. U. F., WANG, T. & VAN HALE, R. 2015. Experimental evidence for sequestering C with biochar by avoidance of CO_2 emissions from original feedstock and protection of native soil organic matter. GCB Bioenergy, 7, 512–526. https://doi.org/10.1111/gcbb.12183.

HONVAULT, N., TIOUCHICHINE, M.-L., SAUZE, J., PIEL, C., LANDAIS, D., DEVIDAL, S., GRITTI, E., BOSCH, D. & MILCU, A. 2024. Additive effects of basalt enhanced weathering and biochar co-application on carbon sequestration, soil nutrient status and plant performance in a mesocosm experiment. Appl Geochem, 169, 106054. https://doi.org/10.1016/j.apgeochem.2024.106054.

HOTHORN, T., BRETZ, F. & WESTFALL, P. 2008. Simultaneous inference in general parametric models. Biometrical J, 50, 346–363. https://doi.org/10.1002/bimj.200810425.

IBRAHIMI, K. & ALGHAMDI, A. G. 2022. Available water capacity of sandy soils as affected by biochar application: A meta-analysis. CATENA, 214, 106281. https://doi.org/10.1016/j.catena.2022.106281.

IDEN, S. C. & DURNER, W. 2014. Comment on "Simple consistent models for water retention and hydraulic conductivity in the complete moisture range" by A. Peters. Water Resour Res, 50, 7530–7534. https://doi.org/10.1002/2014WR015937.

IPCC 2023. Section 2 - Current status and trends. *In:* IPCC (ed.) Climate Change 2023: Synthesis Report. Contribution of Working Groups I, II and III to the Sixth Assessment Report of the Intergovernmental Panel on Climate Change. Geneva, Switzerland. https://doi.org/10.59327/IPCC/AR6-9789291691647.

IPPOLITO, J. A., CUI, L., KAMMANN, C., WRAGE-MÖNNIG, N., ESTAVILLO, J. M., FUERTES-MENDIZABAL, T., CAYUELA, M. L., SIGUA, G., NOVAK, J., SPOKAS, K. & BORCHARD, N. 2020. Feedstock choice, pyrolysis temperature and type influence biochar characteristics: A comprehensive meta-data analysis review. Biochar, 2, 421–438. https://doi.org/10.1007/s42773-020-00067-x.

IUSS WORKING GROUP WRB 2022. World reference base (WRB) for soil resources - International soil classification system for naming soils and creation legends for soil maps. Vienna, Austria., International Union of Soil Sciences (IUSS).

JEFFERY, S., ABALOS, D., PRODANA, M., BASTOS, A., VAN GROENIGEN, J. W., HUNGATE, B. & VERHEIJEN, F. 2017. Biochar boosts tropical but not temperate crop yields. Environ Res Lett, 12. 10.1088/1748-9326/aa67bd.

JEFFERY, S., VERHEIJEN, F. G. A., VAN DER VELDE, M. & BASTOS, A. C. 2011. A quantitative review of the effects of biochar application to soils on crop productivity using meta-analysis. Agr Ecosyst Environ, 144, 175–187. https://doi.org/10.1016/j.agee.2011.08.015.

JIN, X., ZHANG, T., HOU, Y., BOL, R., ZHANG, X., ZHANG, M., YU, N., MENG, J., ZOU, H. & WANG, J. 2024. Review on the effects of biochar amendment on soil microorganisms and enzyme activity. J Soil Sediment. https://doi.org/10.1007/s11368-024-03841-7.

JIN, Y., LIANG, X., HE, M., LIU, Y., TIAN, G. & SHI, J. 2016. Manure biochar influence upon soil properties, phosphorus distribution and phosphatase activities: A microcosm incubation study. Chemosphere, 142, 128–135. https://doi.org/10.1016/j.chemosphere.2015.07.015.

JOERGENSEN, R. G. 1996. The fumigation-extraction method to estimate soil microbial biomass: Calibration of the k_{EC} value. Soil Biol Biochem, 28, 25–31. https://doi.org/10.1016/0038-0717(95)00102-6.

JOSEPH, S., COWIE, A. L., VAN ZWIETEN, L., BOLAN, N., BUDAI, A., BUSS, W., CAYUELA, M. L., GRABER, E. R., IPPOLITO, J. A., KUZYAKOV, Y., LUO, Y., OK, Y. S., PALANSOORIYA, K. N., SHEPHERD, J., STEPHENS, S., WENG, Z. & LEHMANN, J. 2021. How biochar works, and when it doesn't: A review of mechanisms controlling soil and plant responses to biochar. GCB Bioenergy, 13, 1731–1764. https://doi.org/10.1111/gcbb.12885.

JOSEPH, S. D., CAMPS-ARBESTAIN, M., LIN, Y., MUNROE, P., CHIA, C. H., HOOK, J., VAN ZWIETEN, L., KIMBER, S., COWIE, A., SINGH, B. P., LEHMANN, J., FOIDL, N., SMERNIK, R. J. & AMONETTE, J. E. 2010. An investigation into the reactions of biochar in soil. Soil Res, 48, 501–515. https://doi.org/10.1071/SR10009.

JUST, C., POEPLAU, C., DON, A., VAN WESEMAEL, B., KÖGEL-KNABNER, I. & WIESMEIER, M. 2021. A simple approach to isolate slow and fast cycling organic carbon fractions in central european soils — Importance of dispersion method. Front Soil Sci, Volume 1 - 2021. https://doi.org/10.3389/fsoil.2021.692583.

KAHNT, G., PFLEIDERER, H. & HIJAZI, L. A. 1986. Wirkungen meliorativer Gaben von Gesteinsmehlen und Gesteinssanden auf das Wachstum verschiedener landwirtschaftlicher Kulturpflanzen sowie auf physikalische Kennwerte eines Sandbodens und eines Tonbodens. J Agron Crop Sci, 157, 169–180. https://doi.org/10.1111/j.1439-037X.1986.tb00064.x.

KALU, S., SEPPÄNEN, A., MGANGA, K. Z., SIETIÖ, O.-M., GLASER, B. & KARHU, K. 2024. Biochar reduced the mineralization of native and added soil organic carbon: evidence of negative priming and enhanced microbial carbon use efficiency. Biochar, 6, 7. https://doi.org/10.1007/s42773-023-00294-y.

KEMMITT, S. J., WRIGHT, D., GOULDING, K. W. T. & JONES, D. L. 2006. pH regulation of carbon and nitrogen dynamics in two agricultural soils. Soil Biol Biochem, 38, 898–911. https://doi.org/10.1016/j.soilbio.2005.08.006.

KLEBER, M., EUSTERHUES, K., KEILUWEIT, M., MIKUTTA, C., MIKUTTA, R. & NICO, P. S. 2015. Chapter One - Mineral–organic associations: Formation, properties, and relevance in soil environments. *In:* SPARKS, D. L. (ed.) Advances in Agronomy. London: Academic Press. https://doi.org/10.1016/bs.agron.2014.10.005.

KUZYAKOV, Y. 2010. Priming effects: Interactions between living and dead organic matter. Soil Biol Biochem, 42, 1363–1371. https://doi.org/10.1016/j.soilbio.2010.04.003.

KUZYAKOV, Y. 2011. How to link soil C pools with CO_2 fluxes? Biogeosciences, 8, 1523–1537. https://doi.org/10.5194/bg-8-1523-2011.

KUZYAKOV, Y., BOGOMOLOVA, I. & GLASER, B. 2014. Biochar stability in soil: Decomposition during eight years and transformation as assessed by compound-specific ^{14}C analysis. Soil Biol Biochem, 70, 229–236. https://doi.org/10.1016/j.soilbio.2013.12.021.

KUZYAKOV, Y., FRIEDEL, J. K. & STAHR, K. 2000. Review of mechanisms and quantification of priming effects. Soil Biol Biochem, 32, 1485–1498. https://doi.org/10.1016/S0038-0717(00)00084-5.

KUZYAKOV, Y., SUBBOTINA, I., CHEN, H., BOGOMOLOVA, I. & XU, X. 2009. Black carbon decomposition and incorporation into soil microbial biomass estimated by ^{14}C labeling. Soil Biol Biochem, 41, 210–219. https://doi.org/10.1016/j.soilbio.2008.10.016.

LAIRD, D. & ROGOVSKA, N. 2015. Biochar effects on nutrient leaching. *In:* LEHMANN, J. & JOSEPH, S. (eds.) Biochar for environmental management. London, United Kingdom.

LAMMIRATO, C., MILTNER, A. & KAESTNER, M. 2011. Effects of wood char and activated carbon on the hydrolysis of cellobiose by β-glucosidase from *Aspergillus niger*. Soil Biol Biochem, 43, 1936–1942. https://doi.org/10.1016/j.soilbio.2011.05.021.

LAVALLEE, J. M., SOONG, J. L. & COTRUFO, M. F. 2020. Conceptualizing soil organic matter into particulate and mineral-associated forms to address global change in the 21st century. Glob Chang Biol*,* 26**,** 261–273. https://doi.org/10.1111/gcb.14859.

LBEG. 2017. Bodenkarte von Niedersachsen 1 : 50 000. Hannover, Germany: Landesamt für Bergbau Energie und Geologie (LBEG)

LEHMANN, J., ABIVEN, S., KLEBER, M., PAN, G., SINGH, B. P., SOHI, S. P. & ZIMMERMAN, A. R. 2015. Persistence of biochar in soil. *In:* LEHMANN, J. & JOSEPH, S. (eds.) Biochar for environmental management. London, United Kingdom.

LEHMANN, J., COWIE, A., MASIELLO, C. A., KAMMANN, C., WOOLF, D., AMONETTE, J. E., CAYUELA, M. L., CAMPS-ARBESTAIN, M. & WHITMAN, T. 2021. Biochar in climate change mitigation. Nat Geosci*,* 14**,** 883–892. https://doi.org/10.1038/s41561-021-00852-8.

LEHMANN, J., CZIMCZIK, C. I., LAIRD, D. & SOHI, S. P. 2009. Stability of biochar in the soil. *In:* LEHMANN, J. & JOSEPH, S. (eds.) Biochar for environmental management: Science and Technology. London, United Kingdom.

LEHMANN, J. & JOSEPH, S. 2024. Biochar for environmental management: An introduction. *In:* LEHMANN, J. & JOSEPH, S. (eds.) Biochar for environmental management: Science, technology and implementation. 3rd edition ed. London, United Kingdom: Routledge. 10.4324/9780203762264

LEHMANN, J., RILLIG, M. C., THIES, J., MASIELLO, C. A., HOCKADAY, W. C. & CROWLEY, D. 2011. Biochar effects on soil biota – A review. Soil Biol Biochem*,* 43**,** 1812–1836. https://doi.org/10.1016/j.soilbio.2011.04.022.

LEI, K., BUCKA, F. B., TEIXEIRA, P. P. C., BUEGGER, F., JUST, C. & KÖGEL-KNABNER, I. 2025. Balancing organic and inorganic carbon dynamics in enhanced rock weathering: Implications for carbon sequestration. Glob Chang Biol*,* 31**,** e70186. https://doi.org/10.1111/gcb.70186.

LENG, L. & HUANG, H. 2018. An overview of the effect of pyrolysis process parameters on biochar stability. Bioresour Technol*,* 270**,** 627–642. https://doi.org/10.1016/j.biortech.2018.09.030.

LENG, L., XU, X., WEI, L., FAN, L., HUANG, H., LI, J., LU, Q., LI, J. & ZHOU, W. 2019. Biochar stability assessment by incubation and modelling: Methods, drawbacks and recommendations. Sci Total Environ*,* 664**,** 11–23. https://doi.org/10.1016/j.scitotenv.2019.01.298.

LENTH, R. V., PIASKOWSKI, J., BANFAI, B., BOLKER, B., BUERKNER, P., GINÉ-VÁZQUEZ, I., HERVÉ, M., JUNG, M., LOVE, J., MIGUEZ, F., RIEBL, H. & SINGMANN, H. 2025. emmeans: Estimated Marginal Means, aka Least-Squares Means - R package version 1.1.4. [Online].

LFU. 2025. UmweltAtlas Bayern - Bodenübersichtskarte 1:25.000. Augsburg, Germany: Bayerisches Landesamt für Umwelt (LfU).

LI, Z.-B., LI, G., ADAMS, J. M., GUAN, D.-X., ZHAO, L., BIAN, R., HU, Q., LU, X., JI, J. & CHEN, J. 2025. Atmospheric CO_2 removal efficiency through enhanced silicate weathering in croplands: A review with emphasis on the contribution of fungi. J Earth Sci*,* 36**,** 197–211. https://doi.org/10.1007/s12583-024-0101-5.

LIANG, B., LEHMANN, J., SOLOMON, D., KINYANGI, J., GROSSMAN, J., O'NEILL, B., SKJEMSTAD, J. O., THIES, J., LUIZÃO, F. J., PETERSEN, J. & NEVES, E. G. 2006. Black carbon increases cation exchange capacity in soils. Soil Sci Soc Am J*,* 70**,** 1719–1730. https://doi.org/10.2136/sssaj2005.0383.

LIU, S., ZHANG, Y., ZONG, Y., HU, Z., WU, S., ZHOU, J., JIN, Y. & ZOU, J. 2015. Response of soil carbon dioxide fluxes, soil organic carbon and microbial biomass carbon to biochar amendment: a meta-analysis. GCB Bioenergy, 8, 392–406. https://doi.org/10.1111/gcbb.12265.

LIU, Z., WU, X., LIU, W., BIAN, R., GE, T., ZHANG, W., ZHENG, J., DROSOS, M., LIU, X., ZHANG, X., CHENG, K., LI, L. & PAN, G. 2020. Greater microbial carbon use efficiency and carbon sequestration in soils: Amendment of biochar versus crop straws. GCB Bioenergy, 12, 1092–1103. https://doi.org/10.1111/gcbb.12763.

LUGATO, E., LAVALLEE, J. M., HADDIX, M. L., PANAGOS, P. & COTRUFO, M. F. 2021. Different climate sensitivity of particulate and mineral-associated soil organic matter. Nat Geosci, 14, 295–300. 10.1038/s41561-021-00744-x.

LUO, L., MENG, H. & GU, J.-D. 2017a. Microbial extracellular enzymes in biogeochemical cycling of ecosystems. J Environ Manage, 197, 539–549. https://doi.org/10.1016/j.jenvman.2017.04.023.

LUO, Y., DURENKAMP, M., DE NOBILI, M., LIN, Q. & BROOKES, P. C. 2011. Short term soil priming effects and the mineralisation of biochar following its incorporation to soils of different pH. Soil Biol Biochem, 43, 2304–2314. https://doi.org/10.1016/j.soilbio.2011.07.020.

LUO, Y., ZANG, H., YU, Z., CHEN, Z., GUNINA, A., KUZYAKOV, Y., XU, J., ZHANG, K. & BROOKES, P. C. 2017b. Priming effects in biochar enriched soils using a three-source-partitioning approach: ^{14}C labelling and ^{13}C natural abundance. Soil Biol Biochem, 106, 28–35. https://doi.org/10.1016/j.soilbio.2016.12.006.

MAESTRINI, B., NANNIPIERI, P. & ABIVEN, S. 2015. A meta-analysis on pyrogenic organic matter induced priming effect. GCB Bioenergy, 7, 577–590. https://doi.org/10.1111/gcbb.12194.

MALIK, A. A., CHOWDHURY, S., SCHLAGER, V., OLIVER, A., PUISSANT, J., VAZQUEZ, P. G. M., JEHMLICH, N., VON BERGEN, M., GRIFFITHS, R. I. & GLEIXNER, G. 2016. Soil fungal:bacterial ratios are linked to altered carbon cycling. Front Microbiol, Volume 7 - 2016. https://doi.org/10.3389/fmicb.2016.01247.

MANNING, D. A. C., DE AZEVEDO, A. C., ZANI, C. F. & BARNEZE, A. S. 2024. Soil carbon management and enhanced rock weathering: The separate fates of organic and inorganic carbon. Eur J Soil Sci, 75, e13534. https://doi.org/10.1111/ejss.13534.

MANZONI, S. & COTRUFO, M. F. 2024. Mechanisms of soil organic carbon and nitrogen stabilization in mineral-associated organic matter – Insights from modeling in phase space. Biogeosciences, 21, 4077–4098. https://doi.org/10.5194/bg-21-4077-2024.

MARTIN, J. B. 2017. Carbonate minerals in the global carbon cycle. Chem Geol, 449, 58–72. https://doi.org/10.1016/j.chemgeo.2016.11.029.

MARX, M. C., WOOD, M. & JARVIS, S. C. 2001. A microplate fluorimetric assay for the study of enzyme diversity in soils. Soil Biol Biochem, 33, 1633–1640. https://doi.org/10.1016/S0038-0717(01)00079-7.

MEYER ZU DREWER, J., VORRATH, M.-E., AMANN, T., HARTMANN, J., DE LA ROSA, J. M., MÖLLMER, J., PÉREZ-DALÍ, S. M., MEREDITH, W., UGUNA, C., SNAPE, C., KAMMANN, C., SCHMIDT, H.-P. & HAGEMANN, N. 2025. Pyrogenic carbon and carbonating minerals for carbon capture and storage (PyMiCCS) part I: production, physico-chemical characterization and C-sink potential. Front Clim, 7 2025. https://doi.org/10.3389/fclim.2025.1631368.

MICHAELIS, L. & MENTEN, M. L. 1913. Die Kinetik der Invertinwirkung. Biochemische Zeitschrift, 333–369.

MUKHERJEE, A. & ZIMMERMAN, A. R. 2013. Organic carbon and nutrient release from a range of laboratory-produced biochars and biochar–soil mixtures. Geoderma, 193-194, 122–130. https://doi.org/10.1016/j.geoderma.2012.10.002.

MUNERA-ECHEVERRI, J. L., MARTINSEN, V., STRAND, L. T., ZIVANOVIC, V., CORNELISSEN, G. & MULDER, J. 2018. Cation exchange capacity of biochar: An urgent method modification. Sci Total Environ, 642, 190–197. https://doi.org/10.1016/j.scitotenv.2018.06.017.

OELKERS, E. H., DECLERCQ, J., SALDI, G. D., GISLASON, S. R. & SCHOTT, J. 2018. Olivine dissolution rates: A critical review. Chem Geol, 500, 1–19. https://doi.org/10.1016/j.chemgeo.2018.10.008.

PAETSCH, L., MUELLER, C. W., RUMPEL, C., ANGST, Š., WIESHEU, A. C., GIRARDIN, C., IVLEVA, N. P., NIESSNER, R. & KÖGEL-KNABNER, I. 2017. A multi-technique approach to assess the fate of biochar in soil and to quantify its effect on soil organic matter composition. Org Geochem, 112, 177–186. https://doi.org/10.1016/j.orggeochem.2017.06.012.

PETERS, A. 2014. Reply to comment by S. Iden and W. Durner on "Simple consistent models for water retention and hydraulic conductivity in the complete moisture range". Water Resour Res, 50, 7535–7539. https://doi.org/10.1002/2014WR016107.

PLANTE, A. F., FERNÁNDEZ, J. M., HADDIX, M. L., STEINWEG, J. M. & CONANT, R. T. 2011. Biological, chemical and thermal indices of soil organic matter stability in four grassland soils. Soil Biol Biochem, 43, 1051–1058. https://doi.org/10.1016/j.soilbio.2011.01.024.

QIU, H., HU, Z., LIU, J., ZHANG, H. & SHEN, W. 2023. Effect of biochar on labile organic carbon fractions and soil carbon pool management index. Agronomy, 13, 1385. https://doi.org/10.3390/agronomy13051385.

RASMUSSEN, C., SOUTHARD, R. J. & HORWATH, W. R. 2006. Mineral control of organic carbon mineralization in a range of temperate conifer forest soils. Glob Chang Biol, 12, 834–847. https://doi.org/10.1111/j.1365-2486.2006.01132.x.

RATHNAYAKE, D., SCHMIDT, H.-P., LEIFELD, J., BÜRGE, D., BUCHELI, T. D. & HAGEMANN, N. 2024. Quantifying soil organic carbon after biochar application: how to avoid (the risk of) counting CDR twice? Front Clim, 6. https://doi.org/10.3389/fclim.2024.1343516.

RAZZAGHI, F., OBOUR, P. B. & ARTHUR, E. 2020. Does biochar improve soil water retention? A systematic review and meta-analysis. Geoderma, 361, 114055. https://doi.org/10.1016/j.geoderma.2019.114055.

RECHBERGER, M. V., KLOSS, S., RENNHOFER, H., TINTNER, J., WATZINGER, A., SOJA, G., LICHTENEGGER, H. & ZEHETNER, F. 2017. Changes in biochar physical and chemical properties: Accelerated biochar aging in an acidic soil. Carbon, 115, 209–219. https://doi.org/10.1016/j.carbon.2016.12.096.

REGINATO, P. L. 2025. Biotechnology in direct air capture, enhanced weathering, and methane removal: Emerging opportunities and gaps. Front Clim, 6. https://doi.org/10.3389/fclim.2024.1440833

REICHENBACH, M., FIENER, P., GARLAND, G., GRIEPENTROG, M., SIX, J. & DOETTERL, S. 2021. The role of geochemistry in organic carbon stabilization against microbial decomposition in tropical rainforest soils. SOIL, 7, 453–475. https://doi.org/10.5194/soil-7-453-2021.

RENFORTH, P. 2012. The potential of enhanced weathering in the UK. Int J Greenh Gas Control, 10, 229–243. https://doi.org/10.1016/j.ijggc.2012.06.011.

RIAHI, K., SCHAEFFER, R., ARANGO, J., CALVIN, K., GUIVARCH, C., HASEGAWA, T., JIANG, K., KRIEGLER, E., R. MATTHEWS, PETERS, G. P., RAO, A., ROBERTSON, S., SEBBIT, A. M., STEINBERGER, J., TAVONI, M. & VAN VUURE, D. P. 2022. Mitigation pathways compatible with long-term goals. *In:* P.R. SHUKLA, SKEA, J., SLADE, R., AL KHOURDAJIE, A., VAN DIEMEN, R., MCCOLLUM, D., PATHAK, M., SOME, S., VYAS, P., FRADERA, R., BELKACEMI, M., HASIJA, A., LISBOA, G., LUZ, S. & MALLEY, J. (eds.) IPCC, 2022: Climate Change 2022: Mitigation of Climate Change. Contribution of Working Group III to the Sixth Assessment Report of the Intergovernmental Panel on Climate Change. Cambridge, UK and New York, NY, USA: Cambridge University Press. https://doi.org/10.1017/9781009157926.005.

RICHARDSON, J. B. 2025. Basalt rock dust amendment on soil health properties and inorganic nutrients — Laboratory and field study at two organic farm soils in New England, USA. Agriculture*,* 15**,** 52. https://doi.org/10.3390/agriculture15010052.

RITCHIE, J. T. 1981. Water dynamics in the soil-plant-atmosphere system. Plant Soil*,* 58**,** 81–96. https://doi.org/10.1007/BF02180050.

SANEI, H., PETERSEN, H. I., CHIARAMONTI, D. & MASEK, O. 2025. Evaluating the two-pool decay model for biochar carbon permanence. Biochar*,* 7**,** 9. https://doi.org/10.1007/s42773-024-00408-0.

SCHIEDUNG, M., BELLÈ, S. L., SIGMUND, G., KALBITZ, K. & ABIVEN, S. 2020. Vertical mobility of pyrogenic organic matter in soils: a column experiment. Biogeosciences*,* 17**,** 6457–6474. https://doi.org/10.5194/bg-17-6457-2020.

SCHIEDUNG, M., HARRINGTON, K. J., DUPLA, X., MÖLLER, B., FACQ, E., SWEERE, T., DON, A., HILTON, R. G., DOETTERL, S. & HEMINGWAY, J. D. 2026. Uncertainties of enhanced rock weathering for climate-change mitigation. Nat Rev Earth Environ. https://doi.org/10.1038/s43017-026-00761-7.

SCHIMEL, J. 2013. Soil carbon: Microbes and global carbon. Nat Clim Change*,* 3**,** 867–868. https://doi.org/10.1038/nclimate2015.

SCHIMEL, J., BALSER, T. C. & WALLENSTEIN, M. 2007. Microbial stress-response physiology and its implications for ecosystem function. Ecology*,* 88**,** 1386–1394. https://doi.org/10.1890/06-0219.

SCHIMEL, J. & SCHAEFFER, S. M. 2012. Microbial control over carbon cycling in soil. Front Microbiol*,* Volume 3 - 2012. https://doi.org/10.3389/fmicb.2012.00348.

SCHMIDT, H.-P., ABIVEN, S., COWIE, A., GLASER, B., JOSEPH, S., KAMMANN, C., LEHMANN, J., LEIFELD, J., PAN, G., RASSE, D., RUMPEL, C., WOOLF, D., ZIMMERMAN, A. R. & HAGEMANN, N. 2025. Biochar permanence — A policy commentary. GCB Bioenergy*,* 17**,** e70092. https://doi.org/10.1111/gcbb.70092.

SCHWEIZER, S. A., BUCKA, F. B., GRAF-ROSENFELLNER, M. & KÖGEL-KNABNER, I. 2019. Soil microaggregate size composition and organic matter distribution as affected by clay content. Geoderma*,* 355**,** 113901. https://doi.org/10.1016/j.geoderma.2019.113901.

SHEPHERD, J. G., JOSEPH, S., SOHI, S. P. & HEAL, K. V. 2017. Biochar and enhanced phosphate capture: Mapping mechanisms to functional properties. Chemosphere*,* 179**,** 57–74. https://doi.org/10.1016/j.chemosphere.2017.02.123.

SHI, W. 2011. Agricultural and ecological significance of soil enzymes: Soil carbon sequestration and nutrient cycling. *In:* SHUKLA, G. & VARMA, A. (eds.) Soil enzymology. Berlin, Heidelberg: Springer Berlin Heidelberg. https://doi.org/10.1007/978-3-642-14225-3_3.

SINGH, J. S. & GUPTA, V. K. 2018. Soil microbial biomass: A key soil driver in management of ecosystem functioning. Sci Total Environ*,* 634**,** 497–500. https://doi.org/10.1016/j.scitotenv.2018.03.373.

SINGH, N., ABIVEN, S., MAESTRINI, B., BIRD, J. A., TORN, M. S. & SCHMIDT, M. W. I. 2014. Transformation and stabilization of pyrogenic organic matter in a temperate forest field experiment. Glob Chang Biol*,* 20**,** 1629–1642. https://doi.org/10.1111/gcb.12459.

SINSABAUGH, R. L., LAUBER, C. L., WEINTRAUB, M. N., AHMED, B., ALLISON, S. D., CRENSHAW, C., CONTOSTA, A. R., CUSACK, D., FREY, S., GALLO, M. E., GARTNER, T. B., HOBBIE, S. E., HOLLAND, K., KEELER, B. L., POWERS, J. S., STURSOVA, M., TAKACS-VESBACH, C., WALDROP, M. P., WALLENSTEIN, M. D., ZAK, D. R. & ZEGLIN, L. H. 2008. Stoichiometry of soil enzyme activity at global scale. Ecol Lett*,* 11**,** 1252–1264. https://doi.org/10.1111/j.1461-0248.2008.01245.x.

SMITH, S. M., GEDEN, O., GIDDEN, M. J., LAMB, W. F., NEMET, G. F., MINX, J. C., BUCK, H., BURKE, J., COX, E., EDWARDS, M. R., FUSS, S., JOHNSTONE, I., MÜLLER-HANSEN, F., PONGRATZ, J., PROBST, B. S., ROE, S., SCHENUIT, F., SCHULTE, I. & VAUGHAN, N. E. E. 2024. The state of carbon dioxide removal - 2nd Edition. The State of Carbon Dioxide Removal.

SOHNG, J., SOKOL, N. W., WHITEAKER, S., SCHMIDT, R., HOLZER, I., GOERTZEN, H., PEÑA, J., HOULTON, B. Z., MONTAÑEZ, I., O'GEEN, A. & SCOW, K. 2025. Combining organic amendments with enhanced rock weathering shifts soil carbon storage in croplands. Sci Total Environ*,* 998**,** 180179. https://doi.org/10.1016/j.scitotenv.2025.180179.

SOKOL, N. W., SOHNG, J., MORELAND, K., SLESSAREV, E., GOERTZEN, H., SCHMIDT, R., SAMADDAR, S., HOLZER, I., ALMARAZ, M., GEOGHEGAN, E., HOULTON, B., MONTAÑEZ, I., PETT-RIDGE, J. & SCOW, K. 2024. Reduced accrual of mineral-associated organic matter after two years of enhanced rock weathering in cropland soils, though no net losses of soil organic carbon. Biogeochemistry. https://doi.org/10.1007/s10533-024-01160-0.

SOLLINS, P., HOMANN, P. & CALDWELL, B. A. 1996. Stabilization and destabilization of soil organic matter: Mechanisms and controls. Geoderma*,* 74**,** 65–105. https://doi.org/10.1016/S0016-7061(96)00036-5.

STEINER, C., TEIXEIRA, W. G., LEHMANN, J., NEHLS, T., DE MACÊDO, J. L. V., BLUM, W. E. H. & ZECH, W. 2007. Long term effects of manure, charcoal and mineral fertilization on crop production and fertility on a highly weathered Central Amazonian upland soil. Plant Soil*,* 291**,** 275–290. https://doi.org/10.1007/s11104-007-9193-9.

SWOBODA, P., DÖRING, T. F. & HAMER, M. 2022. Remineralizing soils? The agricultural usage of silicate rock powders: A review. Sci Total Environ*,* 807**,** 150976. https://doi.org/10.1016/j.scitotenv.2021.150976.

TE PAS, E. E. E. M., COMANS, R. N. J., BISSELING, S. & HAGENS, M. 2026. Enhanced weathering and biochar co-deployment boosts CO_2 sequestration through changing soil properties. Geoderma*,* 466**,** 117668. https://doi.org/10.1016/j.geoderma.2025.117668.

VAN ZWIETEN, L., KIMBER, S., MORRIS, S., CHAN, K. Y., DOWNIE, A., RUST, J., JOSEPH, S. & COWIE, A. 2010. Effects of biochar from slow pyrolysis of papermill waste on agronomic performance and soil fertility. Plant Soil*,* 327**,** 235–246. https://doi.org/10.1007/s11104-009-0050-x.

VANCE, E. D., BROOKES, P. C. & JENKINSON, D. S. 1987. An extraction method for measuring soil microbial biomass C. Soil Biol Biochem, 19, 703–707. https://doi.org/10.1016/0038-0717(87)90052-6.

VAUGHN, S. F., KENAR, J. A., THOMPSON, A. R. & PETERSON, S. C. 2013. Comparison of biochars derived from wood pellets and pelletized wheat straw as replacements for peat in potting substrates. Ind Crops Prod, 51, 437–443. https://doi.org/10.1016/j.indcrop.2013.10.010.

VDLUFA 1991. Bestimmung von Phosphor und Kalium im Doppellactat(DL)-Auszug. Methodenbuch Band I Böden. Speyer, Germany: Verband Deutscher Landwirtschaftlicher Untersuchungs- und Forschungsanstalten e.V. (VDLUFA).

VICCA, S., GOLL, D. S., HAGENS, M., HARTMANN, J., JANSSENS, I. A., NEUBECK, A., PEÑUELAS, J., POBLADOR, S., RIJNDERS, J., SARDANS, J., STRUYF, E., SWOBODA, P., VAN GROENIGEN, J. W., VIENNE, A. & VERBRUGGEN, E. 2022. Is the climate change mitigation effect of enhanced silicate weathering governed by biological processes? Glob Chang Biol, 28, 711–726. https://doi.org/10.1111/gcb.15993.

VIRET, F. & GRAND, S. 2019. Combined size and density fractionation of soils for investigations of organo-mineral interactions. JoVE, e58927. https://doi.org/10.3791/58927.

VON LÜTZOW, M., KÖGEL-KNABNER, I., EKSCHMITT, K., MATZNER, E., GUGGENBERGER, G., MARSCHNER, B. & FLESSA, H. 2006. Stabilization of organic matter in temperate soils: mechanisms and their relevance under different soil conditions – a review. Eur J Soil Sci, 57, 426–445. https://doi.org/10.1111/j.1365-2389.2006.00809.x.

VON LÜTZOW, M., KÖGEL-KNABNER, I., LUDWIG, B., MATZNER, E., FLESSA, H., EKSCHMITT, K., GUGGENBERGER, G., MARSCHNER, B. & KALBITZ, K. 2008. Stabilization mechanisms of organic matter in four temperate soils: Development and application of a conceptual model. J Plant Nutr Soil Sc, 171, 111–124. https://doi.org/10.1002/jpln.200700047.

VORRATH, M.-E., AMANN, T., MEYER ZU DREWER, J., HAGEMANN, N., ALDRICH, C., BÖRKER, J., SEEDTKE, M., BECKER, J. N., HAGENS, M., ESCHENBACH, A. & HARTMANN, J. 2025. Pyrogenic carbon and carbonating minerals for carbon capture and storage (PyMiCCS) part II: organic and inorganic carbon dioxide removal in an Oxisol. Front Clim, Volume 7 - 2025. https://doi.org/10.3389/fclim.2025.1592454.

WALKER, J. C. G., HAYS, P. B. & KASTING, J. F. 1981. A negative feedback mechanism for the long-term stabilization of Earth's surface temperature. J Geophys Res Ocean, 86, 9776–9782. https://doi.org/10.1029/JC086iC10p09776.

WANG, D., FONTE, S. J., PARIKH, S. J., SIX, J. & SCOW, K. M. 2017. Biochar additions can enhance soil structure and the physical stabilization of C in aggregates. Geoderma, 303, 110–117. https://doi.org/10.1016/j.geoderma.2017.05.027.

WANG, H., NAN, Q., WAQAS, M. & WU, W. 2022. Stability of biochar in mineral soils: Assessment methods, influencing factors and potential problems. Sci Total Environ, 806, 150789. https://doi.org/10.1016/j.scitotenv.2021.150789.

WANG, J., SUN, L., SUN, Y., YANG, S., QIN, Q. & XUE, Y. 2025. Long-term biochar-based fertilizer substitution promotes carbon, nitrogen, and phosphorus acquisition enzymes in dryland soils by affecting soil properties and regulating bacterial community. Appl Soil Ecol, 206, 105801. https://doi.org/10.1016/j.apsoil.2024.105801.

WANG, J., XIONG, Z. & KUZYAKOV, Y. 2016. Biochar stability in soil: meta-analysis of decomposition and priming effects. GCB Bioenergy, 8, 512–523. https://doi.org/10.1111/gcbb.12266.

WEIL, R. R. & BRADY, N. C. 2017. The nature and properties of soils. London, United Kingdom, Pearson.

WENG, Z., VAN ZWIETEN, L., SINGH, B. P., TAVAKKOLI, E., JOSEPH, S., MACDONALD, L. M., ROSE, T. J., ROSE, M. T., KIMBER, S. W. L., MORRIS, S., COZZOLINO, D., ARAUJO, J. R., ARCHANJO, B. S. & COWIE, A. 2017. Biochar built soil carbon over a decade by stabilizing rhizodeposits. Nat Clim Change*,* 7**,** 371–376. https://doi.org/10.1038/nclimate3276.

WHITMAN, T., SINGH, B. P. & ZIMMERMAN, A. R. 2015. Priming effects in biochar-amended soils: Implications of biochar-soil organic matter interactions for carbon storage. *In:* LEHMANN, J. & JOSEPH, S. (eds.) Biochar for environmental management. 2 ed. London, UK: Routledge.

WICKHAM, H. 2016. ggplot2: Elegant graphics for data analysis. New York, USA, Springer.

WICKHAM, H., FRANÇOIS, R., HENRY, L. & MÜLLER, K. 2023. dplyr: A Grammar of Data Manipulation - R package version 1.1.4. [Online].

WIEDNER, K., SCHNEEWEIß, J., DIPPOLD, M. A. & GLASER, B. 2015. Anthropogenic dark earth in Northern Germany — The nordic analogue to *terra preta de Índio* in Amazonia. CATENA*,* 132**,** 114–125. https://doi.org/10.1016/j.catena.2014.10.024.

WU, L., XU, H., XIAO, Q., HUANG, Y., SULEMAN, M. M., ZHU, P., KUZYAKOV, Y., XU, X., XU, M. & ZHANG, W. 2020. Soil carbon balance by priming differs with single versus repeated addition of glucose and soil fertility level. Soil Biol Biochem*,* 148**,** 107913. https://doi.org/10.1016/j.soilbio.2020.107913.

XU, P., WANG, Q., DUAN, C., HUANG, G., DONG, K. & WANG, C. 2024. Biochar addition promotes soil organic carbon sequestration dominantly contributed by macro-aggregates in agricultural ecosystems of China. J Environ Manage*,* 359**,** 121042. https://doi.org/10.1016/j.jenvman.2024.121042.

XU, T., LI, H., VICCA, S., GOLL, D. S., BEERLING, D. J., CHEN, Q., BI, B., YANG, Z., WANG, X. & YUAN, Z. 2025. Enhanced rock weathering promotes soil organic carbon accumulation: A global meta-analysis based on experimental evidence. Glob Chang Biol*,* 31**,** e70483. https://doi.org/10.1111/gcb.70483.

XU, W., WHITMAN, W. B., GUNDALE, M. J., CHIEN, C.-C. & CHIU, C.-Y. 2021. Functional response of the soil microbial community to biochar applications. GCB Bioenergy*,* 13**,** 269–281. https://doi.org/10.1111/gcbb.12773.

YAN, Y., YIN, L., YAN, S., FANG, Y., WANG, A., ZHU, F., BAI, Y., ZHANG, Z. & ZHANG, W. 2025. Similar mineral-associated organic carbon formation but distinct efficiencies by powdered wollastonite addition between two soils. Soil Biol Biochem*,* 211**,** 109979. https://doi.org/10.1016/j.soilbio.2025.109979.

YANG, F., XU, Z., HUANG, Y., TSANG, D. C. W., OK, Y. S., ZHAO, L., QIU, H., XU, X. & CAO, X. 2021. Stabilization of dissolvable biochar by soil minerals: Release reduction and organo-mineral complexes formation. J Hazard Mater*,* 412**,** 125213. https://doi.org/10.1016/j.jhazmat.2021.125213.

YANG, F., ZHAO, L., GAO, B., XU, X. & CAO, X. 2016. The interfacial behavior between biochar and soil minerals and its effect on biochar stability. Environ Sci Technol*,* 50**,** 2264–2271. https://doi.org/10.1021/acs.est.5b03656.

YANG, Y., SUN, K., HAN, L., CHEN, Y., LIU, J. & XING, B. 2022. Biochar stability and impact on soil organic carbon mineralization depend on biochar processing, aging and soil clay content. Soil Biol Biochem*,* 169**,** 108657. https://doi.org/10.1016/j.soilbio.2022.108657.

YOO, G., KIM, H. & CHOI, J. Y. 2017. Soil aggregate dynamics influenced by biochar addition using the ^{13}C natural abundance method. Soil Sci Soc Am J*,* 81**,** 612–621. https://doi.org/10.2136/sssaj2016.09.0313.

YU, Z., CHEN, L., PAN, S., LI, Y., KUZYAKOV, Y., XU, J., BROOKES, P. C. & LUO, Y. 2018. Feedstock determines biochar-induced soil priming effects by stimulating the activity of specific microorganisms. Eur J Soil Sci*,* 69**,** 521–534. https://doi.org/10.1111/ejss.12542.

YU, Z., LING, L., SINGH, B. P., LUO, Y. & XU, J. 2020. Gain in carbon: Deciphering the abiotic and biotic mechanisms of biochar-induced negative priming effects in contrasting soils. Sci Total Environ*,* 746**,** 141057. https://doi.org/10.1016/j.scitotenv.2020.141057.

ZANUTEL, M., GARRÉ, S., SANGLIER, P. & BIELDERS, C. 2024. Biochar modifies soil physical properties mostly through changes in soil structure rather than through its internal porosity. Vadose Zone Journal*,* 23**,** e20301. https://doi.org/10.1002/vzj2.20301.

ZHANG, L., JING, Y., XIANG, Y., ZHANG, R. & LU, H. 2018. Responses of soil microbial community structure changes and activities to biochar addition: A meta-analysis. Sci Total Environ*,* 643**,** 926–935. https://doi.org/10.1016/j.scitotenv.2018.06.231.

ZHANG, Y., WANG, J. & FENG, Y. 2021. The effects of biochar addition on soil physicochemical properties: A review. CATENA*,* 202**,** 105284. https://doi.org/10.1016/j.catena.2021.105284.

ZHAO, L., CAO, X., MAŠEK, O. & ZIMMERMAN, A. 2013. Heterogeneity of biochar properties as a function of feedstock sources and production temperatures. J Hazard Mater*,* 256-257**,** 1–9. https://doi.org/10.1016/j.jhazmat.2013.04.015.

ZHENG, Y., JIN, J., WANG, X., CLARK, G. J., FRANKS, A. & TANG, C. 2023. Nitrogen addition increases the glucose-induced priming effect of the particulate but not the mineral-associated organic carbon fraction. Soil Biol Biochem*,* 184**,** 109106. https://doi.org/10.1016/j.soilbio.2023.109106.

ZIMMERMAN, A. R., GAO, B. & AHN, M.-Y. 2011. Positive and negative carbon mineralization priming effects among a variety of biochar-amended soils. Soil Biol Biochem*,* 43**,** 1169–1179. https://doi.org/10.1016/j.soilbio.2011.02.005.

Manuscripts

Study A:

Effect of combined biochar and basanite applications on chemical and physical properties of a sandy agricultural soil

Maria Ansari[a]*, Joscha N. Becker[a], Susanne E. Hamburger[b], Claudia I. Kammann[b], Johannes Meyer zu Drewer[c,d,e], Nikolas Hagemann[c,d], Annette Eschenbach[a]

[a] Soil Science, Department of Earth System Science, University of Hamburg, Hamburg, Germany

[b] Department of Applied Ecology, Hochschule Geisenheim University, Geisenheim, Germany

[c] Ithaka Institute, Goldbach, Germany

[d] Agroscope, Zurich, Switzerland

[e] Institute of Sustainable Energy Systems, Offenburg University, Offenburg, Germany

*corresponding author

Submitted

A. Abstract

Biochar and silicate rock powder are two soil amendments coupling carbon dioxide removal and soil improvement. Despite potential synergistic effects, their combined effects on soil fertility, soil organic carbon (SOC) stabilization, and soil water dynamics remain poorly constrained. Here, we compare pure wood biochar and pure basanite rock powder with a co-application of both amendments and with rock-enhanced biochar from co-pyrolysis of biomass and basanite. A sandy agricultural topsoil was mixed with these soil amendments and filled in semi-field-based lysimeters planted with cabbage turnip (*Brassica oleracea* var. *gongylodes* L.) for nine weeks. After harvest, we assessed the amendment effects on physical and chemical soil properties, including SOC stabilization.

All biochar-containing amendments increased soil carbon, nitrogen, nutrient availability (P, K), microbial biomass, dissolved organic carbon, soil pH, water holding capacity (WHC), total pore volume, and enhanced the incorporation of SOC in particulate and mineral-associated organic matter. Especially the co-applications effects were mainly determined by biochar. Basanite, both pure and in co-application, showed only nearly no effects on the analyzed soil properties, probably due to limited rock weathering within this short-term experiment. In contrast, rock-enhanced biochar application had less pronounced effects compared to co-application on nutrient availability, WHC, pore volume, and the SOC stabilization in mineral-associations. These differences may result from the inclusion of basanite particles into biochar pores during feedstock preparation or co-pyrolysis. This makes rock-enhanced biochar more resistant to break-down and mineralization, but less effective for soil improvement. Contrary to our hypothesis, both combined applications showed merely additive effects at most, not indicating synergistic effects on soil properties within the nine weeks.

Keywords

carbon dioxide removal (CDR), enhanced rock weathering (ERW), nutrient availability, rock-enhanced biochar, sandy soil, soil fertility, soil organic carbon (SOC) stabilization, soil water dynamics

Highlights

- Combinations: Co-application of biochar and basanite vs. rock-enhanced biochar from co-pyrolysis
- Biochar dominated the effects of both combined applications on soil properties

- Biochar-containing amendments improved soil fertility and increased SOC stabilization
- Rock-enhanced biochar partly less effective in improving soil properties than co-application

A.1 Introduction

Biochar and silicate rock powder are two amendments combining soil-based carbon dioxide removal with soil fertility improvement (BUSS et al., 2021; JOSEPH et al., 2021; BEERLING et al., 2025). While most recent studies investigated both soil amendments separately, their combined application might offer synergistic effects (AMANN & HARTMANN, 2019; JOSEPH et al., 2021; BUSS et al., 2024b). A combined application can be implemented by co-applying biochar and silicate rock powder or co-pyrolyzing biomass and rock powder into rock-enhanced biochar (BUSS et al., 2022; MEYER ZU DREWER et al., 2025; VORRATH et al., 2025). While the effects of a co-application on soils are increasingly studied (HONVAULT et al., 2024; COSTANZO et al., 2025; SOHNG et al., 2025), rock-enhanced biochar has rarely been investigated yet.

Biochar is the carbon-rich product of biomass pyrolysis (HAGEMANN et al., 2018), consisting of highly aromatic and thus barely bioavailable carbon (C) (JOSEPH et al., 2010; AMELOOT et al., 2013). Biochar application can thus enhance the stable pool of soil organic C (SOC) (WANG et al., 2016), but also increase the soil pH (CHAN et al., 2008; VAN ZWIETEN et al., 2010), improve nutrient retention by increasing cation exchange capacity (CEC) (LIANG et al., 2006; ZHANG et al., 2021), and improve soil hydrology (BLANCO-CANQUI, 2017) especially in sandy soils. Additionally, depending on biomass feedstock and pyrolysis conditions, biochar can be an important source of essential nutrients, such as phosphorous (P) and potassium (K) (ANGST & SOHI, 2013; MUKHERJEE & ZIMMERMAN, 2013), which are often scarce in sandy soils. The interplay of these biochar-induced effects can result in increased crop yields (JEFFERY et al., 2011).

While the influence of biochar on soil properties is well studied, the effects of silicate rock powder application for enhanced rock weathering (ERW) on soils remains less investigated (HARTMANN et al., 2013; XU et al., 2024b). Especially effects of silicate rock powder, such as basanite, on soil water dynamics and other physical soil properties are not well understood (SWOBODA et al., 2022; COSTANZO et al., 2025). Previous studies indicate the beneficial effects of silicate rock powder on soil fertility (DUPLA et al., 2024). This includes increasing soil pH (GUO et al., 2023) and enhancing nutrient supply and availability (AMANN et al., 2020; SWOBODA et al., 2022), which potentially increases crop yields (SWOBODA et al., 2022).

Furthermore, the application of both amendments can affect SOC stabilization (WANG et al., 2017; BUSS et al., 2024a). Generally, SOC can be distinguished into particulate and mineral-associated organic matter, which differ in formation pathway and stabilization mechanisms (VON LÜTZOW et al., 2008; KLEBER et al., 2015). Particulate organic matter (POM) originates directly from organic inputs (VON LÜTZOW et al., 2008), is stabilized by its recalcitrance (SOLLINS et al., 1996), and can additionally be stabilized in aggregates (VON LÜTZOW et al., 2006). Mineral-associated organic matter (MAOM) is formed by the adsorption of dissolved organic C (DOC) to mineral surfaces or microbial processing (MANZONI & COTRUFO, 2024), and is stabilized through physical protection (KLEBER et al., 2015). Soil applied biochar remains mostly in the form of POM (KALU et al., 2024), partly occluded in aggregates (YOO et al., 2017; JOSEPH et al., 2021), but can also bind to mineral surfaces as MAOM (YANG et al., 2016; YANG et al., 2021). Additionally, biochar can promote the stabilization of native SOC (WANG et al., 2017; XU et al., 2024a). Weathering of silicate rock powder releases bivalent cations (e.g. Ca and Mg) that can promote aggregate formation via cation bridging and soil particle flocculation (BUSS et al., 2024a; XU et al., 2025), which can further stabilize POM within aggregates. Pristine mineral surfaces and the formation of reactive secondary minerals during weathering can adsorb SOC to form MAOM (REICHENBACH et al., 2021; BUSS et al., 2024a). This might be especially beneficial in sandy soils, which are inherently poor in reactive mineral surfaces (YAN et al., 2025). Both amendments can increase microbial biomass C (MBC) (LEHMANN et al., 2011; XU et al., 2024b), potentially enhancing microbial activity which can on the one hand enhance biogeochemical cycling of SOC and nutrients and the incorporation of microbial necromass in MAOM (CHEN et al., 2023; YAN et al., 2025), and on the other hand stimulate ERW (BUSS et al., 2021; REGINATO, 2025). The combined application of biochar and silicate rock powder may affect both the mechanisms and magnitude of their individual impacts on soil properties. Previous studies mainly observed additive and partly synergistic effects from co-applications on chemical and physical soil properties (HONVAULT et al., 2024; COSTANZO et al., 2025). The mineral surfaces of silicate rock particles may further stabilize biochar-derived SOC (MEYER ZU DREWER et al., 2025). Co-pyrolysis of biomass and minerals can increase the plant-available nutrient content of the pyrolysis product (MEYER ZU DREWER et al., 2025) and the stable C content (BUSS et al., 2022) and could improve the stability of rock-enhanced biochar and create a slow-release fertilizer (LAMMIRATO et al., 2011; BUSS et al., 2022). However, empirical evidence of those combined effects is scarce.Therefore, objective of this study was to compare how either pure or combined applications of biochar and basanite rock powder affect the properties of a sandy agricultural soil. We hypothesized that these amendments (i) improve chemical and physical soil properties and thus general soil fertility and (ii) increase the amount of SOC in POM and MAOM compared to unamended soils. Where biochar and basanite are co-applied or applied as rock-enhanced biochar from co-pyrolysis, (iii) these effects on soil properties might exceed additive effects of both pure amendments, indicating synergistic effects. We conducted a semi-field-based lysimeter-experiment using a sandy agricultural topsoil from Germany, amended with either pure or combined amendments. The lysimeters were planted with cabbage turnip (*Brassica oleracea* var. *gongylodes* L.) and once labeled with ^{13}C-CO_2. After the experiment, the soil samples were analyzed to determine the amendment effects on chemical and physical soil properties, focusing on soil fertility, water dynamics, and SOC pools.

A.2 Material and methods

A2.1 Soils and amendments

This study was conducted using an arable sandy topsoil (0-30 cm; Table A.1). It was collected in Northern Germany (Gartow, Germany, 53°01'26.9"N 11°27'12.7"E) and stored air-dried until further use.

We used the four different soil amendments biochar, basanite rock powder, a co-application of both, and the respective rock-enhanced biochar from co-pyrolysis of biomass and basanite. The biochar was produced from a 1:1 mixture of wood chips and woody sieving residues from green waste composting facility. This feedstock was pyrolyzed at 650 °C for 20 minutes using a PYREG500 commercial pyrolysis unit (PYREG GmbH, Dörth, Germany operated by Sonnenerde GmbH, Riedlingsdorf, Austria) (Table A.1). As silicate rock powder, we used basanite (*"Eifelgold")* with a grain size ranging from 0.5 to 300 µm (further information in Table A.2 in Appendix). To produce rock-enhanced biochar, the woody biomass and basanite were mixed in an 80:20 weight-ratio, pelletized, and co-pyrolyzed at 650 °C for 20 minutes on the same pyrolysis unit (Table A.1). Based on the TOC contents of biochar and rock-enhanced biochar, the latter consisted of ~68% biochar and ~32% basanite. To compare co-pyrolysis with simple mixing of the amendments, we co-applied biochar and basanite in the same ratio as calculated for the rock-enhanced biochar. Further characterizations of the amendments in MEYER ZU DREWER & HAGEMANN (2025).

Table A.1: Properties of sandy agricultural topsoil, biochar, and rock-enhanced biochar.

Properties	**Soil**[a]	**Biochar**[b]	**Rock-enhanced biochar**[b]
pH [$CaCl_2$]	4.7 ± 0.0	9.0	9.2
CEC [$mmol_c\ kg^{-1}$]	21.3 ± 0.4	n.d.	n.d.
C [$g\ kg^{-1}$]	12.4 ± 0.0	494	336
TOC [$g\ kg^{-1}$]	12.0 ± 0.0	482	332
TIC [$g\ kg^{-1}$]	0.4 ± 0.0	12	4
$\delta^{13}C$ [‰]	-26.7 ± 0.0	-27.3 ± 0.4 [a]	-27.0 ± 0.2 [a]
N [$g\ kg^{-1}$]	1.1 ± 0.0	7.0	4.1
P_2O_5 [$g\ kg^{-1}$]	n.d.	9	8
C:N	11.6 ± 0.0	80	82
H:C	n.d.	0.35	0.23
Ash [%]	n.a.	44.3	62.9
Sand [%]	93.8 ± 0.7	n.a.	n.a.
Silt [%]	2.5 ± 0.4	n.a.	n.a.
Clay [%]	3.7 ± 0.3	n.a.	n.a.

[a] Data is presented as mean ± standard error (n = 3), [b] values were measured by Eurofins Umwelt-Ost GmbH (Bobritzsch-Hilbersdorf, Germany) according to the analytical guidelines of the European Biochar Certificate (EBC, 2024). CEC = cation exchange capacity, C = total carbon, TOC = total organic carbon, TIC = total inorganic carbon, N = total nitrogen, n.d. = not determined, n.a. = not applicable.

A2.2 Experimental design

We used 45 lysimeters (each 20 cm inner diameter, 30 cm soil depth, sealed with stainless-steel mesh at the bottom allowing drainage into a catchment vessel below) which were set-up with five treatments (n = 9). The lysimeters and their catchment vessels were embedded in sand beds to achieve closer-to-natural soil temperatures compared to pot experiments. The leachate in the catchment vessel was removed regularly to prevent water accumulation. Inside the lysimeters, PVC bags were installed to contain the samples. For the control treatment, each bag was filled with 9 kg of soil (dry weight equivalent). For the biochar treatment, 379.1 g of biochar (equals ~4.2 wt%) was mixed with the soil before filling and installing the bags in the lysimeters. The rock powder treatment contained soil mixed with 178.2 g of basanite rock powder (~2 wt%). For the co-pyrolysis treatment, the soil was amended with 557.3 g of rock-enhanced biochar (~6.2 wt% of which ~4.2 wt% biochar and ~2 wt% basanite rock powder). For the mass-equivalent co-application, the soil was amended with 379.1 g of biochar (~4.2 wt%) and 178.2 g of basanite rock powder (~2 wt%). All lysimeters were arranged in a randomized complete block design (Figure A.4 in Appendix). Each lysimeter was watered and planted with one cabbage turnip seedling (*Brassica oleracea* var. *gongylodes* L.), selected from a larger batch to ensure similar development and strength of plants. Organic fertilizer (Carbuna AND, Carbuna AG, Memmingen, Germany) based on Vinasse and mineral fertilizer (Ferty 2 Mega, Hauert MANNA Düngerwerke GmbH, Nürnberg, Germany) were applied alternately five times during the nine-week growth period, supplying 0.005 g N, 0.0017 g P_2O_5, and 0.0077 g K_2O in total per lysimeter. The lysimeters were generally rainfed, but supplemented by drip irrigation during dry periods. A pulse-labeling of the experiment was conducted using 99% ^{13}C-CO_2 (Merck, Darmstadt, Germany). Therefore, a transparent tent was placed over the lysimeters for approximately 30 minutes. Perforated tubing was installed along the entire length of the tent at canopy height of the cabbage turnips to ensure homogeneous distribution of the injected ^{13}C-CO_2.

A2.3 Soil sampling and processing

After nine weeks of plant growth, the plants and soils of the lysimeter experiment were carefully harvested in July 2024 (for further information on plant growth see HAMBURGER et al. (2026)). One large (250 cm^3) and two small (100 cm^3) soil cores were taken in the upper 15 cm of each lysimeter to determine physical soil properties in undisturbed samples. The remaining sample was sieved (2 mm) to remove coarse fragments and roots. Since biochar and rock-enhanced biochar have not been crushed prior to application, coarse amendment particles (>2 mm) were also removed during sieving. A representative subsample of this sieved soil was first stored at 4 °C in a sealed plastic bag for later determination of MBC. The remaining sieved sample and all particles >2 mm were air-dried. To comprehensively assess amendment effects on chemical and physical soil properties, we mixed a subsample of the sieved soil with the removed amendment particles. Therefore, amendment particles were separated from other coarse material, carefully crushed, and sieved to 2 mm. For remixing, a subsample of 200 g of the sieved soil (equals 2.2% of total soil weight in lysimeter) was mixed with 2.2% of the crushed and sieved amendments, representing the original weight ratio.

A2.4 Analysis of chemical and physical soil properties

The water content (WC) of the field-moist samples (% dry weight) was determined as the difference between the fresh sample and after drying the sample at 105 °C until constant weight. The field-moist samples were used to determine MBC using the chloroform fumigation extraction (CFE) method after DIN (2011) adapted from VANCE et al. (1987). Two times 12.5 g sample (dry weight equivalent) were weighed in glass flasks. One of the samples was directly extracted with 50 ml of 0.05 M K_2SO_4 solution to quantify DOC. The second sample was fumigated with chloroform to lyse microbial cell walls and was afterwards extracted using K_2SO_4 solution. The extracts were analyzed using a TOC analyzer (TOC-L, Shimadzu Corporation, Kyoto, Japan). The difference between the extracted C in fumigated and non-fumigated samples is interpreted as MBC (mg kg^{-1}), using an extraction factor k_{EC} of 0.45 (JOERGENSEN, 1996).

Air-dried soil samples (including crushed amendment particles) were used to analyze chemical soil properties after the experiment. Plant-available P was extracted using calcium lactate and quantified using a spectrophotometer (DR5000, Hach Lange GmbH, Düsseldorf, Germany) with a wavelength of 580 nm, plant-available K was extracted using hydrochloric acid and quantified using an atomic absorption spectrometer (AAS; AA280FS, Varian, Palo Alto, California, USA), both following VDLUFA (1991). The effective cation exchange capacity (CEC) was determined using a 1 M KCl solution and the extract, containing the released NH_4^+ ions, was measured using a spectrophotometer. Soil pH was measured using a 0.01 M $CaCl_2$ solution (1:2.5 soil:$CaCl_2$ solution mass-ratio) with a pH meter (MP230, Mettler-Toledo GmbH, Gießen, Germany). The electric conductivity (EC) was measured in distilled water (1:2.5 soil:water mass-ratio) using a conductivity meter (Cond 330i, WTW GmbH, Weilheim, Germany). Water holding capacity (WHC) was determined as the amount of water retained against gravity. Soil samples were placed on a filter paper in a funnel and saturated with distilled water. After 24 h, the samples were weighed, dried at 105 °C to constant mass, and weighed again. The WHC (% dry weight) was calculated as the difference between wet and dry mass divided by the dry mass. A part of the air-dried sample was ground and dried at 105 °C to measure the C and N contents using an elemental analyzer (Vario Max Cube, Elementar Analysensysteme GmbH, Langenselbold, Germany). Due to the slightly acidic soil pH of our samples (< 6.6), we consider total and organic C equivalent.

Soil water retention at pressure levels of 3, 20, 60, 130, 300, and 1.000 hPa was determined on the fully saturated, undisturbed 100 cm^3 soil cores using the pressure plates method (DIN, 2014). To quantify the fine pores, disturbed samples were measured at 3.000 and 15.000 hPa. The 250 cm^3 soil cores were used to determine saturated hydraulic conductivity using a KSAT device and unsaturated hydraulic conductivity and water retention using HYPROP® (both Meter Group Inc., Munich, Germany). All soil-core data (100 cm^3 and 250 cm^3) were processed in HYPROP® SoilView based on the van Genuchten bimodal PDI model (IDEN & DURNER, 2014; PETERS, 2014) to calculate air capacity (pF 0-1.8), plant-available water (pF 1.8-4.2), and unavailable water (> pF 4.2). The bulk density (g cm^{-3}) was determined by relating the volume of the undisturbed 100 cm^3 soil cores to the dry soil weight it contained.

A2.5 Sieve fractionation

The POM and MAOM fractions were quantified by sieve fractionation following JUST et al. (2021). Approximately 50 g of air-dried soil was weighed into a glass beaker and 250 ml of distilled water slowly added. To disrupt aggregates, the sample was treated with an ultrasonication probe (450 J ml^{-1}; Bandelin HD-200 with probe UW2070, Bandelin electronic GmbH & Co.KG, Berlin, Germany) for 53 minutes. After dispersion, the sample was wet sieved with 2 l of distilled water using a 53 µm sieve to separate POM (>53 µm) from MAOM (<53 µm) (LUGATO et al., 2021). Both fractions were dried at 60 °C until constant weight, weighed, and grounded. A recovery rate (POM+MAOM) of 98-100% of the initial sample weight was achieved. The sieve fractions were measured at an elemental analyzer (Vario Max Cube, Elementar Analysensysteme GmbH, Langenselbold, Germany) to determine C and N content, and at an isotope ratio mass spectrometer (Delta V Plus, Thermo Fisher Scientific, Bremen, Germany) to determine the $\delta^{13}C$ value (‰). The $\delta^{13}C$ value represents the ratio of ^{13}C:^{12}C relative to the Vienna-PeeDee-Belemniten-Standard, defined as $[(R_{sample} - R_{standard}) / R_{standard}] \times 1000$.

As an indicator for the present stabilization mechanisms, the ratio of SOC in POM to SOC in MAOM ($\mathrm{POM{:}MAOM}$) was calculated according to Equation A1:

$$\mathrm{POM{:}MAOM} = \frac{SOC_{POM}}{SOC_{MAOM}} \qquad \text{(A1)}$$

where SOC_{POM} is the SOC in the sieve fraction >53 µm (mg g^{-1} soil) and SOC_{MAOM} is the SOC in sieve fraction <53 µm (mg g^{-1} soil). Values <1 indicate MAOM as dominant stabilization mechanism, while values >1 show that most of the SOC is present as POM.

A2.6 Statistical analysis

To test for significant differences ($p < 0.05$), we used a linear model with the block as random factor, followed by a Tukey HSD post-hoc test for pairwise comparison. Prior to analysis, model residuals were checked visually for normality and homogeneity of variance. All calculations and statistical tests were conducted in RStudio (version 4.4.2) using 'dplyr' (WICKHAM et al., 2023) for data handling, 'baseR' for linear models, 'emmeans' (LENTH et al., 2025) and 'multcomp' (HOTHORN et al., 2008) for pairwise comparison and compact letter display, 'ggplot2' (WICKHAM, 2016) and 'gridExtra' (AUGUIE & ANTONOV, 2017) for data visualization.

A.3 Results

A3.1 Effects of amendments on soil chemical properties

The application of biochar-containing amendments (biochar, co-application, and co-pyrolysis treatments) almost doubled the soil C content (Figure A.1A). Both pure biochar and co-application increased N contents by up to 14%, while the N contents of the co-pyrolysis treatment did not differ significantly from the control (Figure A.1B). Since the increase in C content was more pronounced than in N content, the C:N ratio increased in all biochar-containing treatments (Figure A.1C).

The content of plant-available P and K, MBC, DOC, as well as soil pH and EC were increased following the application of biochar-containing amendments (Figure A.1E,F,G,H,I,J). For MBC and pH, this increase was equally strong following the application of all three biochar-containing amendments (Figure A.1G,I). For P content and EC, the increase was stronger in pure biochar and co-application than in the co-pyrolysis treatment (Figure A.1E,J). The increase in plant-available K content was more pronounced in the co-application compared to co-pyrolysis treatment (Figure A.1F). The increase in DOC content was stronger in the co-pyrolysis compared to co-application treatment (Figure A.1H).

In contrast to the strong effect of biochar-containing amendments, pure basanite application did not alter any of the analyzed soil properties (Figure A.1). The only parameter analyzed in this study, which was not affected by any of the amendments, was CEC (Figure A.1D).

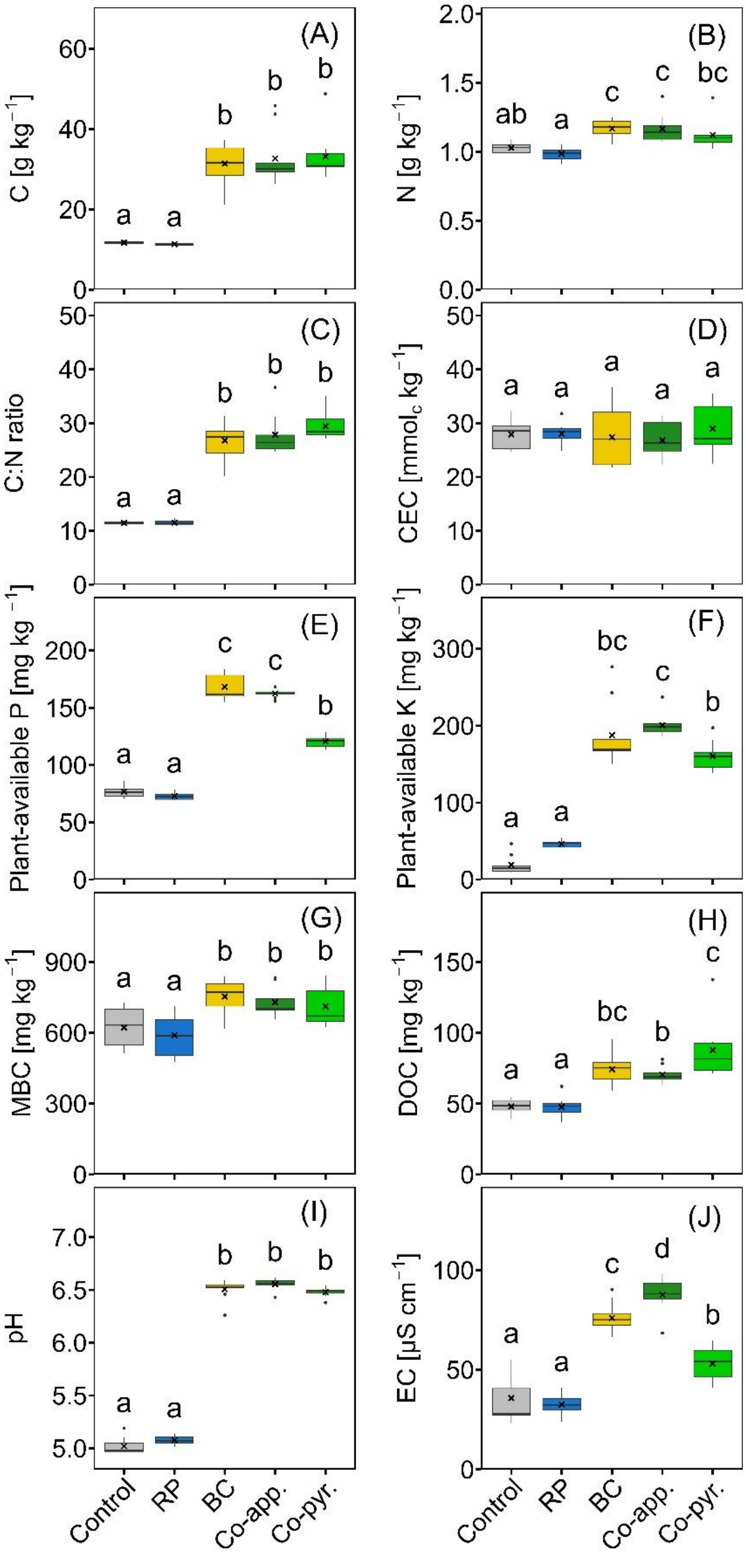

Figure A.1: Total carbon (C) content (Panel A), total nitrogen (N) content (Panel B), C:N ratio (Panel C), effective cation exchange capacity (CEC) (Panel D), plant-available phosphorus (P) content (Panel E), plant-available potassium (K) content (Panel F), microbial biomass C (MBC) (Panel G), dissolved organic C (DOC) (Panel H), pH in $CaCl_2$ (Panel I), and electric conductivity (EC) (Panel J) in five treatments (n = 9). RP = rock powder treatment containing basanite, BC = biochar treatment, Co-app. = co-application treatment containing biochar and basanite, Co-pyr. = co-pyrolysis treatment containing rock-enhanced biochar. Lower case letters indicate significant differences between treatments within one soil property ($p < 0.05$).

A3.2 Effects of amendments on SOC stabilization

The application of biochar-containing amendments significantly increased the C stored in both sieve fractions compared to control (Figure A.2A). The increase in the >53 µm fraction (defined as POM) was more pronounced than in the fraction <53 µm (defined as MAOM), leading to an increase of the ratio between the C in the fractions >53µm : <53µm (POM:MAOM) compared to control (Figure A.2B). In the co-pyrolysis treatment, the increase of C in the >53 µm fraction was stronger compared to both pure biochar and co-application treatments, whereas the C in the <53 µm fraction showed a weaker increase (Figure A.2A). This is reflected in a stronger increase of the ratio between C in the fractions >53µm : <53µm (POM:MAOM) in the co-pyrolysis treatment (Figure A.2B).

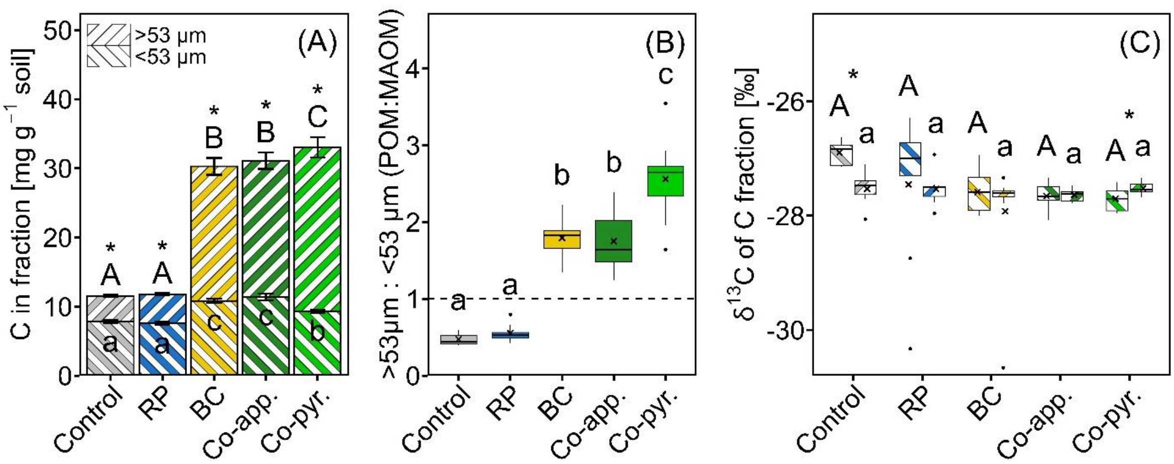

Figure A.2: Carbon (C) content (mg g^{-1} soil excluding amendment weight) of both sieve fractions (Panel A) (<53 µm similar to mineral-associated organic matter (MAOM), >53 µm similar to particulate organic matter (POM); mean and standard error), ratio of C content in sieve fractions >53 µm : <53 µm (POM:MAOM) (Panel B), and the fractions δ^{13}C values (Panel C) in five treatments (n = 9). In (Panel A) and (Panel C), lower case letters indicate significant differences between treatments within the <53 µm sieve fraction, capital letters indicate significant differences between treatments within the >53 µm sieve fraction, * indicate significant differences between both sieve fractions within one treatment ($p < 0.05$). In (Panel B), lower case letters indicate significant differences between treatments. RP = rock powder treatment containing basanite, BC = biochar treatment, Co-app. = co-application treatment containing biochar and basanite, Co-pyr. = co-pyrolysis treatment containing rock-enhanced biochar.

In the control treatment, the fraction <53 µm had a lower δ^{13}C value than the fraction >53 µm (Figure A.2B). In contrast, the fraction <53 µm had a higher δ^{13}C value than the fraction >53 µm in the co-pyrolysis treatment. In pure basanite, pure biochar, and co-application, both fractions had similar δ^{13}C values.

A3.3 Effects of amendments on soil physical properties

The distribution of pore space for air capacity, plant-available water, and unavailable water remained largely unaltered following application of soil amendments (Figure A.3A). Only the proportion of unavailable water in the total pore space was increased in the biochar treatment compared to control. The WHC increased following the application of biochar-containing amendments by up to 19%. This was stronger in the co-application than the co-pyrolysis treatment (Figure A.3B). The soil bulk density was reduced by the biochar-containing amendments by up to 10%, less pronounced in the co-pyrolysis treatment than in biochar and co-application treatment (Figure A.3C). In contrast to the biochar-containing amendments, pure basanite application did neither alter WHC nor bulk density compared to control (Figure A.3B,C).

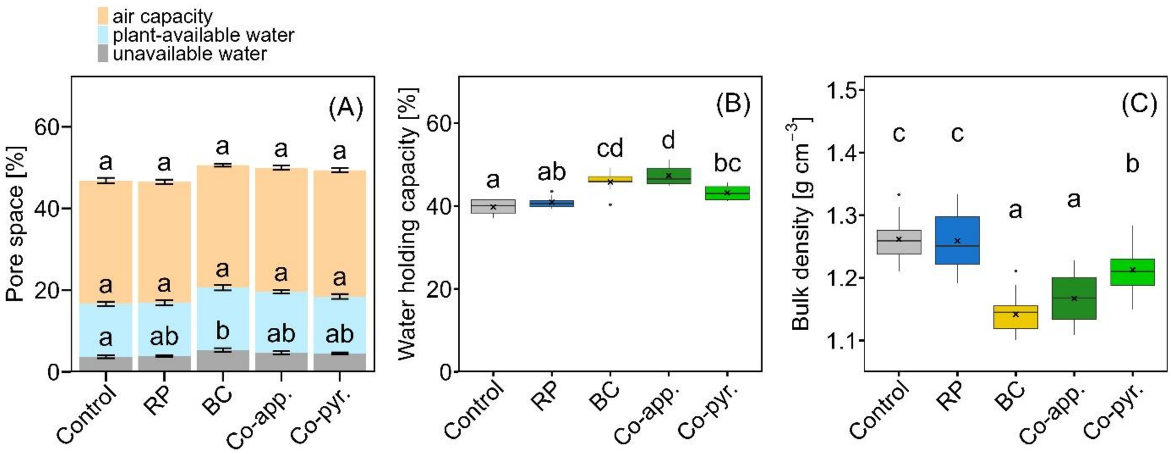

Figure A.3: Pore space availability for air capacity, plant-available water, and unavailable water (Panel A) (mean and standard error), water holding capacity (WHC) (Panel B), and bulk density (Panel C) in five treatments (n = 9). Lower case letters indicate significant differences between treatments within one parameter ($p < 0.05$). RP = rock powder treatment containing basanite, BC = biochar treatment, Co-app. = co-application treatment containing biochar and basanite, Co-pyr. = co-pyrolysis treatment containing rock-enhanced biochar.

A.4 Discussion

A4.1 Effect of pure biochar application on chemical and physical soil properties

The application of biochar improved the overall soil fertility. This is in line with the results of previous studies showing increased nutrient availability (GLASER & LEHR, 2019; GUO et al., 2025), microbial biomass C (LEHMANN et al., 2011), pH, and improved soil structure (ZHANG et al., 2021). The missing effect of biochar-containing amendments on CEC is, however, unexpected, as previous studies often observed an improvement (LIANG et al., 2006; ZHANG et al., 2021). Conventional CEC methods can face limitations in biochar-amended soils (GRABER et al., 2017; MUNERA-ECHEVERRI et al., 2018; LAGO et al., 2021) as high hydrophobicity, heterogeneity, and low density of biochar particles can complicate accurate determination, potentially masking changes in CEC (GRABER et al., 2017). Additionally, biochar CEC has been shown to increase with aging, as progressive oxidation of biochar surfaces leads to the formation of carboxylic functional groups (CHENG et al., 2006; AMELOOT et al., 2013). Thus, the absence of a measurable CEC increase in this study may reflect the relatively short duration of the experiment combined with methodological constraints.

The overall increase in SOC following our biochar application resulted from an increase of SOC in both sieve fractions. The pronounced increase in POM (sieve fraction >53 µm) in our study originates from the remain of biochar-derived SOC in this C pool (HERATH et al., 2014; SINGH et al., 2014; PAETSCH et al., 2017). A noteworthy incorporation of plant-derived C in POM did not occur, since the cabbage turnip showed a strong enrichment in ^{13}C due to the labeling (HAMBURGER & KAMMANN, 2026), which was not found in POM. This strong remain of biochar-derived SOC increased the overall recalcitrance of the otherwise rather labile POM pool, which should be kept in mind when discussing SOC pools following biochar application. Furthermore, the application of biochar-containing amendments increased the SOC in the sieve fraction <53 µm, interpreted as MAOM. This can indicate the stabilization of biochar-derived SOC as MAOM (SINGH et al., 2014; PAETSCH et al., 2017), but also a breaking of biochar in particles <53 µm, a shift of native POM to MAOM (ANSARI et al., 2026), or the stabilization of plant-derived C as MAOM (WENG et al., 2017; KALU et al., 2024). Like POM, an incorporation of plant-derived C in MAOM following biochar application is unlikely, since no enrichment in ^{13}C is found in MAOM. Regardless of the SOC source, the application of biochar led to an increase of SOC in the fine sieve fraction, described as the stable MAOM pool.

An increase in WHC and a reduction of bulk density following biochar application have also been reported in previous studies, especially in sandy soils (BLANCO-CANQUI, 2017; RAZZAGHI et al., 2020; ZHANG et al., 2021). Those improvements in soil physical properties can enhance plant growth and thus increase yield (JOSEPH et al., 2021; ZHANG et al., 2021). However, air capacity and plant-available water, two important physical soil parameters relevant for plant growth (RITCHIE, 1981), remained unaffected by the application of biochar in our experiment. Air capacity is generally high in sandy soils (ARCHER & SMITH, 1972), explaining the limited additional benefit of biochar application. In contrast, plant-available water is often relatively scarce in organic-poor sandy soils, which typically makes biochar in those soils particularly useful to improve water availability (RAZZAGHI et al., 2020; BUSS et al., 2021). However, the high ash content (AURANGZEIB et al., 2025) and larger particle size (IBRAHIMI & ALGHAMDI, 2022) of our (rock-enhanced) biochar could explain why no improvement in plant-available water was observed in the present study. Despite those limitations of biochar for plant-available water, soil physical properties overall remained constant or were improved through the application of biochar-containing amendments.

A4.2 Effect of pure basanite application on chemical and physical soil properties

In contrast to the biochar-containing amendments, pure basanite application had no effect on soil chemical and physical properties. This might either result from limited rock weathering within our nine-week experiment or from uptake and/or leaching of all weathering products. Basanite has rather low weathering rates due to its mineralogical composition and showed the lowest alkalinity export when compared to other silicate rocks and artificial silicates in a two-year pot experiment from HAMMES et al. (2025). The uptake of weathering products by the cabbage turnip in our study seems unlikely, since plant yield was not increased (HAMBURGER et al., 2026). However, basanite application increased the cation load (Na, Si) and total alkalinity in the leachate of a complementary lysimeter experiment, indicating a certain amount of basanite weathering within the nine weeks (VORRATH et al., 2026). Thus, in line with previous studies that observed positive effects of silicate rock powder on longer time scales (KAHNT et al., 1986; RICHARDSON, 2025; SOHNG et al., 2025), improvements of chemical and physical soil properties become more probable in the long-term.

A4.3 Effect of combined applications on chemical and physical soil properties

Both combined applications had comparable effect as pure biochar application on chemical and physical soil properties. Especially the co-application of biochar and basanite strongly mirrored the effects of pure biochar, rarely showing effects of basanite. Thus, adding basanite to the biochar did not compromise the beneficial effects of biochar on our sandy soils, while synergistic effects remain possible in the long-term (HONVAULT et al., 2024).

The effects of rock-enhanced biochar application differed from those of co-applied amendments for several chemical and physical soil parameters, indicating an effect of co-pyrolysis. The reduced release of plant-available nutrients (P, K) and salts from rock-enhanced biochar combined with a less pronounced increase of WHC and a weaker decrease of bulk density suggests the occlusion of basanite particles in biochar pores during feedstock preparation or co-pyrolysis. As described by MEYER ZU DREWER et al. (2025), this process strongly decreases pore space and specific surface area and thus the potential interface of rock-enhanced biochar and soil compared to biochar. On the one hand, this lower exposed surface area of rock-enhanced biochar resulted in a weaker modification of chemical and physical soil properties within our nine-week experiment. On the other hand, this offers the opportunity to use rock-enhanced biochar as a dense, slow-release amendment improving soils over longer time spans (LAMMIRATO et al., 2011; BUSS et al., 2022). Additionally, such inner-pore mineral interactions can further protect the biochar from decomposition, potentially improving its long-term stability and CDR effect (ARCHANJO et al., 2017; SCHMIDT et al., 2025). Further research could include micro- and spectroscopy to gain further insights into these inner-pore processes occurring during co-pyrolysis.

While most chemical soil properties were less strongly increased by rock-enhanced biochar application compared to co-applied biochar, rock-enhanced biochar application led to a more pronounced increase of the soils DOC content. This stronger release of DOC might originate from pyrogenic coating on the surface of rock powder particles, which occurs during co-pyrolysis and forms a layer of pyrogenic C compounds which are ought to be rather labile (MEYER ZU DREWER et al., 2025). These compounds could be released into the soil as DOC, explaining the higher DOC content following rock-enhanced biochar application compared to co-applied biochar. This DOC could be beneficial for MAOM formation (MANZONI & COTRUFO, 2024).

Surprisingly, the application of rock-enhanced biochar led to a less strong increase of SOC in the sieve fraction <53 µm, interpreted as MAOM, than pure and co-applied biochar. This could indicate a reduced stabilization of rock-enhanced biochar-derived SOC as MAOM. Alternatively, the correspondingly higher remain of rock-enhanced biochar-derived SOC in the sieve fraction >53 µm, interpreted as POM, could indicate an increased stability of rock-enhanced biochar particles compared to biochar, resulting in a reduced physical breakdown of rock-enhanced biochar particles below 53 µm. This ambiguity of the results shows a limitation of the sieve fractionation, separating SOC pools by size but not necessarily into conceptual pools (LEUTHOLD et al., 2024). Complementary size- and density fractionations could yield further insights.

Still, a higher stability and thus lower availability of rock-enhanced biochar aligns well with the reduced release of nutrients and salts compared to co-applied biochar.

Commonly, POM has lower $\delta^{13}C$ values compared to MAOM, since POM is similar to the plant material while MAOM is often microbially processed (VOLK et al., 2018; MIDWOOD et al., 2021; LEUTHOLD et al., 2024). The unamended soil as well as the soil amended with rock-enhanced biochar showed significant differences in the $\delta^{13}C$ signal of POM and MAOM. While the soil amended with rock-enhanced biochar showed the common pattern, POM in the unamended soil had significantly higher $\delta^{13}C$ values than MAOM. The pattern in the unamended soil indicates an incorporation of ^{13}C-labeled plant material in POM, increasing its $\delta^{13}C$ value (MIDWOOD et al., 2021; WITZGALL et al., 2021). Due to the high share of rock-enhanced biochar in POM and the thus bigger POM pool, this incorporation of plant-derived C in POM is not visible anymore in the $\delta^{13}C$ value.

A.5 Conclusions

The biochar-containing amendments (pure biochar, co-application, rock-enhanced biochar) improved soil fertility, SOC stabilization, and partly soil water dynamics, highlighting the suitability of these amendments in sandy soils. Co-applications had largely similar effects as pure biochar, showing little effects of basanite rock powder. Comparably, also pure basanite rock powder had no detectable effect during the nine-week semi-field-based lysimeter experiment, likely reflecting limited rock weathering within this time frame. Importantly, basanite rock powder did not negatively affect any measured parameters, supporting its potential as a safe long-term carbon dioxide removal technology. Contrary to our hypothesis, co-application indicated no synergistic effects on soil properties, suggesting that short-term experiments may be insufficient to capture the full potential of basanite-containing amendments and potential long-term effects of basanite rock powder could enhance its relevance.

The improvements in soil fertility, SOC stabilization, and soil water dynamics observed after the application of rock-enhanced biochar were partly less pronounced than those of co-applied biochar and basanite. The potential filling of biochar pore space by basanite particles during co-pyrolysis likely reduced the porosity and thus the surface area available for nutrient release and water retention. Also the increase in MAOM (sieve fraction <53 µm) was weaker following the application of rock-enhanced biochar, with most of the rock-enhanced biochar-derived C remaining in POM (sieve fraction >53 µm). This pattern indicates either a lower effectiveness of rock-enhanced biochar or a higher stability of rock-enhanced biochar, which might develop its potential in the long-term. To disentangle short-term limitations from potential long-term advantages, monitored long-term field experiments across different soil types are required. The findings presented here provide a promising starting point for such studies.

Authors' contributions

Maria Ansari: Conceptualization, Formal analysis, Investigation, Methodology, Visualization, Writing – original draft; **Joscha N. Becker**: Conceptualization, Funding acquisition, Methodology, Supervision, Writing - Review & Editing; **Susanne Hamburger**: Resources; **Claudia Kammann**: Funding acquisition, Resources; **Johannes Meyer zu Drewer**: Resources, Writing - Review & Editing; **Nikolas Hagemann**: Funding acquisition, Resources; **Annette Eschenbach**: Conceptualization, Funding acquisition, Resources, Methodology, Supervision, Writing - Review & Editing.

Acknowledgements

This study was conducted as a part of the PyMiCCS project (Pyrogenic carbon and carbonating Minerals for enhanced plant growth and Carbon Capture and Storage) that is part of the CDRterra consortium and was funded by the German Federal Ministry of Research, Technology and Space (BMFTR, FKZ: 01LS2109A and 01LS2109C). The authors thank Sumita Rui and Josephine Krechel for assisting during sampling as well as Deborah Harms, Annika Naumann, and Jakob Kast for support during lab work.

A.6 References

AMANN, T. & HARTMANN, J. 2019. Ideas and perspectives: Synergies from co-deployment of negative emission technologies. Biogeosciences, 16, 2949–2960. https://doi.org/10.5194/bg-16-2949-2019.

AMANN, T., HARTMANN, J., STRUYF, E., DE OLIVEIRA GARCIA, W., FISCHER, E. K., JANSSENS, I., MEIRE, P. & SCHOELYNCK, J. 2020. Enhanced Weathering and related element fluxes – a cropland mesocosm approach. Biogeosciences, 17, 103–119. https://doi.org/10.5194/bg-17-103-2020.

AMELOOT, N., GRABER, E. R., VERHEIJEN, F. G. A. & DE NEVE, S. 2013. Interactions between biochar stability and soil organisms: review and research needs. Eur J Soil Sci, 64, 379–390. https://doi.org/10.1111/ejss.12064.

ANGST, T. E. & SOHI, S. P. 2013. Establishing release dynamics for plant nutrients from biochar. GCB Bioenergy, 5, 221–226. https://doi.org/10.1111/gcbb.12023.

ANSARI, M., LÜBECK, A., MEYER ZU DREWER, J., HAGEMANN, N., ESCHENBACH, A. & BECKER, J. N. 2026. Rock-enhanced biochar has similar priming effect as pure biochar application, but improves short-term carbon stabilization in agricultural soils. *in prep.*

ARCHANJO, B. S., MENDOZA, M. E., ALBU, M., MITCHELL, D. R. G., HAGEMANN, N., MAYRHOFER, C., MAI, T. L. A., WENG, Z., KAPPLER, A., BEHRENS, S., MUNROE, P., ACHETE, C. A., DONNE, S., ARAUJO, J. R., VAN ZWIETEN, L., HORVAT, J., ENDERS, A. & JOSEPH, S. 2017. Nanoscale analyses of the surface structure and composition of biochars extracted from field trials or after co-composting using advanced analytical electron microscopy. Geoderma, 294, 70–79. https://doi.org/10.1016/j.geoderma.2017.01.037.

ARCHER, J. R. & SMITH, P. D. 1972. The relation between bulk density, available water capacity, and air capacity of soils. J Soil Sci, 23, 475–480. https://doi.org/10.1111/j.1365-2389.1972.tb01678.x.

AUGUIE, B. & ANTONOV, A. 2017. gridExtra: Miscellaneous Functions for "Grid" Graphics - R package version 2.3. [Online].

AURANGZEIB, M., ZHANG, S., YAN, S., WEI, Z., ZHANG, H., NIU, X. & YAN, P. 2025. Does biochar improve acidic soil physical properties and crop yield under varying climatic and soil conditions? A global comprehensive meta-analysis. Soil Use Manage, 41, e70081. https://doi.org/10.1111/sum.70081.

BEERLING, D. J., KANTZAS, E. P., LOMAS, M. R., TAYLOR, L. L., ZHANG, S., KANZAKI, Y., EUFRASIO, R. M., RENFORTH, P., MECURE, J.-F., POLLITT, H., HOLDEN, P. B., EDWARDS, N. R., KOH, L., EPIHOV, D. Z., WOLF, A., HANSEN, J. E., BANWART, S. A., PIDGEON, N. F., REINHARD, C. T., PLANAVSKY, N. J. & VAL MARTIN, M. 2025. Transforming US agriculture for carbon removal with enhanced weathering. Nature, 638, 425–434. https://doi.org/10.1038/s41586-024-08429-2.

BLANCO-CANQUI, H. 2017. Biochar and soil physical properties. Soil Sci Soc Am J, 81, 687–711. https://doi.org/10.2136/sssaj2017.01.0017.

BUSS, W., HASEMER, H., FERGUSON, S. & BOREVITZ, J. 2024a. Stabilisation of soil organic matter with rock dust partially counteracted by plants. Glob Chang Biol, 30, e17052. https://doi.org/10.1111/gcb.17052.

BUSS, W., HASEMER, H., SOKOL, N. W., ROHLING, E. J. & BOREVITZ, J. 2024b. Applying minerals to soil to draw down atmospheric carbon dioxide through synergistic organic and inorganic pathways. Commun Earth Environ, 5, 602. https://doi.org/10.1038/s43247-024-01771-3.

BUSS, W., WURZER, C., MANNING, D. A. C., ROHLING, E. J., BOREVITZ, J. & MAŠEK, O. 2022. Mineral-enriched biochar delivers enhanced nutrient recovery and carbon dioxide removal. Commun Earth Environ, 3, 67. https://doi.org/10.1038/s43247-022-00394-w.

BUSS, W., YEATES, K., ROHLING, E. & BOREVITZ, J. 2021. Enhancing natural cycles in agro-ecosystems to boost plant carbon capture and soil storage. Oxford Open Climate Change, 1, kgab006. https://doi.org/10.1093/oxfclm/kgab006.

CHAN, K. Y., VAN ZWIETEN, L., MESZAROS, I., DOWNIE, A. & JOSEPH, S. 2008. Using poultry litter biochars as soil amendments. Soil Res, 46, 437–444. https://doi.org/10.1071/SR08036.

CHEN, Y., SUN, K., YANG, Y. & ZHENG, H. 2023. Effects of biochar on the accumulation of necromass-derived carbon, the physical protection and microbial mineralization of soil organic carbon. Crit Rev Env Sci Tec, 1–29. https://doi.org/10.1080/10643389.2023.2221155.

CHENG, C.-H., LEHMANN, J., THIES, J. E., BURTON, S. D. & ENGELHARD, M. H. 2006. Oxidation of black carbon by biotic and abiotic processes. Org Geochem, 37, 1477–1488. https://doi.org/10.1016/j.orggeochem.2006.06.022.

COSTANZO, S. A., HOLZER, I. O., MOONILALL, N. I., DAVENPORT, A., HOULTON, B. Z. & NOCCO, M. A. 2025. Preliminary assessment of crushed rock, compost, and biochar amendments on soil physical properties. Agric Environ Lett, 10, e70028. https://doi.org/10.1002/ael2.70028.

DIN 2011. DIN EN ISO 14240-2:2011-09: Soil quality - Determination of soil microbial biomass - Part 2: Fumigation-extraction method. Berlin, Germany: DIN Media GmbH.

DIN 2014. DIN EN ISO 11274:2014-07: Soil quality - Determination of the water-retention characteristic - Laboratory methods. Berlin, Germany: DIN Media GmbH.

DUPLA, X., ROMANE, C., EMMA, B., IRIS, G., RENÉE-CLAIRE, L. B. & STÉPHANIE, G. 2024. Let the dust settle: Impact of enhanced rock weathering on soil biological, physical, and geochemical fertility. Sci Total Environ, 176297. https://doi.org/10.1016/j.scitotenv.2024.176297.

EBC. 2024. Analytical methods - EBC guidelines Version 10.4 [Online]. European Biochar Certificate (EBC). Available: https://www.european-biochar.org/en/ct/8-Analytical-Methods.

GLASER, B. & LEHR, V.-I. 2019. Biochar effects on phosphorus availability in agricultural soils: A meta-analysis. Sci Rep, 9, 9338. https://doi.org/10.1038/s41598-019-45693-z.

GRABER, E. R., SINGH, B., HANLEY, K. & LEHMANN, J. 2017. Determination of cation exchange capacity in biochar. *In:* SINGH, B., CAMPS-ARBESTAIN, M. & LEHMANN, J. (eds.) Biochar: A guide to analytical methods. Australia: CSIRO Publishing

GUO, F., SUN, H., YANG, J., ZHANG, L., MU, Y., WANG, Y. & WU, F. 2023. Improving food security and farmland carbon sequestration in China through enhanced rock weathering: Field evidence and potential assessment in different humid regions. Sci Total Environ, 903, 166118. https://doi.org/10.1016/j.scitotenv.2023.166118.

GUO, H., WU, Z., LI, J., LU, Z., LUAN, S., HU, S., LIU, X., LI, N. & HAN, X. 2025. A nine-year study: continuous application of biochar achieves efficient potassium supply by modifying soil clay mineral composition and its potassium adsorption sites. J Soils Sediments. https://doi.org/10.1007/s11368-025-04035-5.

HAGEMANN, N., SPOKAS, K., SCHMIDT, H.-P., KÄGI, R., BÖHLER, M. A. & BUCHELI, T. D. 2018. Activated carbon, biochar and charcoal: Linkages and synergies across pyrogenic carbon's ABCs. Water, 10, 182. https://doi.org/10.3390/w10020182

HAMBURGER, S. E. & KAMMANN, C. I. 2026. *RE: ^{13}C-signal of plant biomass from a semi-field lysimeter experiment with cabbage turnip under combined biochar and rock powder amendment.*

HAMBURGER, S. E., MEYER ZU DREWER, J., HAGEMANN, N., GEILFUS, C.-M. & KAMMANN, C. I. 2026. A crop yield and nitrate leaching dataset from a semi-field lysimeter experiment with cabbage turnip under combined biochar and rock powder amendment. https://doi.org/10.5281/zenodo.19065555.

HAMMES, J. S., HARTMANN, J., BARTH, J. A. C., LINKE, T., SMET, I., HAGENS, M., POGGE VON STRANDMANN, P. A. E., REERSHEMIUS, T., CASIMIRO, B., VIENNE, A., STOECKEL, A. A., STEFFENS, R. & PAESSLER, D. 2025. Soil processes govern alkalinity and cation retention in enhanced weathering for carbon dioxide removal - *preprint*. EGUsphere, 2025, 1–40. https://doi.org/10.5194/egusphere-2025-5402.

HARTMANN, J., WEST, A. J., RENFORTH, P., KÖHLER, P., DE LA ROCHA, C. L., WOLF-GLADROW, D. A., DÜRR, H. H. & SCHEFFRAN, J. 2013. Enhanced chemical weathering as a geoengineering strategy to reduce atmospheric carbon dioxide, supply nutrients, and mitigate ocean acidification. Rev Geophys, 51, 113–149. https://doi.org/10.1002/rog.20004.

HERATH, H. M. S. K., CAMPS-ARBESTAIN, M., HEDLEY, M., VAN HALE, R. & KAAL, J. 2014. Fate of biochar in chemically- and physically-defined soil organic carbon pools. Org Geochem, 73, 35–46. https://doi.org/10.1016/j.orggeochem.2014.05.001.

HONVAULT, N., TIOUCHICHINE, M.-L., SAUZE, J., PIEL, C., LANDAIS, D., DEVIDAL, S., GRITTI, E., BOSCH, D. & MILCU, A. 2024. Additive effects of basalt enhanced weathering and biochar co-application on carbon sequestration, soil nutrient status and plant performance in a mesocosm experiment. Appl Geochem, 169, 106054. https://doi.org/10.1016/j.apgeochem.2024.106054.

HOTHORN, T., BRETZ, F. & WESTFALL, P. 2008. Simultaneous inference in general parametric models. Biometrical J, 50, 346–363. https://doi.org/10.1002/bimj.200810425.

IBRAHIMI, K. & ALGHAMDI, A. G. 2022. Available water capacity of sandy soils as affected by biochar application: A meta-analysis. CATENA, 214, 106281. https://doi.org/10.1016/j.catena.2022.106281.

IDEN, S. C. & DURNER, W. 2014. Comment on "Simple consistent models for water retention and hydraulic conductivity in the complete moisture range" by A. Peters. Water Resour Res, 50, 7530–7534. https://doi.org/10.1002/2014WR015937.

JEFFERY, S., VERHEIJEN, F. G. A., VAN DER VELDE, M. & BASTOS, A. C. 2011. A quantitative review of the effects of biochar application to soils on crop productivity using meta-analysis. Agr Ecosyst Environ, 144, 175–187. https://doi.org/10.1016/j.agee.2011.08.015.

JOERGENSEN, R. G. 1996. The fumigation-extraction method to estimate soil microbial biomass: Calibration of the k_{EC} value. Soil Biol Biochem, 28, 25–31. https://doi.org/10.1016/0038-0717(95)00102-6.

JOSEPH, S., COWIE, A. L., VAN ZWIETEN, L., BOLAN, N., BUDAI, A., BUSS, W., CAYUELA, M. L., GRABER, E. R., IPPOLITO, J. A., KUZYAKOV, Y., LUO, Y., OK, Y. S., PALANSOORIYA, K. N., SHEPHERD, J., STEPHENS, S., WENG, Z. & LEHMANN, J. 2021. How biochar works, and when it doesn't: A review of mechanisms controlling soil and plant responses to biochar. GCB Bioenergy, 13, 1731–1764. https://doi.org/10.1111/gcbb.12885.

JOSEPH, S. D., CAMPS-ARBESTAIN, M., LIN, Y., MUNROE, P., CHIA, C. H., HOOK, J., VAN ZWIETEN, L., KIMBER, S., COWIE, A., SINGH, B. P., LEHMANN, J., FOIDL, N., SMERNIK, R. J. & AMONETTE, J. E. 2010. An investigation into the reactions of biochar in soil. Soil Res, 48, 501–515. https://doi.org/10.1071/SR10009.

JUST, C., POEPLAU, C., DON, A., VAN WESEMAEL, B., KÖGEL-KNABNER, I. & WIESMEIER, M. 2021. A simple approach to isolate slow and fast cycling organic carbon fractions in central european soils — Importance of dispersion method. Front Soil Sci, Volume 1 - 2021. https://doi.org/10.3389/fsoil.2021.692583.

KAHNT, G., PFLEIDERER, H. & HIJAZI, L. A. 1986. Wirkungen meliorativer Gaben von Gesteinsmehlen und Gesteinssanden auf das Wachstum verschiedener landwirtschaftlicher Kulturpflanzen sowie auf physikalische Kennwerte eines Sandbodens und eines Tonbodens. J Agron Crop Sci, 157, 169–180. https://doi.org/10.1111/j.1439-037X.1986.tb00064.x.

KALU, S., SEPPÄNEN, A., MGANGA, K. Z., SIETIÖ, O.-M., GLASER, B. & KARHU, K. 2024. Biochar reduced the mineralization of native and added soil organic carbon: evidence of negative priming and enhanced microbial carbon use efficiency. Biochar, 6, 7. https://doi.org/10.1007/s42773-023-00294-y.

KLEBER, M., EUSTERHUES, K., KEILUWEIT, M., MIKUTTA, C., MIKUTTA, R. & NICO, P. S. 2015. Chapter One - Mineral–organic associations: Formation, properties, and relevance in soil environments. *In:* SPARKS, D. L. (ed.) Advances in Agronomy. London: Academic Press. https://doi.org/10.1016/bs.agron.2014.10.005.

LAGO, B. C., SILVA, C. A., MELO, L. C. A. & MORAIS, E. G. D. 2021. Predicting biochar cation exchange capacity using Fourier transform infrared spectroscopy combined with partial least square regression. Sci Total Environ, 794, 148762. https://doi.org/10.1016/j.scitotenv.2021.148762.

LAMMIRATO, C., MILTNER, A. & KAESTNER, M. 2011. Effects of wood char and activated carbon on the hydrolysis of cellobiose by β-glucosidase from *Aspergillus niger*. Soil Biol Biochem, 43, 1936–1942. https://doi.org/10.1016/j.soilbio.2011.05.021.

LE BAS, M. J., LE MAITRE, R. W. L., STRECKEISEN, A., ZANETTIN, B. & ROCKS, I. S. O. T. S. O. I. 1986. A chemical classification of volcanic rocks based on the total alkali-silica diagram. J Petrol, 27, 745–750. https://doi.org/10.1093/petrology/27.3.745.

LEHMANN, J., RILLIG, M. C., THIES, J., MASIELLO, C. A., HOCKADAY, W. C. & CROWLEY, D. 2011. Biochar effects on soil biota – A review. Soil Biol Biochem, 43, 1812–1836. https://doi.org/10.1016/j.soilbio.2011.04.022.

LENTH, R. V., PIASKOWSKI, J., BANFAI, B., BOLKER, B., BUERKNER, P., GINÉ-VÁZQUEZ, I., HERVÉ, M., JUNG, M., LOVE, J., MIGUEZ, F., RIEBL, H. & SINGMANN, H. 2025. emmeans: Estimated Marginal Means, aka Least-Squares Means - R package version 1.1.4. [Online].

LEUTHOLD, S., LAVALLEE, J. M., HADDIX, M. L. & COTRUFO, M. F. 2024. Contrasting properties of soil organic matter fractions isolated by different physical separation methodologies. Geoderma, 445, 116870. https://doi.org/10.1016/j.geoderma.2024.116870.

LIANG, B., LEHMANN, J., SOLOMON, D., KINYANGI, J., GROSSMAN, J., O'NEILL, B., SKJEMSTAD, J. O., THIES, J., LUIZÃO, F. J., PETERSEN, J. & NEVES, E. G. 2006. Black carbon increases cation exchange capacity in soils. Soil Sci Soc Am J, 70, 1719–1730. https://doi.org/10.2136/sssaj2005.0383.

LUGATO, E., LAVALLEE, J. M., HADDIX, M. L., PANAGOS, P. & COTRUFO, M. F. 2021. Different climate sensitivity of particulate and mineral-associated soil organic matter. Nat Geosci, 14, 295–300. 10.1038/s41561-021-00744-x.

MANZONI, S. & COTRUFO, M. F. 2024. Mechanisms of soil organic carbon and nitrogen stabilization in mineral-associated organic matter – Insights from modeling in phase space. Biogeosciences, 21, 4077–4098. https://doi.org/10.5194/bg-21-4077-2024.

MEYER ZU DREWER, J. & HAGEMANN, N. 2025. Industrial production and characterization of biochar and rock-enhanced biochar. https://doi.org/10.5281/zenodo.15840176.

MEYER ZU DREWER, J., VORRATH, M.-E., AMANN, T., HARTMANN, J., DE LA ROSA, J. M., MÖLLMER, J., PÉREZ-DALÍ, S. M., MEREDITH, W., UGUNA, C., SNAPE, C., KAMMANN, C., SCHMIDT, H.-P. & HAGEMANN, N. 2025. Pyrogenic carbon and carbonating minerals for carbon capture and storage (PyMiCCS) part I: production, physico-chemical characterization and C-sink potential. Front Clim, 7 2025. https://doi.org/10.3389/fclim.2025.1631368.

MIDWOOD, A. J., HANNAM, K. D., GEBRETSADIKAN, T., EMDE, D. & JONES, M. D. 2021. Storage of soil carbon as particulate and mineral associated organic matter in irrigated woody perennial crops. Geoderma, 403, 115185. https://doi.org/10.1016/j.geoderma.2021.115185.

MUKHERJEE, A. & ZIMMERMAN, A. R. 2013. Organic carbon and nutrient release from a range of laboratory-produced biochars and biochar–soil mixtures. Geoderma, 193-194, 122–130. https://doi.org/10.1016/j.geoderma.2012.10.002.

MUNERA-ECHEVERRI, J. L., MARTINSEN, V., STRAND, L. T., ZIVANOVIC, V., CORNELISSEN, G. & MULDER, J. 2018. Cation exchange capacity of biochar: An urgent method modification. Sci Total Environ, 642, 190–197. https://doi.org/10.1016/j.scitotenv.2018.06.017.

PAETSCH, L., MUELLER, C. W., RUMPEL, C., ANGST, Š., WIESHEU, A. C., GIRARDIN, C., IVLEVA, N. P., NIESSNER, R. & KÖGEL-KNABNER, I. 2017. A multi-technique approach to assess the fate of biochar in soil and to quantify its effect on soil organic matter composition. Org Geochem, 112, 177–186. https://doi.org/10.1016/j.orggeochem.2017.06.012.

PETERS, A. 2014. Reply to comment by S. Iden and W. Durner on "Simple consistent models for water retention and hydraulic conductivity in the complete moisture range". Water Resour Res, 50, 7535–7539. https://doi.org/10.1002/2014WR016107.

RAZZAGHI, F., OBOUR, P. B. & ARTHUR, E. 2020. Does biochar improve soil water retention? A systematic review and meta-analysis. Geoderma, 361, 114055. https://doi.org/10.1016/j.geoderma.2019.114055.

REGINATO, P. L. 2025. Biotechnology in direct air capture, enhanced weathering, and methane removal: Emerging opportunities and gaps. Front Clim, 6. https://doi.org/10.3389/fclim.2024.1440833

REICHENBACH, M., FIENER, P., GARLAND, G., GRIEPENTROG, M., SIX, J. & DOETTERL, S. 2021. The role of geochemistry in organic carbon stabilization against microbial decomposition in tropical rainforest soils. SOIL, 7, 453–475. https://doi.org/10.5194/soil-7-453-2021.

RICHARDSON, J. B. 2025. Basalt rock dust amendment on soil health properties and inorganic nutrients — Laboratory and field study at two organic farm soils in New England, USA. Agriculture, 15, 52. https://doi.org/10.3390/agriculture15010052.

RITCHIE, J. T. 1981. Water dynamics in the soil-plant-atmosphere system. Plant Soil, 58, 81–96. https://doi.org/10.1007/BF02180050.

SCHMIDT, H.-P., ABIVEN, S., COWIE, A., GLASER, B., JOSEPH, S., KAMMANN, C., LEHMANN, J., LEIFELD, J., PAN, G., RASSE, D., RUMPEL, C., WOOLF, D., ZIMMERMAN, A. R. & HAGEMANN,

N. 2025. Biochar permanence — A policy commentary. GCB Bioenergy, 17, e70092. https://doi.org/10.1111/gcbb.70092.

SINGH, N., ABIVEN, S., MAESTRINI, B., BIRD, J. A., TORN, M. S. & SCHMIDT, M. W. I. 2014. Transformation and stabilization of pyrogenic organic matter in a temperate forest field experiment. Glob Chang Biol, 20, 1629–1642. https://doi.org/10.1111/gcb.12459.

SOHNG, J., SOKOL, N. W., WHITEAKER, S., SCHMIDT, R., HOLZER, I., GOERTZEN, H., PEÑA, J., HOULTON, B. Z., MONTAÑEZ, I., O'GEEN, A. & SCOW, K. 2025. Combining organic amendments with enhanced rock weathering shifts soil carbon storage in croplands. Sci Total Environ, 998, 180179. https://doi.org/10.1016/j.scitotenv.2025.180179.

SOLLINS, P., HOMANN, P. & CALDWELL, B. A. 1996. Stabilization and destabilization of soil organic matter: Mechanisms and controls. Geoderma, 74, 65–105. https://doi.org/10.1016/S0016-7061(96)00036-5.

STRECKEISEN, A. 1980. Classification and nomenclature of volcanic rocks, lamprophyres, carbonatites and melilitic rocks IUGS Subcommission on the Systematics of Igneous Rocks. Geol Rundsch, 69, 194–207. https://doi.org/10.1007/BF01869032.

SWOBODA, P., DÖRING, T. F. & HAMER, M. 2022. Remineralizing soils? The agricultural usage of silicate rock powders: A review. Sci Total Environ, 807, 150976. https://doi.org/10.1016/j.scitotenv.2021.150976.

VAN ZWIETEN, L., KIMBER, S., MORRIS, S., CHAN, K. Y., DOWNIE, A., RUST, J., JOSEPH, S. & COWIE, A. 2010. Effects of biochar from slow pyrolysis of papermill waste on agronomic performance and soil fertility. Plant Soil, 327, 235–246. https://doi.org/10.1007/s11104-009-0050-x.

VANCE, E. D., BROOKES, P. C. & JENKINSON, D. S. 1987. An extraction method for measuring soil microbial biomass C. Soil Biol Biochem, 19, 703–707. https://doi.org/10.1016/0038-0717(87)90052-6.

VDLUFA 1991. Bestimmung von Phosphor und Kalium im Doppellactat(DL)-Auszug. Methodenbuch Band I Böden. Speyer, Germany: Verband Deutscher Landwirtschaftlicher Untersuchungs- und Forschungsanstalten e.V. (VDLUFA).

VOLK, M., BASSIN, S., LEHMANN, M. F., JOHNSON, M. G. & ANDERSEN, C. P. 2018. ^{13}C isotopic signature and C concentration of soil density fractions illustrate reduced C allocation to subalpine grassland soil under high atmospheric N deposition. Soil Biol Biochem, 125, 178–184. https://doi.org/10.1016/j.soilbio.2018.07.014.

VON LÜTZOW, M., KÖGEL-KNABNER, I., EKSCHMITT, K., MATZNER, E., GUGGENBERGER, G., MARSCHNER, B. & FLESSA, H. 2006. Stabilization of organic matter in temperate soils: mechanisms and their relevance under different soil conditions – a review. Eur J Soil Sci, 57, 426–445. https://doi.org/10.1111/j.1365-2389.2006.00809.x.

VON LÜTZOW, M., KÖGEL-KNABNER, I., LUDWIG, B., MATZNER, E., FLESSA, H., EKSCHMITT, K., GUGGENBERGER, G., MARSCHNER, B. & KALBITZ, K. 2008. Stabilization mechanisms of organic matter in four temperate soils: Development and application of a conceptual model. J Plant Nutr Soil Sc, 171, 111–124. https://doi.org/10.1002/jpln.200700047.

VORRATH, M.-E., AMANN, T., MEYER ZU DREWER, J., HAGEMANN, N., ALDRICH, C., BÖRKER, J., SEEDTKE, M., BECKER, J. N., HAGENS, M., ESCHENBACH, A. & HARTMANN, J. 2025. Pyrogenic carbon and carbonating minerals for carbon capture and storage (PyMiCCS) part II: organic and inorganic carbon dioxide removal in an Oxisol. Front Clim, Volume 7 - 2025. https://doi.org/10.3389/fclim.2025.1592454.

VORRATH, M.-E., HAMBURGER, S. E., MEYER ZU DREWER, J., KAMMANN, C. I., HAGEMANN, N. & HARTMANN, J. 2026. Water chemistry dataset from two rain events studying enhanced rock weathering and biochar as single and co-application and co-pyrolysis in a semi-field lysimeter experiment. https://doi.org/10.5281/zenodo.19065851.

WANG, D., FONTE, S. J., PARIKH, S. J., SIX, J. & SCOW, K. M. 2017. Biochar additions can enhance soil structure and the physical stabilization of C in aggregates. Geoderma, 303, 110–117. https://doi.org/10.1016/j.geoderma.2017.05.027.

WANG, J., XIONG, Z. & KUZYAKOV, Y. 2016. Biochar stability in soil: meta-analysis of decomposition and priming effects. GCB Bioenergy, 8, 512–523. https://doi.org/10.1111/gcbb.12266.

WENG, Z., VAN ZWIETEN, L., SINGH, B. P., TAVAKKOLI, E., JOSEPH, S., MACDONALD, L. M., ROSE, T. J., ROSE, M. T., KIMBER, S. W. L., MORRIS, S., COZZOLINO, D., ARAUJO, J. R., ARCHANJO, B. S. & COWIE, A. 2017. Biochar built soil carbon over a decade by stabilizing rhizodeposits. Nat Clim Change, 7, 371–376. https://doi.org/10.1038/nclimate3276.

WICKHAM, H. 2016. ggplot2: Elegant graphics for data analysis. New York, USA, Springer.

WICKHAM, H., FRANÇOIS, R., HENRY, L. & MÜLLER, K. 2023. dplyr: A Grammar of Data Manipulation - R package version 1.1.4. [Online].

WITZGALL, K., VIDAL, A., SCHUBERT, D. I., HÖSCHEN, C., SCHWEIZER, S. A., BUEGGER, F., POUTEAU, V., CHENU, C. & MUELLER, C. W. 2021. Particulate organic matter as a functional soil component for persistent soil organic carbon. Nat Commun, 12, 4115. https://doi.org/10.1038/s41467-021-24192-8.

XU, P., WANG, Q., DUAN, C., HUANG, G., DONG, K. & WANG, C. 2024a. Biochar addition promotes soil organic carbon sequestration dominantly contributed by macro-aggregates in agricultural ecosystems of China. J Environ Manage, 359, 121042. https://doi.org/10.1016/j.jenvman.2024.121042.

XU, T., LI, H., VICCA, S., GOLL, D. S., BEERLING, D. J., CHEN, Q., BI, B., YANG, Z., WANG, X. & YUAN, Z. 2025. Enhanced rock weathering promotes soil organic carbon accumulation: A global meta-analysis based on experimental evidence. Glob Chang Biol, 31, e70483. https://doi.org/10.1111/gcb.70483.

XU, T., YUAN, Z., VICCA, S., GOLL, D. S., LI, G., LIN, L., CHEN, H., BI, B., CHEN, Q., LI, C., WANG, X., WANG, C., HAO, Z., FANG, Y. & BEERLING, D. J. 2024b. Enhanced silicate weathering accelerates forest carbon sequestration by stimulating the soil mineral carbon pump. Glob Chang Biol, 30, e17464. https://doi.org/10.1111/gcb.17464.

YAN, Y., YIN, L., YAN, S., FANG, Y., WANG, A., ZHU, F., BAI, Y., ZHANG, Z. & ZHANG, W. 2025. Similar mineral-associated organic carbon formation but distinct efficiencies by powdered wollastonite addition between two soils. Soil Biol Biochem, 211, 109979. https://doi.org/10.1016/j.soilbio.2025.109979.

YANG, F., XU, Z., HUANG, Y., TSANG, D. C. W., OK, Y. S., ZHAO, L., QIU, H., XU, X. & CAO, X. 2021. Stabilization of dissolvable biochar by soil minerals: Release reduction and organo-mineral complexes formation. J Hazard Mater, 412, 125213. https://doi.org/10.1016/j.jhazmat.2021.125213.

YANG, F., ZHAO, L., GAO, B., XU, X. & CAO, X. 2016. The interfacial behavior between biochar and soil minerals and its effect on biochar stability. Environ Sci Technol, 50, 2264–2271. https://doi.org/10.1021/acs.est.5b03656.

YOO, G., KIM, H. & CHOI, J. Y. 2017. Soil aggregate dynamics influenced by biochar addition using the ^{13}C natural abundance method. Soil Sci Soc Am J, 81, 612–621. https://doi.org/10.2136/sssaj2016.09.0313.

ZHANG, Y., WANG, J. & FENG, Y. 2021. The effects of biochar addition on soil physicochemical properties: A review. CATENA, 202, 105284. https://doi.org/10.1016/j.catena.2021.105284.

A.7 Appendix

A7.1 Basanite rock powder properties

The chemical composition of the rock powder (Table A.2) was analyzed using X-ray fluorescence (XRF) at the Mineralogical Institute, University of Hamburg, while the mineralogical composition was determined by Qmineral using X-ray diffraction (XRD), as described in VORRATH et al., 2025. Following the classification of volcanic rocks by STRECKEISEN (1980) or LE BAS et al. (1986), this rock can be classified as a basanite. The basanite was obtained from Rheinische Provinzial-Basalt- u. Lavawerke, Sinzig, Germany.

Table A.2: Main compounds, trace elements, mineral composition and grain size of used basanite rock powder *Eifelgold*. Bdl = below detection limit; LOI = loss on ignition.

Main compounds	[wt%]	Trace Elements	[ppm]	Mineralogy	[wt%]	Grain size [µm]	[wt%]
SiO_2	43.86	As	bdl	Clinopyroxene	44.4	> 300	0.00
TiO_2	2.79	Ba	1026	Plagioclase	15.5	300 - 250	0.13
Al_2O_3	14.15	Bi	bdl	Nepheline	11.2	250 - 210	0.17
Fe_2O_3	11.28	Ce	104	Leucite	9.9	210 - 180	0.14
MnO	0.18	Co	51	Olivine	6.3	180 - 150	0.26
MgO	8.21	Cr	53	2:1 layer silicates	5.1	150 - 120	1.20
CaO	11.63	Cu	66	Hematite	3.1	120 - 100	2.87
Na_2O	3.26	Ga	17	Spinel-type minerals	1.9	100 - 86	4.17
K_2O	3.35	La	52	Apatite	1.1	86 - 74	5.67
P_2O_5	0.6	Nb	52	Analcime	0.9	74 - 62	8.13
SO_3	bdl	Nd	28	Quartz	0.7	62 - 52	8.89
LOI	0.44	Ni	124			52 - 44	8.50
Sum	*99.74*	Pb	5			44 - 36	9.63
		Rb	86			36 - 30	7.86
		Sc	22			30 - 26	5.50
		Sr	882			26 - 22	5.64
		Th	8			22 - 18	5.72
		U	3			18 - 0.5	25.52
		V	302				
		Y	24				
		Zn	90				
		Zr	271				

A7.2 Randomized complete block design

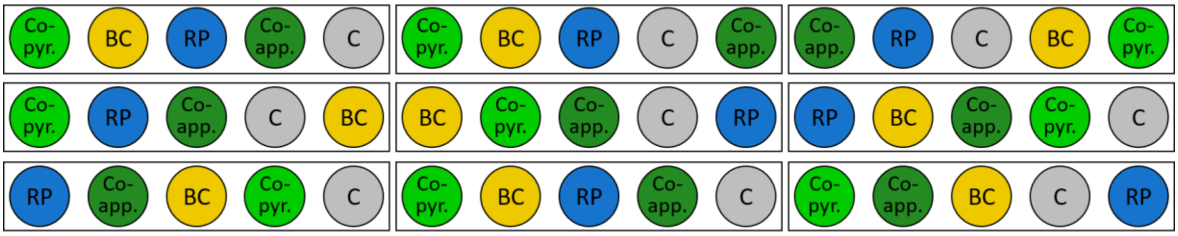

Figure A.4: Visualization of randomized complete block design of lysimeter experiment. Squares represent blocks, circles represent lysimeters. C = control treatment, RP = rock powder treatment containing basanite, BC = biochar treatment, Co-app. = co-application treatment, Co-pyr. = co-pyrolysis treatment containing rock-enhanced biochar.

Study B:

Biochar dominated the combined effect of silicate rock powder and biochar application on extracellular enzyme kinetics and nutrient dynamics in a sandy soil

Maria Ansari[a]*, Svenja Stock[b], Michaela A. Dippold[b], Susanne E. Hamburger[c], Claudia I. Kammann[c], Johannes Meyer zu Drewer[d,e,f], Nikolas Hagemann[d,e], Annette Eschenbach[a], Joscha N. Becker[a]

[a] Institute of Soil Science, University of Hamburg, Hamburg, Germany
[b] Geo-Biosphere Interactions, Department of Geosciences, Eberhard Karls University of Tübingen, Tübingen, Germany
[c] Department of Applied Ecology, Hochschule Geisenheim University, Geisenheim, Germany
[d] Ithaka Institute, Goldbach, Germany
[e] Agroscope, Zurich, Switzerland
[f] Institute of Sustainable Energy Systems, Offenburg University, Offenburg, Germany

*corresponding author

Ansari, M., Stock, S., Dippold, M. A., Hamburger, S. E., Kammann, C. I., Meyer zu Drewer, J., Hagemann, N., Eschenbach, A. & Becker, J. N. (2026). Biochar dominated the combined effect of silicate rock powder and biochar application on extracellular enzyme kinetics and nutrient dynamics in a sandy soil. Soil Till Res, 262, 107234. https://doi.org/10.1016/j.still.2026.107234.

B. Abstract

The application of biochar or silicate rock powder as soil amendments combines carbon dioxide removal with soil improvement. However, their combined short-term effects on nutrient dynamics and microbial activity are poorly understood. Therefore, we combined wood biochar and basanite powder via co-application and via co-pyrolysis of biomass and basanite to rock-enhanced biochar in a nine-week semi-field-based lysimeter experiment with cabbage turnip (*Brassica oleracea* var. *gongylodes* L.). We measured carbon (C), nitrogen (N), available phosphorous (P), mineral N, dissolved organic C (DOC), microbial biomass C (C_{mic}), soil pH, and electric conductivity (EC). We examined extracellular enzyme kinetics of ß-glucosidase (BG), chitinase (CH), leucine-aminopeptidase (LAP), and acid phosphatase (AP) related to C, N, and P cycles. From potential enzyme activity (V_{max}) of BG, LAP, and AP we calculated extracellular enzyme stoichiometry (EES), vector angle and length to assess nutrient limitations.

In combined applications, the influence of biochar was dominant. The application of biochar-containing amendments (biochar, co-application, co-pyrolyzed rock-enhanced biochar) to our sandy topsoil significantly increased C, P, DOC, C_{mic}, pH, and EC. Co-application even exceeded single biochar in increasing N, pH, and EC. Single biochar application resulted in the highest short-term P availability, while combined applications potentially result in a long-term P supply. While LAP's V_{max} increased following biochar-containing amendment application, V_{max} of the other enzymes decreased. Although AP showed the highest V_{max}, indicating a P limitation, the enzyme patterns and EES suggest an increased N demand and a shift from P-limited towards a more balanced microbial nutrient demand following biochar-containing amendment application.

Keywords

basanite, carbon dioxide removal (CDR), nutrient demand, fluorometric enzyme assay, rock-enhanced biochar, enhanced rock weathering (ERW)

Highlights

- Combined applications mainly driven by biochar, not by basanite
- Biochar and combined applications increased P availability and relative N demand
- Co-pyrolysis showed no advantage compared to co-application of biochar and basanite

- No basanite weathering during 9-week planted lysimeter experiment visible in soil
- Basanite application caused no negative effects, highlighting its CDR potential

B.1 Introduction

Biochar is a carbon-rich solid produced from biomass by pyrolysis (HAGEMANN et al., 2018; LEHMANN & JOSEPH, 2024) and is traditionally used as a soil amendment around the world (ALLEN, 1847; GLASER et al., 2001; WIEDNER et al., 2015). Due to its high aromaticity, biochar carbon is barely bioavailable and largely stabilized against decomposition (ZIMMERMAN, 2010; AMELOOT et al., 2013; KUZYAKOV et al., 2014; WANG et al., 2016). Thus, soil-applied biochars are a long-term carbon (C) sink (STEINER et al., 2007; RECHBERGER et al., 2017; LEHMANN et al., 2021) providing carbon dioxide removal (CDR). Nevertheless, biochars contain a labile fraction consisting of more easily available C and nutrients (BAKSHI et al., 2018; ZHAO et al., 2018). Biochars can maintain or improve soil properties (JOSEPH et al., 2010; SCHMIDT et al., 2021), e.g. by increasing soil pH (CHINTALA et al., 2014; DAI et al., 2017) and enhancing nutrient availability (GLASER & LEHR, 2019; HOSSAIN et al., 2020; BEKCHANOVA et al., 2024). The application of biochars often result in an increased microbial biomass C (C_{mic}) as well as microbial activity and can shift microbial community composition, which in turn may alter nutrient cycles and affect plant growth (LEHMANN et al., 2011; BUSS et al., 2021).

Silicate rock powder is applied to agricultural soils for enhanced rock weathering (ERW) as a CDR technology and due to its potential to influence key soil properties and thus increase soil fertility (ABDALQADIR et al., 2024; DUPLA et al., 2024) and yield (HAQUE et al., 2020; SWOBODA et al., 2022). During silicate rock weathering, cations and anions, such as potassium and phosphorus (P), are released (AMANN et al., 2020; GUO et al., 2023; BEERLING et al., 2025), resulting in an increased nutrient content (BUSS et al., 2023). Silicate rock powder application can increase soil pH (SWOBODA et al., 2022; XU et al., 2024a) and by this increase the availability of nutrients, such as P, even further (SWOBODA et al., 2022; BEERLING et al., 2025). These changes in soil properties can result in an altered C_{mic} (SOKOL et al., 2024; XU et al., 2024b) and a shift in microbial community (CARSON et al., 2007; ZHOU et al., 2018). The activity of soil microorganisms can in return stimulate the weathering of silicate rock powder (BUSS et al., 2021; LI et al., 2025; REGINATO, 2025). Even though VICCA et al. (2022) underlined the importance of biological processes for the efficiency of ERW, little is known about the coupling between ERW and soil microorganisms.

Most recent research considered biochar and silicate rock powder separately, while their combined application could offer synergistic effects for CDR as well as for key soil properties and processes, such as nutrient cycles and microbial activity (AMANN & HARTMANN, 2019; BUSS et al., 2021). In addition to simple co-application, co-pyrolysis of biomass and rock powder to rock-enhanced biochar provides another potential approach to combine those soil amendments (MEYER ZU DREWER et al., 2025; VORRATH et al., 2025). The effects of such combined applications of those two amendments on soil properties, including nutrient dynamics and microbial processes, is currently unknown.

Soil microorganisms produce and release extracellular enzymes to meet their nutrient demand (ALLISON et al., 2011; JIN et al., 2024). These extracellular enzymes can trigger the degradation of complex organic substances into smaller molecules (SHI, 2011), thereby enhancing nutrient availability for microbial uptake (ALLISON et al., 2011; JIN et al., 2024). However, after their release, extracellular enzymes can be adsorbed to reactive particle surfaces, such as soil organic matter (ALLISON, 2006; BURNS et al., 2013; LUO et al., 2017) or biochar (LEHMANN et al., 2011). Despite this immobilization, absorbed enzymes remain a significant reservoir of potential enzyme activity, responding rapidly to changes in nutrient availability (BURNS et al., 2013). Consequently, extracellular enzymes serve as valuable indicators for nutrient cycling and availability in soils (LUO et al., 2017). The enzyme ß-glucosidase (BG) is one of the primary catalysts of cellulose degradation to glucose and thus plays an important role in the soil C cycle (BAKSHI & VARMA, 2011; MOORHEAD et al., 2016). Chitinase (CH) is responsible for the degradation of chitin and is part of both C and nitrogen (N) cycle in soils (BAKSHI & VARMA, 2011). Leucine-aminopeptidase (LAP) can catalyze the cleavage of leucine amino acid from peptide substrates, such as proteins, and thus is an indicative part of the soil N cycle (MOORHEAD et al., 2016). Acid phosphatase (AP) can catalyze the hydrolysis of esters and anhydrides of phosphoric acids, leading to a release of inorganic P for soil microbes and plants (BAKSHI & VARMA, 2011; MOORHEAD et al., 2016). The ratios of the potential activities of these enzymes involved in C, N, and P cycling, referred to as extracellular enzyme stoichiometry (EES), and the resulting enzymatic C:N:P ratio can indicate microbial nutrient limitations (SINSABAUGH et al., 2008; YANG et al., 2020).

It has not been studied yet how the combined application of biochar and silicate rock powder, such as basanite, to soils influence nutrient cycles and microbial enzyme kinetics. We hypothesize that the combined application of biochar and basanite (i) significantly improves soil properties relevant to microbial activity, leading to changes in (ii) the extracellular enzyme kinetics of BG, CH, AP, and LAP as well as (iii) EES, compared to unamended soils. We further investigate how these effects compare to those of single biochar or single basanite application. The combined application of biochar and basanite was tested as a simple co-application of both amendments and as rock-enhanced biochar. We conducted a semi-field experiment in lysimeters using sandy agricultural soil (control) amended with either biochar (biochar treatment), basanite powder (rock powder treatment), rock-enhanced biochar (co-pyrolysis treatment), or the co-application of biochar and basanite powder (co-application treatment). We sampled and analyzed the soil samples after the plant harvest for soil properties, such as pH and exchangeable nutrients, and conducted a fluorometric enzyme assay followed by EES calculations.

B.2 Material and methods

B2.1 Soils and amendments

The study was conducted using a sandy arable topsoil (0-30 cm; Table B.1). The soil was collected in summer 2023 in Northern Germany (Gräflich Bernstorff'sche Betriebe, Gartow, Germany, 53°01'26.9"N 11°27'12.7"E) and was air-dried until used in summer 2024.

We used four different soil amendments for this study. The biochar was produced from a mixture of wood chips and woody sieving residues from green waste composting in a weight-ratio of 1:1. This woody biomass was pyrolyzed at 650 °C for 20 minutes on a Pyreg 500 (Pyreg GmbH, Dörth, Germany) full scale commercial pyrolysis unit (Sonnenerde GmbH, Riedlingsdorf, Austria) (Table B.1). As silicate rock powder, we used the locally available basanite *Eifelgold* with a grain size between 0.5 and 300 µm (further information in Table B.2 in Appendix). Additionally, two combined applications of biochar and basanite were used – co-application and co-pyrolysis. For the latter, the woody biomass and basanite were mixed in a weight-ratio of 80:20, pelletized, and afterwards pyrolyzed at 650 °C for 20 minutes to produce rock-enhanced biochar (Table B.1). Based on the TOC contents of biochar and rock-enhanced biochar, we calculated that the rock-enhanced biochar consisted of ~68% biochar and ~32% basanite. To compare the effect of combined pyrolysis to a simple mixing, we co-applied biochar and basanite in the same ratio as found in the rock-enhanced biochar. More detailed information about the amendments can be found in Meyer zu Drewer & Hagemann (2025).

Table B.1: Properties of temperate sandy agricultural topsoil, biochar, and rock-enhanced biochar.

Properties	Soil[a]	Biochar[b]	Rock-enhanced-biochar[b]
pH [$CaCl_2$]	4.7 ± 0.0	9.0	9.2
C [g kg^{-1}]	12.4 ± 0.0	494	336
TOC [g kg^{-1}]	12.0 ± 0.0	482	332
TIC [g kg^{-1}]	0.4 ± 0.0	12	4
N [g kg^{-1}]	1.1 ± 0.0	7.0	4.1
C:N	11.3 ± 0.0	80	82
H:C	n.d.	0.35	0.23
O:C	n.d.	0.14	0.08
P_2O_5 [g kg^{-1}]	n.d.	9	8
Ash [%]	n.d.	44.3	62.9
Sand [%]	93.83 ± 1.15	n.a.	n.a.
Silt [%]	2.47 ± 0.77	n.a.	n.a.
Clay [%]	3.70 ± 0.46	n.a.	n.a.

[a] Values are the mean of analytical replicates (n = 3), [b] values were measured by Eurofins according to the analytical guidelines of the European Biochar Certificate (EBC, 2024). C = total carbon, TOC = total organic carbon, TIC = total inorganic carbon, N = total nitrogen, n.d. = not determined, n.a. = not applicable.

B2.2 Experimental design

We used 45 lysimeters (each 20 cm diameter, 30 cm soil depth, stainless steel mesh allowing drainage into a catchment vessel below) consisting of five treatments (n = 9). The lysimeter tubes with their catchment vessels were embedded in sand beds to enable closer-to-natural soil temperatures compared to pot experiments. The leachate in the catchment vessel was pumped out regularly to prevent water accumulation. Inside the lysimeters, bags consisting of PVC were installed to contain the samples. For the control treatment, the bags inside the lysimeters were filled with 9 kg of soil (dry weight equivalent). For the biochar treatment, 379.1 g of biochar (equals ~4.2 wt%) was mixed with the soil and the mixture was filled into the respective bags and installed in the lysimeters. The rock powder treatment contained soil mixed with 178.2 g of basanite powder (equals ~2 wt%). The co-pyrolysis treatment was filled with a mixture of soil and 557.3 g of rock-enhanced biochar (equals ~6.2 wt% consisting of ~4.2 wt% biochar and ~2 wt% basanite powder). For the equivalent co-application treatment, the bag within the lysimeter was filled with a mixture of soil, 379.1 g of biochar (equals ~4.2 wt%), and 178.2 g of basanite powder (equals ~2 wt%). The lysimeters containing the different treatments were arranged in a randomized complete block design (Figure B.5 in Appendix).

Every lysimeter was planted with one cabbage turnip (*Brassica oleracea* var. *gongylodes* L.) seedling each. The seedlings were as similar as possible in development and strength by selecting them from a larger batch. Fertilizer (CARBUNA AND, Carbuna AG, Memmingen, Germany as organic fertilizer based on Vinasse and mineral fertilizer Ferty 2 Mega, Hauert MANNA Düngerwerke GmbH, Nürnberg, Germany) was applied five times over the nine weeks of plant growth. The lysimeters were watered by rainfall and, if necessary, by drip irrigation.

B2.3 Soil sampling and processing

After nine weeks of plant growth, the lysimeter experiment was harvested in July 2024 (no visible effect of amendment application on plant growth, see HAMBURGER et al. (2026)). The soil was sieved through a 2 mm sieve to remove coarse soil fragments and roots. Since biochar and rock-enhanced biochar have not been crushed prior to application, coarse amendment particles were also removed while sieving. A subsample of the sieved soil material was stored in a 2 ml Eppendorf Tube® at 4 °C until the enzyme assay was conducted (description see chapter B2.5 and appendix chapter B7.3). Another subsample was stored in a plastic bag at 4 °C for further physical and chemical analysis. The remaining sieved soil was air dried.

B2.4 Physical and chemical analysis of soil samples

Dried soil samples were used to measure total C and total N contents using an elemental analyzer (Vario Max Cube, Elementar Analysensysteme GmbH, Langenselbold, Germany). Due to the low soil pH of our samples (< 6.5), we consider total C and TOC as equivalent. Available P content was determined using calcium lactate and hydrochloric acid following VDLUFA (1991) and measured using a spectrophotometer (DR5000, Hach Lange GmbH, Düsseldorf, Germany) with a wavelength of 580 nm. Soil pH was determined in 0.01 M $CaCl_2$ solution (soil : $CaCl_2$ solution = 1:2.5) using a pH meter (MP230, Mettler-Toledo GmbH, Gießen, Germany). The electric conductivity (EC) was measured in deionized water (soil : water = 1:2.5) using a conductivity meter (Cond 330i, WTW GmbH, Weilheim, Germany).

The water content (WC) of the fresh samples was determined by weighing the difference between the cooled sample and after drying the sample at 105 °C until constant weight. Mineral N (N_{min}) of the cooled samples was extracted following DIN (2005) using 0.0125 M $CaCl_2$ and the extract was measured using a spectrophotometer (LLG-unispec 4, Lab Logistics Group GmbH, Meckenheim, Germany) for ammonium and using high performance liquid chromatography (1100 HPLC, Agilent Technologies Inc., Santa Clara, California, USA) for nitrate and nitrite. These field-moist samples were also used to determine C_{mic} using the chloroform fumigation extraction (CFE) method after DIN (2011) adapted from VANCE et al. (1987). Two times 12.5 g dry weight equivalent per sample were weighed in glass flasks. One of the samples was directly extracted with 50 ml of 0.05 M K_2SO_4 solution to quantify dissolved organic carbon (DOC). The second sample was fumigated with chloroform to lyse microbial cell walls and was afterwards also extracted using K_2SO_4 solution. The extracts were analyzed using a TOC analyzer (TOC-L, Shimadzu Corporation, Kyoto, Japan). To be able to measure the CFE extracts also at an isotopic ratio mass spectrometer, we used 0.05 M K_2SO_4 solution (WERTH & KUZYAKOV, 2010). The difference between the extracted C contents in fumigated and non-fumigated samples is interpreted as C_{mic}, using an extraction factor k_{EC} of 0.45 (JOERGENSEN, 1996).

B2.5 Fluorometric enzyme assays

Enzyme activities were determined as a proxy for nutrient dynamics using fluorogenic substrates (). Four fluorogenic substrates were used associated with either 4-methylumbelliferon (MUF) or 7-amido-4-methylcoumarin (AMC): MUF-ß-D-glucoside (for detection of BG), MUF-N-acetyl-ß-D-glucosidase (for detection of CH), MUF-phosphatase (for detection AP), and L-leucine-AMC-hydrochloride (for detection of LAP).

Homogenized cooled (4 °C) soil samples (0.5 g dry weight equivalent) were weighed in sterile 100 ml glass flasks and 50 ml of sterile water was added. Each sample was sonicated using an ultrasonication probe for two minutes with an output energy of 40 J s^{-1}. A volume of 50 µl of the soil suspensions was pipetted into sterile deep-well plates (Nunc™ F96 MicroWell™ plate, black, 96 well, Thermo Scientific™). Afterwards, 50 µl of MES or TRIZMA buffer (for MUF- and AMC-linked substrates respectively) and 100 µl of substrate solution were added. The use of differently concentrated substrate solutions resulted in final concentrations of 0, 1, 2, 3, 4, 5, 10, and 20 µmol g^{-1} dry soil for MUF-linked substrates and of 0, 1, 2, 3, 5, 10, 20, and 40 µmol g^{-1} dry soil for AMC-linked substrates in the deep-well plates. Three analytical replicates were measured for each sample at each substrate concentration.

For calibration, soil suspensions (50 µl per well) and MES or TRIZMA buffer solutions (150, 140, 130, 100, 70, and 30 µl, respectively) were mixed in deep-well plates with either 10 µM MUF or AMC standards (0, 10, 20, 50, 80, and

120 µl, respectively). Fluorescence of all deep-well plates was measured directly and 120 minutes after substrate addition (excitation wavelength of 355 nm, emission wavelength of 460 nm) using a microplate reader (Victor[3] 1420-05 Multi label Counter, PerkinElmer, USA). A more detailed description of the method can be found in appendix chapter B7.3.

B2.6 Data analysis

The kinetic parameters V_{max} and K_m were calculated using the Michaelis Menten equation (Equation B1; after MICHAELIS & MENTEN, 1913), while soil enzyme efficiency K_a was calculated using Equation B2 (after NDOSSI et al., 2020; XIAO et al., 2024):

$$v = (V_{max} * [S]) / (K_m + [S]) \qquad \text{(Equation B1)}$$

$$K_a = V_{max} / K_m \qquad \text{(Equation B2)}$$

where v is the reaction rate of the respective soil enzyme at a certain substrate concentration (nmol MUF/AMC h^{-1} g^{-1} dry soil), V_{max} represents the maximum rate of soil enzyme reaction at saturated substrate concentration at the given temperature (nmol substrate h^{-1} g^{-1} dry soil), K_m is the substrate concentration at ½ Vmax (µmol g^{-1} dry soil) representing the respective enzyme binding affinity to its specific substrate, $[S]$ is the substrate concentration (µM), and K_a is the catalytic enzyme efficiency.

Extracellular enzyme stoichiometry (EES), a proxy for microbial nutrient demand, was calculated as the ratio of C- (BG), N- (LAP), and P-related (AP) enzymes after the concept of SINSABAUGH et al. (2008) following the descriptions of DENG et al. (2019) and YANG et al. (2020):

$$\text{Enzyme C:N ratio} = \ln(V_{max}\,BG)\ /\ \ln(V_{max}\,LAP) \qquad \text{(Equation B3)}$$

$$\text{Enzyme C:P ratio} = \ln(V_{max}\,BG)\ /\ \ln(V_{max}\,AP) \qquad \text{(Equation B4)}$$

$$\text{Enzyme N:P ratio} = \ln(V_{max}\,LAP)\ /\ \ln(V_{max}\,AP) \qquad \text{(Equation B5)}$$

The ratio of the activities of C-, N-, and P-acquiring enzymes is used to assess soil microbial nutrient limitation. While a ratio of C:N:P (lnBG : lnLAP : lnAP) of 1:1:1 represents an equilibrated system, a value >1 indicates a limitation of the respective nutrient. To have comparable ratios for the five treatments, the ratios were standardized to a C-value of 1. In addition, these ratios can be used to calculate the length and the angle of connecting the respective nutrient ratio in a C:N-to-C:P figure relative to the figure origin The vector length indicates the relative C-to-P/N-limitation with an increasing vector length suggesting an increasing C limitation. The vector angle indicates a relative N-to-P-limitation, with a vector angle <45° representing N limitation and >45° representing P limitation (MOORHEAD et al., 2016; DING et al., 2016). Vector length and angle were calculated after MOORHEAD et al. (2016):

$$\text{vector length} = \sqrt{(x^2 + y^2)} \qquad \text{(Equation B6)}$$

$$\text{vector angle} = \arctan(x, y) \qquad \text{(Equation B7)}$$

where x is the enzyme C:P ratio and y the enzyme C:N ratio.

To test for significant differences ($p < 0.05$), we used a linear mixed effects (LME) model and a linear model for enzyme kinetics and soil properties, respectively, followed by a Tukey HSD post-hoc test for pairwise comparison. Outliers of v, V_{max}, K_m, K_a, and EES were detected using the Dixon's Q test to check the measurement accuracy and to check the influence of sample and block on measurement results. P-values < 0.1 are in general interpreted as the tendency towards a difference. All calculations and statistical tests were conducted in RStudio (version 4.4.2) using 'outliers' package (KOMSTA, 2022) to detect outliers, 'lme4' package (BATES et al., 2015) for LME computing, 'multcomp' package (HOTHORN et al., 2008) for compact letter display, 'ggplot2' package (WICKHAM, 2016) for data visualization, and 'ggcorrplot' package (KASSAMBARA, 2023) for correlation matrices.

Differences (%) of amended treatments compared to control were calculated using Equation B8:

$$\text{difference} = \frac{value_{control} - value_{amended}}{value_{amended}} * 100 \qquad \text{(Equation B8)}$$

where $value_{control}$ is the measured or calculated value of the control treatment and $value_{amended}$ is the measured or calculated value of the amended treatments (rock powder, biochar, co-application, and co-pyrolysis treatment).

B.3 Results

B3.1 Effect of amendment application on soil properties

The application of biochar-containing amendments (biochar, co-application, and co-pyrolysis treatments) significantly increased the soil C content by up to 69% (Figure B.1A). The co-application significantly increased N contents by 8%, while neither biochar nor co-pyrolysis treatment altered N contents (Figure B.1B). Since the increase in C content was more pronounced than the increase in N content, the C:N ratio was significantly increased in the biochar-containing treatments (Figure B.1C).

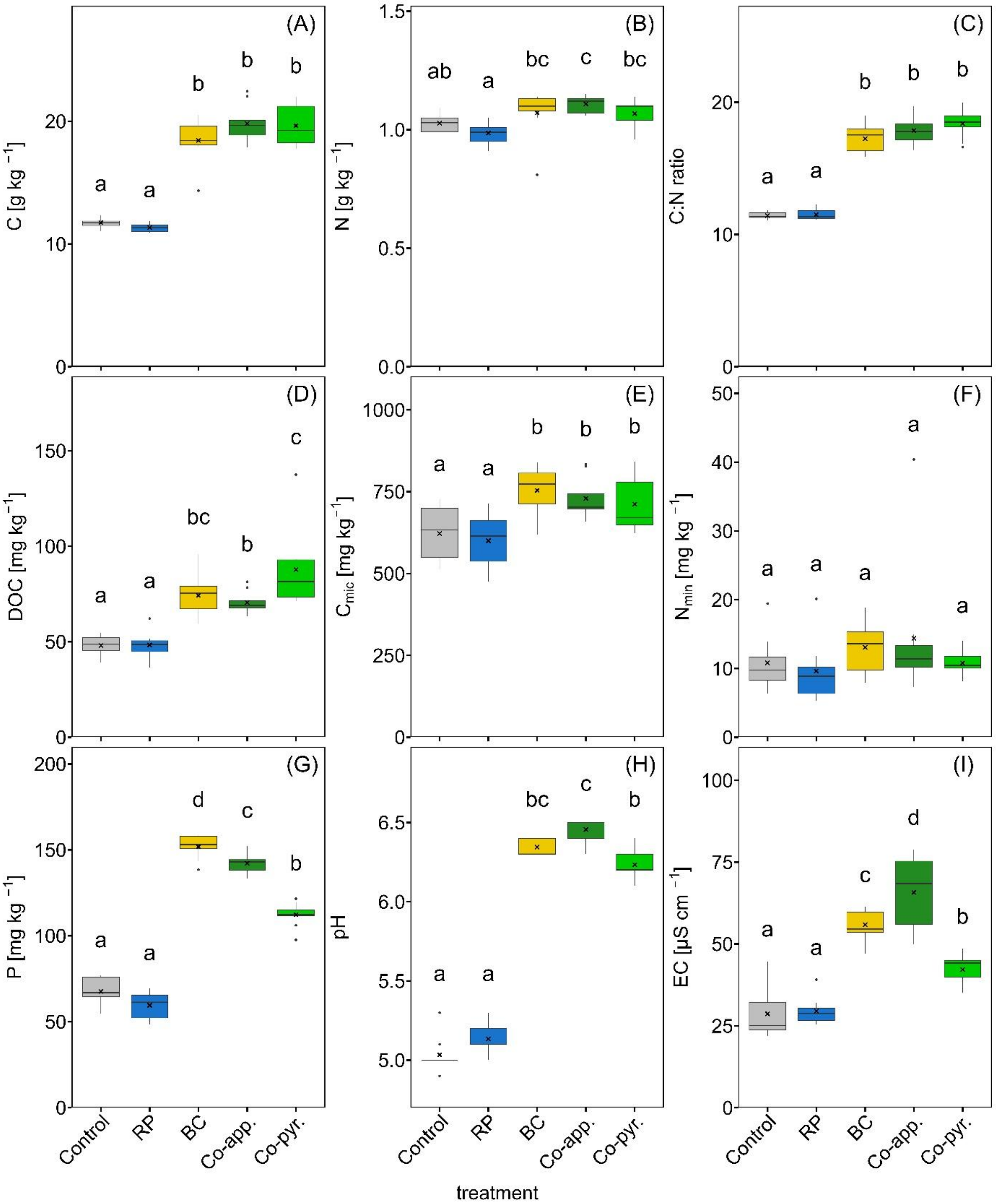

Figure B.1: Total C content (A), total N content (B), C:N ratio (C), dissolved organic carbon (DOC) content (D), microbial biomass C (C_{mic}) content (E), total mineral N (N_{min}) content (F), available P content (G), pH in $CaCl_2$ (H), and electric conductivity (EC) (I) of five treatments of soil with different amendments (n = 9 per treatment). RP = rock powder treatment containing basanite, BC = biochar treatment, Co-app. = co-application treatment, Co-pyr. = co-pyrolysis treatment containing rock-enhanced biochar. Small letters indicate significant differences ($p < 0.05$) between treatments within one soil property.

The application of biochar-containing amendments significantly increased DOC, C_{mic}, P, pH, and EC compared to control (Figure B.1 D, E, G, H, I). Additionally, all of these soil properties except C_{mic} showed significant differences between the three biochar-containing treatments. The available P content was increased by 125% in biochar treatment compared to the control, followed by the co-application treatment with an increase of 110% (Figure B.1G). A lower, but still significant increase in P content of 65% was visible in co-pyrolysis treatment compared to control. For pH and EC, their increase was higher in co-application treatment compared to co-pyrolysis treatment (Figure B.1 H, I). The increase in DOC content by 83% was most pronounced in co-pyrolysis treatment and lowest in co-application treatment (47%; Figure B.1D). For both pH and DOC content the increase following biochar application was not significantly different from both combined amendments (Figure B.1 D, H).

In contrast to the strong effect of biochar-containing amendments, basanite application alone did not alter any of the analyzed soil properties significantly (Figure B.1 A-I). Only the available P content tended to decrease ($p < 0.1$) following basanite application (Figure B.1G). The only soil property analyzed in this study, which was not influenced by any of the amendments, was N_{min} (Figure B.1F).

B3.2 Effect of amendment application on extracellular enzyme kinetics

Potential enzyme activity V_{max} was generally highest for AP with values up to 24 times higher in all treatments compared to the other enzymes ($p < 0.001$), while LAP tended generally to have the lowest V_{max} ($p < 0.1$; Figure B.2 A-D). The application of biochar-containing amendments strongly influenced V_{max} of all four enzymes. Both biochar and co-application treatment resulted in a significant decrease of V_{max} for AP and CH compared to control by up to 57%. The co-pyrolysis treatment had the smallest influence among the three biochar-containing treatments on V_{max}. The co-pyrolysis treatment significantly decreased V_{max} of AP by 35% compared to control but showed a significantly lower effect compared to biochar treatment. While biochar-containing amendments mainly decreased V_{max} of AP and CH, V_{max} of LAP showed the opposite pattern. Both biochar and co-application doubled V_{max} of LAP compared to control treatment and the co-pyrolysis treatment tended to increase V_{max} ($p < 0.1$) compared to control by 45%. In contrast to the strong effect of biochar-containing amendments, basanite application did not influence V_{max} for all four enzymes compared to the control.

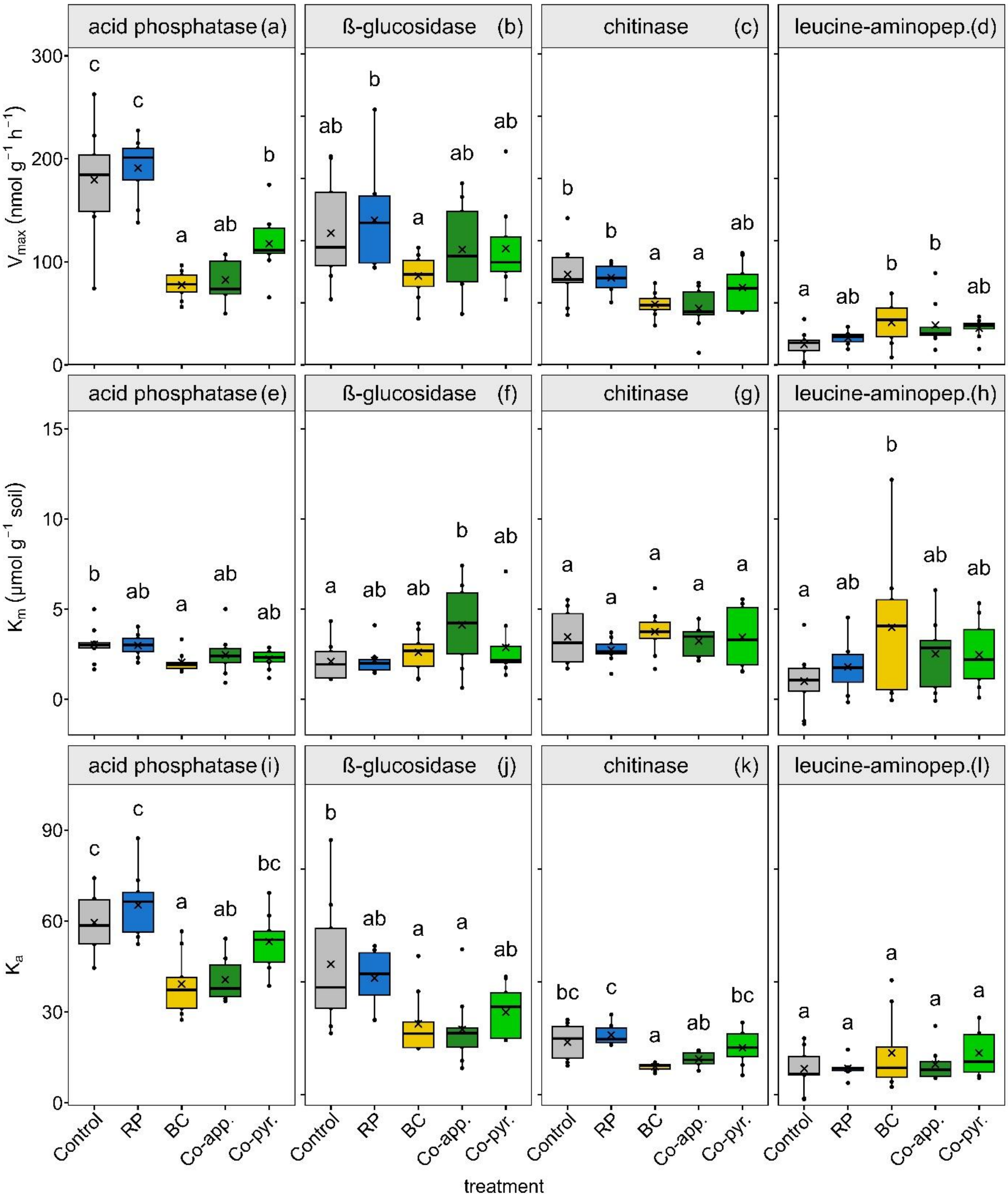

Figure B.2: Potential enzyme activity V_{max} (a-d), enzyme affinity K_m (e-h), and catalytic enzyme efficiency K_a (i-l) of acid phosphatase (AP), ß-glucosidase (BG), chitinase (CH), and leucine-aminopeptidase (LAP) in five treatments of soil with different amendments (n = 9 per treatment). RP = rock powder treatment containing basanite, BC = biochar treatment, Co-app. = co-application treatment, Co-pyr. = co-pyrolysis treatment containing rock-enhanced biochar. Small letters indicate significant differences ($p < 0.05$) between treatments within one parameter and enzyme. To increase readability, the y-axis of BG, CH, and LAP for V_{max} and K_a have a higher resolution than those of AP.

The differences in K_m between enzymes and treatments is less pronounced than the differences between enzyme and treatments we observed in V_{max} (Figure B.2 E-H). The application of biochar decreased K_m of AP by 33% and quadrupled K_m of LAP compared to control, while it did not influence K_m of BG and CH. The co-application increased K_m of BG by 97% compared to control, but had no significant effects on K_m of the AP, CH, and LAP. Both basanite and co-pyrolysis treatments did not alter K_m of any of the enzymes.

In all treatments, AP showed up to 16 times higher enzyme efficiency K_a compared to BG, CH, and LAP (Figure B.2 I-L). Both biochar and co-application significantly decreased K_a of AP and BG by up to 50% and decreased (biochar) or tended to decrease (co-application) K_a of CH by up to 45% compared to control (Figure B.2 I-K). Reflecting the patterns of V_{max}, co-pyrolysis treatment had the smallest influence on K_a of the three biochar-containing amendments (biochar, co-application, and co-pyrolysis treatments). The co-pyrolysis treatment tended to lower the K_a value of BG compared to control ($p < 0.1$), while it did not alter K_a of AP, CH, and LAP. In contrast to AP, BG, and CH, K_a of LAP was not influenced by the application of biochar-containing amendments (Figure B.2L). Basanite application in general did not significantly influence K_a of any of the studied enzymes.

Soil extracellular enzyme stoichiometric C:N and N:P ratio changed signify-cantly through the application of biochar-containing amendments compared to control, while the C:P ratio was not altered (Figure B.3). The enzyme C:N ratio decreased by up to 42% compared to control (Figure B.3A), while the enzyme N:P ratio was up to doubled following the application of biochar-containing amendments (Figure B.3C). Based on those C:N, C:P, and N:P ratios, the combined enzymatic C:N:P ratios reflected the strong influence of biochar-containing amendments on N dynamics. The control treatment had an enzymatic C:N:P ratio of 1:0.28:1.74. Biochar application had the strongest influence and resulted in an enzymatic C:N:P ratio of 1:0.66:1.67, followed by co-pyrolysis and co-application treatments with enzymatic C:N:P ratios of 1:0.62:1.59 and 1:0.60:1.56, respectively. Basanite application did neither alter EES nor the enzymatic C:N:P ratio significantly compared to control.

The control treatment had a calculated vector length of 2.5 ± 0.5 and an angle of 76.4° ± 3.4° (Figure B.4). The application of biochar-containing amendments resulted in a decrease in vector length and angle, most pronounced in the biochar treatment with a calculated vector length of 1.5 ± 0.2 and an angle of 66.4° ± 4.5°. Basanite application did neither alter vector length nor angle compared to control.

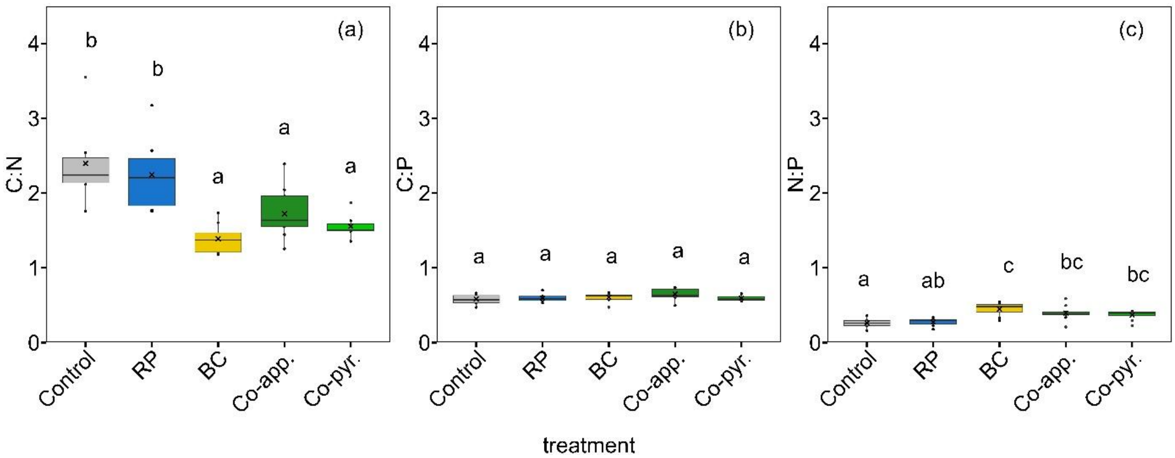

Figure B.3: Extracellular enzyme stoichiometry (EES) ratios of C:N (ln(BG): ln(LAP)) (a), C:P (ln(BG): ln(AP)) (b), and N:P (ln(LAP): ln(AP)) (c) in five treatments of soil with different amendments (n = 9 per treatment). ln(BG) = ln of V_{max} of ß-glucosidase, ln(LAP) = ln of V_{max} of leucine-aminopeptidase, ln(AP) = ln of V_{max} of acid phosphatase. RP = rock powder treatment containing basanite, BC = biochar treatment, Co-app. = co-application treatment, Co-pyr. = co-pyrolysis treatment containing rock-enhanced biochar. Small letters indicate significant differences ($p < 0.05$) between treatments within one stoichiometric ratio.

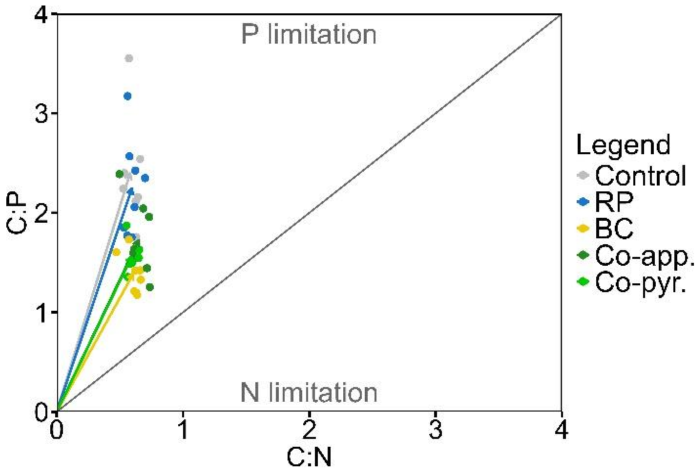

Figure B.4: Relationship between ratios of C:N (ln(BG):ln(LAP)) and C:P (ln(BG):ln(AP)) in five treatments of soil with different amendments (n = 9 per treatment) with arrows indicating the treatment-specific vector length from the figure origin. The angle between the vector and the x axis represents the vector angle. ln(BG) = ln of V_{max} of ß-glucosidase, ln(LAP) = ln of V_{max} of leucine-aminopeptidase, ln(AP) = ln of V_{max} of acid phosphatase. RP = rock powder treatment containing basanite, BC = biochar treatment, Co-app. = co-application treatment, Co-pyr. = co-pyrolysis treatment containing rock-enhanced biochar.

B3.3 Correlation between soil properties and enzyme kinetics

The enzyme kinetics (V_{max}, K_m, K_a) and analyzed soil properties showed strong significant correlations for all four enzymes. For AP, enzyme kinetics showed strong negative correlations with all investigated soil properties across all treatments (Figure B.6 in Appendix). The effects of C, N, P, and C_{mic} content as well as pH and EC were especially pronounced on AP's V_{max} but were often also significant in K_m and K_a. Similarly to AP, V_{max} and K_a (but not K_m) of CH showed negative but less pronounced correlations with C, P, and C_{mic} content as well as pH and EC (Figure B.7 in Appendix). The enzyme kinetics of CH did not correlate significantly with N_{min} and N contents. The enzyme kinetics of BG showed several negative correlations the analyzed soil properties, such as DOC and C_{mic} content as well as pH and P content (Figure B.8 in Appendix). In contrast to AP, BG, and CH, the enzyme kinetics of LAP showed solely positive correlations with the analyzed soil properties (Figure B.9 in Appendix). Both V_{max} and K_m of LAP correlated positively with C, N, and P content as well as C:N ratio and soil pH. Catalytic enzyme efficiency K_a of LAP correlated positively with only DOC content.

B.4 Discussion

B4.1 Influence of amendments on soil C, pH, and nutrients

The application of all three biochar-containing amendments (biochar, co-application, and co-pyrolysis treatments) increased C content, C:N ratio, and C_{mic} content equally strong within our nine-week experiment. Consequently, synergistic or diminishing effects of rock powder on those soil properties were absent in both combined applications (co-application and co-pyrolysis treatments). Increased C content (GROSS et al., 2021; CHAGAS et al., 2022; WANG et al., 2025a), C:N ratio (DING et al., 2023), and C_{mic} content (LEHMANN et al., 2011; LIU et al., 2015; BUSS et al., 2021; CHAGAS et al., 2022) following biochar application align with the results of former studies. Even though amendment particles > 2 mm were removed in our study, a significant increase in C content and C:N was visible, mainly resulting from the high content of stable C in biochar (JOSEPH et al., 2010; GROSS et al., 2021; QIU et al., 2023). The observed enhancement of C_{mic} in our study likely reflects improved microbial habitat and growth conditions due to the application of biochar-containing amendments (GHODSZAD et al., 2021). These are probably driven by increases in soil pH, nutrient and water retention capacity, and labile C availability (VAN ZWIETEN et al., 2010; LIU et al., 2015), e.g. from increased DOC content (AZEEM et al., 2023; CHEN et al., 2024).

Biochar application is generally known to result in increased soil pH (DAI et al., 2017; BUSS et al., 2018) and to potentially increase EC (CHINTALA et al., 2014; HU et al., 2025). The observed increases in soil pH and EC in our study were most pronounced following the co-application of biochar and basanite. This suggests a synergistic effect likely driven by the combined liming and ionic contributions of both amendments. The application of the co-pyrolyzed rock-enhanced biochar showed a less pronounced effect compared to co-application. This attenuation may be attributed to altered mineral availability or reduced soluble salt content resulting from thermal transformation during co-pyrolysis.

By modifying soil pH (SHEPHERD et al., 2017; GHODSZAD et al., 2021) or by increasing cation exchange capacity (CEC; LIANG et al., 2006; KAREEM et al., 2025), biochar application can increase P availability and reduce P leaching. Additionally, biochar application can increase available P content in soils (JIN et al., 2016; GLASER & LEHR, 2019; WANG et al., 2025a) from the dissolution of biochar ash which contains P_2O_5 that is released into the soil over time (GHODSZAD et al., 2021; BUSS et al., 2022). These effects can be short-, mid-, or long-term (GLASER & LEHR, 2019), depending strongly on soil and biochar properties (GHODSZAD et al., 2021). The strong correlation between P content and soil pH in our study highlights the indirect influence of biochar-containing amendment applications on P availability via pH increase. However, the pH increase was similar in biochar and co-application, while the increase in available P content was most pronounced following single biochar application. The reduced increase in P availability following combined applications compared to single biochar could result from reduced biochar ash dissolution, possibly due to clogged biochar pores, or reduced CEC and thus reduced retention of fertilizer P. The pelletizing of the rock-enhanced biochar prior to pyrolysis could explain the even less pronounced increase in available P compared to co-application, due to compressing biomass pores and thus reducing specific surface area. Building on these findings, future work assessing amendment characteristics, such as specific surface area, could deepen our understanding of the mechanisms involved. A reduced ash dissolution in the short-term might lead to a more stable P supply in the long-term following combined application (LAMMIRATO et al., 2011; BUSS et al., 2022).

The application of biochar to sandy soils can have diverse positive and negative impacts on content, retention, and availability of N_{min} (AHMAD et al., 2021; HEMATIMATIN et al., 2024). In our study, the content of Nmin was neither increased nor reduced by the application of the biochar-containing amendments. Since the application of these amendments significantly reduced nitrate leaching (Hamburger et al., 2026), nitrate retention was improved and suggests with the constant Nmin content an increased microbial uptake of Nmin following the application of the biochar-containing amendments.

In contrast to the biochar-containing amendments, the single application of basanite did not influence any of the analyzed soil properties during the nine weeks of plant growth. In contrast, other studies discovered a variety of effects of silicate rock powder application on soil properties, such as altered TOC (AMOAKWAH et al., 2023; BUSS et al., 2023; SOKOL et al., 2024; XU et al., 2024b), C_{mic} (VON MERSI et al., 1992; REIS et al., 2024; SOKOL et al., 2024), and nutrient contents (AMANN et al., 2020; GUO et al., 2023; WANG et al., 2025b) as well as increased soil pH (ABDALQADIR et al., 2024; BEERLING et al., 2025; MEDEIROS et al., 2025). These effects of ERW are often visible in the long-term (SWOBODA et al., 2022; DUPLA et al., 2024), possibly explaining the missing effects of basanite application in our nine-weeks study.

Our results partly confirm our hypothesis that the combined application of biochar and basanite improved soil properties relevant to microbial activity. Key soil properties, such as C and P content, C:N ratio, and C_{mic}, increased significantly following combined application compared to control, indicating positive effects. The observed changes were mainly driven by the biochar component, while potential contributions of basanite may require more time to become effective. Nevertheless, the pronounced changes in pH and EC under co-application compared to co-pyrolysis suggest potential for synergies between biochar and basanite without a significant benefit of combined pyrolysis.

B4.2 Influence of amendments on extracellular enzyme kinetics

All treatments showed, despite the fertilization, a P limitation and, possibly due to the fertilization, a generally low N demand. This is indicated by the high V_{max} of AP, low V_{max} of LAP, vector angles > 45°, and enzymatic C:N:P ratios with P-values > 1 and N-values < 1 (VON MERSI et al., 1992; ALLISON et al., 2007; MOORHEAD et al., 2016). The application of biochar-containing amendments seemed to induce a shift in microbial nutrient demand. The decrease in V_{max} of AP is consistent with the observed increase in available P. This improved P availability, potentially further enhanced by the pH increase (SWOBODA et al., 2022; BEERLING et al., 2025), allowed the microorganisms to down-regulate the production of AP (SINSABAUGH et al., 2008; ALLISON et al., 2011). Simultaneously, the increased V_{max} of LAP indicates an enhanced demand for N, likely driven by the widened soil C:N ratio and the adsorption of N_{min} (CLOUGH et al., 2013) following the application of biochar-containing amendments. This increases the relative stoichiometric imbalance between C and N from the microbial perspective, which can stimulate investment in N-acquiring enzymes such as LAP (SINSABAUGH et al., 2008; ALLISON et al., 2011) and strengthen the microbial community involved in N cycling (ANDERSON et al., 2011). Even though P remained the limiting nutrient for microorganisms, the application of biochar-containing amendments seemed to shift the system towards a more balanced nutrient demand with a relative increase in N demand. The potential enzyme activity V_{max} of AP, CH, and LAP following the application of co-pyrolyzed rock-enhanced biochar was similar to that of control, while both biochar and co-application significantly altered those potential enzyme activities. This can likely be explained by the strong correlation of V_{max} with available P and soil pH, which were also less strongly increased with rock-enhanced biochar application. Despite that, the similar enzymatic C:N:P ratios following all three biochar-containing amendments implies that the rock-enhanced biochar application probably resulted in an equally strong balancing of the nutrient demand as biochar and co-application.

The potential activity V_{max} of the C-cycle-related BG was, contrary to our hypothesis, not affected by the application of biochar-containing amendments. In contrast, several other studies reported increased V_{max} of BG following biochar application (HALMI & SIMARANI, 2021; JIN et al., 2024). However, biochar produced at high temperatures (> 500 °C) has been observed to have minimal or even inhibiting effects on BG activity (JIN et al., 2024; YANG et al., 2024), potentially due to greater porosity and surface area (LIAO et al., 2022). The application of biochar might relocate both C and microorganisms onto biochar surfaces, which may improve microbial efficiency and reduce the need for BG release (LEHMANN et al., 2011). BAMMINGER et al. (2014) interpreted an increase in potential BG activity as a result of insufficient C supply from biochar to support microbial growth. Since we observed an increased C_{mic} content and the calculated vector lengths did not indicate a C limitation following biochar-containing amendment application, the labile biochar part must have provided sufficient C to sustain microbial growth. While our approach provides valuable initial insights into effect of our amendments on C-cycle dynamics, the focus on BG may only reflect part of the microbial response. Including additional C-cycling enzymes, such as β-xylosidase or β-cellobiohydrolase, in future studies could help to broaden the understanding of enzymatic activity patterns in response to combined application of biochars and silicate rock powder (LOEPPMANN et al., 2016).

In contrast to V_{max}, the enzyme affinity K_m of all four enzymes was barely influenced by amendment application. Little is known about the influence of biochar and basanite application of enzyme affinity K_m, but our results indicate robustness against the influence of both amendments. Since K_m has rarely been influenced by the amendments, catalytic enzyme efficiency K_a as the quotient of V_{max} and K_m showed similar patterns as V_{max}. Both biochar and co-application may result in a reduced catalytic enzyme efficiency K_a of AP, BG, and CH, probably due to a strong increase in P and C supply.

The basanite treatment did neither improve nor impair enzyme kinetics and EES, which makes basanite a promising CDR method without a harmful impact on enzymes and microbial processes. Until now, there have been only a few studies investigating the influence of silicate rock powder on soil microbial processes in planted systems. These studies have inconsistent results ranging from increased to decreased V_{max} of different enzymes, strongly depending on soil and rock powder properties as well as the analyzed enzyme (VON MERSI et al., 1992; LI & DONG, 2013; REIS et al., 2024; WANG et al., 2025b). The enzyme kinetics in our study strongly correlated with soil properties, such as nutrient contents and soil pH, which determine nutrient availability and thus affect enzyme activities (SINSABAUGH et al., 2008). Since those parameters were not altered by basanite applied in our study – potentially due to low amounts or insufficient time to weather –, a missing effect on enzyme kinetics, EES, and vector length and angle is not surprising. REIS et al. (2024) showed a significant decrease in AP activity first occurring four months after basalt application. This long-term decrease in AP activity was explained by the low but apparently sufficient content of P_2O_5 in the basalt to supply microorganisms with P, thereby reducing the need for AP release (REIS et al., 2024). Since our basanite had similar P_2O_5 contents (~0.6 wt.%) but did not alter AP activities, this supports the impression of low basanite weathering rates in our experiment. In the long-term, we would expect basanite application to have an impact on enzyme kinetics, especially on AP.

Enzyme kinetics and thus enzyme-based nutrient limitation indices, including EES and vector analysis, provide a valuable framework for comparing microbial nutrient demand. However, these indices are influenced not only by microbial stoichiometry, but also by abiotic factors such as enzyme adsorption to biochar surfaces (LEHMANN et al., 2011; LAMMIRATO et al., 2011) and soil pH and temperature (SINSABAUGH et al., 2008; MOORHEAD et al., 2016). The threshold angle of 45° for distinguishing N from P limitation is an established proxy (VON MERSI et al., 1992; ALLISON et al., 2007; MOORHEAD et al., 2016), but may oversimplify the complex interactions between soils and microbes. Nonetheless, the combined use of enzyme kinetics and stoichiometric ratios applied in this study provides valuable first insights into the effects of single versus combined amendment applications on nutrient dynamics, and future work should complement this approach focusing on the microbial community to further disentangle amendment-specific effects.

B.5 Conclusions

Our experiment, conducted on a sandy agricultural soil, provides an important first step toward understanding effects of the single and combined applications of biochar and basanite on soil properties and microbial processes during a nine-week experiment including plants. The results partly support our hypotheses and reveal distinct short-term responses depending on the applied amendment. Basanite application alone showed no significant effects, likely due to limited weathering over the short experimental duration, which constrained the release of nutrients from the mineral phase. To be able to assess the influence of silicate rock powder application of soil properties and microbial processes, long-term studies are necessary. Nonetheless, basanite application caused no negative impacts within our nine-week experiment, supporting its potential as a safe and promising long-term amendment for CDR and soil improvement.

The combination effect of biochar and basanite was primarily driven by biochar, with co-pyrolyzed rock-enhanced biochar and co-application of biochar and basanite resembling the response of single biochar application. These three biochar-containing amendments significantly improved soil properties, such as soil pH, available P, and C_{mic}, and altered extracellular enzyme kinetics and nutrient stoichiometry. All biochar-containing treatments increased soil C content, C:N ratio, and C_{mic} to a similar extent. While single biochar application enhanced short-term P availability, co-application and especially co-pyrolysis treatments may offer a more sustained long-term P release. Co-application led to the greatest increases in soil N content, pH, and EC, suggesting synergistic effects between biochar and basanite on soil properties within weeks, with the potential to combine the CDR effects of both amendments in the long-term.

Following the application of single biochar and co-application of both amendments to our sandy soil, potential enzyme activity V_{max} of AP, BG, and CH decreased, but increased for LAP. The application of co-pyrolyzed rock-enhanced mainly did not alter V_{max} compared to control, likely due to less pronounced increases in pH and available P. The enzymatic C:N:P ratio varied, indicating a shift from a pure P limitation in the unamended soil to a more balanced nutrient demand in biochar-containing treatments, with increased relative N demand. When applied to agricultural soils, the biochar-containing amendments improved P availability, but could cause long-term N-limitation if not balanced by sufficient N supply.

Authors' contributions

Maria Ansari: Conceptualization, Formal analysis, Investigation, Writing - original draft; **Svenja Stock**: Methodology, Writing - review and editing; **Michaela A. Dippold**: Resources, Writing - review and editing; **Susanne E. Hamburger**: Resources, Writing - review and editing; **Claudia I. Kammann**: Funding acquisition, Resources, Writing - review and editing; **Johannes Meyer zu Drewer**: Resources; **Nikolas Hagemann**: Funding acquisition, Resources, Writing - review and editing; **Annette Eschenbach**: Funding acquisition, Resources, Supervision, Writing - review and editing; **Joscha N. Becker**: Conceptualization, Funding acquisition, Supervision, Writing - review and editing.

Acknowledgements

This study was conducted as a part of the PyMiCCS project (Pyrogenic carbon and carbonating Minerals for enhanced plant growth and Carbon Capture and Storage) that is part of the CDRterra consortium and was funded by the German Federal Ministry of Research, Technology and Space (BMFTR, FKZ: 01LS2109A and 01LS2109C). The authors thank Sumita Rui and Josephine Krechel for assisting during sampling as well as Deborah Harms and Annika Naumann for support during lab work. We particularly thank Moses Ngugi, Elisa Karina Albrecht, and Callum Banfield for support during the fluorometric enzyme assays.

B.6 References

ABDALQADIR, M., HUGHES, D., REZAEI GOMARI, S. & RAFIQ, U. 2024. A state of the art of review on factors affecting the enhanced weathering in agricultural soil: Strategies for carbon sequestration and climate mitigation. Environ Sci Pollut R. https://doi.org/10.1007/s11356-024-32498-5.

AHMAD, Z., MOSA, A., ZHAN, L. & GAO, B. 2021. Biochar modulates mineral nitrogen dynamics in soil and terrestrial ecosystems: A critical review. Chemosphere, 278, 130378. https://doi.org/10.1016/j.chemosphere.2021.130378.

ALLEN, R. L. 1847. A Brief Compend of American Agriculture. Oakland, California, USA, University of California.

ALLISON, S. D. 2006. Soil minerals and humic acids alter enzyme stability: implications for ecosystem processes. Biogeochemistry, 81, 361–373. https://doi.org/10.1007/s10533-006-9046-2.

ALLISON, S. D., GARTNER, T. B., HOLLAND, K., WEINTRAUB, M. & SINSABAUGH, R. L. 2007. Soil enzymes: Linking proteomics and ecological processes. *In:* HURST, C. J., CRAWFORD, R. L., GARLAND, J. L., LIPSON, D. A., MILLS, A. L. & STETZENBACH, L. D. (eds.) Manual of environmental microbiology. ASM Press. https://doi.org/10.1128/9781555815882.ch58.

ALLISON, S. D., WEINTRAUB, M. N., GARTNER, T. B. & WALDROP, M. P. 2011. Evolutionary-economic principles as regulators of soil enzyme production and ecosystem function. *In:* SHUKLA, G. & VARMA, A. (eds.) Soil Enzymology. Berlin, Heidelberg: Springer Berlin Heidelberg. https://doi.org/10.1007/978-3-642-14225-3_12.

AMANN, T. & HARTMANN, J. 2019. Ideas and perspectives: Synergies from co-deployment of negative emission technologies. Biogeosciences, 16, 2949–2960. https://doi.org/10.5194/bg-16-2949-2019.

AMANN, T., HARTMANN, J., STRUYF, E., DE OLIVEIRA GARCIA, W., FISCHER, E. K., JANSSENS, I., MEIRE, P. & SCHOELYNCK, J. 2020. Enhanced Weathering and related element fluxes – a cropland mesocosm approach. Biogeosciences, 17, 103–119. https://doi.org/10.5194/bg-17-103-2020.

AMELOOT, N., GRABER, E. R., VERHEIJEN, F. G. A. & DE NEVE, S. 2013. Interactions between biochar stability and soil organisms: review and research needs. Eur J Soil Sci, 64, 379–390. https://doi.org/10.1111/ejss.12064.

AMOAKWAH, E., SHIM, J., KIM, S., LEE, Y., KWON, S., SANGHO, J. & PARK, S. 2023. Impact of silicate and lime application on soil fertility and temporal changes in soil properties and carbon stocks in a temperate ecosystem. Geoderma, 433, 116431. https://doi.org/10.1016/j.geoderma.2023.116431.

ANDERSON, C. R., CONDRON, L. M., CLOUGH, T. J., FIERS, M., STEWART, A., HILL, R. A. & SHERLOCK, R. R. 2011. Biochar induced soil microbial community change: Implications for biogeochemical cycling of carbon, nitrogen and phosphorus. Pedobiologia, 54, 309–320. https://doi.org/10.1016/j.pedobi.2011.07.005.

AZEEM, M., SUN, T.-R., JEYASUNDAR, P. G. S. A., HAN, R.-X., LI, H., ABDELRAHMAN, H., SHAHEEN, S. M., ZHU, Y.-G. & LI, G. 2023. Biochar-derived dissolved organic matter (BDOM) and its influence on soil microbial community composition, function, and activity: A review. Crit Rev Env Sci Tec, 1–23. https://doi.org/10.1080/10643389.2023.2190333.

BAKSHI, M. & VARMA, A. 2011. Soil enzyme: The state-of-art. *In:* SHUKLA, G. & VARMA, A. (eds.) Soil enzymology. Berlin, Heidelberg: Springer Berlin Heidelberg. https://doi.org/10.1007/978-3-642-14225-3_1.

BAKSHI, S., BANIK, C. & LAIRD, D. A. 2018. Quantification and characterization of chemically-and thermally-labile and recalcitrant biochar fractions. Chemosphere, 194, 247–255. https://doi.org/10.1016/j.chemosphere.2017.11.151.

BAMMINGER, C., MARSCHNER, B. & JÜSCHKE, E. 2014. An incubation study on the stability and biological effects of pyrogenic and hydrothermal biochar in two soils. Eur J Soil Sci, 65, 72–82. https://doi.org/10.1111/ejss.12074.

BATES, D., MÄCHLER, M., BOLKER, B. & WALKER, S. 2015. Fitting linear mixed-effects models using lme4. J Stat Softw, 67, 1 – 48. https://doi.org/10.18637/jss.v067.i01.

BEERLING, D. J., KANTZAS, E. P., LOMAS, M. R., TAYLOR, L. L., ZHANG, S., KANZAKI, Y., EUFRASIO, R. M., RENFORTH, P., MECURE, J.-F., POLLITT, H., HOLDEN, P. B., EDWARDS, N. R., KOH, L., EPIHOV, D. Z., WOLF, A., HANSEN, J. E., BANWART, S. A., PIDGEON, N. F., REINHARD, C. T., PLANAVSKY, N. J. & VAL MARTIN, M. 2025. Transforming US agriculture for carbon removal with enhanced weathering. Nature, 638, 425–434. https://doi.org/10.1038/s41586-024-08429-2.

BEKCHANOVA, M., CAMPION, L., BRUNS, S., KUPPENS, T., LEHMANN, J., JOZEFCZAK, M., CUYPERS, A. & MALINA, R. 2024. Biochar improves the nutrient cycle in sandy-textured soils and increases crop yield: A systematic review. Environ Evid, 13, 3. https://doi.org/10.1186/s13750-024-00326-5.

BURNS, R. G., DEFOREST, J. L., MARXSEN, J., SINSABAUGH, R. L., STROMBERGER, M. E., WALLENSTEIN, M. D., WEINTRAUB, M. N. & ZOPPINI, A. 2013. Soil enzymes in a changing environment: Current knowledge and future directions. Soil Biol Biochem, 58, 216–234. https://doi.org/10.1016/j.soilbio.2012.11.009.

BUSS, W., HASEMER, H., FERGUSON, S. & BOREVITZ, J. 2023. Stabilisation of soil organic matter with rock dust partially counteracted by plants. bioRxiv, https://doi.org/10.1101/2023.06.02.543347. 10.1101/2023.06.02.543347.

BUSS, W., SHEPHERD, J. G., HEAL, K. V. & MAŠEK, O. 2018. Spatial and temporal microscale pH change at the soil-biochar interface. Geoderma, 331, 50–52. https://doi.org/10.1016/j.geoderma.2018.06.016.

BUSS, W., WURZER, C., MANNING, D. A. C., ROHLING, E. J., BOREVITZ, J. & MAŠEK, O. 2022. Mineral-enriched biochar delivers enhanced nutrient recovery and carbon dioxide removal. Commun Earth Environ, 3, 67. https://doi.org/10.1038/s43247-022-00394-w.

BUSS, W., YEATES, K., ROHLING, E. & BOREVITZ, J. 2021. Enhancing natural cycles in agro-ecosystems to boost plant carbon capture and soil storage. Oxford Open Climate Change, 1, kgab006. https://doi.org/10.1093/oxfclm/kgab006.

CARSON, J. K., ROONEY, D., GLEESON, D. B. & CLIPSON, N. 2007. Altering the mineral composition of soil causes a shift in microbial community structure. FEMS Microbiol Ecol, 61, 414–423. https://doi.org/10.1111/j.1574-6941.2007.00361.x.

CHAGAS, J. K. M., FIGUEIREDO, C. C. D. & RAMOS, M. L. G. 2022. Biochar increases soil carbon pools: Evidence from a global meta-analysis. J Environ Manage, 305, 114403. https://doi.org/10.1016/j.jenvman.2021.114403.

CHEN, M., LIU, D., SHAO, X., LI, S., JIN, X., QI, J., LIU, H., LI, C., LI, C. & LI, C. 2024. Effect of biochar types and rates on SOC and its active fractions in tropical farmlands of China. Agronomy, 14, 676. https://doi.org/10.3390/agronomy14040676.

CHINTALA, R., JAVIER, M., E., S. T., D., M. D. & AND JULSON, J. L. 2014. Effect of biochar on chemical properties of acidic soil. Arch Agron Soil Sci, 60, 393–404. https://doi.org/10.1080/03650340.2013.789870.

CLOUGH, T., CONDRON, L. M., KAMMANN, C. & MÜLLER, C. 2013. A review of biochar and soil nitrogen dynamics. Agronomy, 3, 275–293. https://doi.org/10.3390/agronomy3020275.

DAI, Z., ZHANG, X., TANG, C., MUHAMMAD, N., WU, J., BROOKES, P. C. & XU, J. 2017. Potential role of biochars in decreasing soil acidification - A critical review. Sci Total Environ, 581-582, 601–611. https://doi.org/10.1016/j.scitotenv.2016.12.169.

DENG, L., PENG, C., HUANG, C., WANG, K., LIU, Q., LIU, Y., HAI, X. & SHANGGUAN, Z. 2019. Drivers of soil microbial metabolic limitation changes along a vegetation restoration gradient on the Loess Plateau, China. Geoderma, 353, 188–200. https://doi.org/10.1016/j.geoderma.2019.06.037.

DIN 2005. DIN 19746:2005-06: Soil quality - Determination of mineral nitrogen (nitrat and ammonium) in soil profiles (N_{min} laboratory method). Berlin, Germany: DIN Media GmbH.

DIN 2011. DIN EN ISO 14240-2:2011-09: Soil quality - Determination of soil microbial biomass - Part 2: Fumigation-extraction method. Berlin, Germany: DIN Media GmbH.

DING, X., LI, G., ZHAO, X., LIN, Q. & WANG, X. 2023. Biochar application significantly increases soil organic carbon under conservation tillage: An 11-year field experiment. Biochar, 5, 28. https://doi.org/10.1007/s42773-023-00226-w.

DING, Y., LIU, Y., LIU, S., LI, Z., TAN, X., HUANG, X., ZENG, G., ZHOU, L. & ZHENG, B. 2016. Biochar to improve soil fertility. A review. Agron Sustain Dev, 36, 36. https://doi.org/10.1007/s13593-016-0372-z.

DUPLA, X., ROMANE, C., EMMA, B., IRIS, G., RENÉE-CLAIRE, L. B. & STÉPHANIE, G. 2024. Let the dust settle: Impact of enhanced rock weathering on soil biological, physical, and geochemical fertility. Sci Total Environ, 176297. https://doi.org/10.1016/j.scitotenv.2024.176297.

EBC. 2024. Analytical methods - EBC guidelines Version 10.4 [Online]. European Biochar Certificate (EBC). Available: https://www.european-biochar.org/en/ct/8-Analytical-Methods.

GHODSZAD, L., REYHANITABAR, A., MAGHSOODI, M. R., ASGARI LAJAYER, B. & CHANG, S. X. 2021. Biochar affects the fate of phosphorus in soil and water: A critical review. Chemosphere, 283, 131176. https://doi.org/10.1016/j.chemosphere.2021.131176.

GLASER, B., HAUMAIER, L., GUGGENBERGER, G. & ZECH, W. 2001. The 'Terra Preta' phenomenon: a model for sustainable agriculture in the humid tropics. Naturwissenschaften, 88, 37–41. https://doi.org/10.1007/s001140000193.

GLASER, B. & LEHR, V.-I. 2019. Biochar effects on phosphorus availability in agricultural soils: A meta-analysis. Sci Rep, 9, 9338. https://doi.org/10.1038/s41598-019-45693-z.

GROSS, A., BROMM, T. & GLASER, B. 2021. Soil organic carbon sequestration after biochar application: A global meta-analysis. Agronomy, 11, 2474. https://doi.org/10.3390/agronomy11122474.

GUO, F., SUN, H., YANG, J., ZHANG, L., MU, Y., WANG, Y. & WU, F. 2023. Improving food security and farmland carbon sequestration in China through enhanced rock weathering: Field evidence and potential assessment in different humid regions. Sci Total Environ, 903, 166118. https://doi.org/10.1016/j.scitotenv.2023.166118.

HAGEMANN, N., SPOKAS, K., SCHMIDT, H.-P., KÄGI, R., BÖHLER, M. A. & BUCHELI, T. D. 2018. Activated carbon, biochar and charcoal: Linkages and synergies across pyrogenic carbon's ABCs. Water, 10, 182. https://doi.org/10.3390/w10020182

HALMI, M. F. A. & SIMARANI, K. 2021. Responses of soil microbial population and lignocellulolytic enzyme activities to palm kernel shell biochar amendment. Eurasian Soil Sci, 54, 1903–1911. https://doi.org/10.1134/S1064229321120073.

HAMBURGER, S. E., MEYER ZU DREWER, J., HAGEMANN, N., GEILFUS, C.-M. & KAMMANN, C. I. 2026. A crop yield and nitrate leaching dataset from a semi-field lysimeter experiment with cabbage turnip under combined biochar and rock powder amendment. https://doi.org/10.5281/zenodo.19065555.

HAQUE, F., SANTOS, R. M. & CHIANG, Y. W. 2020. Optimizing inorganic carbon sequestration and crop yield with wollastonite soil amendment in a microplot study. Front Plant Sci, 11. https://doi.org/10.3389/fpls.2020.01012.

HEMATIMATIN, N., IGAZ, D., AYDIN, E. & HORÁK, J. 2024. Biochar application regulating soil inorganic nitrogen and organic carbon content in cropland in the Central Europe: A seven-year field study. Biochar, 6, 14. https://doi.org/10.1007/s42773-024-00307-4.

HOSSAIN, M. Z., BAHAR, M. M., SARKAR, B., DONNE, S. W., OK, Y. S., PALANSOORIYA, K. N., KIRKHAM, M. B., CHOWDHURY, S. & BOLAN, N. 2020. Biochar and its importance on nutrient dynamics in soil and plant. Biochar, 2, 379–420. https://doi.org/10.1007/s42773-020-00065-z.

HOTHORN, T., BRETZ, F. & WESTFALL, P. 2008. Simultaneous inference in general parametric models. Biometrical J, 50, 346–363. https://doi.org/10.1002/bimj.200810425.

HU, Y., ABULAIZI, M., TIAN, Y., HU, Y., CHEN, M., LI, K., JIA, Y., KOU, T., ZHOU, J. & JIA, H. 2025. Effects of biochar on soil organic carbon stability in degraded alpine grasslands—A study on arid regions in Central Asia. Land, 14, 1018. https://doi.org/10.3390/land14051018.

JIN, X., ZHANG, T., HOU, Y., BOL, R., ZHANG, X., ZHANG, M., YU, N., MENG, J., ZOU, H. & WANG, J. 2024. Review on the effects of biochar amendment on soil microorganisms and enzyme activity. J Soil Sediment. https://doi.org/10.1007/s11368-024-03841-7.

JIN, Y., LIANG, X., HE, M., LIU, Y., TIAN, G. & SHI, J. 2016. Manure biochar influence upon soil properties, phosphorus distribution and phosphatase activities: A microcosm incubation study. Chemosphere, 142, 128–135. https://doi.org/10.1016/j.chemosphere.2015.07.015.

JOERGENSEN, R. G. 1996. The fumigation-extraction method to estimate soil microbial biomass: Calibration of the k_{EC} value. Soil Biol Biochem, 28, 25–31. https://doi.org/10.1016/0038-0717(95)00102-6.

JOSEPH, S. D., CAMPS-ARBESTAIN, M., LIN, Y., MUNROE, P., CHIA, C. H., HOOK, J., VAN ZWIETEN, L., KIMBER, S., COWIE, A., SINGH, B. P., LEHMANN, J., FOIDL, N., SMERNIK, R. J. & AMONETTE, J. E. 2010. An investigation into the reactions of biochar in soil. Soil Res, 48, 501–515. https://doi.org/10.1071/SR10009.

KAREEM, M. O., LIMAN, A. H., ODOFIN, A. J., AZEEZ, B. A., MUSA, B. M. & JIMOH, L. T. 2025. Soil organic carbon, cation exchange capacity, and maize (*Zea mays*) response to biochar and nitrogen fertilizer amendments. J Sci Res Rep, 31, 278–283. https://doi.org/10.9734/jsrr/2025/v31i53025.

KASSAMBARA, A. 2023. ggcorrplot: Visualization of a correlation matrix using 'ggplot2' - R package version 0.1.4.1 [Online]. Available: https://CRAN.R-project.org/package=ggcorrplot.

KOMSTA, L. 2022. outliers: Tests for outliers - R package version 0.15 [Online]. Available: https://CRAN.R-project.org/package=outliers.

KUZYAKOV, Y., BOGOMOLOVA, I. & GLASER, B. 2014. Biochar stability in soil: Decomposition during eight years and transformation as assessed by compound-specific ^{14}C analysis. Soil Biol Biochem, 70, 229–236. https://doi.org/10.1016/j.soilbio.2013.12.021.

LAMMIRATO, C., MILTNER, A. & KAESTNER, M. 2011. Effects of wood char and activated carbon on the hydrolysis of cellobiose by β-glucosidase from *Aspergillus niger*. Soil Biol Biochem, 43, 1936–1942. https://doi.org/10.1016/j.soilbio.2011.05.021.

LE BAS, M. J., LE MAITRE, R. W. L., STRECKEISEN, A., ZANETTIN, B. & ROCKS, I. S. O. T. S. O. I. 1986. A chemical classification of volcanic rocks based on the total alkali-silica diagram. J Petrol, 27, 745–750. https://doi.org/10.1093/petrology/27.3.745.

LEHMANN, J., COWIE, A., MASIELLO, C. A., KAMMANN, C., WOOLF, D., AMONETTE, J. E., CAYUELA, M. L., CAMPS-ARBESTAIN, M. & WHITMAN, T. 2021. Biochar in climate change mitigation. Nat Geosci, 14, 883–892. https://doi.org/10.1038/s41561-021-00852-8.

LEHMANN, J. & JOSEPH, S. 2024. Biochar for environmental management: An introduction. *In:* LEHMANN, J. & JOSEPH, S. (eds.) Biochar for environmental management: Science, technology and implementation. 3rd edition ed. London, United Kingdom: Routledge. 10.4324/9780203762264

LEHMANN, J., RILLIG, M. C., THIES, J., MASIELLO, C. A., HOCKADAY, W. C. & CROWLEY, D. 2011. Biochar effects on soil biota – A review. Soil Biol Biochem, 43, 1812–1836. https://doi.org/10.1016/j.soilbio.2011.04.022.

LI, J.-G. & DONG, Y.-H. 2013. Effect of a rock dust amendment on disease severity of tomato bacterial wilt. Antonie van Leeuwenhoek, 103, 11–22. https://doi.org/10.1007/s10482-012-9781-4.

LI, Z.-B., LI, G., ADAMS, J. M., GUAN, D.-X., ZHAO, L., BIAN, R., HU, Q., LU, X., JI, J. & CHEN, J. 2025. Atmospheric CO_2 removal efficiency through enhanced silicate weathering in croplands: A review with emphasis on the contribution of fungi. J Earth Sci, 36, 197–211. https://doi.org/10.1007/s12583-024-0101-5.

LIANG, B., LEHMANN, J., SOLOMON, D., KINYANGI, J., GROSSMAN, J., O'NEILL, B., SKJEMSTAD, J. O., THIES, J., LUIZÃO, F. J., PETERSEN, J. & NEVES, E. G. 2006. Black carbon increases cation exchange capacity in soils. Soil Sci Soc Am J, 70, 1719–1730. https://doi.org/10.2136/sssaj2005.0383.

LIAO, X., KANG, H., HAIDAR, G., WANG, W. & MALGHANI, S. 2022. The impact of biochar on the activities of soil nutrients acquisition enzymes is potentially controlled by the pyrolysis temperature: A meta-analysis. Geoderma, 411, 115692. https://doi.org/10.1016/j.geoderma.2021.115692.

LIU, S., ZHANG, Y., ZONG, Y., HU, Z., WU, S., ZHOU, J., JIN, Y. & ZOU, J. 2015. Response of soil carbon dioxide fluxes, soil organic carbon and microbial biomass carbon to biochar amendment: a meta-analysis. GCB Bioenergy, 8, 392–406. https://doi.org/10.1111/gcbb.12265.

LOEPPMANN, S., BLAGODATSKAYA, E., PAUSCH, J. & KUZYAKOV, Y. 2016. Enzyme properties down the soil profile - A matter of substrate quality in rhizosphere and detritusphere. Soil Biol Biochem, 103, 274–283. https://doi.org/10.1016/j.soilbio.2016.08.023.

LUO, L., MENG, H. & GU, J.-D. 2017. Microbial extracellular enzymes in biogeochemical cycling of ecosystems. J Environ Manage, 197, 539–549. https://doi.org/10.1016/j.jenvman.2017.04.023.

MEDEIROS, F. P., THEODORO, S. H., CARVALHO, A. M. X., OLIVEIRA, V. S., OLIVEIRA, L. C., ALMEIDA, R. M. P., VIANA, M. B. & GOMIDE, C. S. 2025. The combination of crushed rock and organic matter enhances the capture of inorganic carbon in tropical soils. J S Am Earth Sci, 152, 105254. https://doi.org/10.1016/j.jsames.2024.105254.

MEYER ZU DREWER, J. & HAGEMANN, N. 2025. Industrial production and characterization of biochar and rock-enhanced biochar. https://doi.org/10.5281/zenodo.15840176.

MEYER ZU DREWER, J., VORRATH, M.-E., AMANN, T., HARTMANN, J., DE LA ROSA, J. M., MÖLLMER, J., PÉREZ-DALÍ, S. M., MEREDITH, W., UGUNA, C., SNAPE, C., KAMMANN, C., SCHMIDT, H.-P. & HAGEMANN, N. 2025. Pyrogenic carbon and carbonating minerals for carbon capture and storage (PyMiCCS) part I: production, physico-chemical characterization and C-sink potential. Front Clim, 7 2025. https://doi.org/10.3389/fclim.2025.1631368.

MICHAELIS, L. & MENTEN, M. L. 1913. Die Kinetik der Invertinwirkung. Biochemische Zeitschrift, 333–369.

MOORHEAD, D. L., SINSABAUGH, R. L., HILL, B. H. & WEINTRAUB, M. N. 2016. Vector analysis of ecoenzyme activities reveal constraints on coupled C, N and P dynamics. Soil Biol Biochem, 93, 1–7. https://doi.org/10.1016/j.soilbio.2015.10.019.

NDOSSI, E. M., BECKER, J. N., HEMP, A., DIPPOLD, M. A., KUZYAKOV, Y. & RAZAVI, B. S. 2020. Effects of land use and elevation on the functional characteristics of soil enzymes at Mt. Kilimanjaro. Eur J Soil Biol, 97, 103167. https://doi.org/10.1016/j.ejsobi.2020.103167.

QIU, H., HU, Z., LIU, J., ZHANG, H. & SHEN, W. 2023. Effect of biochar on labile organic carbon fractions and soil carbon pool management index. Agronomy, 13, 1385. https://doi.org/10.3390/agronomy13051385.

RECHBERGER, M. V., KLOSS, S., RENNHOFER, H., TINTNER, J., WATZINGER, A., SOJA, G., LICHTENEGGER, H. & ZEHETNER, F. 2017. Changes in biochar physical and chemical properties: Accelerated biochar aging in an acidic soil. Carbon, 115, 209–219. https://doi.org/10.1016/j.carbon.2016.12.096.

REGINATO, P. L. 2025. Biotechnology in direct air capture, enhanced weathering, and methane removal: Emerging opportunities and gaps. Front Clim, 6. https://doi.org/10.3389/fclim.2024.1440833

REIS, B. R., VASCONCELOS, A. L. S., SILVA, A. M. M., ANDREOTE, F. D. & AZEVEDO, A. C. 2024. Changes in soil bacterial community structure in a short-term trial with different silicate rock powders. Chem Biol Technol Agric, 11, 61. https://doi.org/10.1186/s40538-024-00586-w.

SCHMIDT, H.-P., KAMMANN, C., HAGEMANN, N., LEIFELD, J., BUCHELI, T. D., SÁNCHEZ MONEDERO, M. A. & CAYUELA, M. L. 2021. Biochar in agriculture – A systematic review of 26 global meta-analyses. GCB Bioenergy, 13, 1708–1730. https://doi.org/10.1111/gcbb.12889.

SHEPHERD, J. G., JOSEPH, S., SOHI, S. P. & HEAL, K. V. 2017. Biochar and enhanced phosphate capture: Mapping mechanisms to functional properties. Chemosphere, 179, 57–74. https://doi.org/10.1016/j.chemosphere.2017.02.123.

SHI, W. 2011. Agricultural and ecological significance of soil enzymes: Soil carbon sequestration and nutrient cycling. *In:* SHUKLA, G. & VARMA, A. (eds.) Soil enzymology. Berlin, Heidelberg: Springer Berlin Heidelberg. https://doi.org/10.1007/978-3-642-14225-3_3.

SINSABAUGH, R. L., LAUBER, C. L., WEINTRAUB, M. N., AHMED, B., ALLISON, S. D., CRENSHAW, C., CONTOSTA, A. R., CUSACK, D., FREY, S., GALLO, M. E., GARTNER, T. B., HOBBIE, S. E., HOLLAND, K., KEELER, B. L., POWERS, J. S., STURSOVA, M., TAKACS-VESBACH, C., WALDROP, M. P., WALLENSTEIN, M. D., ZAK, D. R. & ZEGLIN, L. H. 2008. Stoichiometry of soil enzyme activity at global scale. Ecol Lett, 11, 1252–1264. https://doi.org/10.1111/j.1461-0248.2008.01245.x.

SOKOL, N. W., SOHNG, J., MORELAND, K., SLESSAREV, E., GOERTZEN, H., SCHMIDT, R., SAMADDAR, S., HOLZER, I., ALMARAZ, M., GEOGHEGAN, E., HOULTON, B., MONTAÑEZ, I., PETT-RIDGE, J. & SCOW, K. 2024. Reduced accrual of mineral-associated organic matter after two years of enhanced rock weathering in cropland soils, though no net losses of soil organic carbon. Biogeochemistry. https://doi.org/10.1007/s10533-024-01160-0.

STEINER, C., TEIXEIRA, W. G., LEHMANN, J., NEHLS, T., DE MACÊDO, J. L. V., BLUM, W. E. H. & ZECH, W. 2007. Long term effects of manure, charcoal and mineral fertilization on crop production and fertility on a highly weathered Central Amazonian upland soil. Plant Soil, 291, 275–290. https://doi.org/10.1007/s11104-007-9193-9.

STRECKEISEN, A. 1980. Classification and nomenclature of volcanic rocks, lamprophyres, carbonatites and melilitic rocks IUGS Subcommission on the Systematics of Igneous Rocks. Geol Rundsch, 69, 194–207. https://doi.org/10.1007/BF01869032.

SWOBODA, P., DÖRING, T. F. & HAMER, M. 2022. Remineralizing soils? The agricultural usage of silicate rock powders: A review. Sci Total Environ, 807, 150976. https://doi.org/10.1016/j.scitotenv.2021.150976.

VAN ZWIETEN, L., KIMBER, S., MORRIS, S., CHAN, K. Y., DOWNIE, A., RUST, J., JOSEPH, S. & COWIE, A. 2010. Effects of biochar from slow pyrolysis of papermill waste on agronomic performance and soil fertility. Plant Soil, 327, 235–246. https://doi.org/10.1007/s11104-009-0050-x.

VANCE, E. D., BROOKES, P. C. & JENKINSON, D. S. 1987. An extraction method for measuring soil microbial biomass C. Soil Biol Biochem, 19, 703–707. https://doi.org/10.1016/0038-0717(87)90052-6.

VDLUFA 1991. Bestimmung von Phosphor und Kalium im Doppellactat(DL)-Auszug. Methodenbuch Band I Böden. Speyer, Germany: Verband Deutscher Landwirtschaftlicher Untersuchungs- und Forschungsanstalten e.V. (VDLUFA).

VICCA, S., GOLL, D. S., HAGENS, M., HARTMANN, J., JANSSENS, I. A., NEUBECK, A., PEÑUELAS, J., POBLADOR, S., RIJNDERS, J., SARDANS, J., STRUYF, E., SWOBODA, P., VAN GROENIGEN, J. W., VIENNE, A. & VERBRUGGEN, E. 2022. Is the climate change mitigation effect of enhanced silicate weathering governed by biological processes? Glob Chang Biol, 28, 711–726. https://doi.org/10.1111/gcb.15993.

VON MERSI, W., KUHNERT-FINKERNAGEL, R. & SCHINNER, F. 1992. The influence of rock powders on microbial activity of three forest soils. Z Pflanz Bodenkunde, 155, 29–33. https://doi.org/10.1002/jpln.19921550107.

VORRATH, M.-E., AMANN, T., MEYER ZU DREWER, J., HAGEMANN, N., ALDRICH, C., BÖRKER, J., SEEDTKE, M., BECKER, J. N., HAGENS, M., ESCHENBACH, A. & HARTMANN, J. 2025. Pyrogenic carbon and carbonating minerals for carbon capture and storage (PyMiCCS) part II: organic and inorganic carbon dioxide removal in an Oxisol. Front Clim, Volume 7 - 2025. https://doi.org/10.3389/fclim.2025.1592454.

WANG, J., SUN, L., SUN, Y., YANG, S., QIN, Q. & XUE, Y. 2025a. Long-term biochar-based fertilizer substitution promotes carbon, nitrogen, and phosphorus acquisition enzymes in dryland soils by affecting soil properties and regulating bacterial community. Appl Soil Ecol, 206, 105801. https://doi.org/10.1016/j.apsoil.2024.105801.

WANG, J., XIONG, Z. & KUZYAKOV, Y. 2016. Biochar stability in soil: meta-analysis of decomposition and priming effects. GCB Bioenergy, 8, 512–523. https://doi.org/10.1111/gcbb.12266.

WANG, X., LI, G., ALI, A., ALGORA, C., DELGADO-BAQUERIZO, M., GOLL, D. S., VICCA, S., XU, T., BI, B., CHEN, Q., LIN, L., FANG, Y., HAO, Z., LI, Z. & YUAN, Z. 2025b. Enhanced rock weathering boosts ecosystem multifunctionality via improving microbial networks complexity in a tropical forest plantation. J Environ Manage, 373, 123477. https://doi.org/10.1016/j.jenvman.2024.123477.

WERTH, M. & KUZYAKOV, Y. 2010. ^{13}C fractionation at the root–microorganisms–soil interface: A review and outlook for partitioning studies. Soil Biol Biochem, 42, 1372–1384. https://doi.org/10.1016/j.soilbio.2010.04.009.

WICKHAM, H. 2016. ggplot2: Elegant graphics for data analysis. New York, USA, Springer.

WIEDNER, K., SCHNEEWEIß, J., DIPPOLD, M. A. & GLASER, B. 2015. Anthropogenic dark earth in Northern Germany — The nordic analogue to *terra preta de Índio* in Amazonia. CATENA, 132, 114–125. https://doi.org/10.1016/j.catena.2014.10.024.

XIAO, L., MIN, X., LI, Z. & LI, P. 2024. Kinetic and thermodynamic characteristics of soil enzymes in pure and mixed forest samples on the Loess Plateau of China. J Plant Nutr Soil Sci, n/a. https://doi.org/10.1002/jpln.202400242.

XU, Q., ZHANG, F., SONG, F., GUO, H., WANG, X., BI, F. & XU, M. 2024a. Investigating CO_2 sequestration via enhanced rock weathering: Effects of temperature and citric acid on dolomite and basalt. J Clean Prod, 485, 144414. https://doi.org/10.1016/j.jclepro.2024.144414.

XU, T., YUAN, Z., VICCA, S., GOLL, D. S., LI, G., LIN, L., CHEN, H., BI, B., CHEN, Q., LI, C., WANG, X., WANG, C., HAO, Z., FANG, Y. & BEERLING, D. J. 2024b. Enhanced silicate weathering accelerates forest carbon sequestration by stimulating the soil mineral carbon pump. Glob Chang Biol, 30, e17464. https://doi.org/10.1111/gcb.17464.

YANG, F., WANG, W., WU, Z., PENG, J., XU, H., GE, M., LIN, S., ZENG, Y., SARDANS, J., WANG, C. & PEÑUELAS, J. 2024. Fertilizer reduction and biochar amendment promote soil mineral-associated organic carbon, bacterial activity, and enzyme activity in a jasmine garden in southeast China. Sci Total Environ, 176300. https://doi.org/10.1016/j.scitotenv.2024.176300.

YANG, Y., LIANG, C., WANG, Y., CHENG, H., AN, S. & CHANG, S. X. 2020. Soil extracellular enzyme stoichiometry reflects the shift from P- to N-limitation of microorganisms with grassland restoration. Soil Biol Biochem, 149, 107928. https://doi.org/10.1016/j.soilbio.2020.107928.

ZHAO, S., TA, N., LI, Z., YANG, Y., ZHANG, X., LIU, D., ZHANG, A. & WANG, X. 2018. Varying pyrolysis temperature impacts application effects of biochar on soil labile organic carbon and humic fractions. Appl Soil Ecol, 123, 484–493. https://doi.org/10.1016/j.apsoil.2017.09.007.

ZHOU, X., SHEN, Y., FU, X. & WU, F. 2018. Application of sodium silicate enhances cucumber resistance to fusarium wilt and alters soil microbial communities. Front Plant Sci, 9. https://doi.org/10.3389/fpls.2018.00624.

ZIMMERMAN, A. R. 2010. Abiotic and microbial oxidation of laboratory-produced black carbon (biochar). Environ Sci Technol, 44, 1295–1301. https://doi.org/10.1021/es903140c.

B.7 Appendix

B7.1 Basanite powder properties

The chemical composition of the rock powder (Table B.2) was analyzed using X-ray fluorescence (XRF) at the Mineralogical Institute, University of Hamburg, while the mineralogical composition was determined by Qmineral using X-ray diffraction (XRD), as described in Vorrath et al. *under review*. Following the classification of volcanic rocks by STRECKEISEN (1980) or LE BAS et al. (1986), this rock can be classified as a basanite. The basanite was obtained from Rheinische Provinzial-Basalt- u. Lavawerke, Sinzig, Germany.

Table B.2: Main compounds, trace elements, mineral composition and grain size of used basanite powder *Eifelgold*. bdl = below detection limit; LOI = loss on ignition.

Main compounds	[wt%]	Trace Elements	[ppm]	Mineralogy	[wt%]	Grain size [µm]	[wt%]
SiO_2	43.86	As	bdl	Clinopyroxene	44.4	> 300	0.00
TiO_2	2.79	Ba	1026	Plagioclase	15.5	300 - 250	0.13
Al_2O_3	14.15	Bi	bdl	Nepheline	11.2	250 - 210	0.17
Fe_2O_3	11.28	Ce	104	Leucite	9.9	210 - 180	0.14
MnO	0.18	Co	51	Olivine	6.3	180 - 150	0.26
MgO	8.21	Cr	53	2:1 layer silicates	5.1	150 - 120	1.20
CaO	11.63	Cu	66	Hematite	3.1	120 - 100	2.87
Na_2O	3.26	Ga	17	Spinel-type minerals	1.9	100 - 86	4.17
K_2O	3.35	La	52	Apatite	1.1	86 - 74	5.67
P_2O_5	0.6	Nb	52	Analcime	0.9	74 - 62	8.13
SO_3	bdl	Nd	28	Quartz	0.7	62 - 52	8.89
LOI	0.44	Ni	124			52 - 44	8.50
Sum	*99.74*	Pb	5			44 - 36	9.63
		Rb	86			36 - 30	7.86
		Sc	22			30 - 26	5.50
		Sr	882			26 - 22	5.64
		Th	8			22 - 18	5.72
		U	3			18 - 0.5	25.52
		V	302				
		Y	24				
		Zn	90				
		Zr	271				

B7.2 Randomized complete block design

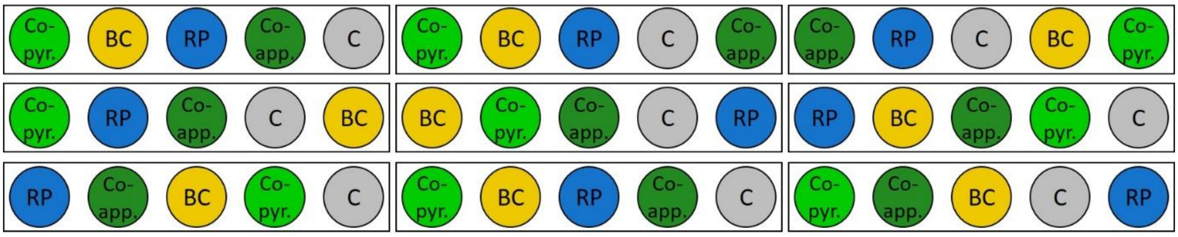

Figure B.5: Visualization of randomized complete block design of lysimeter experiment. Squares represent blocks, circles represent lysimeters. C = control treatment, RP = rock powder treatment containing basanite, BC = biochar treatment, Co-app. = co-application treatment, Co-pyr. = co-pyrolysis treatment containing rock-enhanced biochar.

B7.3 Fluorometric enzyme assay – method description

All equipment was sterilized before usage. Four fluorogenic substrates were used associated with either 4-methylumbelliferon (MUF) or 7-amido-4-methylcoumarin (AMC): MUF-ß-D-glucoside (for detection of BG), MUF-N-acetyl-ß-D-glucosidase (for detection of CH), MUF-phosphatase (for detection AP), and L-leucine-AMC-hydrochloride (for detection of LAP). This fluorogenic method is based on the liberation of fluorescent MUF or AMC once the associated substrate is used. MUF-ß-D-glucoside, MUF-N-acetyl-ß-D-glucosidase, and L-leucine-AMC-hydrochloride were purchased as crystalline material from Sigma Aldrich (Steinheim, Germany), while MUF-phosphatase was purchased as crystalline material from abcr GmbH (Karlsruhe, Germany).

Two sterile buffer solutions were prepared using sterile water. The 0.1 M MES buffer (from 20.673 g of 4-Morpholineethanesulfonic acid hemisodium salt in 1000 ml of sterile water; Sigma Aldrich) was prepared for MUF-based substrates and the 0.05 M TRIZMA buffer (from 0.985 g of Trizma® base and 2.66 g of Trizma® hydrochloride with 500 ml of sterile water; Sigma Aldrich) was prepared for the AMC-based substrate. For preparing 10 mM substrate stock solutions, the crystalline substrates were dissolved in dimethyl sulfoxide and sterile water. These stock solutions were diluted with the respective buffer solutions MES or TRIZMA to reach the desired substrate concentrations for the enzyme assay. For MUF-ß-D-glucoside, MUF-N-acetyl-ß-D-glucosidase, and L-leucine-AMC-hydrochloride, these concentrations were 0, 10, 20, 30, 40, 50, 100, and 200 µM. After a first check of AP enzyme activities, we decided to use higher substrate concentrations of 0, 10, 20, 30, 50, 100, 200, and 400 µM for MUF-phosphatase.

To prepare the soil suspension, homogenized samples of cooled (4 °C) soil were used. An equivalent to 0.5 g of dry soil was weighed in a respective glass bottle and 50 ml of sterile water was added. Each sample was sonicated for 2 minutes with an output energy of 40 J s^{-1}. A volume of 50 µl of the soil suspension were pipetted into sterile deep-well plates (Nunc™ F96 MicroWell™ plate, black, 96 well, Thermo Scientific™) and 50 µl of MES or TRIZMA buffer as well as 100 µl of substrate solution were added. The use of differently concentrated substrate solutions resulted in a gradient of concentrations within a deep-well plate. For MUF-ß-D-glucoside, MUF-N-acetyl-ß-D-glucosidase, and L-leucine-AMC-hydrochloride, these final concentrations were 0, 1, 2, 3, 4, 5, 10, and 20 µmol g^{-1} dry soil, respectively. For MUF-phosphatase this resulted in final substrate concentrations of 0, 1, 2, 3, 5, 10, 20, and 40 µmol g^{-1} dry soil.

For calibration purposes, standard solutions MUF and AMC were used. The 10 mM standard stock solutions were made by dissolving 0.1762 g of MUF or 0.0875 g of AMC, respectively, in 50 ml of methanol and 50 ml of sterile water. For the 10 µM working solutions, the stock solutions were diluted with MES buffer for MUF and TRIZMA buffer for AMC. For the determination of background fluorescence or quenching effects, soil suspensions (50 µl per well) and MES or TRIZMA buffer solutions (150, 140, 130, 100, 70, and 30 µl, respectively) were mixed with either 10 µM MUF or AMC standards (0, 10, 20, 50, 80, and 120 µl, respectively). These soil suspensions were made of a mix out of the nine replicates per treatment.

Fluorescence of the solution in the deep-well plates was measured after 0, 30, 60, and 120 minutes (excitation wavelength of 355 nm, emission wavelength of 460 nm) using a microplate reader (Victor^3 1420-05 Multi label Counter, PerkinElmer, USA). During the experiment, the deep-well plates remained at 22 °C. Before each reading of the plate in the microplate reader, the respective plate was shaken carefully. The soil enzyme activity was quantified by comparing with the plates containing the standard solutions.

B7.4 Correlation matrixes

Figure B.6: Correlation matrix of soil properties and extracellular enzyme kinetics of acid phosphatase (AP). Only significant correlations ($p < 0.05$) are shown. V_{max} = potential enzyme activity [nmol h^{-1} g^{-1} dry soil] , K_m = enzyme affinity [µmol g^{-1} dry soil], K_a = catalytic enzyme efficiency, C = total C content [g kg^{-1}], N = total N content [g kg^{-1}], C:N = total carbon to total N ratio, DOC = dissolved organic C content [mg kg^{-1}], C_{mic} = microbial biomass C content [mg kg^{-1}], N_{min} = mineral N content [mg kg^{-1}], P = available P content [mg kg^{-1}], pH = pH value in $CaCl_2$, EC = electric conductivity [µS cm^{-1}].

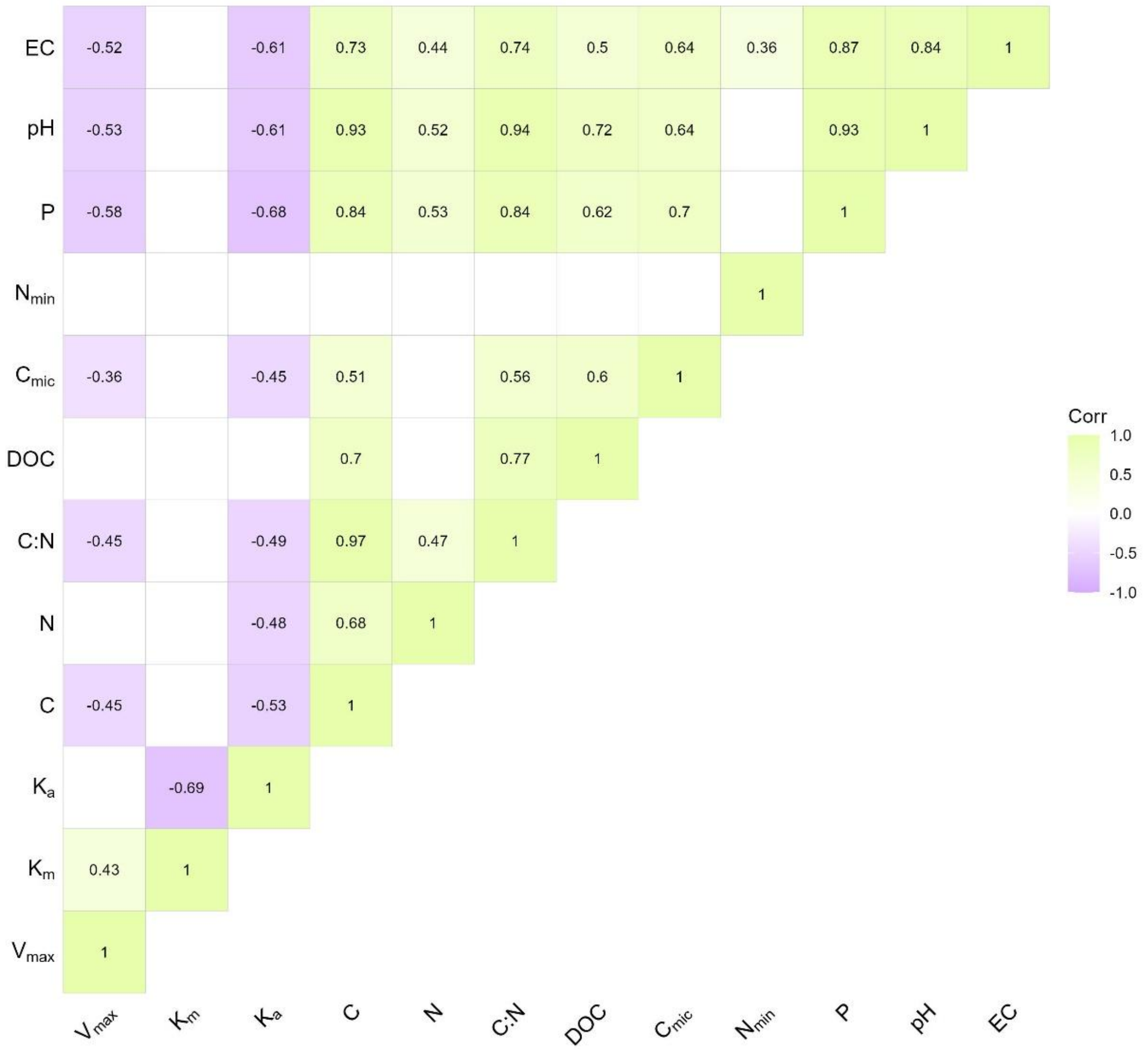

Figure B.7: Correlation matrix of soil properties and extracellular enzyme kinetics of chitinase (CH). Only significant correlations ($p < 0.05$) are shown. V_{max} = potential enzyme activity [nmol h^{-1} g^{-1} dry soil] , K_m = enzyme affinity [µmol g^{-1} dry soil], K_a = catalytic enzyme efficiency, C = total C content [g kg^{-1}], N = total N content [g kg^{-1}], C:N = total carbon to total N ratio, DOC = dissolved organic C content [mg kg^{-1}], C_{mic} = microbial biomass C content [mg kg^{-1}], N_{min} = mineral N content [mg kg^{-1}], P = available P content [mg kg^{-1}], pH = pH value in $CaCl_2$, EC = electric conductivity [µS cm^{-1}].

Figure B.8: Correlation matrix of soil properties and extracellular enzyme kinetics of ß-glucosidase (BG). Only significant correlations ($p < 0.05$) are shown. V_{max} = potential enzyme activity [nmol h^{-1} g^{-1} dry soil] , K_m = enzyme affinity [µmol g^{-1} dry soil], K_a = catalytic enzyme efficiency, C = total C content [g kg^{-1}], N = total N content [g kg^{-1}], C:N = total carbon to total N ratio, DOC = dissolved organic C content [mg kg^{-1}], C_{mic} = microbial biomass C content [mg kg^{-1}], N_{min} = mineral N content [mg kg^{-1}], P = available P content [mg kg^{-1}], pH = pH value in $CaCl_2$, EC = electric conductivity [µS cm^{-1}].

Figure B.9: Correlation matrix of soil properties and extracellular enzyme kinetics of leucine-aminopeptidase (LAP). Only significant correlations ($p < 0.05$) are shown. V_{max} = potential enzyme activity [nmol h^{-1} g^{-1} dry soil] , K_m = enzyme affinity [µmol g^{-1} dry soil], K_a = catalytic enzyme efficiency, C = total C content [g kg^{-1}], N = total N content [g kg^{-1}], C:N = total carbon to total N ratio, DOC = dissolved organic C content [mg kg^{-1}], C_{mic} = microbial biomass C content [mg kg^{-1}], N_{min} = mineral N content [mg kg^{-1}], P = available P content [mg kg^{-1}], pH = pH value in $CaCl_2$, EC = electric conductivity [µS cm^{-1}].

Study C:

Effects of combined biochar and basanite application on short-term glucose-priming and long-term soil carbon stability

Maria Ansari[a,b]*, Annette Eschenbach[a,b], Xavier Rodriguez Lloveras[a,b], Johannes Meyer zu Drewer[c,d,e], Nikolas Hagemann[c,d], Christian Beer[a,b], Joscha N. Becker[a,b]

[a] Department Earth System Sciences, University of Hamburg, Hamburg, Germany

[b] Earth and Society Research Hub (ESRAH), University of Hamburg, Hamburg, Germany

[c] Ithaka Institute, Goldbach, Germany

[d] Agroscope, Zurich, Switzerland

[e] Institute of Sustainable Energy Systems, Offenburg University, Offenburg, Germany

*corresponding author

In preparation for submission

C. Abstract

Biochar and silicate rock powder are soil amendments contributing to terrestrial carbon dioxide removal (CDR). Despite potential synergies, their combined effects on soil organic carbon (SOC) dynamics and thus on net CDR remain poorly understood. We compared pure biochar and basanite applications with their co-application and with rock-enhanced biochar produced via co-pyrolysis of biomass and basanite. Biochar-containing amendments were derived from willow wood and wheat straw and tested in three agricultural topsoils differing in texture, pH, and SOC content. Amendment effects on short-term glucose-induced priming were assessed in a 17-day incubation experiment with ^{13}C-glucose addition, while long-term amendment effects on SOC dynamics, pool sizes, and mean residence times were determined by fitting an exponential decay model to an 874-day incubation.

Short-term glucose-induced priming and its response to amendment application varied strongly between soils, likely depending on initial SOC and nutrient content of the soils and indicating glucose-amendment-interactions. However, reduction of SOC mineralization following biochar-containing amendment application was sustained also following glucose addition. Over time, application of wood-derived biochar-containing amendments consistently reduced overall SOC mineralization across the three investigated soils. The effects of wheat-derived amendments varied between soils, likely driven by initial soil pH. Pure biochar was more effective in reducing SOC mineralization than wheat-derived co-application and wood-derived rock-enhanced biochar. However, the higher long-term stable SOC pool following rock-enhanced biochar application compared to biochar could preserve long-term SOC enhancements, improving the CDR potential of rock-enhanced biochar. Additionally, co-pyrolysis increased the stable SOC pool in wheat-derived rock-enhanced biochar to levels comparable to wood-derived biochar, overwriting feedstock-driven limitations of amendment stability. Weathering of pure basanite became visible over time in both low-pH sandy soils. Overall, feedstock, soil properties, application type, and time since application proved decisive in controlling amendment effects on SOC dynamics, with rock-enhanced biochar being particularly beneficial for long-term SOC storage.

Keywords

rock-enhanced biochar, enhanced rock weathering (ERW), soil organic carbon (SOC) pools, Mean Residence Time (MRT), incubation, ^{13}C labeling, double first-order exponential decay model

Highlights

- Pure vs. combined applications (co-application, rock-enhanced biochar) of biochar and basanite
- Amendment effects on SOC mineralization determined by soil properties and time since application
- Wood-derived amendments reduced SOC mineralization stronger than wheat-derived ones
- Co-pyrolysis to rock-enhanced biochar increased stable SOC pool compared to biochar
- Combined applications partly diminished biochar's reduction of SOC mineralization

Graphical Abstract

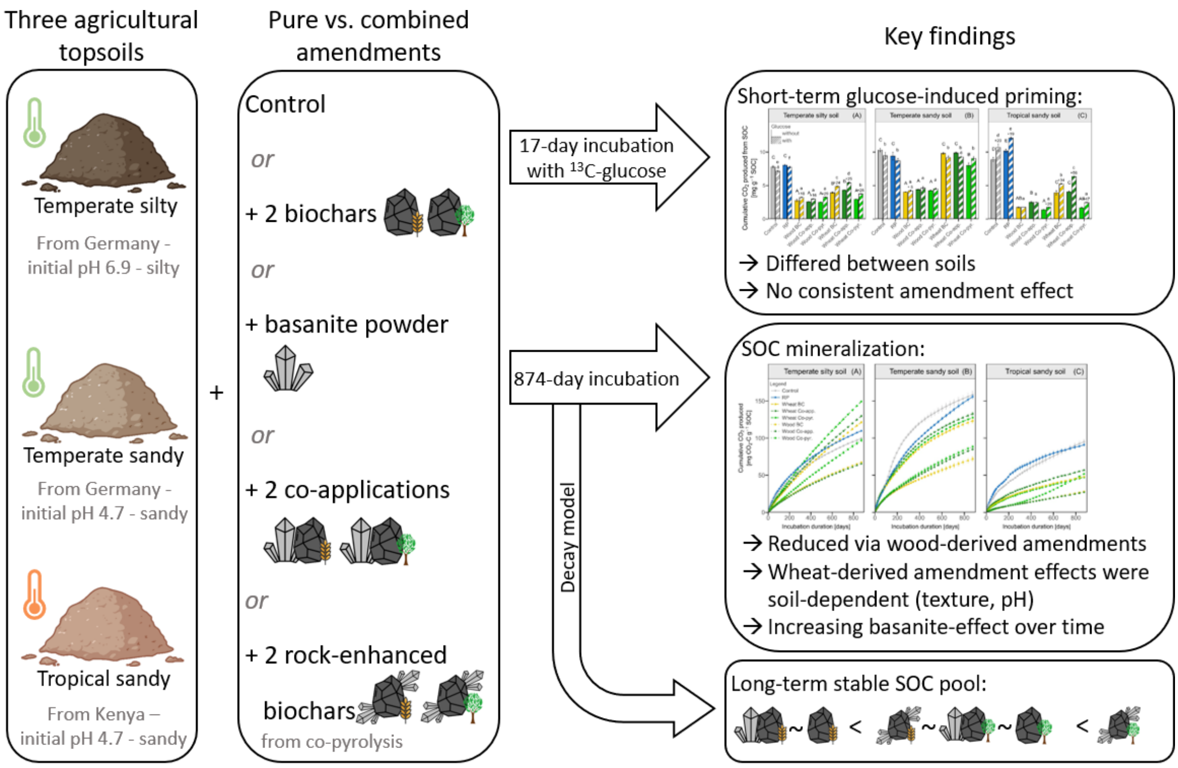

C.1 Introduction

Carbon dioxide removal (CDR) technologies are gaining increasing attention as an important tool to mitigate climate change and to reach long-term climate targets by limiting global warming to 2 °C relative to pre-industrial times (FUSS et al., 2018; RIAHI et al., 2022). The application of silicate rock powder for enhanced rock weathering and biochar are two promising soil-based CDR technologies, removing atmospheric carbon dioxide (CO_2) and enhancing soil carbon (C) storage (BUSS et al., 2021; JOSEPH et al., 2021; BEERLING et al., 2025). While both amendments are often investigated separately, their combined application could have beneficial synergistic effects on soil fertility and CO_2 sequestration (AMANN & HARTMANN, 2019; JOSEPH et al., 2021; ANSARI et al., 2026a; TE PAS et al., 2026). However, their combined effects on soil organic C (SOC) dynamics remain poorly investigated.

The weathering of soil-applied silicate rocks, such as basanite, increases soil C content through the reaction of CO_2-derived acidity with minerals, producing bicarbonate and carbonate (HARTMANN et al., 2013; BEERLING et al., 2025), which can be stored as inorganic soil C for up to centuries (HARTMANN et al., 2013; MARTIN, 2017). The rate of weathering and thus the associated CO_2 removal depend, among other factors, on soil properties, such as texture and soil pH (DIETZEN et al., 2018; ABDALQADIR et al., 2024; TE PAS et al., 2026). In addition to inorganic C storage, silicate rock powder application can enhance the stabilization of SOC in aggregates or on mineral surfaces and thus reduce the mineralizability of SOC (ROWLEY et al., 2018; BUSS et al., 2023). However, the application of silicate rock powder can also stimulate microbial activity (SOKOL et al., 2024; XU et al., 2024), which might enhance SOC mineralization and thus SOC losses, while accelerating weathering and thus increasing CO_2 uptake to unfold the CDR potential of enhanced weathering (BUSS et al., 2021; LI et al., 2025; REGINATO, 2025).

Biochar is the solid product from organic-matter pyrolysis, consisting mainly of highly aromatic pyrogenic compounds (ZHAO et al., 2013; HAGEMANN et al., 2018) that contribute to persistent SOC pools (KUZYAKOV et al., 2014; WANG et al., 2016). These biochar properties, including quantity and quality of biochar C, are governed by pyrolysis conditions and feedstock (ZHAO et al., 2013; LENG & HUANG, 2018; LEHMANN et al., 2021). Wood-derived biochar has often a higher content of aromatic C, while biochar derived from wheat straw contains more low-molecular weight organic substances (VAUGHN et al., 2013; WANG et al., 2016; HAN et al., 2020). Such compositional differences are reflected in biochar stability in soils (HAMER et al., 2004; LEHMANN et al., 2015; LENG & HUANG, 2018) and the effect of biochar on native SOC mineralization (WHITMAN et al., 2015;

WANG et al., 2016). Mineralization of native and biochar-derived SOC is often highest shortly after biochar application and declines over time (KUZYAKOV et al., 2009; AMELOOT et al., 2013; MAESTRINI et al., 2015), varying strongly between soils depending mainly on texture and SOC content (MAESTRINI et al., 2015; WANG et al., 2016; LENG & HUANG, 2018). As early mineralization rates may thus not reflect long-term SOC stability, tracking temporal dynamics is necessary (LEHMANN et al., 2015). To estimate biochar persistence and its effect on SOC mineralization over time, incubations are commonly used (LENG et al., 2019; HAN et al., 2020). Extrapolating incubation data using decay modeling allows the long-term assessment of distinct SOC pools with different mean residence times (MRT) to assess biochar potential for CDR over time (LENG et al., 2019; AZZI et al., 2024).

Beyond its direct effect on SOC mineralization, biochar application can also alter the response of SOC dynamics to inputs of easily degradable organic C compounds, such as root exudates. Such compounds can stimulate co-metabolic mineralization of native and biochar-derived SOC (HAMER et al., 2004; LEHMANN et al., 2009; KUZYAKOV, 2010), commonly simulated using glucose and described as glucose-induced priming effect (KUZYAKOV et al., 2009; KUZYAKOV, 2010; WHITMAN et al., 2015). This glucose-induced priming is often positive, but the magnitude can differ strongly between soils and is typically highest in low-fertility soils (BASTIDA et al., 2019; WU et al., 2020). The application of biochar can affect direction and magnitude of glucose-induced priming, varying with biochar and soil properties (HAMER et al., 2004; KUZYAKOV et al., 2009 ; LEHMANN et al., 2015). How the combined application of biochar and basanite rock powder might affect glucose-induced priming has not been investigated yet.

Combining biochar and silicate rock powder application can be conducted as a simple co-application as well as a co-pyrolysis of biomass and rock powder to produce rock-enhanced biochar (MEYER ZU DREWER et al., 2025; VORRATH et al., 2025). A co-pyrolysis of biomass and minerals could enhance the nutrient content (MEYER ZU DREWER et al., 2025) and the C yield of the pyrolysis product (BUSS et al., 2022). The effect of co-application of biochar and rock powder on SOC sequestration and storage has been increasingly researched (HONVAULT et al., 2024; ANTHONY et al., 2025; SOHNG et al., 2025; TE PAS et al., 2026), indicating additive or even synergistic effects. However, the effects of co-application and rock-enhanced biochar on SOC mineralization over time and their response to labile C input remain unknown.

Therefore, this study investigated how pure and combined amendment applications (co-application and rock-enhanced biochar) derived from two feedstocks (willow wood and wheat straw) affect SOC dynamics over time in contrasting agricultural soils and how these amendments affect glucose-induced priming. We hypothesize that (i) biochar-containing amendments exert a soil- and feedstock-specific effect on short-term glucose-induced priming, (ii) amendment application decreases cumulative CO_2 emissions relative to unamended soils over time, (iii) wood-derived biochar amendments are more resistant to mineralization than wheat-derived amendments, and that (iv) biochar-containing amendments increase the size and persistence of the long-term stable SOC pool. We tested these hypotheses by combining short-term (17 days) ^{13}C-glucose priming with a long-term incubation experiment (874 days). Different soil properties were considered by including three agricultural topsoils (temperate silty, temperate sandy, and tropical sandy) with differing pedogenesis, texture, pH, and SOC content. The CO_2 release and its $\delta^{13}C$ signatures were monitored to quantify SOC mineralization and glucose-induced priming. A decay model was used to extrapolate the measured CO_2 release and estimate long-term SOC pool sizes and MRTs.

C.2 Material and methods

C2.1 Soils and amendments

The study was conducted using three agricultural topsoils (0-30 cm; Table C.1). A temperate silty soil was collected in central Germany (Goldbach, Germany, 49°59'32.4"N 9°09'53.8"E), a temperate sandy soil was collected in Northern Germany (Gartow, Germany, 53°01'26.9"N 11°27'12.7"E), and a tropical sandy soil was collected in central Kenya (Machanga, Kenya, 0°27'26.8"S 37°39'37.4"E). The soil samples were air-dried until used for the incubation. Soils in the respective areas are classified as Cambisol (LFU, 2025), Podzol (LBEG, 2017), and Nitisol (FAO & UNESCO, 1974) according to the world reference base (IUSS WORKING GROUP WRB, 2022).

We tested seven soil amendments for this study. Two biochars (Table C.2), derived from willow wood (*Salix viminalis* L.) and wheat straw (*Triticum aestivum* L.), respectively, were pyrolyzed at 650 °C for 15 minutes. As silicate rock powder, we used the basanite *Eifelgold* (grain size 0.5-300 µm; further information in Table C.4 in Appendix). In addition, two types of combined applications were tested – co-application and co-pyrolysis. For the co-applications, either wood- or wheat-derived biochar, respectively, and basanite powder were mixed before use. To compare the effect of a simple mixing to a combined pyrolysis, biomass (willow wood and wheat straw, respectively) and basanite powder were mixed (90:10, w/w), pelletized, and pyrolyzed at 650 °C for 15 minutes to produce rock-enhanced biochar (Table C.2). Additional information regarding amendment production can be found in MEYER ZU DREWER et al. (2025). Based on the C contents of biochar and rock-enhanced biochar, we calculated that the rock-enhanced biochar derived from willow wood consisted of ~75% biochar and ~25% basanite powder. The rock-enhanced biochar derived from wheat straw consisted of ~77% biochar and ~23% basanite powder. Biochars and rock-enhanced biochars were hand-crushed, sieved to <2 mm, and homogenized as described in TIAN et al. (2016) before further used.

Table C.1: Initial properties of temperate silty, temperate sandy, and tropical sandy agricultural topsoil prior to pre-incubation.

Properties	**Temperate silty soil**	**Temperate sandy soil**	**Tropical sandy soil**
C [g kg^{-1}]	18.5 ± 0.0	12.4 ± 0.0	4.7 ± 0.0
TOC [g kg^{-1}]	13.3 ± 0.1	12.0 ± 0.0	4.6 ± 0.0
TIC [g kg^{-1}]	5.2 ± 0.1	0.4 ± 0.0	0.1 ± 0.0
N [g kg^{-1}]	1.3 ± 0.0	1.1 ± 0.0	0.3 ± 0.0
C:N	13.9 ± 0.0	11.6 ± 0.0	15.0 ± 0.0
$\delta^{13}C$ [‰]	-23.2 ± 0.1	-26.7 ± 0.0	-19.2 ± 0.0
pH [$CaCl_2$]	6.9 ± 0.0	4.7 ± 0.0	4.7 ± 0.0
Sand [%]	28.2 ± 1.0	93.8 ± 0.7	68.9 ± 0.6
Silt [%]	58.0 ± 1.0	2.5 ± 0.4	20.4 ± 0.6
Clay [%]	13.8 ± 0.3	3.7 ± 0.3	10.7 ± 0.2

Data is presented as mean ± standard error (n = 3). C = total carbon, TOC = total organic carbon, TIC = total inorganic carbon, N = total nitrogen.

Table C.2: Initial properties of biochars and rock-enhanced biochars.

Properties	**Wood biochar**	**Rock-enhanced wood biochar**	**Wheat biochar**	**Rock-enhanced wheat biochar**
C [g kg^{-1}] [b]	81.7	61.5	70.0	54.1
TIC [g kg^{-1}] [b]	0.9	0.8	0.7	0.7
TOC [g kg^{-1}] [b]	80.8	60.7	69.3	53.4
N [g kg^{-1}] [b]	0.83	0.69	0.89	0.66
C:N [b]	98	89	79	82
H:C [b]	0.20	0.19	0.20	0.18
O:C [b]	0.052	0.048	0.060	0.047
$\delta^{13}C$ [‰] [a]	-28.2 ± 0.0	-27.7 ± 0.1	-29.7 ± 0.1	-29.9 ± 0.3
Ash content [%] [b]	13.5	35.1	23.7	41.9

[a] Data is presented as mean ± standard error (n = 3), [b] values are based on measurements by Eurofins Umwelt-Ost GmbH (Bobritzsch-Hilbersdorf, Germany) according to the analytical guidelines of the European Biochar Certificate (EBC, 2024). C = total carbon, TOC = total organic carbon, TIC = total inorganic carbon, N = total nitrogen.

C2.2 Experimental design

To assess the effects of the soil amendments on SOC dynamics, we applied the amendments to the different soils in an aerobic incubation experiment (n = 4). For the control treatment, 125 g of air-dried soil (dry-weight equivalent) were used. For the biochar treatments, 4.4 g of wood-derived biochar (~3.5 wt%) or 4.0 g of wheat-derived biochar (~3.2 wt%) were mixed with the soil, respectively. In the rock powder treatment, 2.5 g of basanite rock powder (~2.0 wt%) was added to the soil. For the co-application treatment, 4.4 g of wood-derived biochar (~3.5 wt%) or 4.0 g of wheat-derived biochar (~3.2 wt%), respectively, and 2.5 g of basanite powder (~2.0 wt%) were added. The co-pyrolysis treatment contained a mixture of soil and 6.8 g of wood-derived rock-enhanced biochar (~5.5 wt% consisting of ~4.1 wt% biochar and ~1.4 wt% basanite powder) or 6.5 g of wheat-derived rock-enhanced biochar (~5.2 wt% consisting of ~4.0 wt% biochar and ~1.2 wt% basanite powder), respectively. All results are expressed on a per-gram-SOC basis to ensure comparability across treatments. The samples were adjusted to 40% water holding capacity (WHC) using sterile distilled water and pre-incubated for 7 days at 20 °C.

This set-up of samples was weighed three times for three incubation approaches. One set was used for an 874-day incubation to observe amendment effects over time as follows: after pre-incubation for 7 days, 60 g of each sample (dry-weight soil equivalent excluding amendment weight) was adjusted to 60% WHC using sterile distilled water, transferred into glass flasks sealed with rubber septa, and incubated at 20 °C under aerobic conditions. To maintain a higher pressure within the flasks compared to the surrounding air and to avoid oxygen deficiency by high CO_2 concentrations, flasks were flushed with synthetic air when necessary (>2% CO_2 in headspace). The accumulation of CO_2 in the flask headspace was measured regularly using a gas chromatograph (JAS 6890N GC, Joint Analytical Systems GmbH, Moers, Germany).

The other two incubation sets (glucose and reference set) were incubated for 17 days to observe short-term glucose-induced priming. The glucose set received 60 mM ^{13}C-labeled glucose solution (~566‰), representing labile C inputs (KUZYAKOV et al., 2009; KUZYAKOV, 2010; WHITMAN et al., 2015). The glucose solution consisted of uniformly labeled ^{13}C glucose (99% ^{13}C) and unlabeled glucose (ratio 1:163) and was added quantitatively equivalent to 50% of the present microbial biomass C (MBC). The MBC was determined from the remaining material following the pre-incubation of the 874-day incubation and these values were used as the basis for calculating glucose additions to the glucose set. No glucose was added to the reference set. Both sets were adjusted to 60% WHC and treated as the 874-day incubation set. Additionally, gas samples for $\delta^{13}C$ analysis were taken (days 1, 2, 3, 6, 9, 13, 17), stored in exetainers, and analyzed using an isotope ratio mass spectrometer (IRMS; Delta V Plus, Thermo Fisher Scientific, Bremen, Germany). The sets with (glucose set) and without ^{13}C-labeled glucose (reference set) allowed us to quantify glucose-induced priming and determine amendment effects on this priming by separating glucose-derived CO_2 from CO_2 originating from native and amendment-derived SOC (KUZYAKOV, 2011).

C2.3 Analysis of soil samples

The remaining sample material following the pre-incubation of the 874-day incubation was analyzed for soil sample properties, representing the initial soil conditions prior to incubation applicable to all incubation sets. Air-dried samples were used to determine soil pH in 0.01 M $CaCl_2$ solution (soil:$CaCl_2$ solution = 1:2.5) using a pH meter (MP230, Mettler-Toledo GmbH, Gießen, Germany) and electric conductivity (EC) in deionized water (soil:water = 1:2.5) using a conductivity meter (Cond 330i, WTW GmbH, Weilheim, Germany). A subsample was ground and dried at 105 °C to determine total C and N contents using an elemental analyzer (vario MAX cube, Elementar Analysensysteme GmbH, Langenselbold, Germany). The total inorganic carbon (TIC) content was determined using a TOC analyzer (soli TOC® cube, Elementar Analysensysteme GmbH, Langenselbold, Germany). The total organic carbon (TOC) content was calculated as the difference between total C and TIC. A fresh subsample of the pre-incubated soil was frozen (-20 °C) and used to determine MBC using the chloroform fumigation extraction (CFE) method after DIN (2011), adapted from VANCE et al. (1987). Therefore, two times 12.5 g (dry weight equivalent) were weighed into glass flasks. One was directly extracted with 50 ml of 0.05 M K_2SO_4 solution to quantify DOC. The second was fumigated with chloroform to lyse microbial cell walls and was afterwards extracted using K_2SO_4 solution. To determine C contents, the extracts were measured using a TOC analyzer (TOCL, Shimadzu Corporation, Kyoto, Japan). The difference between the fumigated and non-fumigated extracts is interpreted as MBC, using an extraction factor k_{EC} of 0.45 (JOERGENSEN, 1996). The MBC content after pre-incubation was used to calculate the amount of added ^{13}C-labeled glucose, as described in chapter C2.2. After the 874-day incubation, soil pH as well as C and N content were determined again (Table C.5 in Appendix).

C2.4 Calculation of C mineralization and glucose-induced priming effect

The CO_2 concentration in the headspace of the incubation flasks was used to calculate the cumulative CO_2 release normalized to initial SOC (mg CO_2-C g^{-1} SOC). To trace the fate of SOC (native and amendment-derived SOC) and ^{13}C-labeled glucose and to investigate glucose-induced priming, we determined $\delta^{13}C$ (‰) of soils and amendments prior to the incubations and of the released CO_2 during the 17-day incubations using an IRMS (Delta V Plus, Thermo Fisher Scientific, Bremen, Germany). The abundance of ^{13}C is expressed as $\delta^{13}C$ representing the ratios of ^{13}C:^{12}C relative to the Vienna-PeeDee-Belemnite-Standard, defined as $[(R_{sample} - R_{standard}) / R_{standard}] \times 1000$. The isotopic signatures of glucose and SOC were used to determine the source of the produced CO_2 by using a two-pool mixing model (Equations C1 and C2) following BAMMINGER et al. (2014) and FANG et al. (2015):

$$\mathrm{X} = \frac{(\delta_{treatment} - \delta_{reference})}{(\delta_{glucose} - \delta_{reference})} * 100 \qquad \text{(C1)}$$

$$\mathrm{Y} = 100 - \mathrm{X} \qquad \text{(C2)}$$

where X is the proportion of CO_2 derived from glucose (%), $\delta_{treatment}$ is the $\delta^{13}C$ value (‰) of the samples including soil, amendment, and glucose (glucose set), $\delta_{reference}$ is the $\delta^{13}C$ value (‰) of the respective samples without glucose (reference set), $\delta_{glucose}$ is the $\delta^{13}C$ value (‰) of the glucose solution, and Y is the proportion of CO_2 derived from SOC (%). The mineralized SOC (mg mineralized SOC g^{-1} SOC) was calculated by multiplying the cumulative CO_2 production (mg CO_2-C g^{-1} SOC) with Y.

The glucose-induced priming effect was calculated from the difference in the SOC mineralization between samples with and without glucose addition (Equation C3):

$$PE = \frac{\left(mineralized\ SOC_{glucose} - mineralized\ SOC_{reference}\right)}{mineralized\ SOC_{reference}} * 100 \qquad \text{(C3)}$$

where PE is the priming effect (%), $mineralized\ SOC_{glucose}$ is the SOC mineralized in the glucose-amended treatments (mg mineralized SOC g^{-1} SOC), and $mineralized\ SOC_{reference}$ is SOC mineralized in the reference samples without glucose addition (mg mineralized SOC g^{-1} SOC).

C2.5 Double first-order exponential decay model

To describe and estimate SOC mineralization kinetics, we used a double first-order exponential decay model (Equation C4) based on ANDRÉN & KÄTTERER (1997) following WANG et al. (2016) and LI et al. (2024):

$$C_{cum}(t) = C_f * \left(1 - e^{(-k_f * t)}\right) + C_i * \left(1 - e^{(-k_i * t)}\right) \quad \text{(C4)}$$

where C_{cum} is the total CO_2 respired (mg CO_2-C g^{-1} SOC) at time t of our long-term incubation, C_f and C_i are the fast and intermediate SOC pool (mg C g^{-1} soil), respectively, and k_f and k_i are the respective decomposition rates ($year^{-1}$). The Mean Residence Times MRT_f and MRT_i (years) of both SOC pools are calculated as the reciprocal of both decomposition rates (LENG et al., 2019). Treatments or samples, where no model adaptation was possible, e.g. when the CO_2 production was not decreasing with increasing incubation duration or showed inconsistencies, were excluded.

While both labile and intermediate pools contain native and more labile biochar-derived SOC, a third SOC pool was distinguished to determine the mineralization kinetics on longer time scales. This long-term stable SOC pool contains the stable biochar-derived SOC (Table C.6 in Appendix) and was determined by MEYER ZU DREWER et al. (2025) using hydropyrolysis, as proposed by HAGEMANN et al. (2025). The SOC in this stable pool is considered to remain in the soil for several decades and is not part of the decay model.

C2.6 Statistical analysis

To test for significant differences ($p < 0.05$) between treatments within one soil, a one-way analysis of variance (ANOVA) was conducted. For repeated measurements of CO_2 release during the 874-day incubation, we used a linear mixed effects (LME) model with the sample as a random factor. Both ANOVA and LME were followed by a Tukey HSD post-hoc test for pairwise comparison. Prior to analysis, normality and variance homogeneity of model residues were checked visually. All calculations and statistical tests were conducted in RStudio (version 4.5.1) using 'dplyr' (WICKHAM et al., 2023) for data handling, 'lme4' (BATES et al., 2015) for LME computing, 'multcomp' (HOTHORN et al., 2008) for compact letter display, 'ggplot2' (WICKHAM, 2016) and 'gridExtra' (AUGUIE & ANTONOV, 2017) for data visualization.

C.3 Results

C3.1 Short-term glucose-induced priming

The glucose-induced priming effect during the 17-day incubation depended on soil type and applied amendment (Figure C.1). In the temperate silty soil, the SOC mineralization in the control treatment was reduced by glucose addition, while the treatments containing biochar-containing amendments experienced positive glucose-induced priming (Figure C.1A). In the temperate sandy soil, the amended treatments reacted similar to the control treatments, showing no or only small effects of glucose addition on SOC mineralization (Figure C.1B). In the tropical sandy soil, most amended treatments reacted similar as the control treatments, showing positive glucose-induced priming (Figure C.1C). Following the application of pure and co-applied wood-derived biochar to the tropical sandy soil, glucose addition did not affect SOC mineralization.

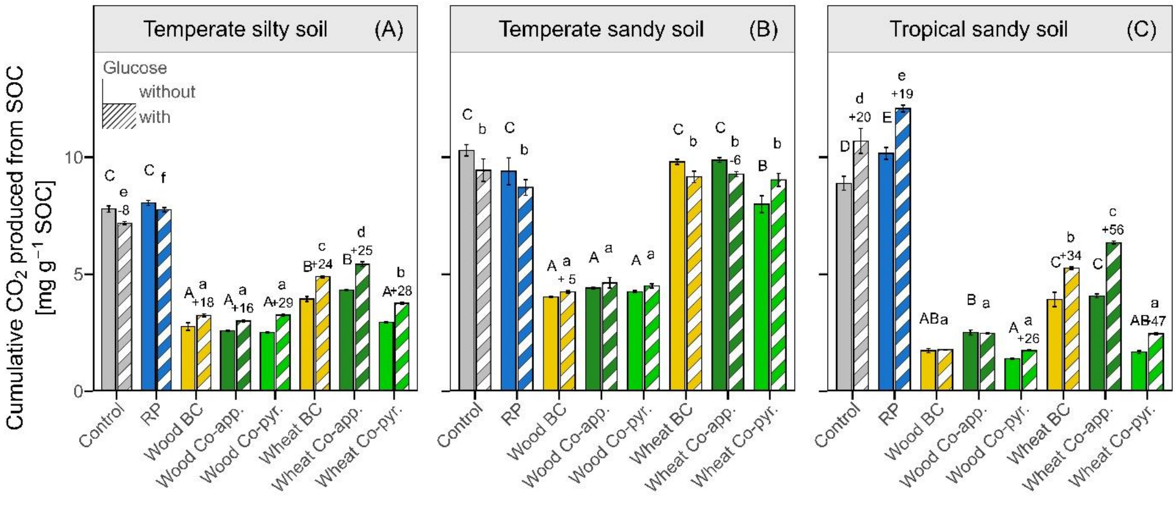

Figure C.1: Cumulative respiration from native and amendment-derived SOC (mg mineralized SOC g^{-1} SOC) of temperate silty (A), temperate sandy (B), and tropical sandy soil (C) per treatment (n = 4, mean and standard error) at the end of the short-term incubation (17 days) with and without glucose addition. Numbers above the bars are the priming effect (%) of the treatment with glucose addition compared to the respective treatment without glucose addition. Only significant priming values ($p < 0.05$) are shown. Capital letters above the bars indicate significant differences between treatments without glucose addition within one soil, lowercase letters above the bars indicate significant differences between treatments with glucose addition within one soil. RP = rock powder treatment containing basanite rock powder, BC = biochar treatment containing biochar derived from either wood or wheat, Co-app. = co-application treatment containing basanite and biochar derived from either wood or wheat, Co-pyr. = co-pyrolysis treatment containing rock-enhanced biochar derived from either wood or wheat.

C3.2 CO_2 release over time following amendment application

The SOC mineralization during the 874-day incubation depended on soil type and applied amendment, particularly amendment feedstock (Figure C.2; Table C.7 in Appendix). Wood-derived amendments reduced the cumulative CO_2 release from all three soils during the 874-day incubation. This reduction of CO_2 release became less pronounced over time following the application of wood-derived rock-enhanced biochar compared to pure biochar (temperate sandy soil) or both pure and co-applied biochar (temperate silty and tropical sandy soil). How fast the CO_2 release from wood-derived rock-enhanced biochar-amended soils began to diverge from that of biochar-amended soils differed between soils, occurring earliest in the tropical sandy soil (significant from day 6 onwards) and latest in the temperate sandy soil (day 447). Differences between pure and co-applied wood-derived biochar occurred solely in the temperate sandy soil from day 447 onward. The reduction of CO2 release following wood-derived amendments was more pronounced than following wheat-derived amendment application. Additionally, wheat-derived amendment effects on the CO_2 release differed between soils. In the temperate silty soil, the application of wheat-derived amendments initially led to a lower or similar CO_2 release as the control but exceeded those of control over time (Figure C.2A; Table C.7 in Appendix). This increase in CO_2 release occurred fastest following the application of wheat-derived rock-enhanced biochar (day 177), followed by co-application (day 279), and latest after the application of pure biochar (day 419). In both sandy soils, the three wheat-derived biochar-containing amendments reduced SOC mineralization compared to the unamended control (Figure C.2B,C; Table C.7 in Appendix). On longer time scales (earliest after 237 days), application of pure wheat-derived biochar led to lower SOC mineralization compared to co-application in all three soils (Figure C.2; Table C.7 in Appendix). Application of wheat-derived rock-enhanced biochar either led to higher (temperate silty soil), similar (temperate sandy soil), or lower (tropical sandy soil) CO_2 release compared to pure and/or co-applied biochar with increasing incubation duration. Basanite rock powder application increased the mineralization of SOC in temperate silty (day 121), while reducing the CO_2 release from the temperate sandy soil (day 77) (Figure C.2A,C; Table C.7 in Appendix). In the tropical sandy soil, basanite powder application initially increased SOC mineralization, but reached a similar cumulative CO_2 release as control on longer time scales (from day 503) (Figure C.2B; Table C.7 in Appendix).

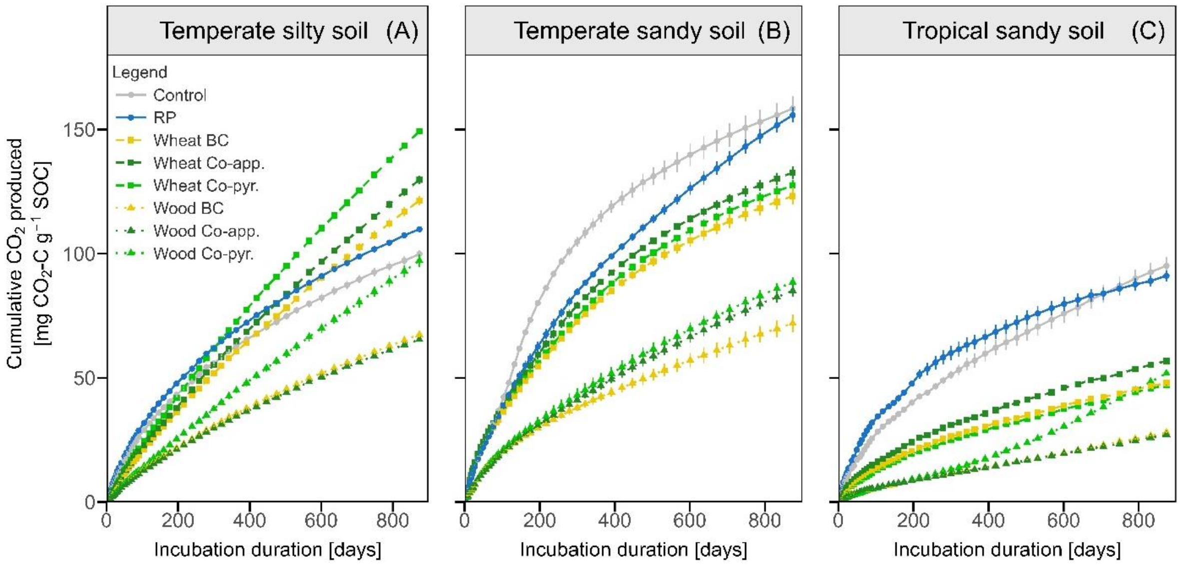

Figure C.2: Cumulative respiration (mg CO_2-C g^{-1} SOC) of temperate silty (A), temperate sandy (B), and tropical sandy soil (C) per treatment (n = 4, mean and standard error) during the 874-day incubation. Significance letters are listed in Table C.7 in Appendix. RP = rock powder treatment containing basanite rock powder, BC = biochar treatment containing biochar derived from either wood or wheat, Co-app. = co-application treatment containing basanite and biochar derived from either wood or wheat, Co-pyr. = co-pyrolysis treatment containing rock-enhanced biochar derived from either wood or wheat.

C3.3 Size and Mean Residence Time of long-term SOC pools

The smallest part of SOC in all treatments can be considered labile with MRTs ranging from 0.06 ± 0.01 to 0.20 ± 0.02 years (Table C.3). While amendment application did not affect the MRT of this labile pool, it partly reduced the labile SOC pool size. While biochar-containing amendments were more likely to reduce the size of the labile SOC pool, rock powder application increased the labile SOC pool in the tropical sandy soil. The intermediate SOC pool contained most SOC in control and rock powder treatments, ranging from 81.8 ± 4.0% to 93.7 ± 3.2% of SOC across soils. Following the application of biochar-containing amendments, the share of SOC in the intermediate pool was reduced, containing between 19.1 ± 0.1% and 43.1 ± 0.2% of SOC. The MRT of this intermediate SOC pool was partly increased, especially following the application of wood-derived amendments in the tropical sandy soil. The stable biochar-derived SOC, forming the stable SOC pool, contained the biggest share of SOC in the treatments with biochar-containing amendments.

Table C.3: Kinetic parameters of the double first-order exponential decay model describing soil organic carbon (SOC; native and biochar-derived) pools and their mean residence time (MRT) in temperate silty, temperate sandy, and tropical sandy soil per treatment based on the long-term incubation (874 days). Lowercase letters indicate significant differences ($p < 0.05$) between SOC pool sizes or MRTs within one SOC pool and one soil.

Soil	Treatment	Labile SOC pool		Intermediate SOC pool		Stable SOC pool
		Size (% SOC)	MRT (years)	Size (% SOC)	MRT (years)	Size (% SOC)
Temperate silty soil	Control	12.5 ± 0.1 [b]	0.19 ± 0.01 [ab]	87.5 ± 0.1 [d]	2.25 ± 0.07 [a]	-
	Rock powder	12.4 ± 0.9 [b]	0.19 ± 0.02 [ab]	87.6 ± 0.9 [d]	2.16 ± 0.15 [a]	-
	Wheat BC	n.a.	n.a.	n.a.	n.a.	n.a.
	Wheat Co-app.	0.7 ± 0.1 [a]	0.19 ± 0.01 [ab]	43.0 ± 0.2 [c]	5.33 ± 0.72 [b]	56.2 ± 0.3 [a]
	Wheat Co-pyr.	0.4 ± 0.0 [a]	0.17 ± 0.02 [ab]	38.7 ± 1.0 [b]	5.45 ± 0.19 [b]	60.9 ± 1.1 [bc]
	Wood BC	1.2 ± 0.1 [a]	0.21 ± 0.02 [b]	36.0 ± 0.5 [ab]	3.70 ± 0.15 [ab]	62.9 ± 0.6 [c]
	Wood Co-app.	1.1 ± 0.0 [a]	0.19 ± 0.01 [b]	38.1 ± 0.2 [b]	3.63 ± 0.24 [ab]	60.8 ± 0.2 [b]
	Wood Co-pyr.	0.1 ± 0.0 [a]	0.14 ± 0.02 [a]	34.3 ± 0.5 [a]	8.26 ± 0.42 [c]	65.6 ± 0.5 [d]
Temperate sandy soil	Control	n.a.	n.a.	n.a.	n.a.	-
	Rock powder	6.3 ± 3.0 [b]	0.13 ± 0.08 [ab]	93.7 ± 3.0 [e]	2.41 ± 0.65 [a]	-
	Wheat BC	3.1 ± 0.1 [ab]	0.07 ± 0.00 [a]	36.9 ± 0.3 [d]	1.37 ± 0.08 [a]	60.0 ± 0.4 [a]
	Wheat Co-app.	2.7 ± 0.1 [a]	0.07 ± 0.01 [a]	38.0 ± 0.3 [d]	1.29 ± 0.10 [a]	59.3 ± 0.3 [a]
	Wheat Co-pyr.	2.7 ± 0.1 [a]	0.07 ± 0.00 [a]	33.9 ± 0.2 [bc]	1.38 ± 0.05 [a]	63.5 ± 0.1 [c]
	Wood BC	3.1 ± 0.4 [ab]	0.20 ± 0.01 [b]	32.7 ± 0.5 [ab]	6.82 ± 1.62 [a]	64.2 ± 0.1 [c]
	Wood Co-app.	1.8 ± 0.2 [a]	0.14 ± 0.02 [ab]	36.0 ± 0.2 [cd]	5.35 ± 1.44 [a]	62.2 ± 0.2 [b]
	Wood Co-pyr.	2.0 ± 0.6 [a]	0.16 ± 0.02 [b]	30.3 ± 0.2 [a]	4.29 ± 0.68 [a]	67.7 ± 0.4 [d]
Tropical sandy soil	Control	7.5 ± 1.3 [b]	0.16 ± 0.03 [abc]	92.5 ± 1.3 [c]	8.09 ± 3.36 [a]	-
	Rock powder	18.5 ± 3.9 [c]	0.12 ± 0.03 [abc]	81.5 ± 3.9 [b]	1.50 ± 0.23 [a]	-
	Wheat BC	2.9 ± 0.1 [ab]	0.18 ± 0.01 [bc]	20.9 ± 0.1 [a]	3.04 ± 0.25 [a]	76.2 ± 0.2 [b]
	Wheat Co-app.	2.7 ± 0.1 [ab]	0.15 ± 0.01 [abc]	22.1 ± 0.4 [a]	2.95 ± 0.42 [a]	75.2 ± 0.5 [a]
	Wheat Co-pyr.	2.1 ± 0.2 [ab]	0.19 ± 0.01 [c]	19.2 ± 0.2 [a]	4.78 ± 0.96 [a]	78.8 ± 0.2 [c]
	Wood BC	0.2 ± 0.0 [a]	0.09 ± 0.01 [a]	21.9 ± 0.1 [a]	39.84 ± 1.69 [b]	78.0 ± 0.1 [c]
	Wood Co-app.	0.2 ± 0.0 [a]	0.11 ± 0.00 [ab]	22.0 ± 0.2 [a]	35.16 ± 1.98 [b]	77.8 ± 0.2 [c]
	Wood Co-pyr.	n.a.	n.a.	n.a.	n.a.	n.a.

Data is presented as mean ± standard error (n = 4). RP = rock powder treatment containing basanite rock powder, BC = biochar treatment containing biochar derived from either wood or wheat, Co-app. = co-application treatment containing basanite and biochar derived from either wood or wheat, Co-pyr. = co-pyrolysis treatment containing rock-enhanced biochar derived from either wood or wheat, n.a. = model not applicable.

C.4 Discussion

C4.1 Amendment effect on short-term glucose-induced priming

The addition of glucose as an easily available C source can enhance the mineralization of native (WU et al., 2020; GAUDEL et al., 2022) and biochar-derived SOC (LEHMANN et al., 2009; FANG et al., 2014) by promoting the co-metabolic decomposition of SOC by microbes (HAMER et al., 2004; KUZYAKOV et al., 2009). We observed that both glucose-induced priming and its response to amendment application differed strongly between soils. In the temperate sandy soil, glucose addition had only minor effects on the mineralization of SOC, regardless of whether and which amendment was applied. This absence of glucose-induced priming could be caused by the higher proportion of POM in this soil (ANSARI et al., 2026b), which is less likely to be primed due to its high recalcitrance (LAVALLEE et al., 2020; ZHENG et al., 2023). In the tropical sandy soil, we observed a positive glucose-induced priming, potentially caused by the initially low SOC content of this soil. In such soils, microbial communities are often C limited and thus respond more strongly to fresh substrate inputs, like glucose, resulting in a more pronounced priming effect (KUZYAKOV et al., 2009; BASTIDA et al., 2019; WU et al., 2020). While this effect was largely independent of the applied amendment, pure and co-applied wood-derived biochar were able to suppress this glucose-induced priming loss of SOC, potentially due to the adsorption of glucose onto the biochar surfaces (WANG et al., 2016; IPPOLITO et al., 2020; KALU et al., 2024). In line with this, TOMCZYK et al. (2020) reported that biochar derived from lignin-rich material, such as wood, has a higher specific surface area. That wood-derived rock-enhanced biochar did not have this reducing effect on glucose-induced priming indicates a lower reactivity, probably due to the occlusion of basanite particles in the biochar pores, reducing its pore volume and specific surface area (MEYER ZU DREWER et al., 2025). In contrast to both sandy soils, the application of biochar-containing amendments increased the systems reaction to glucose in the temperate silty soil. While the SOC mineralization of the unamended soil did not respond to glucose addition, biochar-containing amendments increased the glucose-induced priming. This increased SOC mineralization could result from an interaction between glucose and biochar-containing amendments (HAMER et al., 2004). This interaction could arise from a combined priming induced by glucose and easily available C compounds in biochar (LUO et al., 2017). Alternatively, biochar-containing amendments could adsorb mineral N onto their surfaces (CLOUGH et al., 2013), thus increasing the microbial N demand (ANSARI et al., 2026c) causing an N-mining and thus promoted decomposition of soil organic matter (CRAINE et al., 2007; CHEN et al., 2014). The latter is supported by the pronounced reduction of N during the incubation of the temperate silty soil amended with biochar-containing amendments compared to the unamended soil (Table C.5 in Appendix). The variability of the response of glucose-induced priming to amendment applications indicated complex interactions between soil, amendment, and C inputs. Future studies should thus include the long-term response of amended soils to repeated glucose addition, which could result in more pronounced glucose-induced priming (WU et al., 2020). Nevertheless, all amendments that reduced SOC mineralization in the glucose-free samples compared to the unamended soil continued to reduce SOC mineralization also with glucose addition. This highlights the suitability of biochar-containing amendments as a CDR technology resulting in a long-term SOC increase, even under the input of readily decomposable C.

C4.2 Amendment effect on SOC dynamics over time depend on feedstock, application type, and soil properties

Feedstock in as important factor determining the effect of biochar-containing amendment application on SOC mineralization. As hypothesized, wood-derived biochar-containing amendments consistently reduced SOC mineralization largely independent of soil properties and time since application. This indicates a higher stability of wood-derived amendments compared to wheat-derived amendments (VAUGHN et al., 2013; WANG et al., 2016; WANG et al., 2022) and highlights their potential to lower SOC mineralization and thus to reduce soil-borne CO_2 emissions (LIU et al., 2020). The effects of wheat-derived amendment application on SOC mineralization were driven by soil properties. In the temperate silty soil, wheat-derived amendments increased SOC mineralization on longer time scales compared to the unamended soil, whereas they reduced SOC mineralization in both sandy soils. This contrasting effect might reflect differences in initial soil pH (WANG et al., 2022), which were higher in the temperate silty soil (initial pH 6.9) than in both sandy soils (initial pH 4.7). Consistently, LUO et al. (2011) reported lower biochar stability in high (initial pH 7.6) than in low (initial pH 3.7) pH soils. This indicates that soil properties, such as initial soil pH, can determine biochar-derived amendment-induced changes of SOC mineralization, highlighting the importance of site-specific soil conditions for predicting amendment effects.

Across feedstocks, the effect of biochar-containing amendments on SOC mineralization was affected by the application type. Pure biochar generally was as effective as, or even more effective than, combined applications in reducing

SOC mineralization. Combined application with basanite rock powder, especially as wood-derived rock-enhanced biochar or wheat-derived co-application, partly diminished the reducing effect of biochar on SOC mineralization on longer time scales (earliest after 121 days). Since rock-enhanced biochar generally had a higher stable SOC content than pure and co-applied biochar (MEYER ZU DREWER et al., 2025), the additional released CO_2 likely originated from native SOC. However, these greater losses of native SOC could be offset by the higher stable SOC content in rock-enhanced biochar, thus preserving the long-term positive effect of (rock-enhanced) biochar on total SOC and thus on CDR. Based on these first insights from our study, future studies should systematically compare these application types over extended time scales to better disentangle the mechanisms driving their divergent effects on SOC mineralization.

The combination of wood-derived rock-enhanced biochar in the tropical sandy soil differed from all other soil-amendment-combinations by showing increasing CO_2 emissions after ~250 days. All other combinations had a declining or stable CO_2 release over time, which reflects decreasing SOC mineralization due to depletion of labile C compounds and the slower turnover of more recalcitrant compounds (KUZYAKOV et al., 2009; AMELOOT et al., 2013; WANG et al., 2016; HAN et al., 2020). In contrast, the late SOC mineralization increase observed in the tropical soil amended with wood-derived rock-enhanced biochar suggests activation of an additional mineralization pathway. This might be a shift in microbial dominance as observed by LIU et al. (2020), where fungal activity increases once bacterial mineralization of labile compounds declines and more recalcitrant C sources prevail (LEHMANN et al., 2009; AMELOOT et al., 2013; WANG et al., 2022). That this response occurred only in the tropical soil amended with wood-derived rock-enhanced biochar may relate to an inherently higher fungal:bacterial ratio in this soil (MALIK et al., 2016), the high proportion of recalcitrant compounds in woody feedstock (VAUGHN et al., 2013; WANG et al., 2016; WANG et al., 2022) triggering fungal activity, and/or the reduced availability of labile compounds due to co-pyrolysis. The latter is, however, unlikely since ANSARI et al. (2026a) observed a higher release of DOC following the application of rock-enhanced biochar compared to biochar. While the mechanisms behind this response remain speculative, it shows that feedstock properties and soil-specific microbial dynamics interact.

The effect of basanite rock powder application on the CO_2 release increased with time since application, representing the net gaseous C balance, which is relevant for evaluating CDR via enhanced rock weathering (DIETZEN et al., 2018). The increasing effect on CO_2 release over time points to progressive basanite weathering and associated impacts on soil C dynamics. However, the direction and magnitude of these effects differed between soils. In the temperate silty soil, basanite application increased cumulative CO_2 release, indicating stimulated microbial activity and enhanced SOC mineralization exceeding CO_2 uptake via weathering (DIETZEN et al., 2018; TE PAS et al., 2026). In contrast, both sandy soils showed clear indications of basanite weathering. In the tropical sandy soil, basanite application initially increased CO_2 release, but cumulative emissions decreased over time to the same level as the unamended soil after 503 days. This temporal pattern indicates an initial stimulation of microbial respiration followed by increasing CO_2 uptake via weathering (DIETZEN et al., 2018). In the temperate sandy soil, basanite powder reduced cumulative CO_2 release relative to the unamended control already from day 77 onwards. This could reflect reduced SOC mineralization (BUSS et al., 2023) and/or enhanced CO_2 uptake during weathering (TE PAS et al., 2026). The latter is supported by the observed stable or increased soil pH in both sandy soils at the end of the 874-day incubation (Table C.5 in Appendix), indicating ongoing alkalinity generation through mineral dissolution (HARTMANN et al., 2013; BEERLING et al., 2020), whereas all other treatments exhibited declining pH over time. Given that increasing pH generally rather promotes than suppresses microbial activity (DIETZEN et al., 2018), a reduced microbial respiration alone appears unlikely as the dominant mechanism. Taken together, the results suggest that measurable basanite weathering occurred within the investigated time frame primarily in the sandy soils, indicating a faster or more effective weathering of basanite powder in coarse textured soils with initial low pH (ABDALQADIR et al., 2024).

C4.3 Amendment effect on size and MRT of SOC pools

The application of biochar-containing amendments directly affects amount and composition of SOC, determining the size and MRT of SOC pools (KUZYAKOV et al., 2009; LEHMANN et al., 2009; HAN et al., 2020). In the present study, the fast and intermediate SOC pools contained the native and the more labile biochar-derived SOC. The presence of the stable biochar-derived SOC reduced the relative share of both labile and intermediate SOC pool (% SOC) following the application of biochar-containing amendments. This does not necessarily represent a change in the absolute amount of SOC in labile and intermediate pools but in their relevance for total SOC. Therefore, after the application of biochar-containing amendments, the size and MRT of these SOC pools is often of little interest (LEHMANN et al., 2009). Nonetheless, we observed a partly increase in the MRT of the intermediate pool following the application of biochar-containing amendments compared to the unamended soil. This indicates a broader influence of biochar on SOC cycling beyond the mere addition of recalcitrant C, e.g. via slowdown of mineralization through physicochemical stabilization of SOC (WANG et al., 2017; WENG et al., 2017).

The labile and intermediate SOC pools were distinguished from the stable biochar-derived SOC forming the long-term stable SOC pool, determined by hydropyrolysis from MEYER ZU DREWER et al. (2025) (MEREDITH et al., 2012; HAGEMANN et al., 2025). This approach allowed us to avoid the repeatedly reported underestimation of biochars long-term stability (LEHMANN et al., 2009; WANG et al., 2016; AZZI et al., 2024; LI et al., 2024; SANEI et al., 2025). However, considering this stable SOC pool as inert would also be incorrect (AMELOOT et al., 2013; SCHMIDT et al., 2025) and lead to an overestimation of biochars stability (LI et al., 2024). Even though it is difficult to predict long-term biochar stability (LEHMANN et al., 2009; LENG et al., 2019), an MRT for this stable SOC pool of >1000 years is likely (KUZYAKOV et al., 2009; LEHMANN et al., 2009; LEHMANN et al., 2015; SCHMIDT et al., 2025) and potentially higher for the wood- compared to the wheat-derived amendments (SINGH et al., 2012; WANG et al., 2016; JOSEPH et al., 2021).

The size of the stable SOC pool varied depending on the initial SOC content of the soils and on the applied amendments, differing in feedstock and application type. The higher share of SOC in the stable pool of the amended tropical sandy soil compared to both temperate soils is caused by the lower initial SOC content of the tropical soil, increasing the share of stable SOC in total SOC. The larger stable SOC pool following the application of wood- compared to the respective wheat-derived amendment indicates a higher amount of long-term stable SOC, probably due to the generally higher stability of wood-derived biochars (VAUGHN et al., 2013; WANG et al., 2016; WANG et al., 2022). Irrespective of the feedstock, co-application of biochar and basanite powder reduced the share of SOC in the stable SOC pool compared to pure biochar application. In contrast, co-pyrolysis increased the stability of the amendments, since rock-enhanced biochars led to a larger stable SOC pool as pure and co-applied biochars of the respective feedstock. This increased stability due to co-pyrolysis resulted in a similar or even higher stable SOC pool following the application of wheat-derived rock-enhanced biochar than those of wood-derived pure and co-applied biochar. These findings highlight that co-pyrolysis of biomass and basanite powder can outbalance inherent feedstock limitations and thus represents as an equally important factor as feedstock in controlling long-term biochar stability and thus the biochars' CDR potential. These results form a basis for necessary future long-term experiments, which should focus on validating the effects of rock-enhanced biochar under field conditions (WANG et al., 2022; AZZI et al., 2024).

Basanite rock powder application rarely affected size and MRT of the modeled SOC pools. However, in the tropical sandy soil, basanite powder caused a shift of SOC from the intermediate to the labile SOC pool. This indicates a reduced stability of the SOC, which is already reflected in the higher SOC mineralization during the 874-day incubation. This destabilizing effect of basanite powder in the tropical sandy soil might be caused by a weathering-induced priming, in which the release of rock-derived nutrients and the increase in soil pH stimulated microbial activity and consequently accelerated the decomposition of native SOC (BUSS et al., 2021; FANG et al., 2023; LI et al., 2025). However, TE PAS et al. (2026) expects a compensation of such CO_2 losses through long-term stabilization of SOC in mineral-associations promoted by silicate rock powder, promoting the CDR potential of enhanced rock weathering.

C.5 Conclusions

This study demonstrated that all biochar-containing amendments largely reduced SOC mineralization and enhanced long-term SOC stability, with effects strongly shaped by time, feedstock, application type, and soil-specific properties. Amendments that reduced short-term SOC mineralization (17 days) maintained this effect under glucose addition, highlighting the amendments' resilience to labile C inputs. However, amendments were also able to promote or suppress glucose-induced priming, highlighting the interactions between soil, amendment, and labile C input. Whether these patterns remain following repeated labile C inputs over longer time scales, simulating plant-growth, should be further investigated. Beyond glucose-induced effects, wood-derived amendments consistently reduced SOC mineralization and thus outperformed wheat-derived amendments across timescales and soils. However, co-pyrolysis of wheat straw with basanite rock powder to rock-enhanced biochar increased amendment stability, yielding a long-term stable SOC pool comparable to that of wood-derived biochar. This is especially relevant where agricultural residues are the main biomass for amendment production, suggesting that co-pyrolysis with basanite rock powder can compensate for feedstock-limitations affecting long-term CDR potential. Equally decisive as feedstock and application type were soil properties, particularly pH and texture, for the effects of wheat-derived amendments and basanite rock powder. Basanite effects on SOC dynamics generally increased over time, with progressive weathering reducing cumulative CO_2 release and thus showing basanites' CDR potential, particularly in low-pH sandy soils. Overall, the CDR potential of amendments emerged from the dynamic soil-amendment-interactions over time, underscoring the need for siteadapted strategies and long-term field-scale validation, particularly to assess whether the effect of co-pyrolysis on the amendment's long-term CDR potential remains over time under field conditions.

Authors' contributions

Maria Ansari: Conceptualization, Formal analysis, Investigation, Methodology, Visualization, Writing – original draft; **Annette Eschenbach**: Conceptualization, Funding acquisition, Resources, Supervision, Writing – review and editing; **Xavier Rodriguez Lloveras**: Methodology; **Johannes Meyer zu Drewer**: Resources; **Nikolas Hagemann**: Funding acquisition, Resources; **Christian Beer**: Funding acquisition; **Joscha N. Becker**: Conceptualization, Funding acquisition, Methodology, Supervision, Writing – review and editing.

Acknowledgements

This study was conducted as a part of the PyMiCCS project (Pyrogenic carbon and carbonating Minerals for enhanced plant growth and Carbon Capture and Storage) that is part of the CDRterra consortium and was funded by the German Federal Ministry of Research, Technology and Space (BMFTR, FKZ: 01LS2109A). The authors thank Deborah Harms, Annika Naumann, and Sumita Rui for support during lab work. We acknowledge financial support from the Open Access Publication Fund of Universität Hamburg.

C.6 References

ABDALQADIR, M., HUGHES, D., REZAEI GOMARI, S. & RAFIQ, U. 2024. A state of the art of review on factors affecting the enhanced weathering in agricultural soil: Strategies for carbon sequestration and climate mitigation. Environ Sci Pollut R. https://doi.org/10.1007/s11356-024-32498-5.

AMANN, T. & HARTMANN, J. 2019. Ideas and perspectives: Synergies from co-deployment of negative emission technologies. Biogeosciences*,* 16**,** 2949–2960. https://doi.org/10.5194/bg-16-2949-2019.

AMELOOT, N., GRABER, E. R., VERHEIJEN, F. G. A. & DE NEVE, S. 2013. Interactions between biochar stability and soil organisms: review and research needs. Eur J Soil Sci*,* 64**,** 379–390. https://doi.org/10.1111/ejss.12064.

ANDRÉN, O. & KÄTTERER, T. 1997. ICBM: The introductory carbon balance model for exploration of soil carbon balances. Ecol Appl*,* 7**,** 1226–1236. https://doi.org/10.1890/1051-0761(1997)007[1226:ITICBM]2.0.CO;2.

ANSARI, M., BECKER, J. N., HAMBURGER, S. E., KAMMANN, C. I., MEYER ZU DREWER, J., HAGEMANN, N. & ESCHENBACH, A. 2026a. Effect of combined biochar and basanite applications on chemical and physical properties of a sandy agricultural soil. *in prep.*

ANSARI, M., LÜBECK, A., MEYER ZU DREWER, J., HAGEMANN, N., ESCHENBACH, A. & BECKER, J. N. 2026b. Rock-enhanced biochar has similar priming effect as pure biochar application, but improves short-term carbon stabilization in agricultural soils. *in prep.*

ANSARI, M., STOCK, S., DIPPOLD, M. A., HAMBURGER, S. E., KAMMANN, C. I., MEYER ZU DREWER, J., HAGEMANN, N., ESCHENBACH, A. & BECKER, J. N. 2026c. Biochar dominated the combined effect of silicate rock powder and biochar application on extracellular enzyme kinetics and nutrient dynamics in a sandy soil. Soil Till Res*,* 262**,** 107234. https://doi.org/10.1016/j.still.2026.107234.

ANTHONY, T. L., JONES, A. R. & SILVER, W. L. 2025. Supplementing enhanced weathering with organic amendments accelerates the net climate benefit of soil amendments in rangeland soils. AGU Advances*,* 6**,** e2024AV001480. https://doi.org/10.1029/2024AV001480.

AUGUIE, B. & ANTONOV, A. 2017. gridExtra: Miscellaneous Functions for "Grid" Graphics - R package version 2.3. [Online].

AZZI, E. S., LI, H., CEDERLUND, H., KARLTUN, E. & SUNDBERG, C. 2024. Modelling biochar long-term carbon storage in soil with harmonized analysis of decomposition data. Geoderma*,* 441**,** 116761. https://doi.org/10.1016/j.geoderma.2023.116761.

BAMMINGER, C., MARSCHNER, B. & JÜSCHKE, E. 2014. An incubation study on the stability and biological effects of pyrogenic and hydrothermal biochar in two soils. Eur J Soil Sci*,* 65**,** 72–82. https://doi.org/10.1111/ejss.12074.

BASTIDA, F., GARCÍA, C., FIERER, N., ELDRIDGE, D. J., BOWKER, M. A., ABADES, S., ALFARO, F. D., ASEFAW BERHE, A., CUTLER, N. A., GALLARDO, A., GARCÍA-VELÁZQUEZ, L., HART, S. C., HAYES, P. E., HERNÁNDEZ, T., HSEU, Z.-Y., JEHMLICH, N., KIRCHMAIR, M., LAMBERS, H., NEUHAUSER, S., PEÑA-RAMÍREZ, V. M., PÉREZ, C. A., REED, S. C., SANTOS, F., SIEBE, C., SULLIVAN, B. W., TRIVEDI, P., VERA, A., WILLIAMS, M. A., LUIS MORENO, J. & DELGADO-BAQUERIZO, M. 2019. Global ecological predictors of the soil priming effect. Nat Commun*,* 10**,** 3481. https://doi.org/10.1038/s41467-019-11472-7.

BATES, D., MÄCHLER, M., BOLKER, B. & WALKER, S. 2015. Fitting linear mixed-effects models using lme4. J Stat Softw, 67, 1 – 48. https://doi.org/10.18637/jss.v067.i01.

BEERLING, D. J., KANTZAS, E. P., LOMAS, M. R., TAYLOR, L. L., ZHANG, S., KANZAKI, Y., EUFRASIO, R. M., RENFORTH, P., MECURE, J.-F., POLLITT, H., HOLDEN, P. B., EDWARDS, N. R., KOH, L., EPIHOV, D. Z., WOLF, A., HANSEN, J. E., BANWART, S. A., PIDGEON, N. F., REINHARD, C. T., PLANAVSKY, N. J. & VAL MARTIN, M. 2025. Transforming US agriculture for carbon removal with enhanced weathering. Nature, 638, 425–434. https://doi.org/10.1038/s41586-024-08429-2.

BEERLING, D. J., KANTZAS, E. P., LOMAS, M. R., WADE, P., EUFRASIO, R. M., RENFORTH, P., SARKAR, B., ANDREWS, M. G., JAMES, R. H., PEARCE, C. R., MERCURE, J.-F., POLLITT, H., HOLDEN, P. B., EDWARDS, N. R., KHANNA, M., KOH, L., QUEGAN, S., PIDGEON, N. F., JANSSENS, I. A., HANSEN, J. & BANWART, S. A. 2020. Potential for large-scale CO_2 removal via enhanced rock weathering with croplands. Nature, 583, 242–248. https://doi.org/10.1038/s41586-020-2448-9.

BUSS, W., HASEMER, H., FERGUSON, S. & BOREVITZ, J. 2023. Stabilisation of soil organic matter with rock dust partially counteracted by plants. bioRxiv, https://doi.org/10.1101/2023.06.02.543347. 10.1101/2023.06.02.543347.

BUSS, W., WURZER, C., MANNING, D. A. C., ROHLING, E. J., BOREVITZ, J. & MAŠEK, O. 2022. Mineral-enriched biochar delivers enhanced nutrient recovery and carbon dioxide removal. Commun Earth Environ, 3, 67. https://doi.org/10.1038/s43247-022-00394-w.

BUSS, W., YEATES, K., ROHLING, E. & BOREVITZ, J. 2021. Enhancing natural cycles in agro-ecosystems to boost plant carbon capture and soil storage. Oxford Open Climate Change, 1, kgab006. https://doi.org/10.1093/oxfclm/kgab006.

CHEN, R., SENBAYRAM, M., BLAGODATSKY, S., MYACHINA, O., DITTERT, K., LIN, X., BLAGODATSKAYA, E. & KUZYAKOV, Y. 2014. Soil C and N availability determine the priming effect: microbial N mining and stoichiometric decomposition theories. Glob Chang Biol, 20, 2356–2367. https://doi.org/10.1111/gcb.12475.

CLOUGH, T., CONDRON, L. M., KAMMANN, C. & MÜLLER, C. 2013. A review of biochar and soil nitrogen dynamics. Agronomy, 3, 275–293. https://doi.org/10.3390/agronomy3020275.

CRAINE, J. M., MORROW, C. & FIERER, N. 2007. Microbial nitrogen limitation increases decomposition. Ecology, 88, 2105–2113. https://doi.org/10.1890/06-1847.1.

DIETZEN, C., HARRISON, R. & MICHELSEN-CORREA, S. 2018. Effectiveness of enhanced mineral weathering as a carbon sequestration tool and alternative to agricultural lime: An incubation experiment. Int J Greenh Gas Con, 74, 251–258. https://doi.org/10.1016/j.ijggc.2018.05.007.

DIN 2011. DIN EN ISO 14240-2:2011-09: Soil quality - Determination of soil microbial biomass - Part 2: Fumigation-extraction method. Berlin, Germany: DIN Media GmbH.

EBC. 2024. Analytical methods - EBC guidelines Version 10.4 [Online]. European Biochar Certificate (EBC). Available: https://www.european-biochar.org/en/ct/8-Analytical-Methods.

FANG, Q., LU, A., HONG, H., KUZYAKOV, Y., ALGEO, T. J., ZHAO, L., OLSHANSKY, Y., MORAVEC, B., BARRIENTES, D. M. & CHOROVER, J. 2023. Mineral weathering is linked to microbial priming in the critical zone. Nat Commun, 14, 345. https://doi.org/10.1038/s41467-022-35671-x.

FANG, Y., SINGH, B. & SINGH, B. P. 2015. Effect of temperature on biochar priming effects and its stability in soils. Soil Biol Biochem, 80, 136–145. https://doi.org/10.1016/j.soilbio.2014.10.006.

FANG, Y., SINGH, B., SINGH, B. P. & KRULL, E. 2014. Biochar carbon stability in four contrasting soils. Eur J Soil Sci, 65, 60–71. https://doi.org/10.1111/ejss.12094.

FAO & UNESCO. 1974. Soil map of the world (Scale 1:5.000.000). Rome, Italy: Food and Agriculture Organization (FAO) of the United Nations.

FUSS, S., LAMB, W. F., CALLAGHAN, M. W., HILAIRE, J., CREUTZIG, F., AMANN, T., BERINGER, T., DE OLIVEIRA GARCIA, W., HARTMANN, J., KHANNA, T., LUDERER, G., NEMET, G. F., ROGELJ, J., SMITH, P., VICENTE, J. L. V., WILCOX, J., DEL MAR ZAMORA DOMINGUEZ, M. & MINX, J. C. 2018. Negative emissions - Part 2: Costs, potentials and side effects. Environ Res Lett, 13, 063002. 10.1088/1748-9326/aabf9f.

GAUDEL, G., POUDEL, M., MOSONGO, P. S., XING, L., OLJIRA, A. M., ZHANG, Y., BIZIMANA, F., LIU, B., WANG, Y., DONG, W., UWAMUNGU, J. Y. & HU, C. 2022. Meta-analysis of the priming effect on native soil organic carbon in response to glucose amendment across soil depths. Plant Soil, 479, 107–124. https://doi.org/10.1007/s11104-021-05168-5.

HAGEMANN, N., SCHMIDT, H.-P., BUCHELI, T. D., GRAFMÜLLER, J., VOSSWINKEL, S., HERDEGEN, V., MEREDITH, W., UGUNA, C. N. & SNAPE, C. E. 2025. Proxies for use in biochar decay models: Hydropyrolysis, electric conductivity, and H/C_{org} molar ratio. PLoS ONE, 20, e0330206. https://doi.org/10.1371/journal.pone.0330206.

HAGEMANN, N., SPOKAS, K., SCHMIDT, H.-P., KÄGI, R., BÖHLER, M. A. & BUCHELI, T. D. 2018. Activated carbon, biochar and charcoal: Linkages and synergies across pyrogenic carbon's ABCs. Water, 10, 182. https://doi.org/10.3390/w10020182

HAMER, U., MARSCHNER, B., BRODOWSKI, S. & AMELUNG, W. 2004. Interactive priming of black carbon and glucose mineralisation. Org Geochem, 35, 823–830. https://doi.org/10.1016/j.orggeochem.2004.03.003.

HAN, L., SUN, K., YANG, Y., XIA, X., LI, F., YANG, Z. & XING, B. 2020. Biochar's stability and effect on the content, composition and turnover of soil organic carbon. Geoderma, 364, 114184. https://doi.org/10.1016/j.geoderma.2020.114184.

HARTMANN, J., WEST, A. J., RENFORTH, P., KÖHLER, P., DE LA ROCHA, C. L., WOLF-GLADROW, D. A., DÜRR, H. H. & SCHEFFRAN, J. 2013. Enhanced chemical weathering as a geoengineering strategy to reduce atmospheric carbon dioxide, supply nutrients, and mitigate ocean acidification. Rev Geophys, 51, 113–149. https://doi.org/10.1002/rog.20004.

HONVAULT, N., TIOUCHICHINE, M.-L., SAUZE, J., PIEL, C., LANDAIS, D., DEVIDAL, S., GRITTI, E., BOSCH, D. & MILCU, A. 2024. Additive effects of basalt enhanced weathering and biochar co-application on carbon sequestration, soil nutrient status and plant performance in a mesocosm experiment. Appl Geochem, 169, 106054. https://doi.org/10.1016/j.apgeochem.2024.106054.

HOTHORN, T., BRETZ, F. & WESTFALL, P. 2008. Simultaneous inference in general parametric models. Biometrical J, 50, 346–363. https://doi.org/10.1002/bimj.200810425.

IPPOLITO, J. A., CUI, L., KAMMANN, C., WRAGE-MÖNNIG, N., ESTAVILLO, J. M., FUERTES-MENDIZABAL, T., CAYUELA, M. L., SIGUA, G., NOVAK, J., SPOKAS, K. & BORCHARD, N. 2020. Feedstock choice, pyrolysis temperature and type influence biochar characteristics: A comprehensive meta-data analysis review. Biochar, 2, 421–438. https://doi.org/10.1007/s42773-020-00067-x.

IUSS Working Group WRB 2022. World reference base (WRB) for soil resources - International soil classification system for naming soils and creation legends for soil maps. Vienna, Austria., International Union of Soil Sciences (IUSS).

Joergensen, R. G. 1996. The fumigation-extraction method to estimate soil microbial biomass: Calibration of the k_{EC} value. Soil Biol Biochem*,* 28**,** 25–31. https://doi.org/10.1016/0038-0717(95)00102-6.

Joseph, S., Cowie, A. L., Van Zwieten, L., Bolan, N., Budai, A., Buss, W., Cayuela, M. L., Graber, E. R., Ippolito, J. A., Kuzyakov, Y., Luo, Y., Ok, Y. S., Palansooriya, K. N., Shepherd, J., Stephens, S., Weng, Z. & Lehmann, J. 2021. How biochar works, and when it doesn't: A review of mechanisms controlling soil and plant responses to biochar. GCB Bioenergy*,* 13**,** 1731–1764. https://doi.org/10.1111/gcbb.12885.

Kalu, S., Seppänen, A., Mganga, K. Z., Sietiö, O.-M., Glaser, B. & Karhu, K. 2024. Biochar reduced the mineralization of native and added soil organic carbon: evidence of negative priming and enhanced microbial carbon use efficiency. Biochar*,* 6**,** 7. https://doi.org/10.1007/s42773-023-00294-y.

Kuzyakov, Y. 2010. Priming effects: Interactions between living and dead organic matter. Soil Biol Biochem*,* 42**,** 1363–1371. https://doi.org/10.1016/j.soilbio.2010.04.003.

Kuzyakov, Y. 2011. How to link soil C pools with CO_2 fluxes? Biogeosciences*,* 8**,** 1523–1537. https://doi.org/10.5194/bg-8-1523-2011.

Kuzyakov, Y., Bogomolova, I. & Glaser, B. 2014. Biochar stability in soil: Decomposition during eight years and transformation as assessed by compound-specific ^{14}C analysis. Soil Biol Biochem*,* 70**,** 229–236. https://doi.org/10.1016/j.soilbio.2013.12.021.

Kuzyakov, Y., Subbotina, I., Chen, H., Bogomolova, I. & Xu, X. 2009. Black carbon decomposition and incorporation into soil microbial biomass estimated by ^{14}C labeling. Soil Biol Biochem*,* 41**,** 210–219. https://doi.org/10.1016/j.soilbio.2008.10.016.

Lavallee, J. M., Soong, J. L. & Cotrufo, M. F. 2020. Conceptualizing soil organic matter into particulate and mineral-associated forms to address global change in the 21st century. Glob Chang Biol*,* 26**,** 261–273. https://doi.org/10.1111/gcb.14859.

LBEG. 2017. Bodenkarte von Niedersachsen 1 : 50 000. Hannover, Germany: Landesamt für Bergbau Energie und Geologie (LBEG)

Le Bas, M. J., Le Maitre, R. W. L., Streckeisen, A., Zanettin, B. & Rocks, I. S. o. t. S. o. I. 1986. A chemical classification of volcanic rocks based on the total alkali-silica diagram. J Petrol*,* 27**,** 745–750. https://doi.org/10.1093/petrology/27.3.745.

Lehmann, J., Abiven, S., Kleber, M., Pan, G., Singh, B. P., Sohi, S. P. & Zimmerman, A. R. 2015. Persistence of biochar in soil. *In:* Lehmann, J. & Joseph, S. (eds.) Biochar for environmental management. London, United Kingdom.

Lehmann, J., Cowie, A., Masiello, C. A., Kammann, C., Woolf, D., Amonette, J. E., Cayuela, M. L., Camps-Arbestain, M. & Whitman, T. 2021. Biochar in climate change mitigation. Nat Geosci*,* 14**,** 883–892. https://doi.org/10.1038/s41561-021-00852-8.

Lehmann, J., Czimczik, C. I., Laird, D. & Sohi, S. P. 2009. Stability of biochar in the soil. *In:* Lehmann, J. & Joseph, S. (eds.) Biochar for environmental management: Science and Technology. London, United Kingdom.

Leng, L. & Huang, H. 2018. An overview of the effect of pyrolysis process parameters on biochar stability. Bioresour Technol*,* 270**,** 627–642. https://doi.org/10.1016/j.biortech.2018.09.030.

LENG, L., XU, X., WEI, L., FAN, L., HUANG, H., LI, J., LU, Q., LI, J. & ZHOU, W. 2019. Biochar stability assessment by incubation and modelling: Methods, drawbacks and recommendations. Sci Total Environ, 664, 11–23. https://doi.org/10.1016/j.scitotenv.2019.01.298.

LFU. 2025. UmweltAtlas Bayern - Bodenübersichtskarte 1:25.000. Augsburg, Germany: Bayerisches Landesamt für Umwelt (LfU).

LI, H., AZZI, E. S., SUNDBERG, C., KARLTUN, E. & CEDERLUND, H. 2024. Can inert pool models improve predictions of biochar long-term persistence in soils? Geoderma, 452, 117093. https://doi.org/10.1016/j.geoderma.2024.117093.

LI, Z.-B., LI, G., ADAMS, J. M., GUAN, D.-X., ZHAO, L., BIAN, R., HU, Q., LU, X., JI, J. & CHEN, J. 2025. Atmospheric CO_2 removal efficiency through enhanced silicate weathering in croplands: A review with emphasis on the contribution of fungi. J Earth Sci, 36, 197–211. https://doi.org/10.1007/s12583-024-0101-5.

LIU, Z., WU, X., LIU, W., BIAN, R., GE, T., ZHANG, W., ZHENG, J., DROSOS, M., LIU, X., ZHANG, X., CHENG, K., LI, L. & PAN, G. 2020. Greater microbial carbon use efficiency and carbon sequestration in soils: Amendment of biochar versus crop straws. GCB Bioenergy, 12, 1092–1103. https://doi.org/10.1111/gcbb.12763.

LUO, Y., DURENKAMP, M., DE NOBILI, M., LIN, Q. & BROOKES, P. C. 2011. Short term soil priming effects and the mineralisation of biochar following its incorporation to soils of different pH. Soil Biol Biochem, 43, 2304–2314. https://doi.org/10.1016/j.soilbio.2011.07.020.

LUO, Y., ZANG, H., YU, Z., CHEN, Z., GUNINA, A., KUZYAKOV, Y., XU, J., ZHANG, K. & BROOKES, P. C. 2017. Priming effects in biochar enriched soils using a three-source-partitioning approach: ^{14}C labelling and ^{13}C natural abundance. Soil Biol Biochem, 106, 28–35. https://doi.org/10.1016/j.soilbio.2016.12.006.

MAESTRINI, B., NANNIPIERI, P. & ABIVEN, S. 2015. A meta-analysis on pyrogenic organic matter induced priming effect. GCB Bioenergy, 7, 577–590. https://doi.org/10.1111/gcbb.12194.

MALIK, A. A., CHOWDHURY, S., SCHLAGER, V., OLIVER, A., PUISSANT, J., VAZQUEZ, P. G. M., JEHMLICH, N., VON BERGEN, M., GRIFFITHS, R. I. & GLEIXNER, G. 2016. Soil fungal:bacterial ratios are linked to altered carbon cycling. Front Microbiol, Volume 7 - 2016. https://doi.org/10.3389/fmicb.2016.01247.

MARTIN, J. B. 2017. Carbonate minerals in the global carbon cycle. Chem Geol, 449, 58–72. https://doi.org/10.1016/j.chemgeo.2016.11.029.

MEREDITH, W., ASCOUGH, P. L., BIRD, M. I., LARGE, D. J., SNAPE, C. E., SUN, Y. & TILSTON, E. L. 2012. Assessment of hydropyrolysis as a method for the quantification of black carbon using standard reference materials. Geochim Cosmochim Ac, 97, 131–147. https://doi.org/10.1016/j.gca.2012.08.037.

MEYER ZU DREWER, J., VORRATH, M.-E., AMANN, T., HARTMANN, J., DE LA ROSA, J. M., MÖLLMER, J., PÉREZ-DALÍ, S. M., MEREDITH, W., UGUNA, C., SNAPE, C., KAMMANN, C., SCHMIDT, H.-P. & HAGEMANN, N. 2025. Pyrogenic carbon and carbonating minerals for carbon capture and storage (PyMiCCS) part I: production, physico-chemical characterization and C-sink potential. Front Clim, 7 2025. https://doi.org/10.3389/fclim.2025.1631368.

REGINATO, P. L. 2025. Biotechnology in direct air capture, enhanced weathering, and methane removal: Emerging opportunities and gaps. Front Clim, 6. https://doi.org/10.3389/fclim.2024.1440833

RIAHI, K., SCHAEFFER, R., ARANGO, J., CALVIN, K., GUIVARCH, C., HASEGAWA, T., JIANG, K., KRIEGLER, E., R. MATTHEWS, PETERS, G. P., RAO, A., ROBERTSON, S., SEBBIT, A. M., Steinberger, J., Tavoni, M. & van Vuure, D. P. 2022. Mitigation pathways compatible with long-term goals. *In:* P.R. Shukla, Skea, J., Slade, R., Al Khourdajie, A., van Diemen, R., McCollum, D., Pathak, M., Some, S., Vyas, P., Fradera, R., Belkacemi, M., Hasija, A., Lisboa, G., Luz, S. & Malley, J. (eds.) IPCC, 2022: Climate Change 2022: Mitigation of Climate Change. Contribution of Working Group III to the Sixth Assessment Report of the Intergovernmental Panel on Climate Change. Cambridge, UK and New York, NY, USA: Cambridge University Press. https://doi.org/10.1017/9781009157926.005.

Rowley, M. C., Grand, S. & Verrecchia, É. P. 2018. Calcium-mediated stabilisation of soil organic carbon. Biogeochemistry, 137, 27–49. https://doi.org/10.1007/s10533-017-0410-1.

Sanei, H., Petersen, H. I., Chiaramonti, D. & Masek, O. 2025. Evaluating the two-pool decay model for biochar carbon permanence. Biochar, 7, 9. https://doi.org/10.1007/s42773-024-00408-0.

Schmidt, H.-P., Abiven, S., Cowie, A., Glaser, B., Joseph, S., Kammann, C., Lehmann, J., Leifeld, J., Pan, G., Rasse, D., Rumpel, C., Woolf, D., Zimmerman, A. R. & Hagemann, N. 2025. Biochar permanence — A policy commentary. GCB Bioenergy, 17, e70092. https://doi.org/10.1111/gcbb.70092.

Singh, B. P., Cowie, A. L. & Smernik, R. J. 2012. Biochar carbon stability in a clayey soil as a function of feedstock and pyrolysis temperature. Environ Sci Technol, 46, 11770–11778. https://doi.org/10.1021/es302545b.

Sohng, J., Sokol, N. W., Whiteaker, S., Schmidt, R., Holzer, I., Goertzen, H., Peña, J., Houlton, B. Z., Montañez, I., O'Geen, A. & Scow, K. 2025. Combining organic amendments with enhanced rock weathering shifts soil carbon storage in croplands. Sci Total Environ, 998, 180179. https://doi.org/10.1016/j.scitotenv.2025.180179.

Sokol, N. W., Sohng, J., Moreland, K., Slessarev, E., Goertzen, H., Schmidt, R., Samaddar, S., Holzer, I., Almaraz, M., Geoghegan, E., Houlton, B., Montañez, I., Pett-Ridge, J. & Scow, K. 2024. Reduced accrual of mineral-associated organic matter after two years of enhanced rock weathering in cropland soils, though no net losses of soil organic carbon. Biogeochemistry. https://doi.org/10.1007/s10533-024-01160-0.

Streckeisen, A. 1980. Classification and nomenclature of volcanic rocks, lamprophyres, carbonatites and melilitic rocks IUGS Subcommission on the Systematics of Igneous Rocks. Geol Rundsch, 69, 194–207. https://doi.org/10.1007/BF01869032.

te Pas, E. E. E. M., Comans, R. N. J., Bisseling, S. & Hagens, M. 2026. Enhanced weathering and biochar co-deployment boosts CO_2 sequestration through changing soil properties. Geoderma, 466, 117668. https://doi.org/10.1016/j.geoderma.2025.117668.

Tian, J., Wang, J., Dippold, M., Gao, Y., Blagodatskaya, E. & Kuzyakov, Y. 2016. Biochar affects soil organic matter cycling and microbial functions but does not alter microbial community structure in a paddy soil. Sci Total Environ, 556, 89–97. https://doi.org/10.1016/j.scitotenv.2016.03.010.

Tomczyk, A., Sokołowska, Z. & Boguta, P. 2020. Biochar physicochemical properties: Pyrolysis temperature and feedstock kind effects. Rev Environ Sci Biotechnol, 19, 191–215. https://doi.org/10.1007/s11157-020-09523-3.

VANCE, E. D., BROOKES, P. C. & JENKINSON, D. S. 1987. An extraction method for measuring soil microbial biomass C. Soil Biol Biochem, 19, 703–707. https://doi.org/10.1016/0038-0717(87)90052-6.

VAUGHN, S. F., KENAR, J. A., THOMPSON, A. R. & PETERSON, S. C. 2013. Comparison of biochars derived from wood pellets and pelletized wheat straw as replacements for peat in potting substrates. Ind Crops Prod, 51, 437–443. https://doi.org/10.1016/j.indcrop.2013.10.010.

VORRATH, M.-E., AMANN, T., MEYER ZU DREWER, J., HAGEMANN, N., ALDRICH, C., BÖRKER, J., SEEDTKE, M., BECKER, J. N., HAGENS, M., ESCHENBACH, A. & HARTMANN, J. 2025. Pyrogenic carbon and carbonating minerals for carbon capture and storage (PyMiCCS) part II: organic and inorganic carbon dioxide removal in an Oxisol. Front Clim, Volume 7 - 2025. https://doi.org/10.3389/fclim.2025.1592454.

WANG, D., FONTE, S. J., PARIKH, S. J., SIX, J. & SCOW, K. M. 2017. Biochar additions can enhance soil structure and the physical stabilization of C in aggregates. Geoderma, 303, 110–117. https://doi.org/10.1016/j.geoderma.2017.05.027.

WANG, H., NAN, Q., WAQAS, M. & WU, W. 2022. Stability of biochar in mineral soils: Assessment methods, influencing factors and potential problems. Sci Total Environ, 806, 150789. https://doi.org/10.1016/j.scitotenv.2021.150789.

WANG, J., XIONG, Z. & KUZYAKOV, Y. 2016. Biochar stability in soil: meta-analysis of decomposition and priming effects. GCB Bioenergy, 8, 512–523. https://doi.org/10.1111/gcbb.12266.

WENG, Z., VAN ZWIETEN, L., SINGH, B. P., TAVAKKOLI, E., JOSEPH, S., MACDONALD, L. M., ROSE, T. J., ROSE, M. T., KIMBER, S. W. L., MORRIS, S., COZZOLINO, D., ARAUJO, J. R., ARCHANJO, B. S. & COWIE, A. 2017. Biochar built soil carbon over a decade by stabilizing rhizodeposits. Nat Clim Change, 7, 371–376. https://doi.org/10.1038/nclimate3276.

WHITMAN, T., SINGH, B. P. & ZIMMERMAN, A. R. 2015. Priming effects in biochar-amended soils: Implications of biochar-soil organic matter interactions for carbon storage. *In:* LEHMANN, J. & JOSEPH, S. (eds.) Biochar for environmental management. 2 ed. London, UK: Routledge.

WICKHAM, H. 2016. ggplot2: Elegant graphics for data analysis. New York, USA, Springer.

WICKHAM, H., FRANÇOIS, R., HENRY, L. & MÜLLER, K. 2023. dplyr: A Grammar of Data Manipulation - R package version 1.1.4. [Online].

WU, L., XU, H., XIAO, Q., HUANG, Y., SULEMAN, M. M., ZHU, P., KUZYAKOV, Y., XU, X., XU, M. & ZHANG, W. 2020. Soil carbon balance by priming differs with single versus repeated addition of glucose and soil fertility level. Soil Biol Biochem, 148, 107913. https://doi.org/10.1016/j.soilbio.2020.107913.

XU, T., YUAN, Z., VICCA, S., GOLL, D. S., LI, G., LIN, L., CHEN, H., BI, B., CHEN, Q., LI, C., WANG, X., WANG, C., HAO, Z., FANG, Y. & BEERLING, D. J. 2024. Enhanced silicate weathering accelerates forest carbon sequestration by stimulating the soil mineral carbon pump. Glob Chang Biol, 30, e17464. https://doi.org/10.1111/gcb.17464.

ZHAO, L., CAO, X., MAŠEK, O. & ZIMMERMAN, A. 2013. Heterogeneity of biochar properties as a function of feedstock sources and production temperatures. J Hazard Mater, 256-257, 1–9. https://doi.org/10.1016/j.jhazmat.2013.04.015.

ZHENG, Y., JIN, J., WANG, X., CLARK, G. J., FRANKS, A. & TANG, C. 2023. Nitrogen addition increases the glucose-induced priming effect of the particulate but not the mineral-associated organic carbon fraction. Soil Biol Biochem, 184, 109106. https://doi.org/10.1016/j.soilbio.2023.109106.

C.7 Appendix

C7.1 Basanite powder properties

The chemical composition of the rock powder (Table C.4) was analyzed using X-ray fluorescence (XRF) at the Mineralogical Institute, University of Hamburg, while the mineralogical composition was determined by Qmineral using X-ray diffraction (XRD), as described in VORRATH et al. (2025). Following the classification of volcanic rocks by STRECKEISEN (1980) or LE BAS et al. (1986), this rock can be classified as a basanite. The basanite was obtained from Rheinische Provinzial-Basalt- u. Lavawerke, Sinzig, Germany.

Table C.4: Main compounds, trace elements, mineral composition and grain size of used basanite rock powder *Eifelgold*. bdl = below detection limit; LOI = loss on ignition.

Main compounds	[wt%]	Trace Elements	[ppm]	Mineralogy	[wt%]	Grain size [µm]	[wt%]
SiO_2	43.86	As	bdl	Clinopyroxene	44.4	> 300	0.00
TiO_2	2.79	Ba	1026	Plagioclase	15.5	300 - 250	0.13
Al_2O_3	14.15	Bi	bdl	Nepheline	11.2	250 - 210	0.17
Fe_2O_3	11.28	Ce	104	Leucite	9.9	210 - 180	0.14
MnO	0.18	Co	51	Olivine	6.3	180 - 150	0.26
MgO	8.21	Cr	53	2:1 layer silicates	5.1	150 - 120	1.20
CaO	11.63	Cu	66	Hematite	3.1	120 - 100	2.87
Na_2O	3.26	Ga	17	Spinel-type minerals	1.9	100 - 86	4.17
K_2O	3.35	La	52	Apatite	1.1	86 - 74	5.67
P_2O_5	0.6	Nb	52	Analcime	0.9	74 - 62	8.13
SO_3	bdl	Nd	28	Quartz	0.7	62 - 52	8.89
LOI	0.44	Ni	124			52 - 44	8.50
Sum	*99.74*	Pb	5			44 - 36	9.63
		Rb	86			36 - 30	7.86
		Sc	22			30 - 26	5.50
		Sr	882			26 - 22	5.64
		Th	8			22 - 18	5.72
		U	3			18 - 0.5	25.52
		V	302				
		Y	24				
		Zn	90				
		Zr	271				

C7.2 Soil pH as well as C and N content prior and after 874-day incubation experiment

Table C.5: Soil pH ($CaCl_2$), total C and total N content prior and after 874-day incubation. Lower case letters indicate significant differences ($p < 0.05$) between treatments in one parameter of one soil at one time point, while * indicates significant differences between the two time points of one parameter and one treatment.

Soil	Treatment	Total C content [mg kg^{-1}]		Total N content [mg kg^{-1}]		Soil pH [$CaCl_2$]	
		Prior to incubation	After incubation	Prior to incubation	After incubation	Prior to incubation	After incubation
Temperate silty soil	Control	18.1 ± 0.5 ^{a}	16.6 ± 0.3 ^{a} *	0.13 ± 0.01 ^{a}	0.12 ± 0.00 ^{a}	6.9 ± 0.0 ^{a}	6.5 ± 0.1 ^{a} *
	Rock powder	16.8 ± 0.4 ^{a}	16.2 ± 0.1 ^{a}	0.12 ± 0.00 ^{a}	0.11 ± 0.00 ^{a}	6.9 ± 0.0 ^{a}	6.4 ± 0.3 ^{a} *
	Wheat BC	37.0 ± 0.9 ^{bc}	36.5 ± 0.5 ^{b}	0.15 ± 0.00 ^{b}	0.13 ± 0.00 ^{b} *	7.8 ± 0.1 ^{cd}	6.8 ± 0.0 ^{b} *
	Wheat Co-app.	36.2 ± 0.2 ^{b}	35.1 ± 0.4 ^{b}	0.14 ± 0.00 ^{b}	0.13 ± 0.00 ^{b} *	7.9 ± 0.0 ^{cd}	6.8 ± 0.0 ^{b} *
	Wheat Co-pyr.	40.1 ± 0.8 ^{cd}	39.9 ± 0.9 ^{cd}	0.16 ± 0.00 ^{b}	0.14 ± 0.00 ^{b} *	8.0 ± 0.0 ^{d}	6.9 ± 0.0 ^{b} *
	Wood BC	43.4 ± 0.8 ^{ef}	41.0 ± 1.1 ^{cd}	0.16 ± 0.00 ^{b}	0.13 ± 0.00 ^{b} *	7.6 ± 0.1 ^{b}	6.8 ± 0.0 ^{b} *
	Wood Co-app.	40.7 ± 0.3 ^{de}	40.8 ± 0.3 ^{c}	0.15 ± 0.00 ^{b}	0.13 ± 0.00 ^{b} *	7.5 ± 0.0 ^{b}	6.8 ± 0.0 ^{b} *
	Wood Co-pyr.	45.9 ± 1.0 ^{f}	44.0 ± 0.8 ^{d}	0.16 ± 0.00 ^{b}	0.13 ± 0.00 ^{b} *	7.7 ± 0.0 ^{bc}	6.8 ± 0.0 ^{b} *
Temperate sandy soil	Control	11.2 ± 0.1 ^{a}	10.2 ± 0.2 ^{a} *	0.10 ± 0.00 ^{a}	0.08 ± 0.00 ^{a} *	4.7 ± 0.0 ^{a}	4.1 ± 0.0 ^{a} *
	Rock powder	11.4 ± 0.1 ^{a}	10.2 ± 0.0 ^{a} *	0.11 ± 0.00 ^{b}	0.08 ± 0.00 ^{a} *	4.9 ± 0.0 ^{b}	4.9 ± 0.0 ^{b}
	Wheat BC	31.6 ± 0.4 ^{b}	29.1 ± 0.4 ^{b} *	0.13 ± 0.00 ^{de}	0.10 ± 0.00 ^{b} *	7.4 ± 0.0 ^{e}	6.4 ± 0.0 ^{c} *
	Wheat Co-app.	30.8 ± 0.3 ^{b}	28.5 ± 0.5 ^{b} *	0.13 ± 0.00 ^{de}	0.10 ± 0.00 ^{b} *	7.3 ± 0.0 ^{e}	6.4 ± 0.0 ^{cd} *
	Wheat Co-pyr.	34.8 ± 0.1 ^{c}	32.4 ± 0.3 ^{c} *	0.13 ± 0.00 ^{d}	0.11 ± 0.00 ^{b} *	7.5 ± 0.0 ^{f}	6.5 ± 0.0 ^{cd} *
	Wood BC	37.6 ± 0.2 ^{d}	35.9 ± 0.8 ^{d}	0.13 ± 0.00 ^{de}	0.11 ± 0.00 ^{b} *	6.8 ± 0.0 ^{c}	6.6 ± 0.0 ^{e} *
	Wood Co-app.	34.9 ± 0.3 ^{c}	33.8 ± 0.5 ^{cd}	0.12 ± 0.00 ^{c}	0.10 ± 0.00 ^{b} *	6.8 ± 0.0 ^{c}	6.5 ± 0.0 ^{d} *
	Wood Co-pyr.	41.2 ± 0.7 ^{e}	39.0 ± 0.9 ^{e}	0.13 ± 0.00 ^{e}	0.11 ± 0.00 ^{b} *	7.1 ± 0.0 ^{d}	6.7 ± 0.0 ^{e} *
Tropical sandy soil	Control	4.5 ± 0.1 ^{a}	4.4 ± 0.1 ^{a}	0.04 ± 0.00 ^{a}	0.03 ± 0.00 ^{a} *	4.7 ± 0.0 ^{a}	4.5 ± 0.1 ^{a} *
	Rock powder	4.4 ± 0.1 ^{a}	4.3 ± 0.1 ^{a}	0.04 ± 0.00 ^{a}	0.03 ± 0.00 ^{a} *	5.0 ± 0.0 ^{b}	5.1 ± 0.0 ^{b} *
	Wheat BC	25.5 ± 0.3 ^{b}	25.0 ± 0.3 ^{b}	0.07 ± 0.00 ^{bc}	0.04 ± 0.00 ^{bc} *	7.9 ± 0.0 ^{e}	6.8 ± 0.1 ^{de} *
	Wheat Co-app.	24.0 ± 0.7 ^{b}	24.7 ± 0.2 ^{b}	0.07 ± 0.00 ^{b}	0.04 ± 0.00 ^{b} *	8.0 ± 0.0 ^{e}	6.8 ± 0.0 ^{de} *
	Wheat Co-pyr.	29.0 ± 0.3 ^{c}	29.1 ± 0.0 ^{c}	0.07 ± 0.00 ^{bc}	0.05 ± 0.00 ^{bc} *	8.0 ± 0.0 ^{e}	6.8 ± 0.0 ^{e} *
	Wood BC	30.8 ± 0.2 ^{d}	30.4 ± 0.3 ^{d}	0.07 ± 0.00 ^{bc}	0.05 ± 0.00 ^{bc} *	7.0 ± 0.0 ^{c}	6.5 ± 0.0 ^{cd} *
	Wood Co-app.	30.4 ± 0.4 ^{cd}	30.2 ± 0.2 ^{cd}	0.07 ± 0.00 ^{bc}	0.04 ± 0.00 ^{b} *	7.0 ± 0.0 ^{c}	6.5 ± 0.0 ^{c} *
	Wood Co-pyr.	35.1 ± 0.3 ^{e}	31.1 ± 0.4 ^{d} *	0.08 ± 0.00 ^{c}	0.05 ± 0.00 ^{c} *	7.3 ± 0.0 ^{d}	6.7 ± 0.1 ^{cde} *

Data is presented as mean ± standard error (n = 4). RP = rock powder treatment containing basanite rock powder, BC = biochar treatment containing biochar derived from either wood or wheat, Co-app. = co-application treatment containing basanite and biochar derived from either wood or wheat, Co-pyr. = co-pyrolysis treatment containing rock-enhanced biochar derived from either wood or wheat.

C7.3 Stable biochar fraction determined by hydropyrolysis

The stable biochar fraction of the used amendments (Table C.6) was determined by MEYER ZU DREWER et al. (2025) using hydropyrolysis. The stable fraction of the co-application treatments is the same as in the respective biochar treatment.

Table C.6: Stable fraction of biochars and rock-enhanced biochars, determined by hydropyrolysis.

	Wood biochar	**Rock-enhanced wood biochar**	**Wheat biochar**	**Rock-enhanced wheat biochar**
Stable biochar fraction (% biochar-derived C)	90.8	92.4	92.0	92.7

C7.4 Significance letters of respiration during long-term incubation

Table C.7: Significance letters for cumulative respiration displayed in Figure C.2. Letters indicate significant differences (p < 0.05) between treatment within one soil.

soil	treatment	day																																															
		1	2	3	6	10	15	17	20	23	27	30	34	41	50	55	62	69	76	83	90	105	121	132	146	160	177	196	216	239	259	279	300	321	342	363	391	419	447	475	503	531	566	601	636	672	706	748	790	832	874
temperate silty soil	Control	c	c	c	c	c	c	c	d	d	c	c	c	c	c	c	c	c	c	cd	de	de	e	de	de	de	d	c	c	cd	cd	c	c	c	c	c	c	c	c	c	c	c	c	c	c	c	c	c	c	c	c
	RP	c	c	c	c	c	c	c	d	d	c	c	c	c	c	c	c	c	c	d	e	e	f	f	f	f	e	d	d	e	e	d	d	d	d	d	d	e	e	de	d	d	d	d	d	d	d	d	d	d	d
	Wheat BC	ab	ab	ab	b	b	b	b	bc	bc	b	b	b	b	b	b	b	b	b	b	b	b	c	c	c	c	c	c	c	c	c	c	c	c	c	c	c	d	d	d	d	d	d	d	d	d	d	d	d	d	d
	Wheat Co-app.	b	b	b	b	b	b	b	c	c	b	b	b	b	b	b	b	b	b	b	bc	bc	cd	cd	cd	cd	cd	c	c	d	de	d	d	d	d	d	d	e	e	e	e	e	e	e	e	e	e	e	e	e	e
	Wheat Co-pyr.	ab	ab	ab	b	b	b	b	c	c	b	b	b	b	b	b	b	b	b	bc	cd	cd	de	ef	ef	ef	e	d	d	e	f	e	e	e	e	e	e	f	f	f	f	f	f	f	f	f	f	f	f	f	f
	Wood BC	ab	ab	ab	ab	ab	ab	ab	ab	ab	a	a	a	a	a	a	a	a	a	a	a	a	ab	a	a	a	a	a	a	a	a	a	a	a	a	a	a	a	a	a	a	a	a	a	a	a	a	a	a	a	a
	Wood Co-app.	ab	ab	ab	ab	ab	ab	ab	ab	ab	a	a	a	a	a	a	a	a	a	a	a	a	a	a	a	a	a	a	a	a	a	a	a	a	a	a	a	a	a	a	a	a	a	a	a	a	a	a	a	a	a
	Wood Co-pyr.	a	a	a	a	a	a	a	a	a	a	a	a	a	a	a	a	a	a	a	a	a	b	b	b	b	b	b	b	b	b	b	b	b	b	b	b	b	b	b	b	b	b	b	b	b	b	b	b	b	b

soil	treatment	day																																												
		1	6	8	13	17	20	22	27	35	42	49	56	64	70	77	85	90	104	118	133	146	162	175	195	217	237	258	279	300	321	342	363	391	419	447	475	503	532	566	601	637	672	706	748	787	832	874
temperate sandy soil	Control	b	b	b	b	b	b	b	b	b	b	c	c	c	c	c	c	c	c	c	c	c	c	c	d	d	d	d	d	d	e	e	e	f	f	f	f	f	f	f	f	f	f	f	f	f	f	f
	RP	b	b	b	b	b	b	b	b	b	b	bc	bc	bc	bc	b	b	b	b	b	b	b	b	b	c	c	c	c	c	c	d	d	d	e	e	e	e	e	e	e	e	e	e	e	e	e	e	e
	Wheat BC	b	b	b	b	b	b	b	b	b	b	b	b	b	b	b	b	b	b	b	b	b	b	b	b	b	b	b	b	b	c	c	c	c	c	c	c	c	c	c	c	c	c	c	c	c	c	c
	Wheat Co-app.	b	b	b	b	b	b	b	b	b	b	bc	bc	bc	bc	bc	b	b	b	b	b	b	b	b	bc	bc	bc	bc	bc	bc	c	c	c	d	d	d	d	d	d	d	d	d	d	d	d	d	d	d
	Wheat Co-pyr.	b	b	b	b	b	b	b	b	b	b	bc	b	b	b	b	b	b	b	b	b	b	b	b	bc	b	b	b	b	b	c	c	c	cd	cd	cd	cd	cd	cd	cd	cd	cd	cd	cd	cd	cd	cd	cd
	Wood BC	a	a	a	a	a	a	a	a	a	a	a	a	a	a	a	a	a	a	a	a	a	a	a	a	a	a	a	a	a	a	a	a	a	a	a	a	a	a	a	a	a	a	a	a	a	a	a
	Wood Co-app.	a	a	a	a	a	a	a	a	a	a	a	a	a	a	a	a	a	a	a	a	a	a	a	a	a	a	a	a	a	ab	ab	ab	ab	ab	b	b	b	b	b	b	b	b	b	b	b	b	b
	Wood Co-pyr.	a	a	a	a	a	a	a	a	a	a	a	a	a	a	a	a	a	a	a	a	a	a	a	a	a	a	a	a	a	b	b	b	b	b	b	b	b	b	b	b	b	b	b	b	b	b	b

soil	treatment	day																																															
		1	2	3	6	9	13	17	20	23	27	36	42	49	57	62	69	76	83	90	105	118	134	147	160	175	196	216	237	258	259	279	300	321	342	363	391	419	447	475	503	531	568	601	638	673	706	749	791	832	874
tropical sandy soil	Control	d	d	d	c	c	c	c	c	c	c	c	c	c	c	c	c	c	c	c	c	c	c	c	d	d	d	d	d	e	e	e	e	e	e	e	e	e	e	e	e	e	e	e	e	e	e	e	e	e	e
	RP	e	e	e	d	d	d	d	d	d	d	d	d	d	d	d	d	d	d	d	d	d	d	d	e	e	e	e	e	f	f	f	f	f	f	f	f	f	f	f	e	e	e	e	e	e	e	e	e	e	e
	Wheat BC	c	c	c	b	b	b	b	b	b	b	b	b	b	b	b	b	b	b	b	b	b	b	b	bc	bc	bc	bc	b	c	c	c	c	c	c	c	c	c	c	c	c	c	c	c	c	c	c	c	c	c	c
	Wheat Co-app.	c	c	c	b	b	b	b	b	b	b	b	b	b	b	b	b	b	b	b	b	b	b	b	c	c	c	c	c	d	d	d	d	d	d	d	d	d	d	d	d	d	d	d	d	d	d	d	d	d	d
	Wheat Co-pyr.	bc	bc	bc	b	b	b	b	b	b	b	b	b	b	b	b	b	b	b	b	b	b	b	b	b	b	b	b	b	c	c	c	c	c	c	c	c	c	c	c	c	c	c	c	c	c	c	c	c	c	c
	Wood BC	ab	ab	ab	a	a	a	a	a	a	a	a	a	a	a	a	a	a	a	a	a	a	a	a	a	a	a	a	a	a	a	a	a	a	a	a	a	a	a	a	a	a	a	a	a	a	a	a	a	a	a
	Wood Co-app.	ab	ab	ab	a	a	a	a	a	a	a	a	a	a	a	a	a	a	a	a	a	a	a	a	a	a	a	a	a	a	a	a	a	a	a	a	a	a	a	a	a	a	a	a	a	a	a	a	a	a	a
	Wood Co-pyr.	bc	bc	bc	b	b	b	b	b	b	b	b	b	b	b	b	b	b	b	b	b	b	b	b	b	b	b	b	b	c	c	c	c	c	c	c	c	c	c	c	c	c	c	c	c	c	c	c	c	c	c

RP = rock powder treatment containing basanite rock powder, BC = biochar treatment containing biochar derived from either wood or wheat, Co-app. = co-application treatment containing basanite and biochar derived from either wood or wheat, Co-pyr. = co-pyrolysis treatment containing rock-enhanced biochar derived from either wood or wheat.

Study D:

Rock-enhanced biochar has similar priming effect as pure biochar application, but improves short-term carbon stabilization in agricultural soils

Maria Ansari[a,b]*, Annemarie Lübeck[a], Johannes Meyer zu Drewer[c,d,e], Nikolas Hagemann[c,d], Annette Eschenbach[a,b], Joscha N. Becker[a,b]

[a] Department Earth System Sciences, University of Hamburg, Hamburg, Germany
[b] Earth and Society Research Hub (ESRAH), University of Hamburg, Hamburg, Germany
[c] Ithaka Institute, Goldbach, Germany
[d] Agroscope, Zurich, Switzerland
[e] Institute of Sustainable Energy Systems, Offenburg University, Offenburg, Germany

*corresponding author

Submitted

D. Abstract

Combined soil-applied biochar and silicate rock powder might have synergistic effects on both combine carbon dioxide removal with soil improvement. However, it remains unknown how their combined application affects mineralization and stabilization of soil organic carbon (SOC). We tested ^{13}C-labeled wheat-straw biochar and basanite rock powder either pure, co-applied, or as rock-enhanced biochar from co-pyrolysis. Pure and combined amendments were incubated for 66 days with three agricultural topsoils (temperate silty, temperate sandy, tropical sandy). We monitored the $\delta^{13}C$-signal of the respired CO_2 to determine the priming effect of the amendments. After incubation, we conducted a density fractionation to investigate the potential stabilization of native and biochar-derived SOC as free particulate organic matter (fPOM), occluded POM (oPOM), and mineral-associated organic matter (MAOM). Pure basanite application did not influence short-term SOC dynamics, probably due to limited weathering within the 66-day incubation. In combined applications (co-application, rock-enhanced biochar), the effect of biochar was dominant. The effects of biochar-containing amendments were mainly controlled by texture and pH. Both sandy soils experienced positive priming following the application of biochar-containing amendments. In both temperate soils, positive priming occurred in MAOM, while native fPOM was partly shifted to oPOM. Losses of native SOC in fPOM and MAOM were smaller than biochar-derived carbon input, resulting in overall SOC gains in most fractions. While priming intensity was similar for biochar-containing amendments, rock-enhanced biochar most strongly increased in HF, interpreted as MAOM, and had a higher short-term stability. Our findings highlight the potential of co-pyrolysis for short-term SOC stabilization.

Keywords

silicate rock powder, carbon dioxide removal (CDR), enhanced rock weathering (ERW), mineral-associated organic matter (MAOM), particulate organic matter (POM), biochar stability

D.1 Introduction

To mitigate climate change and meet long-term climate targets, the removal of atmospheric carbon dioxide plays an important role (RIAHI et al., 2022). Soil-application of both biochar and silicate rock powder for enhanced rock weathering are approaches, which combine carbon dioxide removal with soil fertility improvement (BUSS et al., 2021; JOSEPH et al., 2021; BEERLING et al., 2025). While most recent research considered both carbon dioxide removal technologies separately, their combined application could offer synergistic effects (AMANN & HARTMANN, 2019; JOSEPH et al., 2021). A combined application can include a co-application of biochar and silicate rock powder as well as the co-pyrolysis of biomass and rock powder to produce rock-enhanced biochar (MEYER ZU DREWER et al., 2025; VORRATH et al., 2025). Such a co-pyrolysis of biomass and minerals can increase the carbon (C) yield (BUSS et al., 2024b) and improve the nutrient content of the pyrolysis product (MEYER ZU DREWER et al., 2025). The co-application of biochar and rock powder gained increasing attention and its effects on SOC sequestration and storage were investigated (e.g. HONVAULT et al., 2024; SOHNG et al., 2025; TE PAS et al., 2026), indicating additive or even synergistic effects. However, co-application effects on SOC mineralization and stabilization and the effects of rock-enhanced biochar on general SOC dynamics remain unknown.

Biochar application enhances soil organic C (SOC) storage (STEINER et al., 2007; LEHMANN et al., 2021; KALU et al., 2024), while maintaining or improving soil functions (JOSEPH et al., 2010). Biochar is the solid product from biomass pyrolysis and consists mainly of highly aromatic pyrogenic C compounds (HAGEMANN et al., 2018; XIE et al., 2025). Due to its low degradability, biochar contributes to the persistent SOC pool (KUZYAKOV et al., 2014; WANG et al., 2016; XIE et al., 2025) and its application provides a considerable carbon dioxide removal potential (LEHMANN et al., 2021). However, biochar also contains minor amounts of more easily degradable organic compounds (BRUUN et al., 2014; BAKSHI et al., 2018). This labile C can either stimulate or suppress native SOC mineralization, resulting in a positive or negative priming effect, respectively (KUZYAKOV et al., 2000; YU et al., 2018). Direction and magnitude of biochar-induced priming vary depending on several parameters, such as soil and biochar properties (ZIMMERMAN et al., 2011; WHITMAN et al., 2015; JOSEPH et al., 2021) as well as the observed time span after application (BLANCO-CANQUI et al., 2020). In particular, biochar-induced priming is often positive in sandy soils (FANG et al., 2015; LIU et al., 2015; WANG et al., 2016) with lower pH (LUO et al., 2011; ZHANG et al., 2018; XU et al., 2021) and organic matter content (ZIMMERMAN et al., 2011; WANG et al., 2016).

Applying silicate rock powder, such as basanite, to agricultural soils can couple carbon dioxide removal with improvements of soil properties (SWOBODA et al., 2022; DUPLA et al., 2024; XU et al., 2025). Weathering of silicate rocks directly enhances soil C content through the reaction between CO_2-derived acidity and minerals, forming bicarbonate and carbonate (HARTMANN et al., 2013; BEERLING et al., 2025), which can be stored as inorganic C in the soil (HARTMANN et al., 2013; MARTIN, 2017). The effect of enhanced rock weathering on SOC dynamics, such as SOC mineralization, is less well understood. Even though silicate rock powder does not contain labile C to directly induce a priming effect, it still has the potential to alter SOC mineralization, e.g. via an increase in soil pH (AMANN et al., 2020; LEI et al., 2025) or nutrient availability (HARLEY & GILKES, 2000; HARTMANN et al., 2013).

Soil organic C is stabilized through the biochemical low bioavailability and chemical complexity of particulate organic matter (POM), by spatial inaccessibility through the occlusion of POM in aggregates (oPOM), or the association to mineral surfaces (SOLLINS et al., 1996; VON LÜTZOW et al., 2006; VON LÜTZOW et al., 2008). Aggregate occlusion and mineral-association limit the accessibility of SOC for microbes, thus reducing its biodegradation (VON LÜTZOW et al., 2006; KLEBER et al., 2015). Both biochar and silicate rock powder have the potential to influence the stabilization of native SOC. The weathering of silicate rock powder can enhance aggregate formation by releasing bivalent cations, such as Ca and Mg, which promote cation bridging and flocculation of soil particles (CLOUGH & SKJEMSTAD, 2000; BUSS et al., 2024a; XU et al., 2025). Additionally, fresh mineral surfaces and reactive secondary minerals, which are formed during weathering, can directly adsorb dissolved organic carbon (DOC) forming mineral-associated organic matter (MAOM; REICHENBACH et al., 2021; BUSS et al., 2024a). While most biochar-derived C remains as highly recalcitrant free POM (fPOM; KALU et al., 2024), it can also be further stabilized by occlusion in aggregates (YOO et al., 2017; JOSEPH et al., 2021) or mineral-association (YANG et al., 2016; YANG et al., 2021). Additionally, biochar has the potential to accelerate the formation of aggregates and the stabilization of native SOC as MAOM (WANG et al., 2017; WENG et al., 2017; XU et al., 2024). When applying biochar and silicate rock powder combined, the additional minerals may further stabilize the biochar-derived C (MEYER ZU DREWER et al., 2025), especially if it is directly bound to mineral surfaces during co-pyrolysis.

The influence of pure biochar and silicate rock powder application on the mineralization of native SOC and the stabilization of SOC are relatively well understood And initial research indicated additive or synergistic effects of co-application on SOC storage (SOHNG et al., 2025) and sequestration (HONVAULT et al., 2024; TE PAS et al., 2026). However, co-applications effect on SOC mineralization and stabilization as well as the general effects of rock-enhanced biochar on SOC dynamics are currently unknown. Therefore, our objective was to identify combined effects of both amendments on SOC (both native SOC and biochar-derived C) dynamics in contrasting agricultural soils and assess how these effects differ from those of pure biochar or basanite application. We tested biochar, basanite, a co-application of both amendments as well as rock-enhanced biochar as soil amendments. Incubation experiments were set-up using three agricultural soils from Germany (sandy, silty) and Kenia (sandy), representing temperate and tropical soil properties. We hypothesized that the combined application of biochar and basanite (i) affects the mineralization rate of native SOC depending on soil properties with coarser texture, lower pH, and SOC content likely causing positive amendment-induced priming, and (ii) increases the amount of SOC in oPOM and MAOM via the enhancement of aggregate occlusion and mineral-association, compared to unamended soils. Head-space CO_2 concentrations and its $\delta^{13}C$ signals were monitored to calculate the priming effect of the amendments. After the incubation, the soil samples were fractionated to quantify the potential of the amendments for SOC stabilization.

D.2 Material and methods

D2.1 Soils and amendments

The study was conducted using three different topsoils from agricultural fields (0-30 cm; Table D.1). One of them was collected in central Germany (Goldbach, Germany, 49°59'32.4"N 9°09'53.8"E), referred to as temperate silty soil. The second soil was collected in northern Germany (Gartow, Germany, 53°01'26.9"N 11°27'12.7"E), referred to as temperate sandy soil. The third soil was collected in central Kenia (Machanga, Kenia, 0°27'26.8"S 37°39'37.4"E), referred to as tropical sandy soil. The soils were air-dried until used in spring 2024. The soils in the respective areas are classified as Cambisol (LFU, 2025), Podzol (LBEG, 2017), and Nitisol (FAO & UNESCO, 1974) according to the world reference base (IUSS WORKING GROUP WRB, 2022).

These soils were incubated with four different soil amendments. The biochar was produced from a mixture of ^{13}C-labeled and unlabeled wheat straw (*Triticum aestivum* L.). The ^{13}C-labeled wheat straw was derived from field-grown plants exposed to repeated $^{13}CO_2$ flushing under a hood during the growing season. The homogenized mixture of labeled and unlabeled wheat straw was pelletized to 6 mm without additional binder (WK230 pellet press, Evertec, Dieburg, Germany) and pyrolyzed at 650 °C for 15 minutes in a continuously operating auger reactor (HAGEMANN et al., 2020; Table D.2 and further information in Table D.4 in Appendix). As silicate rock powder, we used the locally available basanite *Eifelgold* (grain size 0.5-300 µm as described in VORRATH et al. (2025); further information in Table D.3 in Appendix). In addition, two combined applications of biochar and basanite were tested – co-application and co-pyrolyzed rock-enhanced biochar. For the co-application, biochar and basanite were mixed before use. To compare the effect of a co-pyrolysis to post-pyrolysis mixing, wheat straw (mix of labeled and unlabeled straw) and basanite were mixed (90:10, w/w), pelletized, and pyrolyzed at 650 °C for 15 minutes to produce rock-enhanced biochar following MEYER ZU DREWER et al. (2025) (Table D.2 and further information in Table D.4 in Appendix). Based on the TC contents of biochar and rock-enhanced biochar, we calculated the proportion of biochar (~71%) and basanite (~29%) in rock-enhanced biochar. Both biochar and rock-enhanced biochar were hand-crushed and sieved to <2 mm.

Table D.1: Initial soil properties of temperate silty, temperate sandy, and tropical sandy agricultural topsoil prior to pre-incubation.

Properties	**Temperate silty soil**	**Temperate sandy soil**	**Tropical sandy soil**
pH [$CaCl_2$]	6.9 ± 0.0	4.7 ± 0.0	4.7 ± 0.0
TC [g kg^{-1}]	18.5 ± 0.0	12.4 ± 0.0	4.7 ± 0.0
TOC [g kg^{-1}]	13.3 ± 0.1	12.0 ± 0.0	4.6 ± 0.0
TIC [g kg^{-1}]	5.2 ± 0.1	0.4 ± 0.0	0.1 ± 0.0
N [g kg^{-1}]	1.3 ± 0.0	1.1 ± 0.0	0.3 ± 0.0
TC:N	13.9 ± 0.0	11.6 ± 0.0	15.0 ± 0.0
$\delta^{13}C$ [‰]	-23.2 ± 0.1	-26.7 ± 0.0	-19.2 ± 0.0
Sand [%]	28.2 ± 1.0	93.8 ± 0.7	68.9 ± 0.6
Silt [%]	58.0 ± 1.0	2.5 ± 0.4	20.4 ± 0.6
Clay [%]	13.8 ± 0.3	3.7 ± 0.3	10.7 ± 0.2

Data is presented as mean ± standard error (n = 3). TC = total carbon, TOC = total organic carbon, TIC = total inorganic carbon, N = total nitrogen.

Table D.2: Initial properties of biochar and rock-enhanced biochar. Further information listed in Table D.4 in Appendix.

Properties	Biochar	Rock-enhanced biochar
TC [g kg^{-1}]	705.5 ± 1.6 [a]	502.7 ± 4.3 [a]
TOC [g kg^{-1}]	703.7	501.3
TIC [g kg^{-1}]	1.8 ± 0.1 [a]	1.4 ± 0.3 [a]
N [g kg^{-1}]	8.9 ± 0.0 [a]	6.3 ± 0.1 [a]
TC:N	79 ± 0.0 [a]	80 ± 0.6 [a]
$\delta^{13}C$ [‰]	140.8 ± 15.9 [a]	146.8 ± 3.4 [a]
H:TC	0.14 [b]	0.14 [b]
O:TC	0.64 [b]	0.70 [b]
pH	9.4 [b]	9.4 [b]
Ash [%]	20.4 [b]	42.2 [b]
Specific surface area [m^2 g^{-1}]	92.6 [b]	48.6 [b]

[a] Values are the mean of analytical replicates (n = 3, mean ± standard error), [b] values (n = 1) were measured by Ruhr Lab GmbH according to the analytical guidelines of the European Biochar Certificate (EBC, 2024). TOC is calculated as difference between TC and TIC. TC = total carbon, TOC = total organic carbon, TIC = total inorganic carbon, N = total nitrogen.

D2.2 Experimental design

To assess the amendment effects on mineralization and stabilization of SOC, we set up an aerobic incubation experiment (n = 4). For the control treatment, 120 g of air-dried soil (dry-weight equivalent) were used. For the biochar treatment, 4.71 g of biochar (~3.93 wt%) was mixed with the soil. In the rock powder treatment, 2.38 g of basanite rock powder (~1.98 wt%) were added to the soil. For the co-application treatment, 4.71 g of biochar (~3.93 wt%) and 2.38 g of basanite rock powder (~1.98 wt%) were added to the soil. The co-pyrolysis treatment contained a mixture of soil and 6.70 g of rock-enhanced biochar (~5.58 wt% consisting of ~3.98 wt% biochar and ~1.60 wt% basanite rock powder). After mixing, the samples were adjusted to 40% water holding capacity (WHC) using sterile distilled water and pre-incubated for 7 days at 20 °C to reactive microorganisms and buffer potential effects from previous drying.

Following the pre-incubation, 60 g of each sample (dry-weight soil equivalent excluding amendment weight) was adjusted to 60% WHC using sterile distilled water. Moist samples were then transferred into glass flasks, sealed with rubber septa, and incubated at 20 °C for 66 days. This incubation duration allows to determine the amendment effects primarily on short-term SOC dynamics. The accumulation of CO_2 in the flask headspace was monitored as a proxy for SOC mineralization using gas chromatography (JAS 6890N GC, Joint Analytical Systems GmbH, Moers, Germany; 7890 A GC, Agilent Technologies, Santa Clara, United States). To maintain a higher pressure within the flasks (~1100 mbar) compared to the surrounding air and to avoid oxygen deficiency due to high CO_2 concentrations (> 2% in headspace), flasks were flushed with synthetic air when necessary. Additional gas samples for $\delta^{13}C$ analysis were taken on selected days (1, 2, 3, 6, 9, 13, 17, 27, 42, 66) throughout the incubation and analyzed using an isotope ratio mass spectrometer (Delta V Plus, Thermo Fisher Scientific, Bremen, Germany).

D2.3 Chemical analysis of soil samples

The remaining material of each sample after the pre-incubation was further analyzed, describing initial sample properties at the beginning of the incubation. Soil pH was determined in 0.01 M $CaCl_2$ solution (soil : $CaCl_2$ solution = 1:2.5) using a pH meter (MP230, Mettler-Toledo GmbH, Gießen, Germany). The electric conductivity (EC) was measured in deionized water (soil : water = 1:2.5) using a conductivity meter (Cond 330i, WTW GmbH, Weilheim, Germany).

After pre-incubation and incubation, a subsample was ground and dried at 105 °C to determine total C and N contents using an elemental analyzer (vario MAX cube, Elementar Analysensysteme GmbH, Langenselbold, Germany). The total inorganic C (TIC) content was determined using a TOC analyzer (soli TOC® cube, Elementar Analysensysteme GmbH, Langenselbold, Germany). The TOC content was calculated as the difference between total C and TIC. Additionally, a subsample was frozen (-20°C) after pre-incubation and incubation and used to determine microbial biomass C (MBC) at the end of the incubation using the chloroform fumigation extraction method according to DIN (2011), adapted from VANCE et al. (1987). Two subsamples of 12.5 g (dry weight equivalent) were weighed into glass flasks. One of the subsamples was directly extracted with 50 ml of 0.05 M K_2SO_4 solution to quantify DOC. The second subsample was fumigated with chloroform to lyse microbial cell walls and was afterwards extracted using K_2SO_4 solution. To determine C contents, the extracts were measured using a TOC analyzer (TOC-L, Shimadzu Corporation, Kyoto, Japan). The difference between the fumigated and non-fumigated extracts is interpreted as MBC, using an extraction factor k_{EC} of 0.45 (JOERGENSEN, 1996). The 0.05 M K_2SO_4 solution allowed $\delta^{13}C$ determination of MBC using an isotope ratio mass spectrometer (WERTH & KUZYAKOV, 2010).

D2.4 Density fractionation

To separate SOC into differently stabilized fractions, we conducted a density fractionation after the incubation following GOLCHIN et al. (1994) and VIRET & GRAND (2019). We used a sodium polytungstate (3 $Na_2WO_4 \cdot 9\ WO_3 \cdot H_2O$) solution with a density of 1.8 g cm^{-3} following BEER et al. (2022). Approximately 10 g of air-dried sample was weighed into a centrifuge tube and 40 ml of sodium polytungstate solution was slowly added. The suspension was carefully stirred and after 30 min sedimentation time was centrifuged at 2500*g* for 60 minutes. The supernatant, containing the free light fraction (fLF; considered as fPOM), was filtered (cellulose acetate filter, 0.45 µm) using vacuum where necessary. The fLF was washed with distilled water to remove the remaining sodium polytungstate solution until the supernatant had an EC of <50 µS cm^{-1}. Afterwards, the fLF was dried at 65 °C and weighed. To disrupt aggregates and separate the occluded light fraction (oLF; considered as oPOM), 40 ml of sodium polytungstate were added to the remaining sample in the centrifuge tube and the sample was treated with an ultrasonication probe (280 J ml^{-1}; Bandelin HD-200 with probe UW2070, Bandelin electronic GmbH & Co.KG, Berlin, Germany) for 12 minutes. Afterwards the oLF was extracted, washed, and dried in the same way as the fLF. The remaining heavy fraction (HF; containing MAOM) was also washed with distilled water until the EC of the supernatant was <50 µS cm^{-1}, dried at 105 °C, and weighed. The recovery rate of the initial sample weight was in a range of 94-100%, the recovery rate of the initial SOC was 98.5% ± 1.7% (ranging from 81 to 138%). The dried fractions were ground and measured at an elemental analyzer (Euro EA 3000, EuroVector, Pavia, Italy) to determine C and N content, and at an isotope ratio mass spectrometer to determine the $\delta^{13}C$ value of the density fractions.

D2.5 Calculation of C mineralization and priming effect

The CO_2 concentration in the flask headspace was corrected for gas pressure (measured during the incubation using a manometer) and volume (based on flask volume and gas pressure), and used to calculate the cumulative CO_2 production per initial sample mass (mg CO_2-C g^{-1} dry weight excluding amendment mass) and per initial TOC (mg CO_2-C g^{-1} TOC including biochar-derived C).

The use of ^{13}C-labeled amendments enabled the distinction between amendment-derived SOC and native SOC (KUZYAKOV, 2011). To trace their fate and to investigate the priming effect of the amendments, we determined the

$\delta^{13}C$ values (‰) of the amendment-C prior to incubation, of the released CO_2 during incubation, of the MBC and of density fractions after incubation using an isotope ratio mass spectrometer (Delta V Plus, Thermo Fisher Scientific, Bremen, Germany). The abundance of ^{13}C is expressed as $\delta^{13}C$ representing the ratios of ^{13}C:^{12}C relative to the Vienna-PeeDee-Belemnite-Standard, defined as *$[(R_{sample} - R_{standard}) / R_{standard}] \times 1000$*. The $\delta^{13}C$ values of the ^{13}C-labeled amendments and native SOC were used to determine the contributions of amendment-C and native SOC to CO_2, MBC, and density fractions by using a two-pool mixing model (Equations D1 and D2) following BAMMINGER et al. (2014) and FANG et al. (2015):

$$\mathrm{X} = \frac{(\delta_{treatment} - \delta_{control})}{(\delta_{amendment} - \delta_{control})} * 100 \quad \text{(D1)}$$

$$\mathrm{Y} = 100 - \mathrm{X} \quad \text{(D2)}$$

where X is the proportion of SOC derived from the amendments (%), $\delta_{treatment}$ is the $\delta^{13}C$ value from the sample including soil and amendment (‰), $\delta_{control}$ is the $\delta^{13}C$ value from the control soils (‰) containing only native SOC, $\delta_{amendment}$ is the $\delta^{13}C$ value of the amendment (biochar or rock-enhanced biochar) (‰), and Y is the proportion of SOC derived from native SOC (%). Both X and Y were calculated for produced CO_2, MBC, and density fractions.

The mineralized amendment-C (mg mineralized amendment-C g^{-1} amendment-C) was calculated by multiplying the cumulative CO_2 production (mg CO_2-C g^{-1} TOC) with X and by normalizing to one gram of initial amendment-C. The mineralized native SOC (mg mineralized native SOC g^{-1} native SOC) was calculated by multiplying the cumulative CO_2 production (mg CO_2-C g^{-1} TOC) with Y and by normalizing to one gram of initial native SOC (FANG et al., 2015).

Priming effects of the amendments were calculated from the difference in the native SOC mineralization between amended and unamended samples (control):

$$PE_{absolute} = mineralized\,SOC_{treatment} - mineralized\,SOC_{control} \quad \text{(D3)}$$

$$PE_{relative} = \frac{(mineralized\,SOC_{treatment} - mineralized\,SOC_{control})}{mineralized\,SOC_{control}} * 100 \quad \text{(D4)}$$

where $PE_{absolute}$ is the absolute priming effect (mg mineralized native SOC g^{-1} native SOC), $mineralized\,SOC_{treatment}$ is the native SOC mineralized in the amended treatments (mg mineralized native SOC g^{-1} native SOC), $mineralized\,SOC_{control}$ is native SOC mineralized in the control (mg mineralized native SOC g^{-1} native SOC), and $PE_{relative}$ is the priming effect (%) relative to the amount of mineralized SOC in the control at the end of the incubation. For control and basanite treatments, the total CO_2 production was assumed to result from the release of native C, since no amendment-C was added.

The TOC (mg C g^{-1} soil) stored in the density fractions ($normalized\ TOC_{fraction}$) was calculated to determine the fractions' contributions to the overall SOC pool following Equation D5:

$$normalized\ TOC_{fraction} = \frac{mass_{fraction} * relative\ TOC_{fraction}}{mass_{soil}} \quad \text{(D5)}$$

where $mass_{fraction}$ and $relative\ TOC_{fraction}$ are mass (g) and the TOC content (%) of the fraction, respectively, and $mass_{soil}$ is the soil mass (excluding the weight of the amendments).

Additionally to the overall priming effect, we calculated the priming effect (%) of the amendments for the density fractions. Therefore, the SOC in each density fraction was distinguished in native and amendment-derived as described in Equation D1 and D2, and calculated the fraction-specific priming ($PE_{fraction}$) following Equation D6:

$$PE_{fraction} = \frac{(SOC_{treatment} - SOC_{control})}{SOC_{control}} * 100 \quad \text{(D6)}$$

$SOC_{treatment}$ is the native SOC in the density fractions of the amended treatments (mg native SOC g^{-1} soil) and $SOC_{control}$ is native SOC in the density fractions of the control (mg native SOC g^{-1} soil) at the end of the incubation.

Differences (%) of amended treatments compared to control, e.g. in CO_2 production, were calculated using Equation D7:

$$\text{difference} = \frac{value_{amended} - value_{control}}{value_{control}} * 100 \quad \text{(D7)}$$

where $value_{control}$ is the measured or calculated value of the control treatment and $value_{amended}$ is the measured or calculated value of the amended treatments.

D2.6 Statistical analysis

To test for significant differences ($p < 0.05$) between treatments within one soil for repeated measurements, such as CO_2 production, we used a linear mixed effects -model with the sample as a random factor as well as treatment, incubation day, and their interaction as fixed factors. For C mineralization, MBC, and density fractions, a one-way analysis of variance (ANOVA) was conducted. Both statistical analyses were conducted separately for each soil, since the large baseline differences among soil types masked treatment effects, which were our primary objective. Both linear mixed effects model and ANOVA were followed by a Tukey HSD post-hoc test for pairwise comparison. For all analyses, normality and variance homogeneity of model residues were checked visually using qqplots. All calculations and statistical tests were conducted in RStudio (version 4.4.2) using 'dplyr' package (WICKHAM et al., 2023) for data handling, 'lme4' package (BATES et al., 2015) for linear mixed effects model computing, 'multcomp' package (HOTHORN et al., 2008) for compact letter display, 'ggplot2' package (WICKHAM, 2016) and 'gridExtra' (AUGUIE & ANTONOV, 2017) for data visualization.

D.3 Results

D3.1 Carbon mineralization and priming effect

The relative priming effect following amendment application compared to control was soil dependent and varied during the incubation (Figure D.1). In the temperate silty soil, during the course of the incubation the biochar-containing amendments initially induced a negative priming, which switched to a cumulative positive priming latest at day 42 (Figure D.6 in Appendix). Overall, only the co-pyrolysis treatment increased the native SOC mineralization in the temperate silty soil ($p = 0.03$), while biochar and co-application did not differ from control (Figure D.1a). In both sandy soils, the application of the three biochar-containing amendments increased the mineralization of native SOC (Figure D.1b,c) and induced cumulative positive priming throughout the entire incubation period (Figure D.6 in Appendix). This effect was more pronounced in the temperate sandy soil with priming up to ~109% compared to control (Figure D.1b). In contrast to the biochar-containing amendments, the application of rock powder did not affect native SOC mineralization within the 66 days of incubation in all three soils (Figure D.1).

Between 0.0345% ± 0.0008% and 0.0843%± 0.0011% of amendment-C was mineralized within the 66-day incubation, most pronounced in the temperate sandy soil (Figure D.2). In both sandy soils, both pure biochar and co-application had higher mineralization of amendment-C than the co-pyrolysis treatment (Figure D.2b,c). In the temperate silty soil, co-application treatment showed higher amendment-C mineralization than the co-pyrolysis treatment ($p = 0.014$) (Figure D.2a).

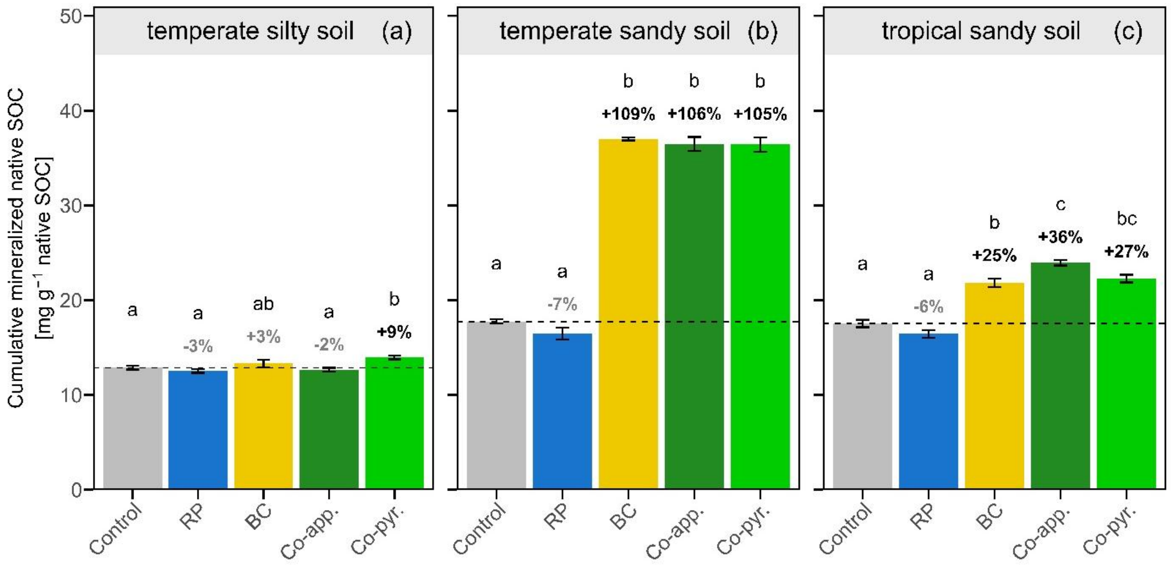

Figure D.1: Cumulative mineralized native SOC (mg mineralized native SOC g^{-1} native SOC) of temperate silty (A), temperate sandy (B), and tropical sandy soil (C) in five treatments (n = 4, mean and standard error) after 66 days of incubation (temporal cumulative mineralized native SOC in Figure D.7 in Appendix). The dashed black line shows the cumulative mineralized native SOC in the control. Numbers above the bars are the relative priming effect (%) of the respective treatment compared to control (black = significant, grey = insignificant; mean amendment-induced priming effect ± standard error in Table D.5 in Appendix; temporal cumulative priming effect in Figure D.6 in Appendix). Lower case letters indicate significant differences in cumulative mineralized native SOC between treatments within one soil ($p < 0.05$). RP = rock powder treatment containing basanite, BC = biochar treatment, Co-app. = co-application treatment containing biochar and basanite, Co-pyr. = co-pyrolysis treatment containing rock-enhanced biochar.

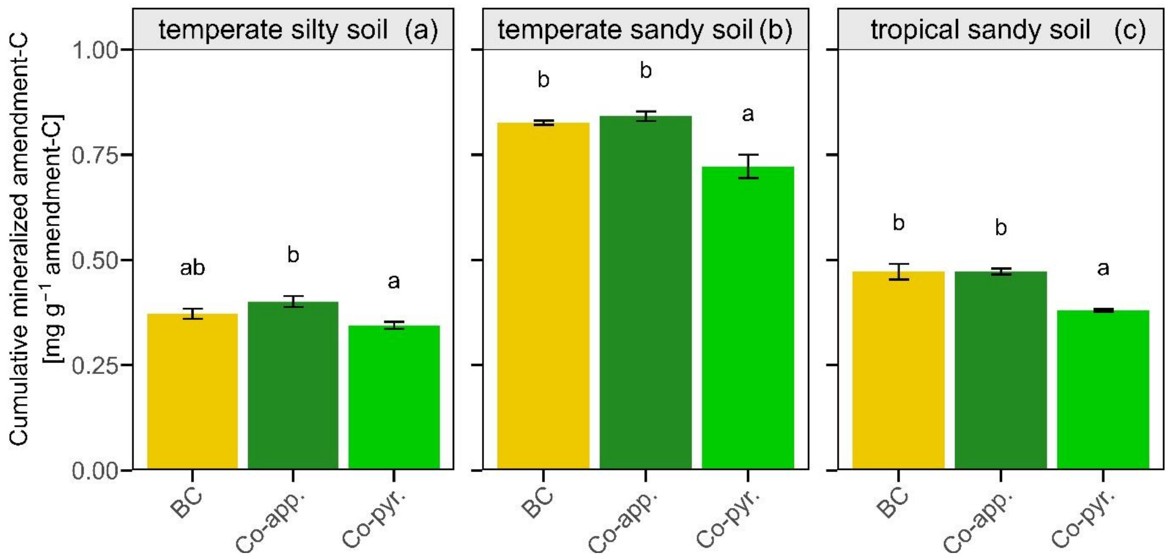

Figure D.2: Cumulative mineralized amendment-C (mg mineralized amendment-C g^{-1} amendment-C) of temperate silty (A), temperate sandy (B), and tropical sandy soil (C) in three treatments (n = 4, mean and standard error) after 66 days of incubation (temporal cumulative mineralized amendment-C in Figure D.6 in Appendix). Lower case letters indicate significant differences in cumulative mineralized amendment-C between treatments within one soil ($p < 0.05$). BC = biochar treatment, Co-app. = co-application treatment containing biochar and basanite, Co-pyr. = co-pyrolysis treatment containing rock-enhanced biochar.

D3.2 Carbon in density fractions: amount and origin

The incorporation of SOC in the density fractions of the unamended controls differed strongly between soils (Figure D.3). In the temperate silty and the tropical sandy soil, most of the SOC was recovered in the HF. In the temperate sandy soil, the oLF contained most of the SOC. The application of biochar-containing amendments increased the overall SOC stored in all density fractions in all three soils compared to the unamended control except the HF in the temperate sandy soil. In the biochar-containing treatments, the SOC stored in the fLF increased strongest compared to control, now containing most of the SOC in the three soils. The increase in SOC stored in the oLF following the application of biochar-containing amendments was most pronounced in the tropical sandy soil. Biochar-containing amendments increased SOC storage in the HF by 11-33% in temperate soils, and by more than 300% in the tropical sandy soil. The co-pyrolysis treatment led to larger SOC incorporation into HF across all soils, compared to biochar and co-application. In contrast, pure rock powder application alone did not significantly alter the SOC stored in any of the three density fractions.

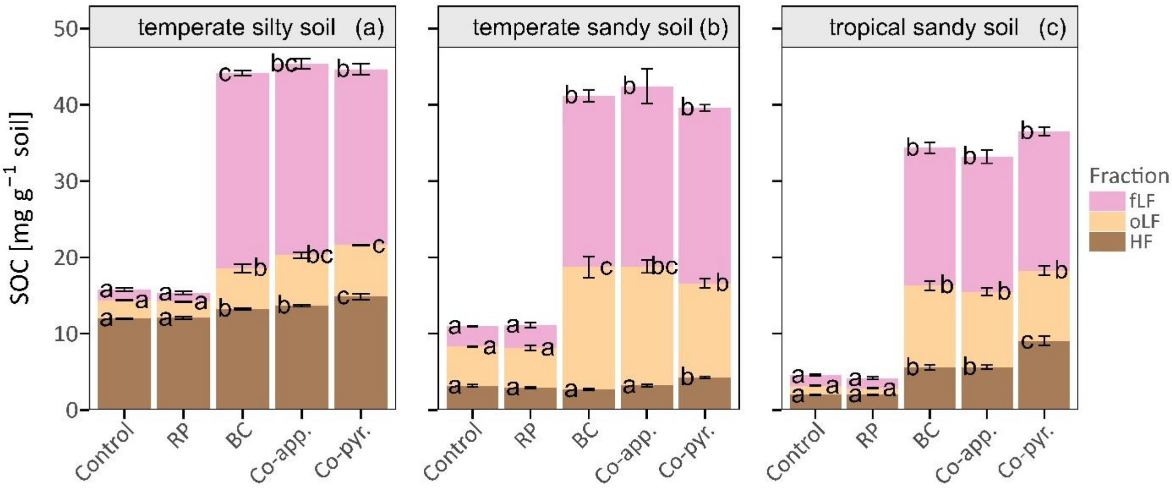

Figure D.3: Soil organic carbon (SOC) content (mg g^{-1} soil excluding amendment weight) of the free light fraction (fLF, similar to fPOM), occluded light fraction (oLF, similar to oPOM), and heavy fraction (HF, similar to MAOM) of temperate silty (A), temperate sandy (B), and tropical sandy soil (C) in five treatments (n = 4, mean and standard error) after 66 days of incubation. Lower case letters indicate significant differences between treatments within one density fraction and one soil ($p < 0.05$). RP = rock powder treatment containing basanite, BC = biochar treatment, Co-app. = co-application treatment containing biochar and basanite, Co-pyr. = co-pyrolysis treatment containing rock-enhanced biochar.

The proportion of native SOC in the density fractions was influenced by the biochar-containing amendments differing between the soils and the amendments at the end of the 66-day incubation (Figure D.4). The native SOC in fLF was reduced in the temperate silty soil following biochar and co-application and in the temperate sandy soil in the co-application treatment (Figure D.4a,b). The co-pyrolysis treatment did not alter the native SOC content in the fLF of both temperate soils and even increased the native SOC in fLF of the tropical sandy soil (Figure D.4a,b,c). Compared to the control, native SOC contents in the oLF increased (negative priming) or remained constant following the application of biochar-containing amendments (Figure D.4d,e,f). The negative priming was most pronounced in the co-application treatment of the temperate silty soil (-81%; Figure D.4e). Native SOC in the HF of both temperate soils was often reduced following the application of biochar-containing amendments (Figure D.4g,h). This positive priming of HF was most pronounced in the biochar treatment of the temperate sandy soil (+41%). In the tropical sandy soil, only the co-pyrolysis treatment altered the native SOC content in the HF and led to a negative priming (-45%) (Figure D.4i). In contrast to the biochar-containing treatments, rock powder application did not significantly alter the amount of native SOC in the three density fractions.

The application of biochar-containing amendments changed the composition of the SOC stored in the three density fractions by incorporating amendment-C (Figure D.4). Biochar-derived SOC from all three amendments was incorporated to a similar extent. In all soils, the co-pyrolysis treatment led to the highest incorporation of amended-C into the HF fraction (Figure D.4g,h,i).

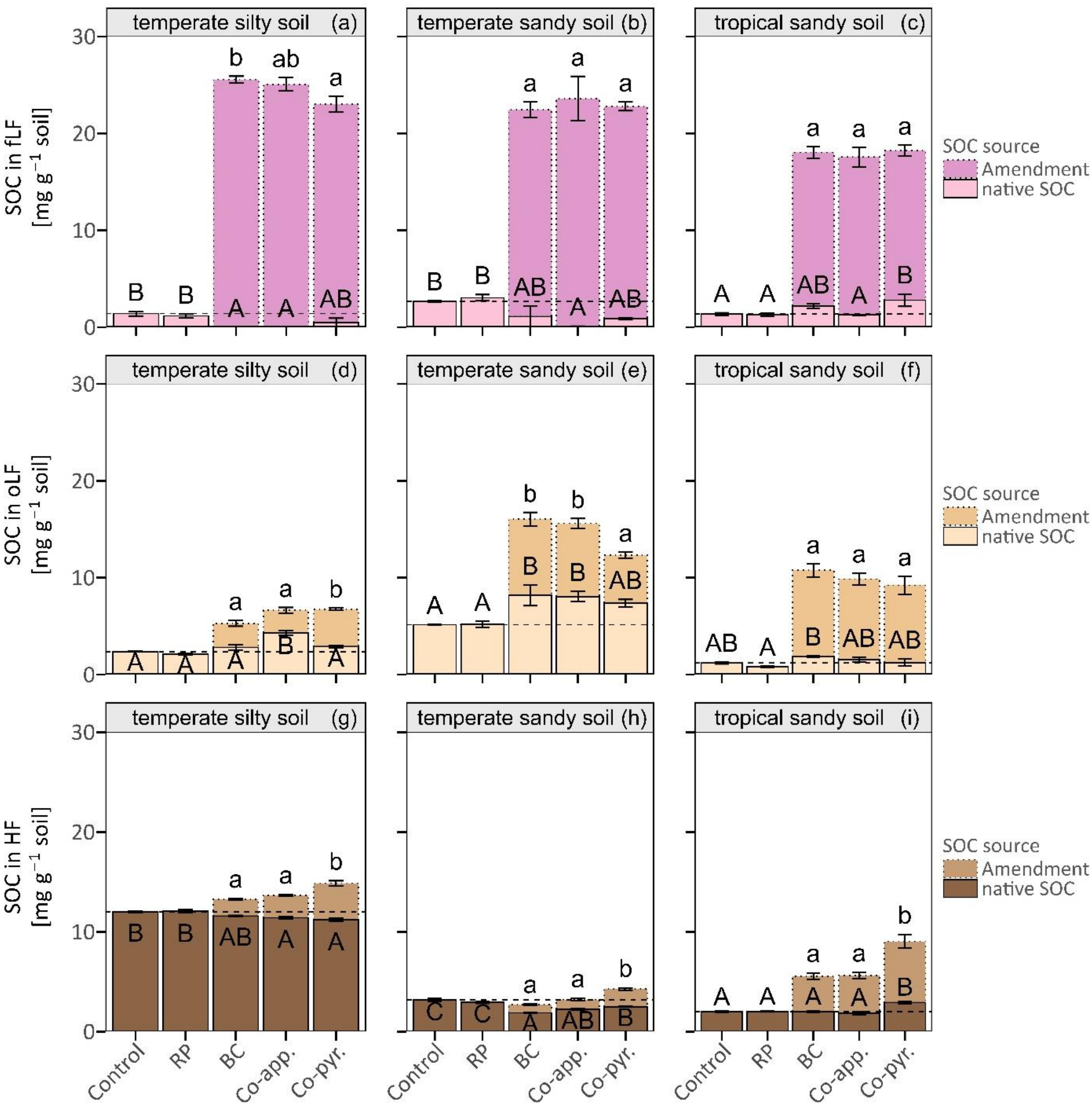

Figure D.4: Source of the soil organic carbon (SOC) content (mg g^{-1} soil excluding amendment weight) in the free light fraction (fLF, similar to fPOM), occluded light fraction (oLF, similar to oPOM), and heavy fraction (HF, similar to MAOM) of temperate silty (a, d, g), temperate sandy (b, e, h), and tropical sandy (c, f, i) soil in five treatments (n = 4, mean and standard error) after 66 days of incubation. The black dashed line shows the content of native SOC in the respective control treatment. Lower case letters indicate significant differences in amendment-C content between treatments within one fraction and one soil ($p < 0.05$). Capital letters indicate significant differences in native SOC content between treatments within one fraction and one soil ($p < 0.05$). RP = rock powder treatment containing basanite, BC = biochar treatment, Co-app. = co-application treatment containing biochar and basanite, Co-pyr. = co-pyrolysis treatment containing rock-enhanced biochar.

D3.3 Microbial biomass C: amount and origin

The effect of the amendments on MBC at the end of the 66-day incubation differed between soils. In the temperate silty soil, both combined applications reduced the MBC compared to control ($p < 0.001$), while pure biochar application had no reducing effect (Figure D.5a). In the temperate sandy soil, only the co-pyrolysis treatment showed significantly higher MBC compared to control ($p = 0.03$) (Figure D.5b). In the tropical sandy soil, rock powder, biochar, and co-pyrolysis treatments significantly increased MBC compared to control ($p < 0.01$), while co-application had no increasing effect (Figure D.5c).

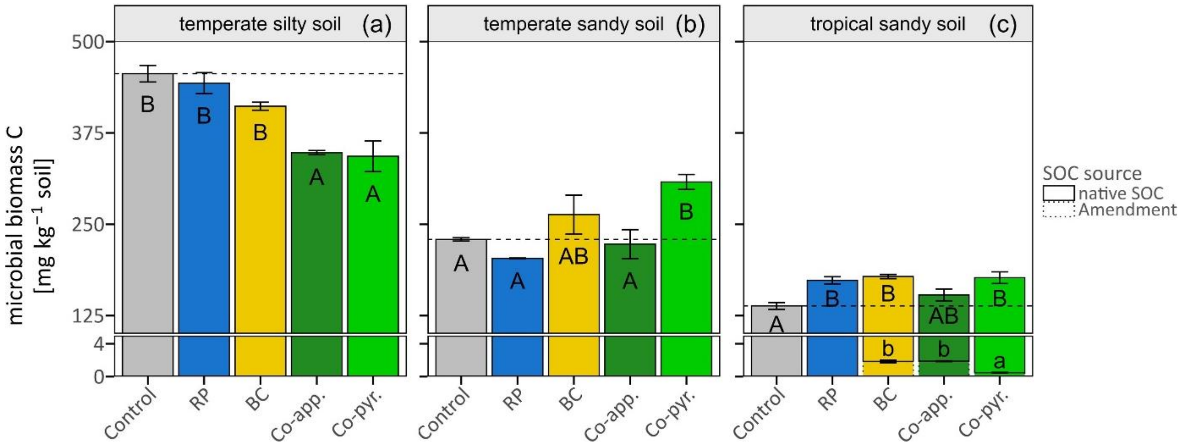

Figure D.5: Content and source of the microbial biomass C (MBC; mg kg^{-1} soil weight) of the temperate silty (a), temperate sandy (b), and tropical sandy soil (c) in five treatments (n = 4, mean and standard error) after 66 days of incubation. Lower case letters indicate significant differences in amendment-C content in MBC between biochar-containing treatments within one soil ($p < 0.05$). Capital letters indicate significant differences in native SOC content in MBC between treatments within one soil ($p < 0.05$). RP = rock powder treatment containing basanite, BC = biochar treatment, Co-app. = co-application treatment containing biochar and basanite, Co-pyr. = co-pyrolysis treatment containing rock-enhanced biochar.

In both temperate soils, amendment-C was not incorporated in the MBC (measurement accuracy for used standards ±0.1 ‰; Figure D.5a,b). In contrast, an incorporation of amendment-C in MBC was visible in the tropical sandy soil, accounting for ~0.3% (co-pyrolysis treatment) up to ~1.2% (co-application treatment) of the overall MBC (Figure D.5c).

D.4 Discussion

D4.1 Soil properties control amendment effects on SOC dynamics

The effects of biochar-containing amendments (pure biochar, co-application with basanite rock powder, rock-enhanced biochar) on SOC dynamics differed between the three agricultural soils used in this study, suggesting that soil type was the dominant factor controlling how biochar-containing amendments affected native SOC mineralization and stabilization. In line with our first hypothesis, this soil-effect was especially visible in the amendment-induced priming. Clay-rich soils often show negative priming following biochar application (BRUUN et al., 2014; HERATH et al., 2015; YU et al., 2020), whereas clay-poor or sandy soils commonly experience positive priming (FANG et al., 2015; LIU et al., 2015; WANG et al., 2016). Consistent with this pattern occurring in incubations between 28 days (YU et al., 2020) and 2 years (FANG et al., 2015), we observed minimal priming in the finer-textured temperate silty soil but positive amendment-induced priming in both sandy soils during the 66-day incubation. In our three soils, the texture effect coincided with the soils' pH response to the application of biochar-containing amendments, making it difficult to attribute the observed priming effect to either factor independently. The temperate silty soil showed a weak pH increase (6.9 to 7.5 during pre-incubation) and almost no priming, while both sandy soils experienced a strong pH increase (4.7 to 7.2-7.4 during pre-incubation), coinciding with positive priming. Both pH increase (LUO et al., 2011; ZHANG et al., 2018; XU et al., 2021) and the input of labile biochar compounds, especially to sandy soils poor in organic matter (ZIMMERMAN et al., 2011; WANG et al., 2016), can enhance microbial activity and modify the microbial community composition (LI et al., 2026). Thus, the application of biochar-containing amendments can potentially enhance native SOC mineralization, resulting in positive priming. The pronounced positive priming in our temperate sandy soil probably mainly originated from a loss of native MAOM (up to 45%). Even though the fraction-specific priming was not measured over the course of the incubation and the exact mechanisms causing the amendment-induced priming could not be observed, the losses of native MAOM during the 66-day incubation were likely a consequence of the amendment-induced priming since this the SOC fraction showed the biggest losses of native SOC in the temperate sandy soil. The typically stable native MAOM may respond to released labile biochar-derived C (KLEBER et al., 2015; JILLING et al., 2021) and could be mobilized due to the high sorption affinity of biochar-derived C, particularly in sandy soils with limited sorption capacity, which potentially leads to the mineralization of native MAOM (SCHIEDUNG et al., 2020).

Soil texture not only affected the response of native SOC to biochar-containing amendments, but also the stability of those amendments. Biochar contains a wide range of C compounds, including readily available compounds, such as aliphatic compounds, as well as highly stable aromatic clusters (KEILUWEIT et al., 2010). During a 66-day incubation, only readily available C compounds can be mineralized. Thus, our set-up does not allow conclusions about the behavior of the persistent majority of biochar-derived C (AZZI et al., 2024; HAGEMANN et al., 2025; SANEI et al., 2025). However, we observed the highest mineralization of biochar-derived C in the temperate sandy soil, indicating a lower stability of labile biochar components in clay-poor soils and showing the importance of soil texture for biochars' persistence (BRUUN et al., 2014; YANG et al., 2022; SCHMIDT et al., 2025). Once the labile compounds are mineralized, we expect a reduction of amendment mineralization (AMELOOT et al., 2013; WANG et al., 2016; AZZI et al., 2024), indicating the potential of biochar-containing amendments to store SOC in the long-term.

Regarding both native SOC and biochar-derived C, their stabilization in oPOM and MAOM was more pronounced in the SOC-poor tropical sandy soil compared to both temperate soils. This indicates a connection between initial SOC content and SOC stabilization potential following biochar-containing amendment application. Overall, our results demonstrate that soil type regulates both the response of native SOC and the stability of labile biochar components, and should therefore be explicitly considered when predicting the effect of biochar-containing amendments on SOC dynamics.

D4.2 Effects on SOC dynamics driven by biochar

Both combined applications followed the trends observed following pure biochar application for most analyzed parameters. Biochar-induced priming often shifts from positive to negative over time (MAESTRINI et al., 2015; DING et al., 2018; JOSEPH et al., 2021), as the release of labile biochar-derived C declines within days or weeks (BRUUN et al., 2008; BRUUN et al., 2014). In line with this, our biochar-containing amendments induced strong positive priming in both sandy soils during the first days of incubation (Figure D.6 in Appendix). Afterwards, cumulative priming slowed down and even declined in the tropical sandy soil, indicating potential negative priming in the long-term (ZIMMERMAN et al., 2011). The amendment-induced priming likely originated from a loss of native MAOM, especially in the temperate sandy soil (Figure D.4). The observed positive priming of native fPOM in both sandy soils turned out to be, at least partly, a shift of native SOC from fPOM to oPOM caused by the application of biochar-containing amendments, increasing the amount of native SOC stabilized in aggregates. While the priming effect of pure biochar application is well researched, that of combined biochar and silicate rock powder application remains poorly understood. Our findings differ from previous, already inconsistent results (HONVAULT et al., 2024; VIENNE et al., 2025), underlining the importance of further research into the underlying mechanisms of a combined application.

Supporting our second hypothesis, the application of biochar-containing amendments led to either constant or often increased SOC stored in all three density fractions (Figure D.3). This increase in fraction SOC often resulted from the incorporation of biochar-derived C (Figure D.4). The partial loss of native SOC in fPOM and MAOM was similar or smaller than the biochar-derived C input, often resulting in an overall increase of SOC in those pools. As previously observed (HERATH et al., 2014; SINGH et al., 2014; PAETSCH et al., 2017; SCHIEDUNG et al., 2020; KALU et al., 2024), the main part of our biochar-derived C remained in the fPOM. This alters the properties of the otherwise rather unstable fPOM, which should be kept in mind when discussing SOC fractions following biochar application. Additionally, biochar-derived C was recovered in both oPOM and MAOM, as observed in previous studies (BRODOWSKI et al., 2006; SINGH et al., 2014; PAETSCH et al., 2017; SCHIEDUNG et al., 2020). The association to mineral surfaces can either occur through the direct sorption of labile biochar-derived DOC (YANG et al., 2016; YANG et al., 2021) or via an in-vivo microbial turnover pathway (SOKOL et al., 2018; MANZONI & COTRUFO, 2024). For the tropical sandy soil, where we also observed the incorporation of biochar-derived C into MBC, the latter pathway might contribute to the stabilization of biochar-derived C as MAOM. Since the microbial incorporation of biochar-derived C into MAOM and thus also in MBC is likely during the 66-day incubation, the absence of biochar-derived C in MBC of both sandy soils could be explained by the detection limit of the used TOC analyzer of 1‰. However, the observed incorporation of biochar-derived C in MAOM may partly reflect our density-based definition of MAOM. Since biochar can reach particle densities of up to 2 g cm^{-3} (BREWER et al., 2014), biochar particles with a density >1.8 g cm^{-3} may be recovered in the HF fraction (representing MAOM) even in the absence of mineral-associations. This is particularly relevant for rock-enhanced biochar, since it has a higher ash content and mineral association can already occur during pyrolysis, so certain carbonaceous fractions can have a particle density >2.5 g cm^{-3} (MEYER ZU DREWER et al., 2025). Although density fractionation is commonly used to assess SOC stabilization after biochar application (e.g. GRUNWALD et al., 2017; KALU et al., 2024), this methodological effect could contribute to the occurrence of biochar-derived C in MAOM. Nonetheless, this effect cannot fully explain our results, since we observed clear differences in the amount of biochar-derived C in MAOM among soils. In line with this, TE PAS et al. (2026) observed the formation of secondary minerals during weathering and suggests that this might be beneficial for the long-term stabilization of co-applied biochar. Moreover, even though not conducted in this study, the association of biochar-derived C to minerals has been observed rather directly using thermal analysis (BURGEON et al., 2021; FOUCHÉ et al., 2023), supporting the association of biochar-derived C to mineral surfaces. While FANG et al. (2018) and SCHIEDUNG et al. (2020) identified fine soil texture as the main driver of biochar-C stabilization in field and column experiments, we observed strong interactions between biochar-derived C and soil minerals unaffected by texture in our incubation study. The magnitude of those interactions in this relatively short period of 66 days underlines the potential for a further stabilization of biochar-derived C in soils.

D4.3 Effect of basanite rock powder in pure and combined application on SOC dynamics

Basanite rock powder application had no short-term effect on most soil properties, neither pure nor in both combined applications, within 66 days. The potential effects of silicate rock powder application on SOC dynamics depend on several factors, including the observed time span following application (XU et al., 2025). Since previous studies found effects of silicate rock powder application on both SOC mineralization (BUSS et al., 2024a; ANTHONY et al., 2025) and stabilization (BUSS et al., 2024a; COSTANZO et al., 2025) on longer time scales. Thus, even though we cannot confirm this by measured pH or alkalinity release after the incubation, the missing effect in our study probably results from low basanite weathering rates during our 66-day incubation (SOKOL et al., 2024; XU et al., 2025). While most previous studies show the potential of enhanced rock weathering to improve SOC dynamics in the long-term, also positive priming (LEI et al., 2025) and reduced SOC accrual (SOKOL et al., 2024) have been reported.

Differences between biochar-containing amendments could be caused by application rates or compositional differences. When co-pyrolyzed with wheat straw to rock-enhanced biochar, basanite rock powder had a pronounced positive effect on SOC stabilization. The application of rock-enhanced biochar led to an overall higher content of SOC in the HF, interpreted as MAOM, compared to pure biochar application and co-application of both amendments, thus more strongly increasing the stable SOC pool (Figure D.3). The short-term increase in MAOM originated from a more pronounced occurrence of rock-enhanced biochar-C in the heavy fraction, defined as mineral-associations, compared to biochar-derived C from pure and co-application (Figure D.4). This indicates either a density-driven recovery of rock-enhanced biochar in the HF interpreted as MAOM, a higher affinity of rock-enhanced biochar-C to form MAOM, or direct formation of mineral-associations during co-pyrolysis of biomass and basanite rock powder. Such mineral-associations could include coating of rock particles with biochar-derived C, as observed in MEYER ZU DREWER et al. (2025). The pronounced stabilization of rock-enhanced biochar-C was reflected in a significantly lower mineralization and thus higher stability of its labile compounds compared to pure and co-applied biochar (Figure D.2). This is potentially supported by the initially greater stability of rock-enhanced biochar (determined via hydropyrolysis from MEYER ZU DREWER et al., 2025) and the lower specific surface area compared to biochar, probably reducing interactions between soil and rock-enhanced biochar. This difference in the stability of the labile rock-enhanced biochar components highlights the potential of co-pyrolyzing biomass and basanite to further improve the persistence of biochar-derived C.

D.5 Conclusions

Basanite rock powder, applied pure or combined with biochar, had negligible effects on the short-term mineralization and stabilization of native SOC, likely due to limited rock weathering during our 66-day incubation. In contrast, all biochar-containing amendments (pure biochar, co-application, rock-enhanced biochar) had strong effects on short-term SOC dynamics, although responses varied across soils, depending on texture, soil pH, and initial SOC content.

Across treatments and soils, increasing SOC was mainly driven by the incorporation of biochar-derived C into all fractions (fPOM, oPOM, MAOM) during 66 days. While the application of biochar-containing amendments induced positive priming and SOC losses in fPOM and MAOM, these losses were consistently offset by biochar-derived C. Notably, our observations indicate a redistribution of native SOC from fPOM to oPOM rather than net mineralization. Rock-enhanced biochar led to the largest increase in the HF, defined as the stable MAOM fraction, suggesting enhanced short-term SOC stabilization potential compared to pure and co-applied biochar. This pattern hints to the formation of organo-mineral complexes during co-pyrolysis of biomass and basanite, which is reflected in a higher short-term stability of the otherwise labile rock-enhanced biochar compounds. These findings indicate the short-term potential of co-pyrolysis as a promising strategy to enhance the stabilization of labile biochar-derived C in agricultural topsoils, beyond the effect of co-application. However, confirming these mechanisms on long-term field scales require further studies, including soil-plant-interactions, different application rates, and spectroscopic analyses as a next step in understanding the interactions between amendments and SOC dynamics.

Authors' contributions

Maria Ansari: Conceptualization, Formal analysis, Investigation, Methodology, Visualization, Writing – original draft; **Annemarie Lübeck**: Investigation; **Johannes Meyer zu Drewer**: Resources, Writing – review and editing; **Nikolas Hagemann**: Funding acquisition, Resources, Writing – review and editing; **Annette Eschenbach**: Conceptualization, Funding acquisition, Resources, Supervision, Writing – review and editing; **Joscha N. Becker**: Conceptualization, Funding acquisition, Methodology, Resources, Supervision, Writing – review and editing.

Acknowledgements

This work was conducted within the PyMiCCS project (Pyrogenic carbon and carbonating Minerals for enhanced plant growth and Carbon Capture and Storage) as part of the CDRterra consortium and was supported by the German Federal Ministry of Research, Technology and Space (BMFTR, FKZ: 01LS2109A). The authors thank Deborah Harms, Sumita Rui, Annika Naumann, Jakob Kast, and Jannis Löchte (all University of Hamburg) for support during lab work as well as Jochen Mayer and Jannis Grafmüller (both Agroscope) for providing the ^{13}C labeled straw.

D.6 References

AMANN, T. & HARTMANN, J. 2019. Ideas and perspectives: Synergies from co-deployment of negative emission technologies. Biogeosciences, 16, 2949–2960. https://doi.org/10.5194/bg-16-2949-2019.

AMANN, T., HARTMANN, J., STRUYF, E., DE OLIVEIRA GARCIA, W., FISCHER, E. K., JANSSENS, I., MEIRE, P. & SCHOELYNCK, J. 2020. Enhanced Weathering and related element fluxes – a cropland mesocosm approach. Biogeosciences, 17, 103–119. https://doi.org/10.5194/bg-17-103-2020.

AMELOOT, N., GRABER, E. R., VERHEIJEN, F. G. A. & DE NEVE, S. 2013. Interactions between biochar stability and soil organisms: review and research needs. Eur J Soil Sci, 64, 379–390. https://doi.org/10.1111/ejss.12064.

ANTHONY, T. L., JONES, A. R. & SILVER, W. L. 2025. Supplementing enhanced weathering with organic amendments accelerates the net climate benefit of soil amendments in rangeland soils. AGU Advances, 6, e2024AV001480. https://doi.org/10.1029/2024AV001480.

AUGUIE, B. & ANTONOV, A. 2017. gridExtra: Miscellaneous Functions for "Grid" Graphics - R package version 2.3. [Online].

AZZI, E. S., LI, H., CEDERLUND, H., KARLTUN, E. & SUNDBERG, C. 2024. Modelling biochar long-term carbon storage in soil with harmonized analysis of decomposition data. Geoderma, 441, 116761. https://doi.org/10.1016/j.geoderma.2023.116761.

BAKSHI, S., BANIK, C. & LAIRD, D. A. 2018. Quantification and characterization of chemically-and thermally-labile and recalcitrant biochar fractions. Chemosphere, 194, 247–255. https://doi.org/10.1016/j.chemosphere.2017.11.151.

BAMMINGER, C., MARSCHNER, B. & JÜSCHKE, E. 2014. An incubation study on the stability and biological effects of pyrogenic and hydrothermal biochar in two soils. Eur J Soil Sci, 65, 72–82. https://doi.org/10.1111/ejss.12074.

BATES, D., MÄCHLER, M., BOLKER, B. & WALKER, S. 2015. Fitting linear mixed-effects models using lme4. J Stat Softw, 67, 1 – 48. https://doi.org/10.18637/jss.v067.i01.

BEER, C., KNOBLAUCH, C., HOYT, A. M., HUGELIUS, G., PALMTAG, J., MUELLER, C. W. & TRUMBORE, S. 2022. Vertical pattern of organic matter decomposability in cryoturbated permafrost-affected soils. Environ Res Lett, 17, 104023. https://doi.org/10.1088/1748-9326/ac9198.

BEERLING, D. J., KANTZAS, E. P., LOMAS, M. R., TAYLOR, L. L., ZHANG, S., KANZAKI, Y., EUFRASIO, R. M., RENFORTH, P., MECURE, J.-F., POLLITT, H., HOLDEN, P. B., EDWARDS, N. R., KOH, L., EPIHOV, D. Z., WOLF, A., HANSEN, J. E., BANWART, S. A., PIDGEON, N. F., REINHARD, C. T., PLANAVSKY, N. J. & VAL MARTIN, M. 2025. Transforming US agriculture for carbon removal with enhanced weathering. Nature, 638, 425–434. https://doi.org/10.1038/s41586-024-08429-2.

BLANCO-CANQUI, H., LAIRD, D., HEATON, E., RATHKE, S. & ACHARYA, B. 2020. Soil carbon increased by twice the amount of biochar carbon applied after 6 years: Field evidence of negative priming. GCB Bioenergy, 12. 10.1111/gcbb.12665.

BREWER, C. E., CHUANG, V. J., MASIELLO, C. A., GONNERMANN, H., GAO, X., DUGAN, B., DRIVER, L. E., PANZACCHI, P., ZYGOURAKIS, K. & DAVIES, C. A. 2014. New approaches to measuring biochar density and porosity. Biomass Bioenergy, 66, 176–185. https://doi.org/10.1016/j.biombioe.2014.03.059.

BRODOWSKI, S., JOHN, B., FLESSA, H. & AMELUNG, W. 2006. Aggregate-occluded black carbon in soil. Eur J Soil Sci, 57, 539–546. https://doi.org/10.1111/j.1365-2389.2006.00807.x.

BRUUN, S., CLAUSON-KAAS, S., BOBUĽSKÁ, L. & THOMSEN, I. K. 2014. Carbon dioxide emissions from biochar in soil: Role of clay, microorganisms and carbonates. Eur J Soil Sci, 65, 52–59. https://doi.org/10.1111/ejss.12073.

BRUUN, S., JENSEN, E. S. & JENSEN, L. S. 2008. Microbial mineralization and assimilation of black carbon: Dependency on degree of thermal alteration. Org Geochem, 39, 839–845. https://doi.org/10.1016/j.orggeochem.2008.04.020.

BURGEON, V., FOUCHÉ, J., LEIFELD, J., CHENU, C. & CORNÉLIS, J.-T. 2021. Organo-mineral associations largely contribute to the stabilization of century-old pyrogenic organic matter in cropland soils. Geoderma, 388, 114841. https://doi.org/10.1016/j.geoderma.2020.114841.

BUSS, W., HASEMER, H., FERGUSON, S. & BOREVITZ, J. 2024a. Stabilisation of soil organic matter with rock dust partially counteracted by plants. Glob Chang Biol, 30, e17052. https://doi.org/10.1111/gcb.17052.

BUSS, W., HASEMER, H., SOKOL, N. W., ROHLING, E. J. & BOREVITZ, J. 2024b. Applying minerals to soil to draw down atmospheric carbon dioxide through synergistic organic and inorganic pathways. Commun Earth Environ, 5, 602. https://doi.org/10.1038/s43247-024-01771-3.

BUSS, W., YEATES, K., ROHLING, E. & BOREVITZ, J. 2021. Enhancing natural cycles in agro-ecosystems to boost plant carbon capture and soil storage. Oxford Open Climate Change, 1, kgab006. https://doi.org/10.1093/oxfclm/kgab006.

CLOUGH, A. & SKJEMSTAD, J. O. 2000. Physical and chemical protection of soil organic carbon in three agricultural soils with different contents of calcium carbonate. Soil Res, 38, 1005–1016. https://doi.org/10.1071/SR99102.

COSTANZO, S. A., HOLZER, I. O., MOONILALL, N. I., DAVENPORT, A., HOULTON, B. Z. & NOCCO, M. A. 2025. Preliminary assessment of crushed rock, compost, and biochar amendments on soil physical properties. Agric Environ Lett, 10, e70028. https://doi.org/10.1002/ael2.70028.

DIN 2011. DIN EN ISO 14240-2:2011-09: Soil quality - Determination of soil microbial biomass - Part 2: Fumigation-extraction method. Berlin, Germany: DIN Media GmbH.

DING, F., VAN ZWIETEN, L., ZHANG, W., WENG, Z., SHI, S., WANG, J. & MENG, J. 2018. A meta-analysis and critical evaluation of influencing factors on soil carbon priming following biochar amendment. J Soil Sediment, 18, 1507–1517. https://doi.org/10.1007/s11368-017-1899-6.

DUPLA, X., ROMANE, C., EMMA, B., IRIS, G., RENÉE-CLAIRE, L. B. & STÉPHANIE, G. 2024. Let the dust settle: Impact of enhanced rock weathering on soil biological, physical, and geochemical fertility. Sci Total Environ, 176297. https://doi.org/10.1016/j.scitotenv.2024.176297.

EBC. 2024. Analytical methods - EBC guidelines Version 10.4 [Online]. European Biochar Certificate (EBC). Available: https://www.european-biochar.org/en/ct/8-Analytical-Methods.

FANG, Y., SINGH, B. & SINGH, B. P. 2015. Effect of temperature on biochar priming effects and its stability in soils. Soil Biol Biochem, 80, 136–145. https://doi.org/10.1016/j.soilbio.2014.10.006.

FANG, Y., SINGH, B. P., LUO, Y., BOERSMA, M. & VAN ZWIETEN, L. 2018. Biochar carbon dynamics in physically separated fractions and microbial use efficiency in contrasting soils under temperate pastures. Soil Biol Biochem, 116, 399–409. https://doi.org/10.1016/j.soilbio.2017.10.042.

FAO & UNESCO. 1974. Soil map of the world (Scale 1:5.000.000). Rome, Italy: Food and Agriculture Organization (FAO) of the United Nations.

FOUCHÉ, J., BURGEON, V., MEERSMANS, J., LEIFELD, J. & CORNELIS, J.-T. 2023. Accumulation of century-old biochar contributes to carbon storage and stabilization in the subsoil. Geoderma, 440, 116717. https://doi.org/10.1016/j.geoderma.2023.116717.

GOLCHIN, A., OADES, J., SKJEMSTAD, J. & CLARKE, P. 1994. Study of free and occluded particulate organic matter in soils by solid state ^{13}C Cp/MAS NMR spectroscopy and scanning electron microscopy. Soil Res, 32, 285–309. https://doi.org/10.1071/SR9940285.

GRUNWALD, D., KAISER, M., JUNKER, S., MARHAN, S., PIEPHO, H.-P., POLL, C., BAMMINGER, C. & LUDWIG, B. 2017. Influence of elevated soil temperature and biochar application on organic matter associated with aggregate-size and density fractions in an arable soil. Agr Ecosyst Environ, 241, 79–87. https://doi.org/10.1016/j.agee.2017.02.029.

HAGEMANN, N., SCHMIDT, H.-P., BUCHELI, T. D., GRAFMÜLLER, J., VOSSWINKEL, S., HERDEGEN, V., MEREDITH, W., UGUNA, C. N. & SNAPE, C. E. 2025. Proxies for use in biochar decay models: Hydropyrolysis, electric conductivity, and H/C_{org} molar ratio. PLoS ONE, 20, e0330206. https://doi.org/10.1371/journal.pone.0330206.

HAGEMANN, N., SCHMIDT, H.-P., KÄGI, R., BÖHLER, M., SIGMUND, G., MACCAGNAN, A., MCARDELL, C. S. & BUCHELI, T. D. 2020. Wood-based activated biochar to eliminate organic micropollutants from biologically treated wastewater. Sci Total Environ, 730, 138417. https://doi.org/10.1016/j.scitotenv.2020.138417.

HAGEMANN, N., SPOKAS, K., SCHMIDT, H.-P., KÄGI, R., BÖHLER, M. A. & BUCHELI, T. D. 2018. Activated carbon, biochar and charcoal: Linkages and synergies across pyrogenic carbon's ABCs. Water, 10, 182. https://doi.org/10.3390/w10020182

HARLEY, A. D. & GILKES, R. J. 2000. Factors influencing the release of plant nutrient elements from silicate rock powders: a geochemical overview. Nutr Cycl Agroecosys, 56, 11–36. https://doi.org/10.1023/A:1009859309453.

HARTMANN, J., WEST, A. J., RENFORTH, P., KÖHLER, P., DE LA ROCHA, C. L., WOLF-GLADROW, D. A., DÜRR, H. H. & SCHEFFRAN, J. 2013. Enhanced chemical weathering as a geoengineering strategy to reduce atmospheric carbon dioxide, supply nutrients, and mitigate ocean acidification. Rev Geophys, 51, 113–149. https://doi.org/10.1002/rog.20004.

HERATH, H. M. S. K., CAMPS-ARBESTAIN, M., HEDLEY, M., VAN HALE, R. & KAAL, J. 2014. Fate of biochar in chemically- and physically-defined soil organic carbon pools. Org Geochem, 73, 35–46. https://doi.org/10.1016/j.orggeochem.2014.05.001.

HERATH, H. M. S. K., CAMPS-ARBESTAIN, M., HEDLEY, M. J., KIRSCHBAUM, M. U. F., WANG, T. & VAN HALE, R. 2015. Experimental evidence for sequestering C with biochar by avoidance of CO_2 emissions from original feedstock and protection of native soil organic matter. GCB Bioenergy, 7, 512–526. https://doi.org/10.1111/gcbb.12183.

HONVAULT, N., TIOUCHICHINE, M.-L., SAUZE, J., PIEL, C., LANDAIS, D., DEVIDAL, S., GRITTI, E., BOSCH, D. & MILCU, A. 2024. Additive effects of basalt enhanced weathering and biochar co-application on carbon sequestration, soil nutrient status and plant performance in a mesocosm experiment. Appl Geochem, 169, 106054. https://doi.org/10.1016/j.apgeochem.2024.106054.

HOTHORN, T., BRETZ, F. & WESTFALL, P. 2008. Simultaneous inference in general parametric models. Biometrical J, 50, 346–363. https://doi.org/10.1002/bimj.200810425.

IUSS WORKING GROUP WRB 2022. World reference base (WRB) for soil resources - International soil classification system for naming soils and creation legends for soil maps. Vienna, Austria., International Union of Soil Sciences (IUSS).

JILLING, A., KEILUWEIT, M., GUTKNECHT, J. L. M. & GRANDY, A. S. 2021. Priming mechanisms providing plants and microbes access to mineral-associated organic matter. Soil Biol Biochem, 158, 108265. https://doi.org/10.1016/j.soilbio.2021.108265.

JOERGENSEN, R. G. 1996. The fumigation-extraction method to estimate soil microbial biomass: Calibration of the k_{EC} value. Soil Biol Biochem, 28, 25–31. https://doi.org/10.1016/0038-0717(95)00102-6.

JOSEPH, S., COWIE, A. L., VAN ZWIETEN, L., BOLAN, N., BUDAI, A., BUSS, W., CAYUELA, M. L., GRABER, E. R., IPPOLITO, J. A., KUZYAKOV, Y., LUO, Y., OK, Y. S., PALANSOORIYA, K. N., SHEPHERD, J., STEPHENS, S., WENG, Z. & LEHMANN, J. 2021. How biochar works, and when it doesn't: A review of mechanisms controlling soil and plant responses to biochar. GCB Bioenergy, 13, 1731–1764. https://doi.org/10.1111/gcbb.12885.

JOSEPH, S. D., CAMPS-ARBESTAIN, M., LIN, Y., MUNROE, P., CHIA, C. H., HOOK, J., VAN ZWIETEN, L., KIMBER, S., COWIE, A., SINGH, B. P., LEHMANN, J., FOIDL, N., SMERNIK, R. J. & AMONETTE, J. E. 2010. An investigation into the reactions of biochar in soil. Soil Res, 48, 501–515. https://doi.org/10.1071/SR10009.

KALU, S., SEPPÄNEN, A., MGANGA, K. Z., SIETIÖ, O.-M., GLASER, B. & KARHU, K. 2024. Biochar reduced the mineralization of native and added soil organic carbon: evidence of negative priming and enhanced microbial carbon use efficiency. Biochar, 6, 7. https://doi.org/10.1007/s42773-023-00294-y.

KEILUWEIT, M., NICO, P. S., JOHNSON, M. G. & KLEBER, M. 2010. Dynamic molecular structure of plant biomass-derived black carbon (biochar). Environ Sci Technol, 44, 1247–1253. https://doi.org/10.1021/es9031419.

KLEBER, M., EUSTERHUES, K., KEILUWEIT, M., MIKUTTA, C., MIKUTTA, R. & NICO, P. S. 2015. Chapter One - Mineral–organic associations: Formation, properties, and relevance in soil environments. *In:* SPARKS, D. L. (ed.) Advances in Agronomy. London: Academic Press. https://doi.org/10.1016/bs.agron.2014.10.005.

KUZYAKOV, Y. 2011. How to link soil C pools with CO_2 fluxes? Biogeosciences, 8, 1523–1537. https://doi.org/10.5194/bg-8-1523-2011.

KUZYAKOV, Y., BOGOMOLOVA, I. & GLASER, B. 2014. Biochar stability in soil: Decomposition during eight years and transformation as assessed by compound-specific ^{14}C analysis. Soil Biol Biochem, 70, 229–236. https://doi.org/10.1016/j.soilbio.2013.12.021.

KUZYAKOV, Y., FRIEDEL, J. K. & STAHR, K. 2000. Review of mechanisms and quantification of priming effects. Soil Biol Biochem, 32, 1485–1498. https://doi.org/10.1016/S0038-0717(00)00084-5.

LBEG. 2017. Bodenkarte von Niedersachsen 1 : 50 000. Hannover, Germany: Landesamt für Bergbau Energie und Geologie (LBEG)

LE BAS, M. J., LE MAITRE, R. W. L., STRECKEISEN, A., ZANETTIN, B. & ROCKS, I. S. O. T. S. O. I. 1986. A chemical classification of volcanic rocks based on the total alkali-silica diagram. J Petrol, 27, 745–750. https://doi.org/10.1093/petrology/27.3.745.

LEHMANN, J., COWIE, A., MASIELLO, C. A., KAMMANN, C., WOOLF, D., AMONETTE, J. E., CAYUELA, M. L., CAMPS-ARBESTAIN, M. & WHITMAN, T. 2021. Biochar in climate change mitigation. Nat Geosci, 14, 883–892. https://doi.org/10.1038/s41561-021-00852-8.

LEI, K., BUCKA, F. B., TEIXEIRA, P. P. C., BUEGGER, F., JUST, C. & KÖGEL-KNABNER, I. 2025. Balancing organic and inorganic carbon dynamics in enhanced rock weathering: Implications for carbon sequestration. Glob Chang Biol, 31, e70186. https://doi.org/10.1111/gcb.70186.

LFU. 2025. UmweltAtlas Bayern - Bodenübersichtskarte 1:25.000. Augsburg, Germany: Bayerisches Landesamt für Umwelt (LfU).

LI, J., PEDURUHEWA, J. H., BROWN, R. W., CHADWICK, D. R., GRIFFITHS, R. I., FU, H., BIAN, H., SHENG, L., MA, Q. & JONES, D. L. 2026. Biochar reshapes soil bacterial community composition and survival strategies: A meta-analysis revealing trade-offs between microbial stability and functional complexity. Biol Fert Soils, 62, 251–266. https://doi.org/10.1007/s00374-025-01971-9.

LIU, S., ZHANG, Y., ZONG, Y., HU, Z., WU, S., ZHOU, J., JIN, Y. & ZOU, J. 2015. Response of soil carbon dioxide fluxes, soil organic carbon and microbial biomass carbon to biochar amendment: a meta-analysis. GCB Bioenergy, 8, 392–406. https://doi.org/10.1111/gcbb.12265.

LUO, Y., DURENKAMP, M., DE NOBILI, M., LIN, Q. & BROOKES, P. C. 2011. Short term soil priming effects and the mineralisation of biochar following its incorporation to soils of different pH. Soil Biol Biochem, 43, 2304–2314. https://doi.org/10.1016/j.soilbio.2011.07.020.

MAESTRINI, B., NANNIPIERI, P. & ABIVEN, S. 2015. A meta-analysis on pyrogenic organic matter induced priming effect. GCB Bioenergy, 7, 577–590. https://doi.org/10.1111/gcbb.12194.

MANZONI, S. & COTRUFO, M. F. 2024. Mechanisms of soil organic carbon and nitrogen stabilization in mineral-associated organic matter – Insights from modeling in phase space. Biogeosciences, 21, 4077–4098. https://doi.org/10.5194/bg-21-4077-2024.

MARTIN, J. B. 2017. Carbonate minerals in the global carbon cycle. Chem Geol, 449, 58–72. https://doi.org/10.1016/j.chemgeo.2016.11.029.

MEYER ZU DREWER, J., VORRATH, M.-E., AMANN, T., HARTMANN, J., DE LA ROSA, J. M., MÖLLMER, J., PÉREZ-DALÍ, S. M., MEREDITH, W., UGUNA, C., SNAPE, C., KAMMANN, C., SCHMIDT, H.-P. & HAGEMANN, N. 2025. Pyrogenic carbon and carbonating minerals for carbon capture and storage (PyMiCCS) part I: production, physico-chemical characterization and C-sink potential. Front Clim, 7 2025. https://doi.org/10.3389/fclim.2025.1631368.

PAETSCH, L., MUELLER, C. W., RUMPEL, C., ANGST, Š., WIESHEU, A. C., GIRARDIN, C., IVLEVA, N. P., NIESSNER, R. & KÖGEL-KNABNER, I. 2017. A multi-technique approach to assess the fate of biochar in soil and to quantify its effect on soil organic matter composition. Org Geochem, 112, 177–186. https://doi.org/10.1016/j.orggeochem.2017.06.012.

REICHENBACH, M., FIENER, P., GARLAND, G., GRIEPENTROG, M., SIX, J. & DOETTERL, S. 2021. The role of geochemistry in organic carbon stabilization against microbial decomposition in tropical rainforest soils. SOIL, 7, 453–475. https://doi.org/10.5194/soil-7-453-2021.

RIAHI, K., SCHAEFFER, R., ARANGO, J., CALVIN, K., GUIVARCH, C., HASEGAWA, T., JIANG, K., KRIEGLER, E., R. MATTHEWS, PETERS, G. P., RAO, A., ROBERTSON, S., SEBBIT, A. M., STEINBERGER, J., TAVONI, M. & VAN VUURE, D. P. 2022. Mitigation pathways compatible with long-term goals. *In:* P.R. SHUKLA, SKEA, J., SLADE, R., AL

KHOURDAJIE, A., VAN DIEMEN, R., MCCOLLUM, D., PATHAK, M., SOME, S., VYAS, P., FRADERA, R., BELKACEMI, M., HASIJA, A., LISBOA, G., LUZ, S. & MALLEY, J. (eds.) IPCC, 2022: Climate Change 2022: Mitigation of Climate Change. Contribution of Working Group III to the Sixth Assessment Report of the Intergovernmental Panel on Climate Change. Cambridge, UK and New York, NY, USA: Cambridge University Press. https://doi.org/10.1017/9781009157926.005.

SANEI, H., PETERSEN, H. I., CHIARAMONTI, D. & MASEK, O. 2025. Evaluating the two-pool decay model for biochar carbon permanence. Biochar*,* 7**,** 9. https://doi.org/10.1007/s42773-024-00408-0.

SCHIEDUNG, M., BELLÈ, S. L., SIGMUND, G., KALBITZ, K. & ABIVEN, S. 2020. Vertical mobility of pyrogenic organic matter in soils: a column experiment. Biogeosciences*,* 17**,** 6457–6474. https://doi.org/10.5194/bg-17-6457-2020.

SCHMIDT, H.-P., ABIVEN, S., COWIE, A., GLASER, B., JOSEPH, S., KAMMANN, C., LEHMANN, J., LEIFELD, J., PAN, G., RASSE, D., RUMPEL, C., WOOLF, D., ZIMMERMAN, A. R. & HAGEMANN, N. 2025. Biochar permanence — A policy commentary. GCB Bioenergy*,* 17**,** e70092. https://doi.org/10.1111/gcbb.70092.

SINGH, N., ABIVEN, S., MAESTRINI, B., BIRD, J. A., TORN, M. S. & SCHMIDT, M. W. I. 2014. Transformation and stabilization of pyrogenic organic matter in a temperate forest field experiment. Glob Chang Biol*,* 20**,** 1629–1642. https://doi.org/10.1111/gcb.12459.

SOHNG, J., SOKOL, N. W., WHITEAKER, S., SCHMIDT, R., HOLZER, I., GOERTZEN, H., PEÑA, J., HOULTON, B. Z., MONTAÑEZ, I., O'GEEN, A. & SCOW, K. 2025. Combining organic amendments with enhanced rock weathering shifts soil carbon storage in croplands. Sci Total Environ*,* 998**,** 180179. https://doi.org/10.1016/j.scitotenv.2025.180179.

SOKOL, N., SANDERMAN, J. & BRADFORD, M. 2018. Pathways of mineral-associated soil organic matter formation: Integrating the role of plant carbon source, chemistry, and point of entry. Glob Chang Biol*,* 25. https://doi.org/10.1111/gcb.14482.

SOKOL, N. W., SOHNG, J., MORELAND, K., SLESSAREV, E., GOERTZEN, H., SCHMIDT, R., SAMADDAR, S., HOLZER, I., ALMARAZ, M., GEOGHEGAN, E., HOULTON, B., MONTAÑEZ, I., PETT-RIDGE, J. & SCOW, K. 2024. Reduced accrual of mineral-associated organic matter after two years of enhanced rock weathering in cropland soils, though no net losses of soil organic carbon. Biogeochemistry. https://doi.org/10.1007/s10533-024-01160-0.

SOLLINS, P., HOMANN, P. & CALDWELL, B. A. 1996. Stabilization and destabilization of soil organic matter: Mechanisms and controls. Geoderma*,* 74**,** 65–105. https://doi.org/10.1016/S0016-7061(96)00036-5.

STEINER, C., TEIXEIRA, W. G., LEHMANN, J., NEHLS, T., DE MACÊDO, J. L. V., BLUM, W. E. H. & ZECH, W. 2007. Long term effects of manure, charcoal and mineral fertilization on crop production and fertility on a highly weathered Central Amazonian upland soil. Plant Soil*,* 291**,** 275–290. https://doi.org/10.1007/s11104-007-9193-9.

STRECKEISEN, A. 1980. Classification and nomenclature of volcanic rocks, lamprophyres, carbonatites and melilitic rocks IUGS Subcommission on the Systematics of Igneous Rocks. Geol Rundsch*,* 69**,** 194–207. https://doi.org/10.1007/BF01869032.

SWOBODA, P., DÖRING, T. F. & HAMER, M. 2022. Remineralizing soils? The agricultural usage of silicate rock powders: A review. Sci Total Environ*,* 807**,** 150976. https://doi.org/10.1016/j.scitotenv.2021.150976.

TE PAS, E. E. E. M., COMANS, R. N. J., BISSELING, S. & HAGENS, M. 2026. Enhanced weathering and biochar co-deployment boosts CO_2 sequestration through changing soil properties. Geoderma, 466, 117668. https://doi.org/10.1016/j.geoderma.2025.117668.

VANCE, E. D., BROOKES, P. C. & JENKINSON, D. S. 1987. An extraction method for measuring soil microbial biomass C. Soil Biol Biochem, 19, 703–707. https://doi.org/10.1016/0038-0717(87)90052-6.

VIENNE, A., NEWELL, J., ROUSSARD, J., DOHERTY, R., COX, S. F., LYONS, G. & VICCA, S. 2025. Increased soil CO_2 emissions after basalt amendment were partly offset by biochar addition in an urban field experiment. EGUsphere [preprint], 2025, 1–24. https://doi.org/10.5194/egusphere-2025-3232, 2025. .

VIRET, F. & GRAND, S. 2019. Combined size and density fractionation of soils for investigations of organo-mineral interactions. JoVE, e58927. https://doi.org/10.3791/58927.

VON LÜTZOW, M., KÖGEL-KNABNER, I., EKSCHMITT, K., MATZNER, E., GUGGENBERGER, G., MARSCHNER, B. & FLESSA, H. 2006. Stabilization of organic matter in temperate soils: mechanisms and their relevance under different soil conditions – a review. Eur J Soil Sci, 57, 426–445. https://doi.org/10.1111/j.1365-2389.2006.00809.x.

VON LÜTZOW, M., KÖGEL-KNABNER, I., LUDWIG, B., MATZNER, E., FLESSA, H., EKSCHMITT, K., GUGGENBERGER, G., MARSCHNER, B. & KALBITZ, K. 2008. Stabilization mechanisms of organic matter in four temperate soils: Development and application of a conceptual model. J Plant Nutr Soil Sc, 171, 111–124. https://doi.org/10.1002/jpln.200700047.

VORRATH, M.-E., AMANN, T., MEYER ZU DREWER, J., HAGEMANN, N., ALDRICH, C., BÖRKER, J., SEEDTKE, M., BECKER, J. N., HAGENS, M., ESCHENBACH, A. & HARTMANN, J. 2025. Pyrogenic carbon and carbonating minerals for carbon capture and storage (PyMiCCS) part II: organic and inorganic carbon dioxide removal in an Oxisol. Front Clim, Volume 7 - 2025. https://doi.org/10.3389/fclim.2025.1592454.

WANG, D., FONTE, S. J., PARIKH, S. J., SIX, J. & SCOW, K. M. 2017. Biochar additions can enhance soil structure and the physical stabilization of C in aggregates. Geoderma, 303, 110–117. https://doi.org/10.1016/j.geoderma.2017.05.027.

WANG, J., XIONG, Z. & KUZYAKOV, Y. 2016. Biochar stability in soil: meta-analysis of decomposition and priming effects. GCB Bioenergy, 8, 512–523. https://doi.org/10.1111/gcbb.12266.

WENG, Z., VAN ZWIETEN, L., SINGH, B. P., TAVAKKOLI, E., JOSEPH, S., MACDONALD, L. M., ROSE, T. J., ROSE, M. T., KIMBER, S. W. L., MORRIS, S., COZZOLINO, D., ARAUJO, J. R., ARCHANJO, B. S. & COWIE, A. 2017. Biochar built soil carbon over a decade by stabilizing rhizodeposits. Nat Clim Change, 7, 371–376. https://doi.org/10.1038/nclimate3276.

WERTH, M. & KUZYAKOV, Y. 2010. ^{13}C fractionation at the root–microorganisms–soil interface: A review and outlook for partitioning studies. Soil Biol Biochem, 42, 1372–1384. https://doi.org/10.1016/j.soilbio.2010.04.009.

WHITMAN, T., SINGH, B. P. & ZIMMERMAN, A. R. 2015. Priming effects in biochar-amended soils: Implications of biochar-soil organic matter interactions for carbon storage. *In:* LEHMANN, J. & JOSEPH, S. (eds.) Biochar for environmental management. 2 ed. London, UK: Routledge.

WICKHAM, H. 2016. ggplot2: Elegant graphics for data analysis. New York, USA, Springer.

WICKHAM, H., FRANÇOIS, R., HENRY, L. & MÜLLER, K. 2023. dplyr: A Grammar of Data Manipulation - R package version 1.1.4. [Online].

XIE, N., FAN, Y., DUAN, N., YANG, L., RADOSEVICH, M., ZHANG, Y., WANG, Y., WANG, J. & LIANG, X. 2025. Interactive effects of straw and biochar amendments on soil organic carbon stabilization and bacterial community dynamics. Biol Fert Soils*,* 61**,** 1423–1437. https://doi.org/10.1007/s00374-025-01947-9.

XU, P., WANG, Q., DUAN, C., HUANG, G., DONG, K. & WANG, C. 2024. Biochar addition promotes soil organic carbon sequestration dominantly contributed by macro-aggregates in agricultural ecosystems of China. J Environ Manage*,* 359**,** 121042. https://doi.org/10.1016/j.jenvman.2024.121042.

XU, T., LI, H., VICCA, S., GOLL, D. S., BEERLING, D. J., CHEN, Q., BI, B., YANG, Z., WANG, X. & YUAN, Z. 2025. Enhanced rock weathering promotes soil organic carbon accumulation: A global meta-analysis based on experimental evidence. Glob Chang Biol*,* 31**,** e70483. https://doi.org/10.1111/gcb.70483.

XU, W., WHITMAN, W. B., GUNDALE, M. J., CHIEN, C.-C. & CHIU, C.-Y. 2021. Functional response of the soil microbial community to biochar applications. GCB Bioenergy*,* 13**,** 269–281. https://doi.org/10.1111/gcbb.12773.

YANG, F., XU, Z., HUANG, Y., TSANG, D. C. W., OK, Y. S., ZHAO, L., QIU, H., XU, X. & CAO, X. 2021. Stabilization of dissolvable biochar by soil minerals: Release reduction and organo-mineral complexes formation. J Hazard Mater*,* 412**,** 125213. https://doi.org/10.1016/j.jhazmat.2021.125213.

YANG, F., ZHAO, L., GAO, B., XU, X. & CAO, X. 2016. The interfacial behavior between biochar and soil minerals and its effect on biochar stability. Environ Sci Technol*,* 50**,** 2264–2271. https://doi.org/10.1021/acs.est.5b03656.

YANG, Y., SUN, K., HAN, L., CHEN, Y., LIU, J. & XING, B. 2022. Biochar stability and impact on soil organic carbon mineralization depend on biochar processing, aging and soil clay content. Soil Biol Biochem*,* 169**,** 108657. https://doi.org/10.1016/j.soilbio.2022.108657.

YOO, G., KIM, H. & CHOI, J. Y. 2017. Soil aggregate dynamics influenced by biochar addition using the ^{13}C natural abundance method. Soil Sci Soc Am J*,* 81**,** 612–621. https://doi.org/10.2136/sssaj2016.09.0313.

YU, Z., CHEN, L., PAN, S., LI, Y., KUZYAKOV, Y., XU, J., BROOKES, P. C. & LUO, Y. 2018. Feedstock determines biochar-induced soil priming effects by stimulating the activity of specific microorganisms. Eur J Soil Sci*,* 69**,** 521–534. https://doi.org/10.1111/ejss.12542.

YU, Z., LING, L., SINGH, B. P., LUO, Y. & XU, J. 2020. Gain in carbon: Deciphering the abiotic and biotic mechanisms of biochar-induced negative priming effects in contrasting soils. Sci Total Environ*,* 746**,** 141057. https://doi.org/10.1016/j.scitotenv.2020.141057.

ZHANG, L., JING, Y., XIANG, Y., ZHANG, R. & LU, H. 2018. Responses of soil microbial community structure changes and activities to biochar addition: A meta-analysis. Sci Total Environ*,* 643**,** 926–935. https://doi.org/10.1016/j.scitotenv.2018.06.231.

ZIMMERMAN, A. R., GAO, B. & AHN, M.-Y. 2011. Positive and negative carbon mineralization priming effects among a variety of biochar-amended soils. Soil Biol Biochem*,* 43**,** 1169–1179. https://doi.org/10.1016/j.soilbio.2011.02.005.

D.7 Appendix

D7.1 Basanite rock powder properties

The chemical composition of the rock powder (Table D.3) was analyzed using X-ray fluorescence (XRF) at the Mineralogical Institute, University of Hamburg, while the mineralogical composition was determined by Qmineral using X-ray diffraction (XRD), as described in VORRATH et al. (2025). Following the classification of volcanic rocks by STRECKEISEN (1980) or LE BAS et al. (1986), this rock can be classified as a basanite. The basanite was obtained from Rheinische Provinzial-Basalt- u. Lavawerke, Sinzig, Germany.

Table D.3: Main compounds, trace elements, mineral composition and grain size of used basanite rock powder *Eifelgold*. Bdl = below detection limit; LOI = loss on ignition.

Main compounds	**[wt%]**	**Trace Elements**	**[ppm]**	**Mineralogy**	**[wt%]**	**Grain size [µm]**	**[wt%]**
SiO_2	43.86	As	bdl	Clinopyroxene	44.4	> 300	0.00
TiO_2	2.79	Ba	1026	Plagioclase	15.5	300 - 250	0.13
Al_2O_3	14.15	Bi	bdl	Nepheline	11.2	250 - 210	0.17
Fe_2O_3	11.28	Ce	104	Leucite	9.9	210 - 180	0.14
MnO	0.18	Co	51	Olivine	6.3	180 - 150	0.26
MgO	8.21	Cr	53	2:1 layer silicates	5.1	150 - 120	1.20
CaO	11.63	Cu	66	Hematite	3.1	120 - 100	2.87
Na_2O	3.26	Ga	17	Spinel-type minerals	1.9	100 - 86	4.17
K_2O	3.35	La	52	Apatite	1.1	86 - 74	5.67
P_2O_5	0.6	Nb	52	Analcime	0.9	74 - 62	8.13
SO_3	bdl	Nd	28	Quartz	0.7	62 - 52	8.89
LOI	0.44	Ni	124			52 - 44	8.50
Sum	*99.74*	Pb	5			44 - 36	9.63
		Rb	86			36 - 30	7.86
		Sc	22			30 - 26	5.50
		Sr	882			26 - 22	5.64
		Th	8			22 - 18	5.72
		U	3			18 - 0.5	25.52
		V	302				
		Y	24				
		Zn	90				
		Zr	271				

D7.2 Properties of biochar and rock-enhanced biochar

Table D.4: Further information on initial composition of biochar and rock-enhanced biochar.

Properties	**Biochar**	**Rock-enhanced biochar**
Oxygen [%]	3.79	2.95
Hydrogen [%]	0.83	0.60
Sulfur [%]	0.62	0.45
Trace elements		
Ag [mg kg^{-1}]	<1.1	<1.1
As [mg kg^{-1}]	0.3	0.6
B [mg kg^{-1}]	13.9	11.6
Cd [mg kg^{-1}]	0.15	0.13
Cr [mg kg^{-1}]	39.5	40.0
Cu [mg kg^{-1}]	829.4	515.2
Hg [mg kg^{-1}]	0.016	0.020
Mn [mg kg^{-1}]	84.4	233.4
Ni [mg kg^{-1}]	15.0	28.4
Pb [mg kg^{-1}]	2.0	2.1
Zn [mg kg^{-1}]	62.0	58.9
Chemical composition of ash		
CaO [%]	15.07	12.53
Fe_2O_3 [%]	1.61	7.26
K_2O [%]	24.50	10.69
MgO [%]	2.50	6.30
Na_2O [%]	1.00	2.15
P_2O_5 [%]	5.00	1.93
SO_3 [%]	4.29	1.62
SiO_2 [%]	32.40	36.60

Measured by Ruhr Lab GmbH according to the analytical guidelines of the European Biochar Certificate (EBC, 2024).

D7.3 Cumulative priming effect during incubation

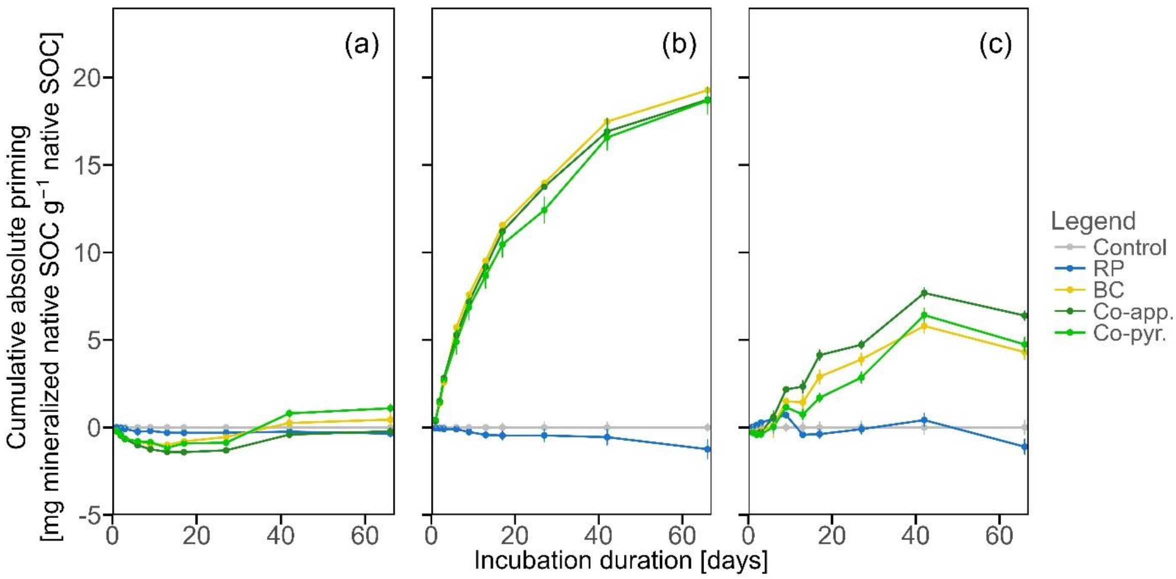

Figure D.6: Cumulative absolute priming relative to control (mg mineralized native SOC g^{-1} native SOC) of temperate silty (a), temperate sandy (b), and tropical sandy (c) soil in five treatments (n = 4, mean and standard error) during the 66 days of incubation. RP = rock powder treatment containing basanite, BC = biochar treatment, Co-app. = co-application treatment containing biochar and basanite, Co-pyr. = co-pyrolysis treatment containing rock-enhanced biochar.

D7.4 Mineralization of native SOC and amendment-C during the incubation

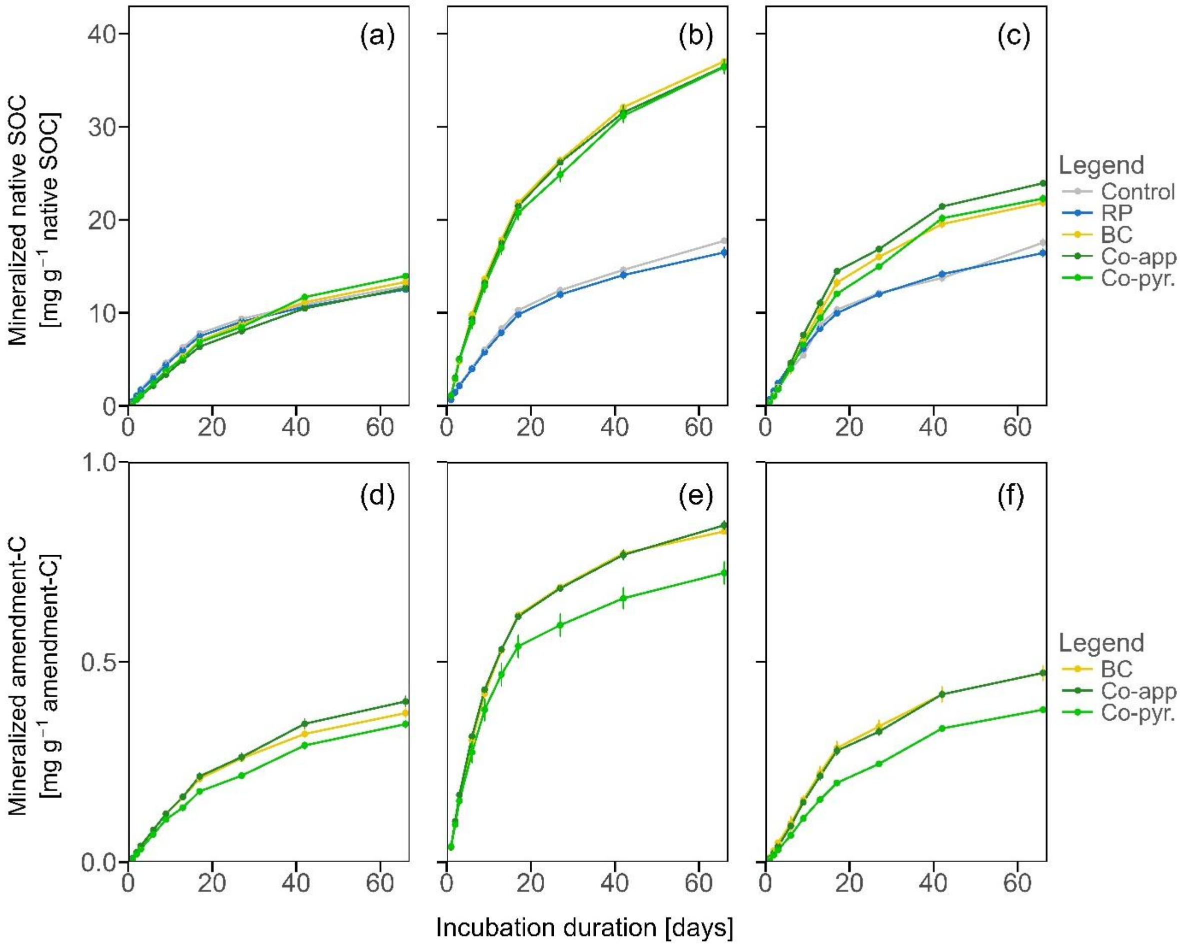

Figure D.7: Cumulative mineralized native SOC (mg mineralized native SOC g^{-1} native SOC) and amendment-C (mg mineralized amendment-C g^{-1} amendment-C) of temperate silty (a, d), temperate sandy (b, e), and tropical sandy soil (c, f) in five treatments (n = 4, mean and standard error) during the 66-day incubation. RP = rock powder treatment containing basanite, BC = biochar treatment, Co-app. = co-application treatment containing biochar and basanite, Co-pyr. = co-pyrolysis treatment containing rock-enhanced biochar.

D7.5 Mean and standard deviation of relative amendment-induced priming effect

Table D.5: Relative cumulative amendment-induced priming effect at the end of the 66-day incubation.

Soil	Treatment	Relative priming [%]
Temperate silty soil	RP	-2.74 ± 1.48 [a]
	BC	3.48 ± 3.03 [ab]
	Co-app.	-1.72 ± 1.63 [a]
	Co-pyr.	8.51 ± 1.69 [b]
Temperate sandy soil	RP	7.02 ± 3.55 [a]
	BC	108.61 ± 0.95 [b]
	Co-app.	105.54 ± 4.15 [b]
	Co-pyr.	105.23 ± 4.30 [b]
Tropical sandy soil	RP	-6.30 ± 2.45 [a]
	BC	24.54 ± 2.46 [b]
	Co-app.	36.43 ± 1.60 [c]
	Co-pyr.	27.03 ± 2.29 [bc]

Data is presented as mean ± standard error (n = 4). Lower case letters indicate significant differences in relative amendment-induced priming between treatments within one soil ($p < 0.05$). RP = rock powder treatment containing basanite, BC = biochar treatment, Co-app. = co-application treatment containing biochar and basanite, Co-pyr. = co-pyrolysis treatment containing rock-enhanced biochar.

Acknowledgments

Vielen Dank an meine Betreuerin, **Annette Eschenbach**, die mir diese Promotion ermöglicht und mich über die gesamte Zeit hinweg begleitet hat. Ihre positive Bestärkung und ihr Vertrauen in mich und meine Arbeit haben mir, besonders in der Endphase der Dissertation, viel bedeutet. Sie hat es mir ermöglicht, mich sowohl persönlich als auch fachlich, wie bei Konferenzteilnahmen oder Aufenthalten an anderen Forschungseinrichtungen, weiterzuentwickeln.

Vielen Dank an meinen Betreuer, **Joscha Becker**, für seine wissenschaftliche Expertise und seine offene Tür bei alltäglichen fachlichen Fragen, besonders zu methodischen und statistischen Belangen, während der gesamten Promotionszeit. Durch ihn war mir der Aufenthalt an der Universität Tübingen möglich und ich danke ihm darüber hinaus für seine Hilfe bei der Probenahme in Geisenheim.

Ich danke **Jörn Peckmann** für seine Unterstützung als mein Panel Chair. Sein großes Interesse an meinem Forschungsthema und seine engagierte Teilnahme an den Panel Meetings haben diese sehr bereichert.

Dem **PyMiCCS-Team** danke ich für die Möglichkeit, Teil eines interdisziplinären Forschungsverbundes zu sein. Der Austausch mit Expert:innen aus unterschiedlichen Fachbereichen hat mir sehr geholfen und mir den Blick für unterschiedliche Perspektiven eröffnet. Besonders danke ich **Susanne Hamburger** für den engen wissenschaftlichen Austausch, die Mühe, die sie in das Feldexperiments gesteckt hat, und die Unterstützung bei der Probenahme am Ende dieses Feldexperiments vor Ort in Geisenheim. Ich schätze unsere freundschaftliche Verbindung, die sich daraus entwickelt hat.

Ich danke außerdem meinen **Co-Autor:innen**, ohne deren Beiträge diese Arbeit nicht möglich gewesen wäre. Ein besonderer Dank gilt **Annemarie** für ihre Unterstützung meiner Forschung im Rahmen ihrer Masterarbeit.

Meiner **Arbeitsgruppe** danke ich für den fachlichen und vor allem persönlichen Austausch, der die Zeit am Institut für mich ganz besonders gemacht hat und mir vor Augen geführt hat, wie viel ein tolles Kollegium wert ist. Die gemeinsamen Mittagessen und Kaffeepausen haben meinen Promotionsalltag deutlich aufgelockert. Ich danke **Sumita**, **Volker**, **Andreas**, **Annika** und insbesondere **Deborah** sowie allen **studentischen Hilfskräften** für ihre Unterstützung im Labor. **Sumita** danke ich darüber hinaus für ihre Hilfe bei der Probenahme in Geisenheim. Außerdem danke ich **Deborah** und **Sumita** für ihre Unterstützung und den persönlichen Austausch, aus dem sich eine tolle Freundschaft entwickelt hat. Ich danke **Rike** für ihr stets offenes Ohr und ihre Empathie sowie **Mathias** und **Liz** für ihre Hilfsbereitschaft und ihre aufmunternden Worte. Ich bin dankbar für die Zeit, die sich **Rike** und **Elisa** für das sorgfältige Korrekturlesen meiner Dissertation genommen haben.

Bei **Elisa** möchte ich mich besonders bedanken – aus unserem Dasein als Bürokolleginnen hat sich eine enge Freundschaft entwickelt. Sie hat mich während der gesamten Promotionszeit begleitet, einschließlich der Höhen und Tiefen unserer Arbeit – von Fehlschlägen im Labor, abgelehnten Manuskripten, und der Panik vor Präsentationen bis hin zu unvergesslichen Konferenzreisen, abgeschlossenen Experimenten, und der Abgabe unserer Dissertationen. Ihre unermüdliche Unterstützung und ihr Rat auf fachlicher und persönlicher Ebene haben mir durch diese Promotion geholfen.

Meiner Familie danke ich von Herzen für ihre Unterstützung und ihren Rückhalt. Insbesondere danke ich meiner **Mama**, die mir immer das Gefühl gegeben hat, stolz auf mich zu sein. Mein größter Dank gilt meinem Mann **Daniel**. Er hat mich nicht nur im Alltag entlastet und versucht, auch inhaltlich in mein Thema einzusteigen, sondern mich vor allem mental unterstützt und an mich geglaubt, sodass meine Selbstzweifel nie zu laut werden konnten.